Investigating Fork Rotation and DNA Pre-catenation in *Saccharomyces cerevisiae*

Sahar Mansoubi

Thesis submitted for the degree of Doctor of Philosophy

University of Sussex

May 2017

Declaration

I hereby declare that this thesis has not been and will not be submitted in whole or in part to another university for the award of any other degree.

Signature:

Sahar Mansoubi

Acknowledgements

I would like to thank my supervisor, Dr. Jon Baxter, for giving me the opportunity to conduct my PhD work in his laboratory. I am deeply grateful for all his patience, rigorous training, guidance, and support throughout the years, without which the completion of this project would have been impossible.

I would also like to thank my co-supervisor, Dr. Jo Murray, for her support, particularly in the beginning of my PhD. I also wish to extend special thanks to Dr. Stephanie Schalbetter for all her guidance, help, and support during my work on this PhD project (both inside the lab and outside). In addition, I wish to express my deepest appreciation to Dr. Andrea Keszthelyi for the helpful discussions about my project. I am also grateful to all the members of the Baxter lab, including Dr. Catrina Miles, Nicola, and Rose, for their continued support and encouragement, for keeping me smiling throughout my project, and most importantly for being the best friends I could have asked for.

I also wish to thank the Zegerman lab, our collaborators at Cambridge University, for sharing their knowledge about ChIP-Seq and quantification of the corresponding data. I thank the Watts and Hochegger labs for making the lab environment so friendly and Dr. Farimah Gholami and Dr. Nisha Peter for being a constant source of support over the past few years. I am also grateful to all the GDSC staff for their support and care.

Finally, I am deeply grateful to my parents and my sister, who despite being so far away, showered me with lots of love and encouragement and were the utmost source of inspiration for me to finish my PhD successfully. I could not have done this without their support!

I would like to dedicate this work to the memory of my elder sister, Najmeh.

پدر بزرگوار و مادر مهربانم همیشه دست بوس و قدردان زحمات شما دو عزیزم هستم.

UNIVERSITY OF SUSSEX

Sahar Mansoubi

Doctor of Philosophy (Genome Damage and Stability)

Investigating Fork Rotation and DNA Pre-catenation in *Saccharomyces cerevisiae*

Summary

During DNA replication, the intertwining between the two strands of the parental DNA double helix needs to be resolved. This is achieved in two ways: by the action of topoisomerases ahead of the replication fork or by fork rotation and pre-catenation of the newly replicated DNA helixes. However, the factors that influence fork rotation and pre-catenation remain unknown. In this thesis, I used classical genetics and high-resolution two-dimensional agarose gel electrophoresis to identify the replisome-associated factors important for fork rotation and DNA pre-catenation during DNA replication in the yeast *Saccharomyces cerevisiae*. The results indicate that fork rotation and pre-catenation are impeded by two non-essential evolutionarily conserved replisome components: the Timeless and Tipin homologs, Tof1 and Csm3. Tof1/Csm3 are required for maintaining genome integrity during unperturbed and perturbed DNA replication. Similarly, checkpoint activation is also thought to stabilize the replisome in both unchallenged and challenged cells. However, none of the checkpoint kinases were found to alter the frequency of fork rotation during DNA replication in our study. Finally, constitutive DNA damage was found to be dramatically increased on newly replicated chromatids in the absence of Top2 and/or Tof1 as a consequence of excessive fork rotation and DNA pre-catenation during DNA replication in both western blot and ChIp-Seq experiments. This led to the activation of the DNA damage checkpoint and extensive DNA repair. These results suggest that although fork rotation and pre-catenation facilitate DNA unwinding under certain chromosomal contexts, excessive fork rotation and pre-catenation lead to defects on the newly replicated chromatids and therefore must be inhibited by Tof1/Csm3. In conclusion, I showed that Tof1/Timeless and Csm3/Tipin proteins regulate DNA replication and prevent chronic genome instability by minimizing pre-catenation during DNA replication.

Contents

SCHALBETTER, S. A., MANSOUBI, S., CHAMBERS, A. L., DOWNS, J. A. & BAXTER, J. 2015. Fork rotation and DNA pre-catenation are restricted during DNA replication to prevent chromosomal instability. 112**,** E4565-70.

List of Figures

List of Tables

Abbreviations

2D	Two-dimensional
Å	Ångstrom
APC	Anaphase promoting complex
APS	Ammonium persulphate
ARS	Autonomously replicating sequence
ATP	Adenosine triphosphate
ATR	Ataxia-Telangiectasia Mutated and Rad3 related
bp	Base pair
CDK	Cyclin-dependent kinase
ChIP	Chromatin immunoprecipitation
DAPI	4,6-diaminidino-2-phenylindole
dATP	Deoxyadenosine triphosphate
DMSO	Dimethyl sulphoxide
DNA	Deoxyribonucleic acid
dNTPs	Deoxyribonucleoside triphosphate
DSB	Double strand break
dsDNA	Double-stranded DNA
ECL	Enhanced chemiluminescence
E. coli	*Escherichia coli*
EDTA	Ethylenediaminetetraacetic acid
FACS	Fluorescence-activated cell sorting
g	Gram
G1	Growth 1
G2	Growth 2

G418	Geneticin
GCR	Gross chromosomal rearrangement
h	Hour(s)
HA	Hemagglutinin
HCl	Hydrochloric acid
hph	Hygromycin B
HR	Homologous recombination
H. s	*Homo sapiens*
HU	Hydroxyurea
IB	Immunoblotting
IP	Immunoprecipitation
kb	Kilo base
LB	Luria-bertani
LiOAc	Lithium acetate
M	Mitosis
MCM	Minichromosome maintenance
µg	Microgram
min	Minute(s)
µl	Microlitre
MMS	Methyl methanesulphonate
NAT	Nourseothricin sulphate
NHEJ	Non-homologous end joining
ORC	Origin recognition complex
PBS	Phosphate buffered saline
PBS-T	Phosphate buffered saline- Tween20

PCR	Polymerase chain reaction
PEG	Polyethylene glycol
pH	Negative log of the hydrogen ion concentration
pre-IC	Pre-initiation complex
pre-RC	Pre-replication complex
PRR	Post Replicative Repair
rDNA	Ribosomal DNA
RNA	Ribonucleic acid
rpm	Revolutions per minute
SAC	Spindle assembly checkpoint
S. cerevisiae	*Saccharomyces cerevisiae*
SDS	Sodium dodecyl sulphate
SDS-PAGE	SDS polyacrylamide gel electrophoresis
S. pombe	*Saccharomyces pombe*
ssDNA	Single-stranded DNA
TBE	Tris-Borate-EDTA
TCA	Trichloroacetic acid
TE	Tris-EDTA
TEMED	N,N,N0, N0-tetramethylpropane-1,3-diol
Tris	Tris(hydroxymethyl)aminomethane
tRNA	Transfer RNA
V	Volt
WT	Wild-type
YNB	Yeast nitrogen base
YPD	Yeast extract peptone dextrose

Chapter 1

Introduction

1.1 DNA Topology

1.1.1 DNA Double Helix

The discovery of the structure of the DNA double helix by Watson, Crick, and Franklin was one of the most important scientific findings of the twentieth century (Watson and Crick, 1953a). In their model, Watson and Crick described that the DNA (a negatively charged polymer) is made up of repeating units known as nucleotides and that each nucleotide consists of three components: one of four heterocyclic bases, a five-carbon sugar (2'-deoxyribose) and a phosphate. These nucleotides are linked by phosphodiester linkages and form the polynucleotide backbone of the DNA. The formation of hydrogen bonds between purines (A: adenine, G: guanosine) and pyrimidines (C: cytosine, T: thymine) is the essence of the double-stranded DNA (ds) structure of the DNA helix. The two strands in the helix run in opposite directions and are hence said to be antiparallel (Figure 1.1) (Watson and Crick, 1953a).

The most common DNA conformation identified in living cells is the B-DNA confirmation, which is most stable at high humidity (e.g. 92%). The two strands forming the nucleotide backbone of a B-DNA helix are coiled around each other in a right-handed fashion, and this helix has been shown to have an average of 10.5 base pairs per turn. The double helix structure of the DNA consists of a major groove and minor groove. In B-DNA, the major groove is wider and deeper than the minor groove, and this feature makes it more accessible for interactions with proteins that can identify specific DNA sequences. The average distance between base pairs is 3.3 Å; therefore, the average distance between each turn is about 34 Å and the width of the double helix is around 20 Å. The bases are on the inner side of the double helix and are perpendicular to the helix axis; however, the sugar-phosphate backbones of the two strands are on the outer side of the double helix and carry negative charges on their phosphate groups (Watson and Crick, 1953a).

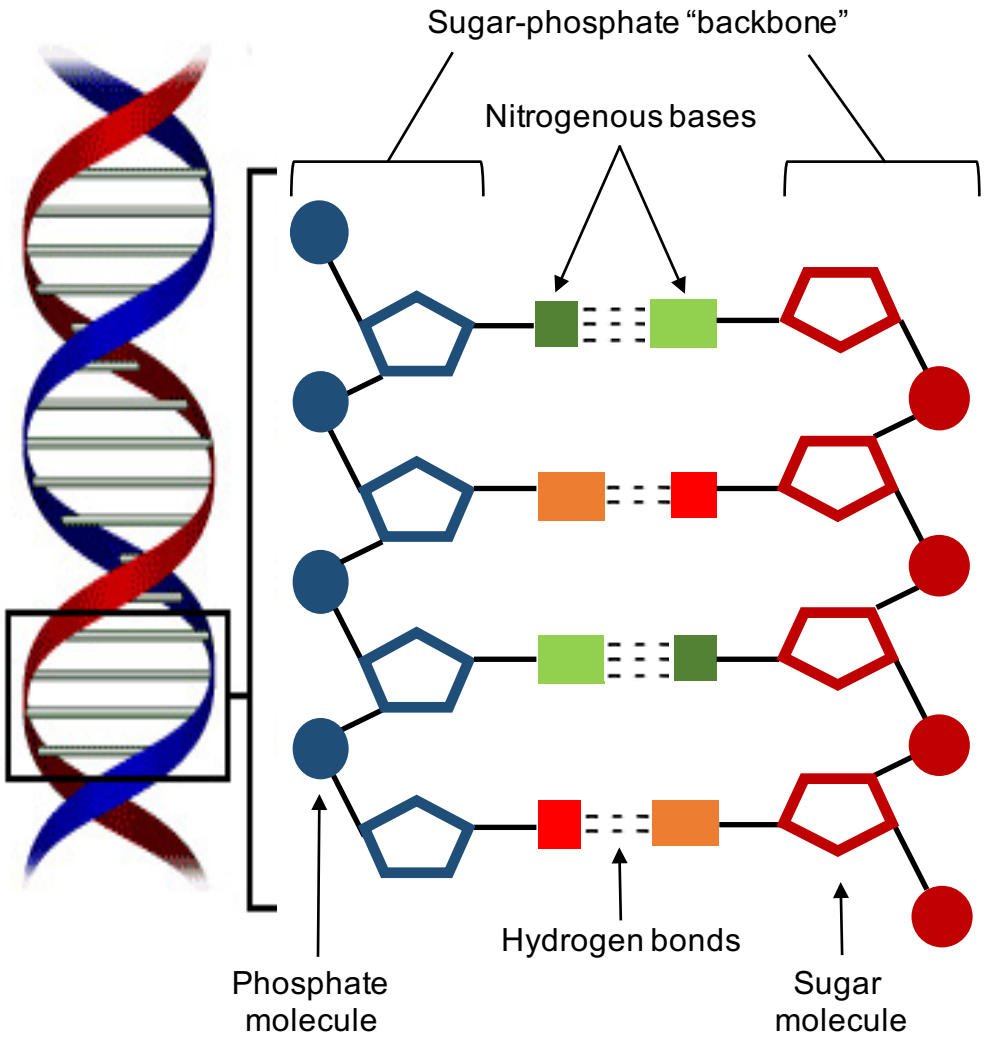

Figure 1.1: Structure of the DNA double helix.
This figure was adapted from (Watson and Crick, 1953a).

1.1.2 DNA Supercoiling

1.1.2.1 Linking Number

The extent of intertwining of a DNA molecule is often defined by its linking number (Lk). The Lk is composed of two components the twisting number (Tw) and the writhing number (Wr) and can be defined by the following equation (reviewed by Postow et al., 2001a):

$$Lk=Tw + Wr$$

Where Lk refers to the number of times and the handedness of one strand crossing over the other when the axis is constrained in a plane, Tw is the measure of the helical winding of the DNA strands around each other, and Wr is the measure of the coiling of the axis of the double helix. A right-handed coil is assigned a negative number (negative supercoiling) and a left-handed coil is assigned a positive number (positive supercoiling) (Bates and Maxwell, 2005). When the DNA helix has a normal number of base pairs per helical turn, it is in the relaxed state. Processes that read genetic codes, such as DNA replication, homologous recombination, and gene expression, need access to internal nucleotide bases. Cells permit access to the genetic code by holding the DNA in an underwound state. This helix underwinding means that the Lk of the DNA is less than that in the lowest free energy state (Berg et al., 2002).

The Lk of the strands of a right-handed DNA is defined as positive. For instance, in circular and relaxed B-DNA of 260 base pairs (bp), the Lk is 260/10.4 = 25 turns without supercoiling; then, Wr = 0, and Lk = Tw = 25 (where 10.4 is the number of bp per turn for B-DNA) (Figure 1.2A). A different circular DNA can be produced by unwinding the DNA duplex by two turns, and this unwinding must involve cutting and resealing the DNA. In this case, the DNA can either fold into a structure possessing 23 turns of B-helix and an unwound loop (Figure 1.2B) or adopt a supercoiled structure with 25 turns of B-helix and 2 turns of right-handed (negative) superhelix (Figure 1.2C). Hence, closed DNA molecules of the same sequence can have different Lks, indicating different levels of supercoiling; such DNA molecules are known as *topological isomers* or topoisomers. Topoisomers

of DNA can be interconverted, i.e. the Lk of a specific closed molecule can only be altered by nicking one or both strands, thereby allowing the free end to let one strand pass around the other, and subsequently re-joining the broken ends. Thus, this reaction alters the Lk, and this value is identified as a characteristic of the reaction. The unwound DNA and supercoiled DNA shown in Figure 1.2B and 1.2C are topologically identical, but geometrically different. They have the same value of Lk but differ in their Tw and Wr. In Figure 1.2B, the partly unwound circular DNA has Tw = 23 and Wr = 0; however, the supercoiled DNA has Tw = 25 and Wr = -2 (Figure 1.2C). These conformations can be interconverted without breaking the DNA chain because they have the same Lk value. Thus, as mentioned earlier, negative supercoiling provides DNA for processes requiring separation of the DNA strands, such as replication and transcription. Positive supercoiling makes strand separation more difficult (Berg et al., 2002).

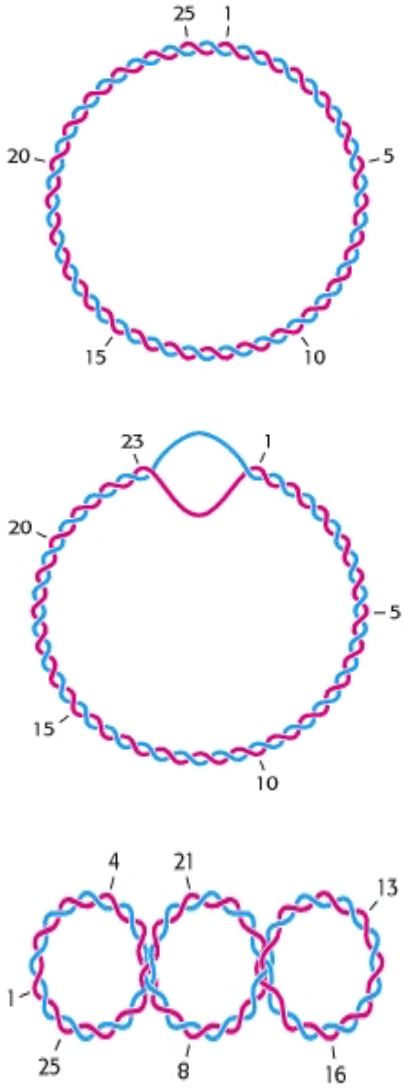

Figure 1.2: Schematic representation of the relationship between the linking number (Lk), twisting number (Tw), and writhing number (Wr) of a circular DNA molecule.
This figure was taken from (Berg et al., 2002).

1.1.2.2 The Problem of the Double Helix

The two strands of the double-stranded DNA (dsDNA) have to be separated for the DNA to be able to carry out all of its functions (replication, transcription and recombination). Figure 1.3 shows some of the consequences of unwinding by the replicative helicase. No problems seem to arise during the unwinding of a short linear DNA, since the rotation of the ends of the DNA strands is freely carried out around the axis of the double helix to relax any tension. However, linear eukaryotic chromosomes are coated with proteins that anchor the DNA at many points, thus making it difficult for the DNA to rotate freely. In this case, when two intertwined strands are separated, it increases the winding along the DNA molecule, leading to supercoiling of the fibre (see section 1.1.2.3) to balance the under-winding in the single-stranded region. If the DNA cannot rotate to relieve the stress that builds up, further separation of the strands can stop. This issue was discussed by Watson and Crick after they described their DNA model (Watson and Crick, 1953b, Watson and Crick, 1993). In 1954, Delbruck proposed that this problem can be solved by introducing a transient break in one or both DNA strands, which will cause the nicked strand to pass around the intact strand; this can then be followed by re-joining of the broken ends, so that one superhelical turn is released by each cycle of nicking and sealing (delbruck, 1954). We now know that this breaking and rejoining is carried out by DNA topoisomerases; the details of the mechanisms of action of these enzymes will be discussed in the following sections.

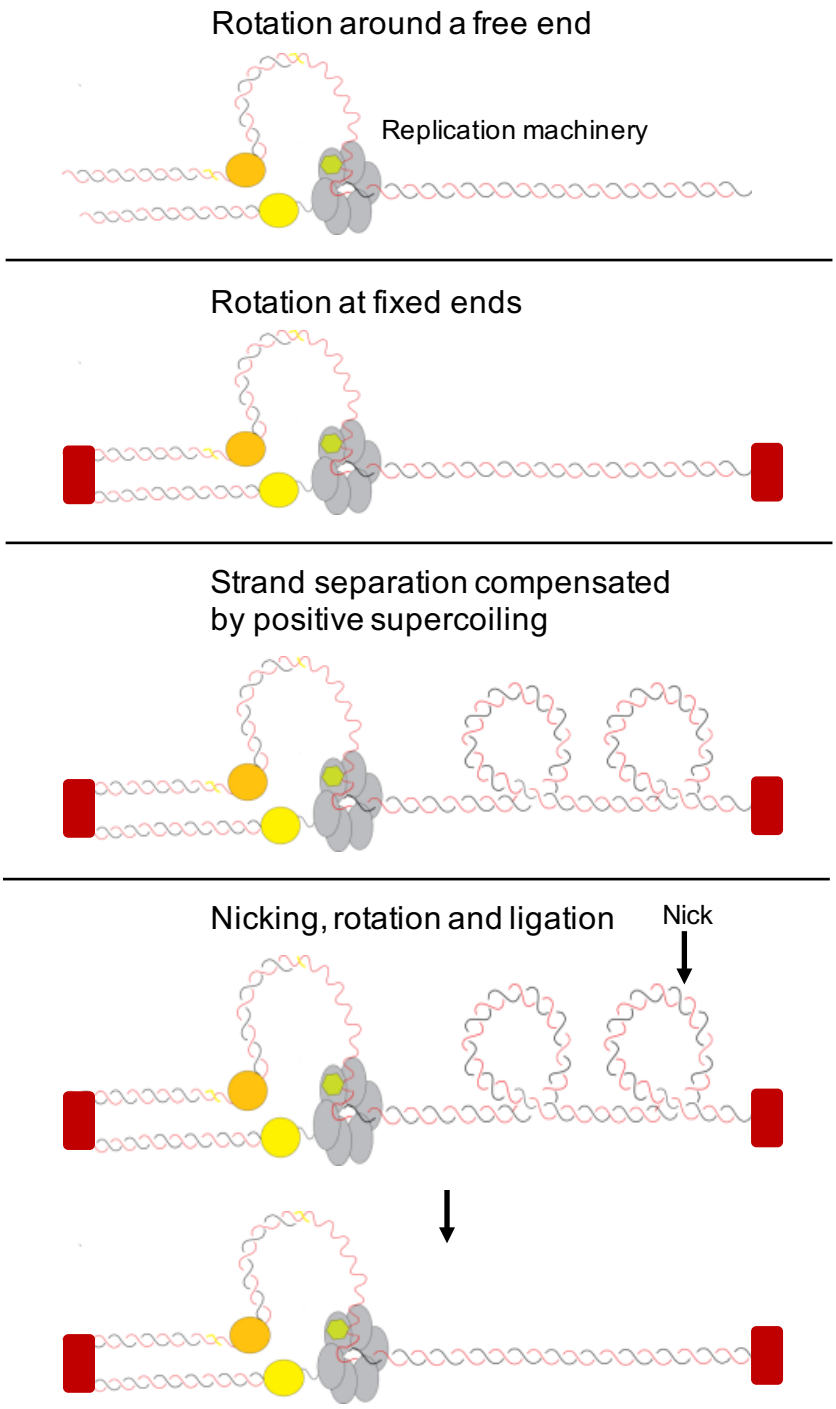

Figure 1.3: Topological consequences of the separation of the strands of the DNA double helix and their resolution.
This figure was adapted from (Krebs et al., 2011).

1.1.2.3 Closed Circular DNA and Supercoiling

In a “relaxed” double-helical segment of a B-DNA, the two strands are wound around each other once every 10.4 bp. The whole conformation can be altered when the double helix winds around itself, which is known as supercoiling. Thus, topological tension can result in supercoiling of the structure of the DNA, and it can only occur either in linear DNA when it is anchored to a protein scaffold, like in eukaryotic chromosomes, or in DNA that has no free ends, such as a circular DNA molecule, as the free ends can rotate to relieve the tension. The right-handed DNA helix rotates in the clockwise direction (right-handed). Over-twisting of the helix results in an anti-clockwise (left-handed) writhe (between dsDNAs), which forms positive supercoiling. In contrast, untwisting of the helix is referred to as opposite motion, which forms negative supercoiling. Thus, adding or subtracting twists, as some enzymes do, imposes a strain (Figure 1.4) (Bates and Maxwell, 2005).

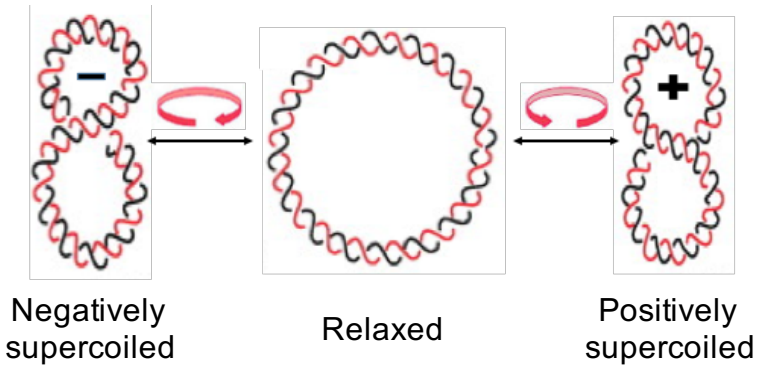

Figure 1.4: Direction of the twisting of the two strands of the DNA determines whether the supercoiling is negative or positive.
This figure was taken from (Baxter and Aragon, 2012).

1.1.3 DNA Catenanes

Circular DNA molecules that are linked together are known as DNA catenanes. Catenated DNA molecules were first found *in vivo* in 1967 in human cells (Hudson and Vinograd, 1967) and are routinely detected *in vivo* as a result of DNA replication. In simplistic terms, a catenated DNA node refers to the intertwining of two DNA duplexes such that they cannot be pulled apart without one of the molecules being broken. Therefore, catenated DNA molecules are produced from the intertwining of two intact DNA duplexes, as the breakage of one strand of either duplex is not sufficient to resolve the dimers into their subsequent monomeric states. To achieve this, breakage of both backbones of one of the two intertwined duplexes is required (Marini et al., 1980). The generation of a DNA catenane during replication is one of the potential topological consequences of replication and will be discussed further in the following sections. DNA catenanes can occur in three different conformations (Figure 1.5): CatAs are created by two nicked rings; CatBs are created by one nicked ring and another covalently closed ring; and CatCs are created by two covalently closed rings. Furthermore, the DNA rings can be catenated either once ($Ca = 1$) or multiple times ($Ca \geq 2$) (Sundin and Varshavsky, 1980, Sundin and Varshavsky, 1981). The sum of the intermolecular nodes is defined as the catenation number (Ca) (Martinez-Robles et al., 2009).

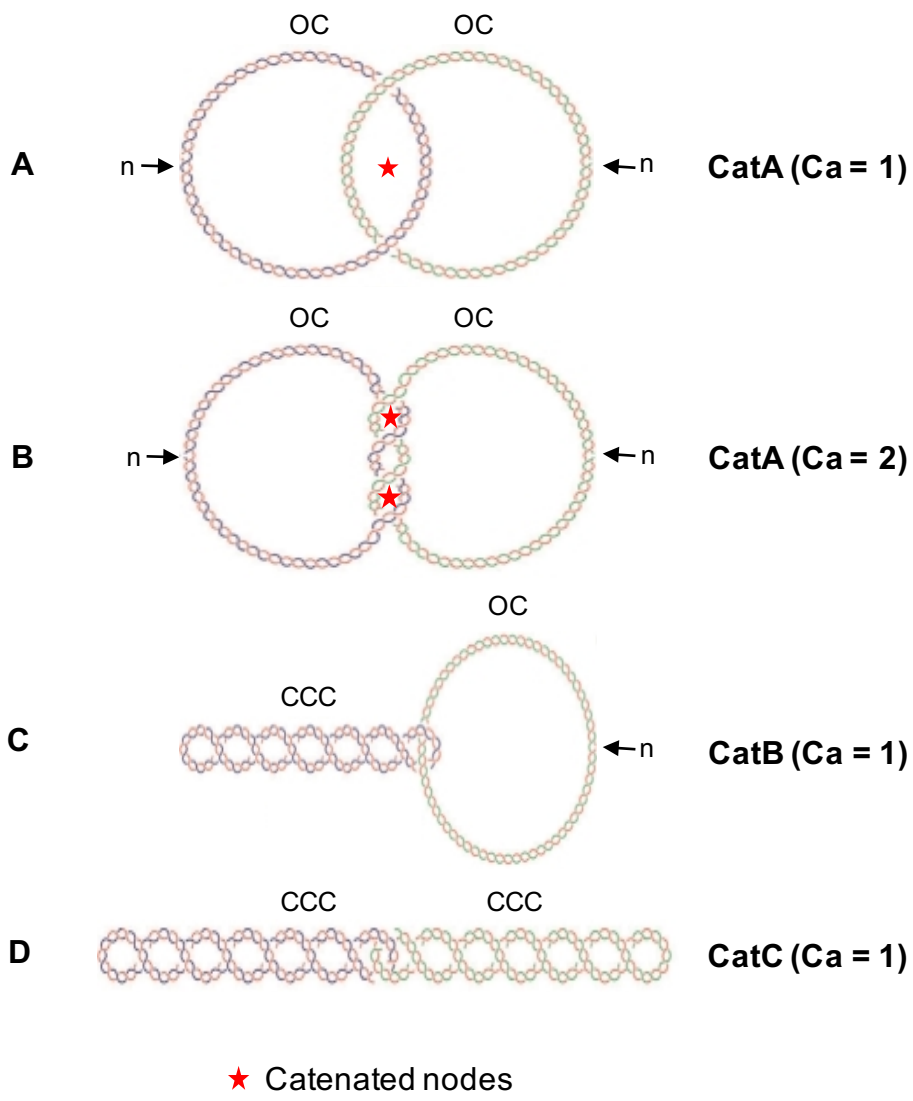

Figure 1.5: Different forms of DNA catenanes with varying node numbers. **A**) One pair of nicked DNA rings catenated once (one catenated node). **B**) One pair of nicked DNA rings catenated twice (two catenated nodes). **C**) One pair of DNA rings catenated once, where one ring is nicked and the other is covalently closed and supercoiled. **D**) One pair of DNA rings catenated once, where both rings are covalently closed and supercoiled. n = nick; *Ca* = catenation number; OC = open circle; CCC = covalently closed circle. Parental DNA strands are shown in blue and green; newly synthesised strands are shown in red. Figure taken from (Martinez-Robles et al., 2009).

1.1.4 DNA Topoisomerases

The inter-conversion of different topoisomers is catalysed by a group of enzymes known as DNA topoisomerases in living organisms. Topoisomerases can overcome all topological obstacles and constraints arising from the double helical structure of the DNA molecule. Topoisomerases have been found in all organisms from bacteria to higher eukaryotes (Bates and Maxwell, 2005). James Wang in 1971 discovered the first DNA topoisomerase called ω protein from *Escherichia coli*. This enzyme is now known as DNA topoisomerase I, and its function is to decrease the number of negative supercoils in bacterial DNA (Wang, 1971). Following this discovery by Wang, James Champoux found an enzyme capable of catalysing a 'nicking-closing' reaction in nuclear extracts of mouse cells, which removed supercoils from closed-circular polyoma virus DNA. At the time, this enzyme was also called DNA topoisomerase I (Champoux and Dulbecco, 1972). However, the mechanisms of action of these two enzymes were different; therefore, they were divided into two different categories: the first category was type IA for the prokaryotic enzyme and the second one was type IB for the eukaryotic enzyme (Bates and Maxwell, 2005). Thereafter, Martin Gellert and co-workers discovered an enzyme called DNA gyrase, which was capable of introducing supercoils. This enzyme was the first type II topoisomerase discovered (Gellert et al., 1976).

The function of DNA topoisomerases is to transiently break and re-join DNA strands in a manner that changes the extent of linkage either within one duplex or between different DNA molecules. DNA topoisomerases carry out this function by the simple chemical reaction of transesterification. In this reaction, the tyrosyl oxygen of the enzyme attacks the phosphorus group of the DNA, i.e. it breaks a DNA phosphodiester bond and then generates a covalent phosphotyrosine linkage. Re-joining is carried out via the opposite reaction; in this case, the oxygen of the DNA hydroxyl group, which is formed in the first reaction, attacks the phosphorus of the phosphotyrosine link, leading to the breakage of the covalent bond between the protein and DNA, which then facilitates formation of the bond in the DNA backbone. These reactions form transient enzyme-mediated

gates in the DNA to allow the passage of another DNA strand or a double helix (Figure 1.6) (Wang, 2002).

Figure 1.6: Catalysis of the transient breakage of DNA by DNA topoisomerases.
Transesterification between the tyrosyl group of an enzyme and the phosphate group of the DNA causes a breakage in the DNA backbone and leads to the formation of a covalent enzyme-DNA intermediate. Re-joining of the DNA backbone occurs in the opposite manner. In a type IA or type II enzyme-catalysed reaction, 3'-OH is the leaving group and the active-site tyrosyl group becomes covalently linked to a 5'-phosphoryl group. Reversely, in a type IB enzyme-catalysed reaction, 5'-OH is the leaving group and the active site of tyrosyl becomes covalently linked to a 3'-phosphoryl group (not shown). Figure taken from (Wang, 2002).

DNA topoisomerases are segregated into two categories: type I and type II. The function of type I enzymes is to break only one strand of the DNA. However, type II enzymes break both strands. With this mode of action, type II enzymes can both catenate and decatenate ds circular DNA molecules as well as relax supercoiling. Type II topoisomerases are the primary topoisomerases to decatenate/catenate DNA, although some type I enzymes can also catalyse such decatenation/catenation reactions when one of the circular DNA molecules possesses a nick in a strand. The two types of DNA isomerases have been further divided into four subfamilies: IA, IB, IIA, and IIB (Table 1.1). Members of the same subfamilies are mechanistically and structurally similar (Wang, 2002). Throughout the introduction, I will use *sc* as a prefix to refer to *Saccharomyces*

cerevisiae proteins, *h* to refer to human proteins, and *sp* to refer to *Schizosaccharomyces pombe* proteins.

Table 1.1: Subfamilies of DNA topoisomerases.

Subfamily	Representative members
IA	• Bacterial DNA topoisomerases I (ω protein) and III • Yeast DNA topoisomerase III • Mammalian DNA topoisomerases IIIα and IIIβ • Eubacterial and archaeal reverse DNA gyrase (*Sulfolobus acidocaldarius*)
IB	• Eukaryotic DNA topoisomerase I • Mammalian mitochondrial DNA topoisomerase I
IIA	• Bacterial gyrase, DNA topoisomerase IV • Yeast DNA topoisomerase II • Mammalian DNA topoisomerases IIα and IIβ
IIB	• Archaeal DNA topoisomerase VI (e.g. *Sulfolobus shibatae*) (subunit A homologous to yeast Spo11)

Table adapted from (Wang, 2002).

1.1.4.1 Type IA Topoisomerases

Type IA topoisomerase enzymes can relax an underwound or negatively supercoiled DNA (Figure 1.7), but a short stretch of dsDNA must first be pulled apart by the binding of the enzyme, after which a transient break is introduced in the single-stranded region (Wang, 1996, Kirkegaard and Wang, 1985). The enzyme can unwind dsDNA with more ease when the DNA is highly negatively supercoiled, i.e. the efficiency of the enzyme reduces when the DNA is less negatively supercoiled. Type IA topoisomerases cannot relax overwound or positively supercoiled DNA unless a single-stranded region is already present (Kirkegaard and Wang, 1985). An additional ability of type IA enzymes is that they pass one double helix through another, but this can occur only when at least one of the pair has a nick or a gap (Tse and Wang, 1980).

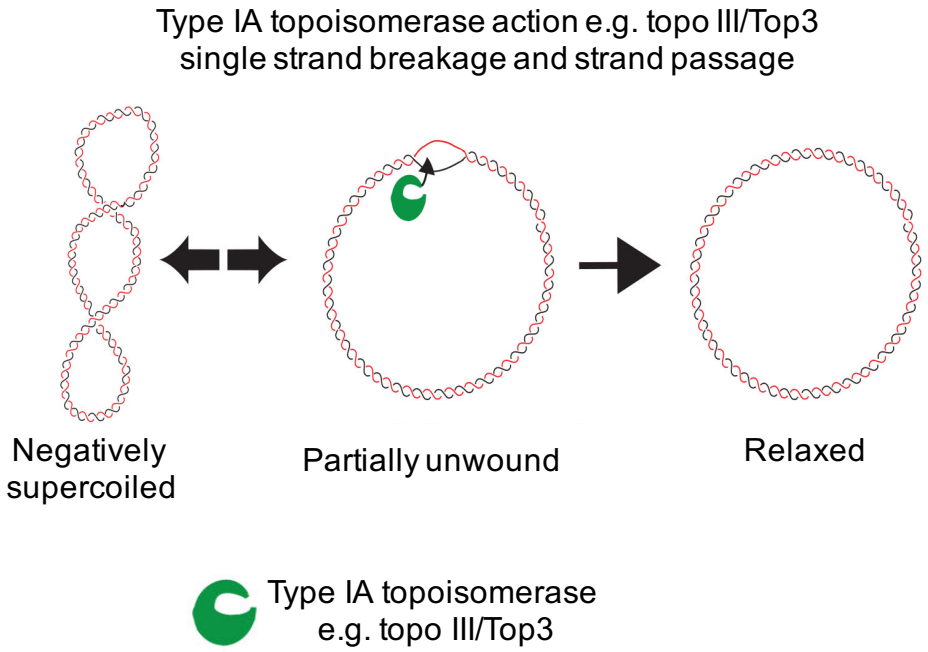

Figure 1.7: Topoisomerase action in supercoil relaxation.
Type IA topoisomerases such as topo III relax negative supercoiling/ underwinding by catalysing a strand passage reaction on unwound regions. Figure taken from (Baxter, 2015).

Type IA topoisomerases act through cleavage of a single-stranded segment, after which the DNA (single-stranded or ds) is passed through the break into the

central cavity of the enzyme. Such a cavity is a highly conserved feature of this class of topoisomerases and is large enough to accommodate a segment of dsDNA. The active-site tyrosine is located at the opening of this cavity between two domains. This mechanism known as strand passage is a main step in the mechanism of action of type IA topoisomerases. Finally, the break is re-ligated and the strand is released. This process results in relaxation of the DNA molecule (Figure 1.8) (Bates and Maxwell, 2005).

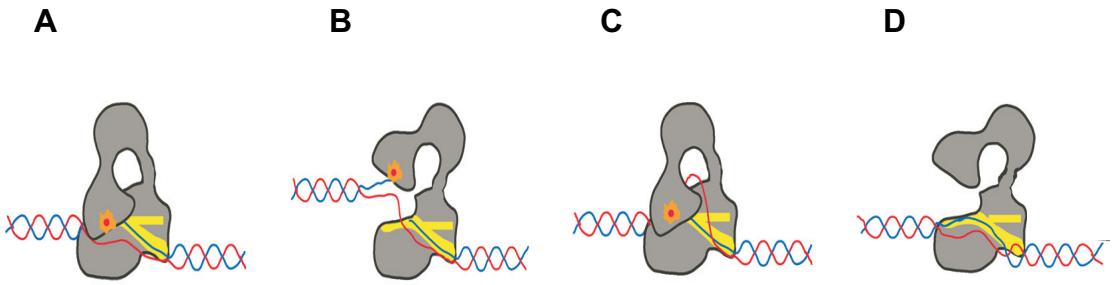

Figure 1.8: The proposed mechanism of DNA relaxation by type IA topoisomerases.
A) Type IA topoisomerases bind DNA and cleave one strand, **B**) thus generating a 5'-phosphotyrosine linkage (orange circle). **C**) The complementary strand is passed through the gap and into the central cavity of the enzyme. **D**) Next, the nick is resealed and the passed strand is released, which changes the linking number by ±1 and cause relaxation of the DNA. Figure taken and modified from (Baker et al., 2009).

Type IA topoisomerases consist of three different subfamilies: bacterial topo I (protein ω), bacterial and eukaryotic topo III, and bacterial and archaeal reverse gyrase. Bacterial topoisomerase I is not involved in relaxing positive supercoils, since it cannot bind with positively supercoiled DNA; therefore the primary activity of bacterial topo I is to relax negatively supercoiled DNA (Kirkegaard and Wang, 1985). However, bacterial topo III is thought to resolve single-stranded DNA entanglements that can occur during DNA replication (Hiasa et al., 1994). *E. coli* Rec-Q helicase, a member of superfamily 2 of helicases, and *E. coli* topo III interact with each other, and this interaction is required for maintaining genome stability. Here, the likely function of the helicase is to form a region that acts as a substrate for the topo III, since topo III requires single-stranded regions as a substrate (Harmon et al., 1999). One particular member of the type IA topoisomerase family does not function in the same way as the other members.

Reverse gyrase is an enzyme found in thermophilic bacteria and archaea, and this enzyme introduces positive supercoils into the genome instead of relaxing negative supercoils, which helps to counteract thermal denaturation. In addition to the type IA topoisomerase domain, the reverse gyrase enzyme also contains a helicase domain. However, this enzyme is not a DNA gyrase homologue (Table 1.2) (Duguet, 1997, Bates and Maxwell, 2005).

1.1.4.2 Type IB Topoisomerases

In contrast to type IA topoisomerases, type IB topoisomerases can relax both overwound and underwound DNA (also known as positively or negatively supercoiled DNA) (Figure 1.9). For instance, eukaryotic topoisomerase I is a member of the topoisomerase type IB family and can relax both positive and negative supercoils (Table 1.2) (Baxter, 2015).

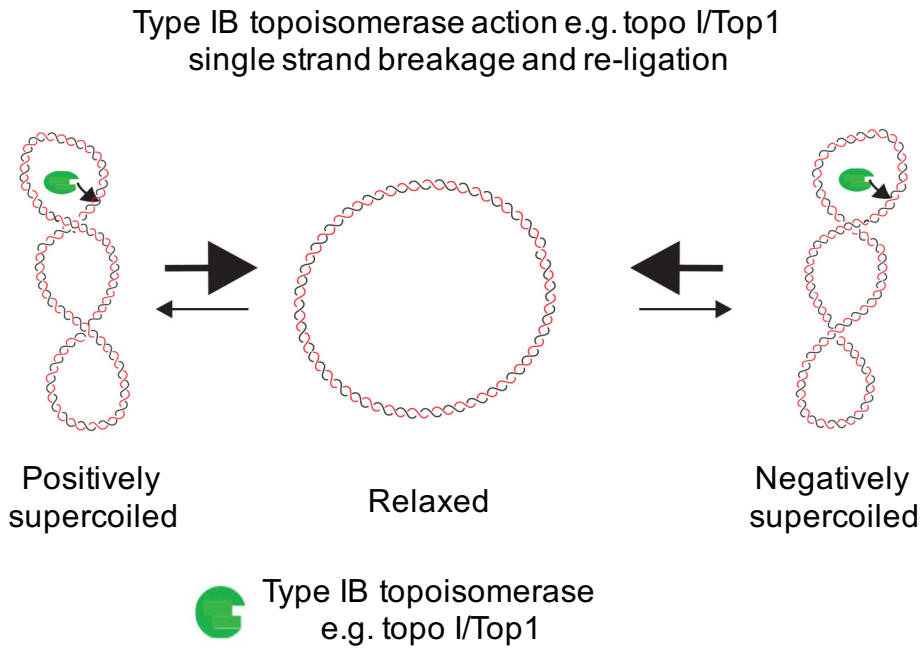

Figure 1.9: Topoisomerase type IB action in supercoil relaxation.
Type IB topoisomerases such as top1 relax negative and positive supercoiling by transient nicking of one of the two strands, leading them to rotate relative to one another. Figure taken from (Baxter, 2015).

Type IB topoisomerases act differently compared to type IA topoisomerases in that they initially surround the DNA double helix (Figure 1.10) and cleave a single

strand of the duplex. The 3'-phosphate is then covalently attached to the protein, thus forming a 3'-phosphotyrosine intermediate. The 5' end is then free to rotate and is twisted around the other strand to relax the DNA until the topoisomerase religates the broken strands. Type IB enzymes show no structural features resembling the internal cavity that is seen in type IA topoisomerases, which indicates that type IB topoisomerases do not act through a strand passage mechanism. The model for the mechanism of action of type IB topoisomerases is called 'controlled rotation'. Another mechanistically crucial difference between the two kinds of type I enzymes is that breakage and re-joining of the DNA strand takes place in a single-stranded region in type IA enzyme-catalysed reactions, but a nick is formed in a dsDNA segment in type IB enzyme-catalysed reactions (Champoux, 2001, Bates and Maxwell, 2005).

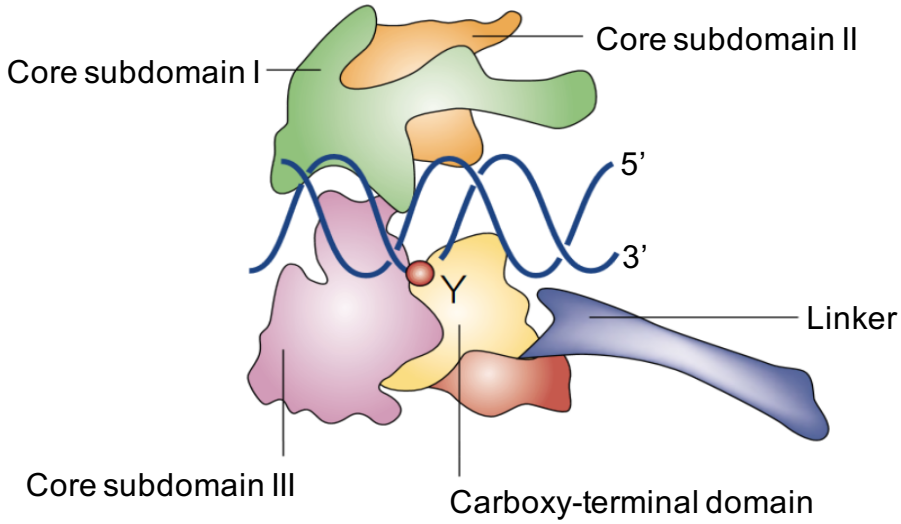

Figure 1.10: The proposed mechanism of DNA relaxation by type IB topoisomerases.
Type IB topoisomerases surround the DNA double helix and cleave one strand, thus forming a 3'-phosphotyrosine linkage (red circle). The free 5'-OH can then rotate (controlled rotation) before the break is resealed, resulting in DNA relaxation. Figure taken from (Wang, 2002).

1.1.4.3 Type II Topoisomerases

Type IIA and type IIB topoisomerases, like type IA enzymes, carry out an active strand passage mechanism for causing topological changes in DNA. Moreover, these enzymes (type IA, type IIA, and type IIB) have the same catalytic domains

that they use for DNA cleavage (Berger et al., 1998). However, unlike type IA and type IB topoisomerases, type IIA and type IIB topoisomerases cleave both strands of a DNA duplex and pass a second intact duplex through the transient break using ATP to power strand passage (Gellert et al., 1976, Goto and Wang, 1982). Such a mechanism allows type IIA and type IIB topoisomerases to resolve both positive and negative DNA supercoils and to unwind long intertwined chromosomes and DNA catenanes (Figure 1.11) (Champoux, 2001).

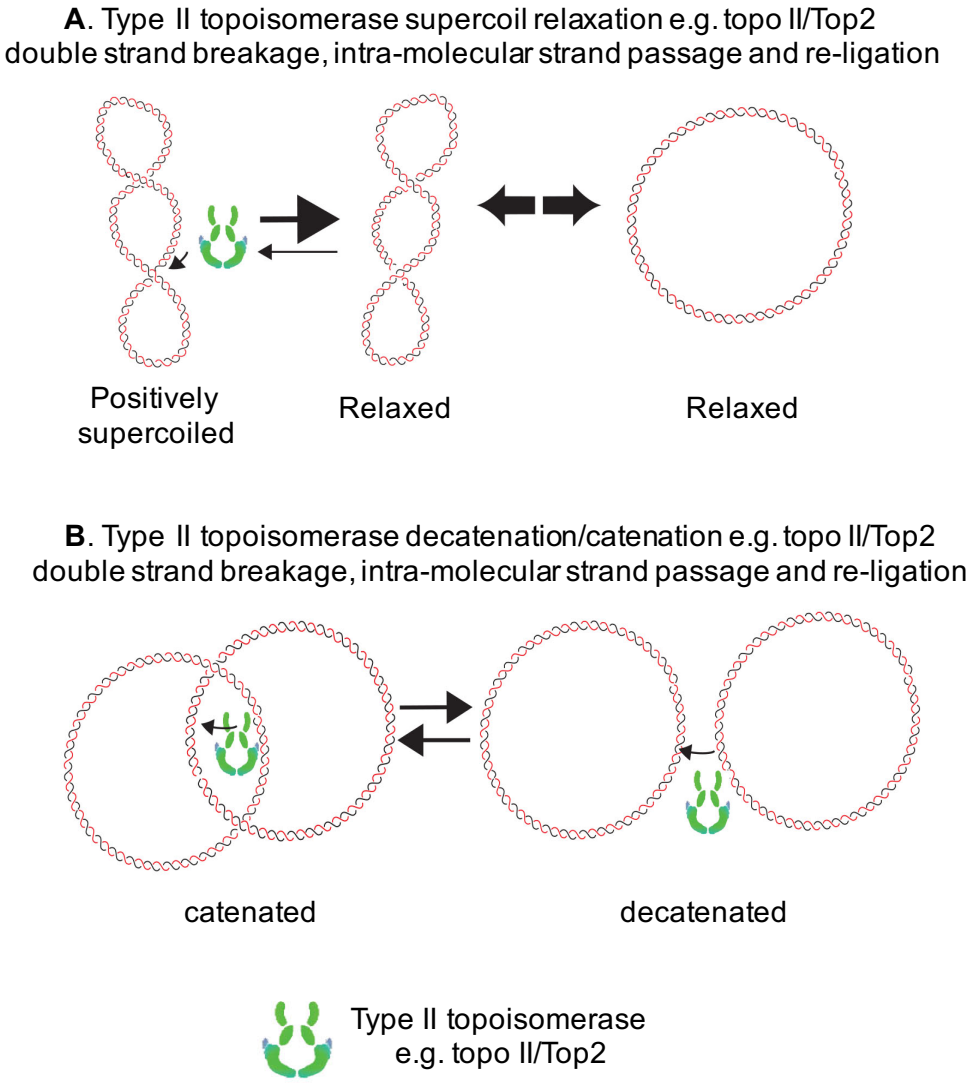

Figure 1.11: Topoisomerase action in supercoil relaxation and DNA decatenation/catenation.
A) Type II topoisomerases such as Top2 relax supercoiling tension by a double strand breakage and strand passage. **B**) Type II topoisomerases can also remove/add catenated intertwines by a double strand breakage and strand passage. Figure taken from (Baxter, 2015).

As mentioned above, type IIB enzymes possess many common features with type IIA enzymes. A comparison of the structures of type IIA and type IIB enzymes show that they share significant structural similarity in their B-subunit, suggesting that these proteins maybe evolutionary related and therefore share similar mechanisms for strand cleavage and strand passage (Berger et al., 1998). In contrast to the B-subunit, the A-subunit of type IIA and type IIB topoisomerases show no structural or sequence similarity (Nichols et al., 1999).

The creation of double strand breaks (DSBs) is harmful to the cell; therefore, the action of topoisomerase II is potentially very dangerous. However, type II topoisomerases have the ability to protect the ends of DSBs. This is achieved by the formation of a reversible covalent bond between the tyrosine hydroxyl group of the enzyme and the phosphate at the break site, which enables the enzyme to protect the cell from the DSB (Bates and Maxwell, 2005). Figure 1.12 shows a molecular model for the transport of one DNA double helix through another by a type IIA and type IIB enzyme.

A. Type IIA topoisomerase mechanism

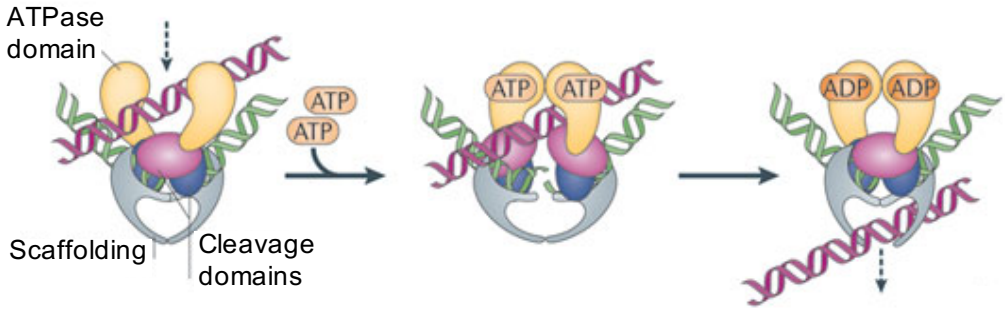

B. Type IIB topoisomerase mechanism

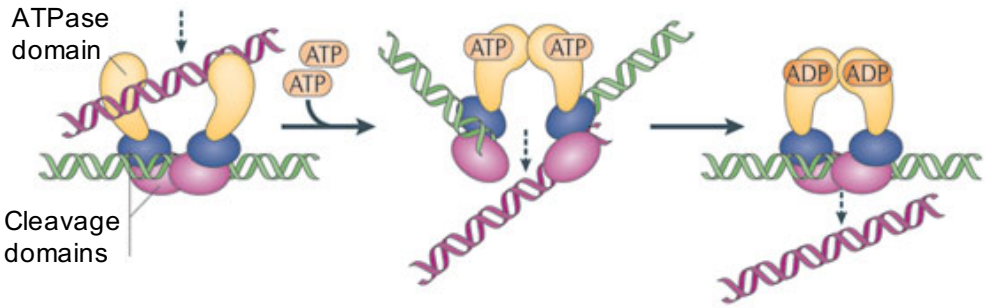

Figure 1.12: The proposed mechanism of DNA relaxation and DNA decatenation/catenation by type IIA and IIB topoisomerases.
A) Type IIA topoisomerases cleave both strands of a duplex DNA (green) and pass another duplex DNA (pink) through the transient break in a reaction that is coupled to ATP turnover. The cleaved strands are then re-ligated, and the products of the reaction are released from the enzyme. **B**) Type IIB topoisomerases use a duplex strand passage mechanism like that used by type IIA enzymes and have the same ATPase and cleavage domains, but differ in their overall tertiary structure. Figure taken from (Vos et al., 2011).

Type IIA topoisomerases are found in all cellular organisms (e.g. bacterial and archaeal gyrase, bacterial topo IV and eukaryotic topo II) and show different functional properties (Table 1.2) (Forterre et al., 2007). For example, gyrase is the only enzyme in bacteria that can actively add negative supercoils to DNA using the free energy from ATP hydrolysis, and therefore is responsible for global formation of negative supercoils in the bacterial chromosome. It can also weakly unlink catenanes; moreover, gyrase effectively removes positive supercoils ahead of the fork (Zechiedrich and Cozzarelli, 1995). The enzyme topo IV (with a sequence similarity to gyrase) both relaxes supercoils in the cell and has a specific decatenation role (Zechiedrich et al., 2000, Peng and Marians, 1993, Crisona et al., 2000). Type IIB topoisomerases include Topo VI from archaea, plants, and a few bacteria (Table 1.2). It should be noted that type IIB enzymes are evolutionally associated with SPO11, which is the factor responsible for forming DSBs in DNA that initiate meiotic recombination (Vos et al., 2011, Corbett and Berger, 2003, Lichten, 2001).

1.1.4.4 *Saccharomyces cerevisiae* Topoisomerases

Three DNA topoisomerases exist in *S. cerevisiae*, but only two of them efficiently influence superhelicity: topoisomerase I (Top1) of the IB subfamily and topoisomerase II (Top2) of the IIA subfamily. *In vitro*, both these enzymes can relax both positive and negative supercoiling, but eukaryotic topoisomerase II preferentially relaxes positive supercoiling. Deletion of either Top1 or Top2 does not change the kinetics of DNA replication, suggesting that Top1 and Top2 can substitute for one another in terms of their ability to relax supercoiling. However, the deletion of both topoisomerases prevents immediate DNA replication fork progression, indicating that either topoisomerase can resolve intertwines during

DNA replication and that there is no other enzyme in the cell that can substitute for the loss of both topoisomerases (Brill et al., 1987, Bermejo et al., 2007). Top2 is not as efficient as Top1 in relaxing supercoils *in vitro;* therefore, it was proposed that Top2 cooperates with the removal of torsional stress by resolving pre-catenanes (Postow et al., 2001a, Wang, 2002). Top2 is also involved in chromosomal segregation during mitosis, where it is presumed to be required to ensure complete removal of double-stranded intertwines before chromosome segregation (Holm et al., 1985, Baxter and Diffley, 2008). Top2 is therefore necessary for cell growth, but a Top1 deletion strain can remain viable (Champoux, 2001, Wang, 2002). The third topoisomerase in *S. cerevisiae* is a class IA enzyme called Top3, which is mainly believed to function in DNA homologous recombination. Top3 is important for growth in *S. cerevisiae*; cells grow slowly in its absence, show increased levels of mitotic recombination and cannot sporulate due to a defect in mitotic recombination (Gangloff et al., 1999, Wallis et al., 1989). In yeast, the RecQ homolog, *sgs1*, acts as a suppressor of the slow growth phenotype of *top3* knockouts, indicating that these two enzymes function in the same pathway (Gangloff et al., 1994).

Yeast cells containing Top2 as the only active topoisomerase (Top1 ablation) are viable and can perform normal DNA replication (Brill et al., 1987, Kim and Wang, 1989) without the activation of any S phase-dependent checkpoints (Bermejo et al., 2007). Deletion of both topoisomerases blocks replication fork progression and leads to the formation of checkpoint signals that result in Rad53 activation in S phase (Bermejo et al., 2007). Interestingly, the influence of the depletion of Top2 activity on DNA replication in yeast cells completely lacking Top2 protein is different from that observed in yeast cells that have an enzymatically inactive protein. Cells depleted of Top2 using a conditionally degradable Top2 protein were able to complete the S, G2 and M phases with normal kinetics, but could not perform chromosome decatenation. This result indicated that chromosome missegregation, DNA damage and cell lethality take place when cells enter cytokinesis. However, when catalytically inactive Top2 was expressed in the cells (Top2Y-F), the cells could progress through S phase with normal kinetics but could not complete DNA replication, which caused checkpoint induction and prevented their entry into mitosis (Baxter and Diffley, 2008).

1.1.4.5 Topoisomerases in Higher Eukaryotes

Like yeasts, all higher eukaryotes possess a single topoisomerase I enzyme that has an important function of supporting fork progression during DNA replication. Topo I is essential during development and perhaps during cell division (reviewed by Champoux, 2001). However, unlike yeasts, most higher eukaryotes seem to have two type IIA isoforms known as topoisomerase IIα and IIβ. Topoisomerase IIα is essential for the viability of all dividing cells and for unlinking intertwined daughter duplexes during DNA replication; it is therefore required in chromosome segregation. Topoisomerase IIβ is required for normal development and supports recombination or transcription. Higher eukaryotes also have two types III (type IA subfamily) isoforms known as topoisomerases IIIα and IIIβ. The role of topoisomerase IIIα is likely to resolve homologous recombination intermediates and topoisomerase IIIβ may not be important for cell viability or development. There is also an interaction between topoisomerase IIIα and the mammalian homologue of the *SGS1* gene, *BLM*, which is similar to that observed in yeast; mutation in *BLM* leads to Bloom's syndrome (reviewed by Champoux, 2001).

Table 1.2: DNA Topoisomerases.

Enzyme	type	Source	Remarks
Bacterial topoisomerase I (ω protein)	IA	Bacteria (e.g. *E. coli*)	Cannot relax positive supercoils
Eukaryotic topoisomerase I	IB	Eukaryotes (e.g. human)	Can relax both positive and negative supercoils
Topoisomerase III	IA	Bacteria (e.g. *E. coli*)	Potent decatenating activity
Topoisomerase III	IA	Eukaryotes (e.g. human topoisomerase IIIα)	Resolve DNA homologous recombination intermediates
Reverse gyrase	IA	Thermophilic Archaea (*Sulfolobus acidocaldarius*)	Can introduce positive supercoils into DNA (ATP-dependent)
DNA gyrase	IIA	Bacteria (e.g. *E. coli*)	Can introduce negative supercoils into DNA (ATP-dependent)
Topoisomerase IV	IIA	Bacteria (e.g. *E. coli*)	Can relax, but not supercoil, DNA, potent decatenase (ATP-dependent)
Eukaryotic topoisomerase II	IIA	Eukaryotes (e.g. human topoisomerase IIα)	Can relax, but not supercoil, DNA (ATP-dependent)
Topoisomerase VI	IIB	Archaea (e.g. *Sulfolobus shibatae*)	Can relax, but not supercoil, DNA (ATP-dependent)

Table taken from (Bates and Maxwell, 2005).

1.2 The Cell Cycle

Cells have to undergo cell division once every cell cycle in order to proliferate. The cell cycle contains three basic processes that are conserved from bacteria to human cells: cell growth, genome duplication, and cell division. Although cell growth and genome duplication take place concomitantly during most of the cell cycle in bacteria, the cell cycle in eukaryotic cells is divided into four major phases. The DNA is replicated and chromosomes are duplicated in the S phase early in the cell cycle. The second main phase of the cell cycle is the M phase, which is typically divided into two main events: nuclear division (mitosis) and cell division (cytokinesis). The S and M phases are divided by two gap phases. The first gap phase, G1, occurs between the M and S phases, during which the cells prepare for DNA replication. The G2 phase occurs before the M phase and during this time, the cells continue to grow and ensure that the replication of genetic material is complete and error free. The length of G2 can change significantly between organisms, where some have very long G2 phases, while others have no detectable G2 phase at all (as is the case in *S. cerevisiae*). In these cases, the end of the S phase appears to overlap with the start of the M phase. The G1, S, and G2 phases are often collectively called the interphase (Forsburg and Nurse, 1991, Cooper, 2000). Once the cells have passed a certain point in the G1 phase (called the “start point” in budding yeast or “restriction point” in mammalian cells), they become committed to a new cell cycle. Cells can also exit the cell cycle and enter into a prolonged non-dividing state, called the G0 phase, if the environment is unfavourable (Alberts, 2002). The length of a typical cell cycle changes significantly between different eukaryotic cells. In this study, I used *S. cerevisiae* as the model organism, where the typical cell cycle can be as short as 90 minutes. *S. cerevisiae* is also known as budding yeast due to the formation of buds during the cell cycle. It is commonly used as a model organism owing to the large number of conserved genes and cellular mechanisms. *S. cerevisiae* shows a fast growth rate and provides the advantage of easy genetic manipulation. Moreover, entire cultures can be arrested at specific cell cycle stages. All of these factors make *S. cerevisiae* a fantastically versatile tool for studying the underlying mechanisms of the eukaryotic cell cycle (Forsburg and Nurse, 1991).

1.2.1 Cell Cycle Control

In eukaryotes, cell cycle progression is tightly regulated by cyclin-dependent kinases (Cdks) to generate two daughter cells, each containing an exact copy of the genome. However, in cases where the genetic material is damaged, the progression of the cell cycle is inhibited to allow the cells time to overcome the damage. In the yeasts, *S. pombe* and *S. cerevisiae*, a single Cdk, leads to cell cycle progression (Cdc2 and Cdc28, respectively). However, in higher eukaryotes, different Cdks control the passage of the cells through different phases of the cell cycle. The levels of Cdks are fairly constant throughout the cell cycle, and changes in their activity mostly rely on changes in the levels of the regulatory subunits called cyclins, which bind tightly to the Cdks. Cdks can be roughly divided into three subgroups: G1-Cdk, S-Cdk, and M-Cdk. Each phase of the cell cycle has specific cyclins; for instance, in budding yeast, Cdc28 associates with Cln1-3 in the G1 phase, Clb 5/6 in the S phase, and Clb1-4 in the M phase to drive cell cycle progression. The activities of the cyclin-Cdk complexes are further altered by the addition or removal of inhibitory phosphorylation and by alternations in the levels of Cdk inhibitor proteins. Cdk activity is high during the S phase and early mitosis to initiate replication and chromosome segregation. In the late M phase, M-Cdks lead to the activation of the ubiquitin protein ligase APC (Anaphase Promoting Complex), where one of its roles is to destroy S and M cyclins. Consequently, all the main Cdks in late mitosis are inactivated, which leads to mitosis and cytokinesis completion. APC remains active in the G1 phase until G1/S-Cdk activity increases again and commits the cell to the next cycle (Nurse, 1997, Bloom and Cross, 2007, Harashima et al., 2013, Morgan, 1995).

Another level of cell cycle control is achieved by cell cycle checkpoints, which monitor critical cell cycle events. They often ensure the completion of the relevant cell cycle stages before allowing the cells to enter the next stage. In budding yeast, the S phase checkpoint and the spindle assembly checkpoint (SAC) represent two major checkpoints. The S phase checkpoint monitors the replicative status in the S phase and responds to replication defects; on the other

hand, the SAC ensures proper segregation of sister chromatids in the M phase (Hartwell and Weinert, 1989).

The regulation of the cell cycle is important for maintenance of genomic integrity, where it acts by guaranteeing high-fidelity replication, accurate chromosome distribution, and proper cell cycle progression. Failure to do so causes accumulation of genome instability, which is a prominent feature of cancer cells (Shen, 2011).

1.2.2 Principles and Mechanisms of DNA Replication

Chromosome duplication occurs in the S phase of the cell cycle, and DNA replication is the central event of this phase. To begin with, the DNA helix has to be unwound before DNA replication initiation. This takes place at particular sites known as replication origins, where the initiator protein complex binds to and unwinds the DNA. Two Y-shaped DNA structures known as replication forks are then created. At each fork, a complex assembly of proteins known as the replisome carries out the enzymatic process of DNA replication. The replisomes move from one origin until they meet the fork coming from another origin or reach the end of the chromosome, until the completion of duplication of the entire chromosome. Chromosomal DNA replication can be divided into three distinct steps: initiation, elongation and termination. Initiation sets up the two replisome complexes capable of unwinding and duplicating the parental DNA strands. During elongation, the replisomes synthesize new strands by unwinding the parental strands and then synthesizing complementary nascent strands. Following termination of DNA replication, the duplicated chromosomes have to be separated from one another. Once DNA replication starts, it normally proceeds to completion; otherwise, the incompletely replicated chromosomes might break during mitosis (Bell and Dutta, 2002, Waga and Stillman, 1998). The principles of the molecular mechanism of DNA replication are conserved amongst eukaryotes, and the basic replication machineries are similar between yeast and metazoans (Masai et al., 2010, O'Donnell et al., 2013, Zegerman, 2015). The molecular mechanism of DNA replication in the model organism *S. cerevisiae* is explained in the following paragraphs. An overview of the homologous counterparts of some

of the most important proteins involved in replication is also shown in Table 1.3.

Table 1.3: Homology of different replication proteins.
Dash indicates that a higher eukaryotic homolog has not been clearly identified.

S. cerevisiae	*S. pombe*	*H. sapiens*
Proteins in the pre-RC		
Orc1-6	Orc1-6	ORC1-6
Cdc6	Cdc18	CDC6
Cdt1/Tah11/Sid2	Cdt1	CDT1
Mcm2	Mcm2/Cdc19/Nda1	MCM2
Mcm3	Mcm3	MCM3
Cdc54/Mcm4	Cdc21	MCM4
Cdc46/Mcm5	Mcm5/Nda4	MCM5
Mcm6	Mcm6/Mis5	MCM6
Cdc47/Mcm7	Mcm7	MCM7
Homologs of Cdc7 and Dbf4		
Cdc7	Hsk1	CDC7
Dbf4	Dfp1	DBF4/ASK
Proteins in the pre-IC		
Mcm10	Cdc23	MCM10
Cdc45 complex		
Cdc45	Cdc45	CDC45
Sld3	Sld3	TICRR
Dpb11 complex		
Dpb11	Cut5/Rad4	TopBP1
Sld2	Drc1	RECQL4
GINS complex		
Sld5	Sld5	SLD5
Psf1	Psf1	PSF1
Psf2	Psf2	PSF2
Psf3	Psf3	PSF3
Replisome associated factors		
Mrc1	Mrc1	CLASPIN
Tof1	Swi1	TIMELESS
Csm3	Swi3	TIPIN
Ctf4	Mcl1	AND-1

Ctf18 – RFC complex	Ctf18	Ctf18 – RFC
Chl1	Chl1	ChLR1
Dpb3	Dpb3	p17
Pol32	Cdc27	p66
Dia2	Pof3	–

1.2.2.1 Replication Origin

The replication origin is a stretch of DNA where replisomes are assembled and replication is initiated. Unlike bacteria where only one replication origin is used to replicate the whole genome (e.g. *OriC* in *E. coli*), eukaryotes have large chromosomes that contain multiple origins of replication, which are distributed along the chromosomes so that many different regions can be duplicated simultaneously in the same chromosome. Thus, DNA replication is completed in a limited time; for example, replication is initiated at hundreds of replication origins in budding yeast and at up to thousands of replication origins in mammalian cells (Yabuki et al., 2002, Raghuraman et al., 2001, Wyrick et al., 2001, Nieduszynski et al., 2007).

In most eukaryotes, replication origins do not have well-defined DNA sequences; however, in budding yeast, the origin encompasses a short stretch of DNA known as autonomously replicating sequence (ARS), which allows DNA replication in the S phase when transferred to any piece of DNA. Therefore, replication origins in budding yeast possess the ability to support the replication of a plasmid (Stinchcomb et al., 1979, Vallet et al., 1984, Dhar et al., 2012). Other eukaryotes do not exhibit strong sequence-specific origins of replication. It has been shown that replication origins in *S. pombe* are preferentially located in AT-rich regions (Dai et al., 2005, Segurado et al., 2003). With regard to humans, studies aimed at identifying sequence specificity for origin replication complex (ORC) binding have remained unsuccessful, although it has been proposed that replication origins are located in CG-rich regions (Fragkos et al., 2015). It is likely that origins are often determined by chromatin organization rather than by DNA sequence in these organisms (Leonard and Mechali, 2013).

In budding yeast, each ARS is about 100–200 bp long and contains the important and highly conserved AT-rich ARS consensus sequence (ACS). The ACS contains two elements. The *A element* includes a 11-bp long ACS, whose sequence is highly conserved among all origins, and it is highly important for origin function (Bell and Dutta, 2002, Theis and Newlon, 1997). The second part, the *B elements* (B1, B2, and B3), is close to the A element but includes less-conserved sequences. Like the A element, the B1 element also generates central binding sites for the ORC (Rao and Stillman, 1995, Rowley et al., 1995). The other two B elements are thought to increase origin efficiency (Miyake et al., 2002). In the budding yeast genome, 12,000 ACSs exist, but only about 400 are used (Nieduszynski et al., 2006). This suggests that factors other than the ACS, such as chromatin organization or the mentioned B element, contribute to ARS activity. Budding yeast origins are also determined by their chromatin environment, since most of them are found in intergenic regions lacking nucleosomes (Eaton et al., 2010).

The deletion of a few origins from a chromosome is not lethal, as replication forks from other origins can still duplicate the DNA. However, in the absence of large numbers of origins, chromosomal replication might become so slow that it may lead to chromosome damage and loss as some cells might enter mitosis with incompletely replicated chromosomes (Marahrens and Stillman, 1992, Gilbert, 2001). The origins are not all fired at the same time in the S phase; some origins are fired early and others later. If replication is inhibited during the S phase, for example due to nucleotide depletion, DNA damage response will inhibit the firing of other replication origins and block entry into mitosis (Bell and Dutta, 2002).

1.2.2.2 DNA Replication Initiation

The initiation of DNA replication can be divided into two distinct steps: first, a large complex of initiator proteins, known as the *pre-replicative complex* (pre-RC), is assembled on DNA origins during late mitosis and in the early G1 phase, which prepares the origins for firing. This process is called **origin licensing**. Second, the pre-RC is activated (**origin activation**) and transformed into the active *pre-initiation complex* (pre-IC) by two protein kinases, cyclin-dependent

kinase (CDK) and Dbf4-dependent kinase (DDK), during G1 to S phase transition. The DNA synthesis machinery is then loaded on to the DNA origins for initiation of DNA synthesis. Once the replication origin has been fired, the pre-RC is dispersed, and its rejoining is halted until the next G1 phase. Hence, each origin can only be fired once per cell cycle. The pre-RC cannot be assembled in the S and M phases as S- and M-Cdks are active in these phases, and the assembly cannot occur until all Cdk activities are decreased in late mitosis (Bell and Dutta, 2002, Waga and Stillman, 1998).

1.2.2.2.1 Origin Licensing

During the first phase of replication initiation, origins are licensed by the formation of the pre-RC complex. The core component in pre-RC assembly is the ORC containing six subunits known as *sc*Orc1-6 (*sp*Orc1-6, *h*ORC1-6) (Bell and Dutta, 2002). This multi-protein complex remains bound at the replication origins throughout the cell cycle in budding yeast, but is only active in late mitosis and early G1. Mutations in ORC genes lead to defects in DNA replication initiation. The ORC recognizes the origins based on a combination of DNA sequence recognition and chromatin context and is ATP-dependent (Figure 1.13) (Bell and Kaguni, 2013). It has been shown that the ORC is bound to around 400 origins in budding yeast, which are typically separated by approximately 20 to 30 kb (Bell and Dutta, 2002, Sclafani and Holzen, 2007).

Replication origin licensing is initiated by the recruitment of *sc*Cdc6 (*sp*Cdc18 and *h*Cdc6), Cdt1 (*sp*Cdt1 and *h*Cdt1), and *sc*Mcm2-7 (MCM, for minichromosome maintenance) to the ORC located at the origins of replication. These four proteins are sufficient for pre-RC assembly. Several findings have indicated that the order of recruitment of these proteins is not random; Cdc6 first binds to the ORC and then a complex of Cdt1 and the hexameric Mcm2-7 helicase is recruited (Bell and Kaguni, 2013, Speck et al., 2005, Remus et al., 2009). After Mcm2-7 recruitment, Cdt1 and Cdc6 are rapidly destroyed; therefore, a new Mcm complex cannot be loaded at a fired origin. This shows that one origin cannot be used twice in the same cell cycle. Further, the ORC-Cdc6-Cdt1-Mcm2-7 complex cannot be detected *in vivo*, which indicates that this complex is very short-lived (Figure 1.13)

(Randell et al., 2006).

The Mcm2-7 double hexamers exist in a ring structure and encircle the dsDNA in a head-to-head conformation. The loaded, but inactive, Mcm2-7 helicase is known as pre-RC (Figure 1.13) (Bell and Kaguni, 2013, Sclafani and Holzen, 2007, Siddiqui et al., 2013). Interestingly, a large number of Mcm2-7s are recruited in budding yeast, *Xenopus* egg extracts, and human cells (Zegerman and Diffley, 2009), but only around 10% of all Mcm2-7 complexes loaded onto the DNA in the G1 phase are activated in the S phase, and the remaining origins are replicated passively and hence are known as dormant replication origins (McIntosh and Blow, 2012).

1.2.2.2.2 Origin Activation

The second phase of replication initiation begins in the S phase and leads to Mcm2-7 helicase activation. In this step, the pre-RC is transformed into the very transient pre-IC immediately prior to the start of replication. The pre-IC contains Cdc45, GINS, Dpb11, Sld2, Sld3, Sld7, Mcm10, and DNA polymerase ε in addition to the Mcm2-7 complex. The formation of the pre-IC can be divided into two essential and distinct steps: one is DDK-dependent and the other is S phase CDK-dependent (Tanaka and Araki, 2013, Li and Araki, 2013). The activity of these two kinases is essential for the assembly of replication factors and the activation of the replicative helicase (Labib, 2010).

*sc*Cdc7 (*sp*Hsk1 and *h*Cdc7), an essential protein kinase, is activated in the late G1 phase, probably because of Cdk activation, and remains active throughout the S phase for the firing of late origins. A mutation in the *CDC7* gene in budding yeast will prevent DNA replication initiation. Cdks and Cdc7 work together in the firing of origins by promoting the formation of the pre-IC at the origin. Like Cdks, the activation of Cdc7 is associated with a specific regulatory protein, *sc*Dbf4 (*sp*Dfp1 and *h*Dbf4), whose levels oscillate during the cell cycle. Therefore, Cdc7 is also not active throughout the cell cycle. Changes in Cdc7 activity are caused by a change in the level of Dbf4, which increases in the late G1 phase and stays high until the exit from mitosis. Cdc7 is sometimes also known as Dbf4-dependent

kinase, or DDK. Reduction in the levels of Dbf4 in G1 can be due to reduction in the transcription of the *DBF4* gene or due to increased degradation of the Dbf4 protein, which is carried out by the ubiquitin-protein ligase, APC. In budding yeast, APC is inactivated late in G1 due to Cdk activation. Thus, it is likely that Dbf4 stabilization and Cdc7 activation is the indirect result of Cdk activation (Bousset and Diffley, 1998, Donaldson et al., 1998).

As mentioned, DDK contains the catalytic subunit Cdc7 and the regulatory subunit Dbf4. DDK is required for the phosphorylation of the Mcm2-7 double hexamers, which is in turn important for the recruitment of Cdc45 and Sld3 onto the pre-RC (Tanaka and Araki, 2013). However, it is still not clear as to which subunits are phosphorylated by DDK. DDK has been shown to phosphorylate Mcm2, Mcm4, and Mcm6 *in vitro* (Randell et al., 2010), and Mcm4 and Mcm5 can be mutated to bypass the requirement of DDK (Sheu and Stillman, 2010, Hardy et al., 1997).

CDK phosphorylates Sld2 and Sld3 (Zegerman and Diffley, 2007, Tanaka et al., 2007), which leads to the interaction of the two proteins with the BRCT domains of the protein *sc*Dpb11 (*sp*Rad4 and *h*TopBP1). This interaction promotes the loading of additional proteins such as the leading strand polymerase ε and GINS (Sld5 and Psf1-3). Next, Cdc45, MCM, and GINS interact with each other to form the CMG complex, which then encircles single-stranded DNA (ssDNA). The CMG complex is an active form of DNA helicase and acts at replication forks, unwinding the DNA helix at the replication origin and then moving along the DNA with other ancillary replisome components. Although it has been shown that Mcm10 has a crucial function in DNA unwinding by the CMG helicase, its role is not very clear (Thu and Bielinsky, 2014). Sld2, Sld3, Sld7, and Dpb11 are not parts of the replisome and disassemble after replication starts at the forks (Figure 1.13) (Tanaka and Araki, 2013). Besides MCM, which is thought to be the main replicate helicase, other helicases such as Rrm3, RecQ helicases (*sc*Sgs1 and *sp*Rqh1), Pif1 (*sp*Pfh1), and Dna2 have been identified to play a role in DNA replication (Labib and Diffley, 2001).

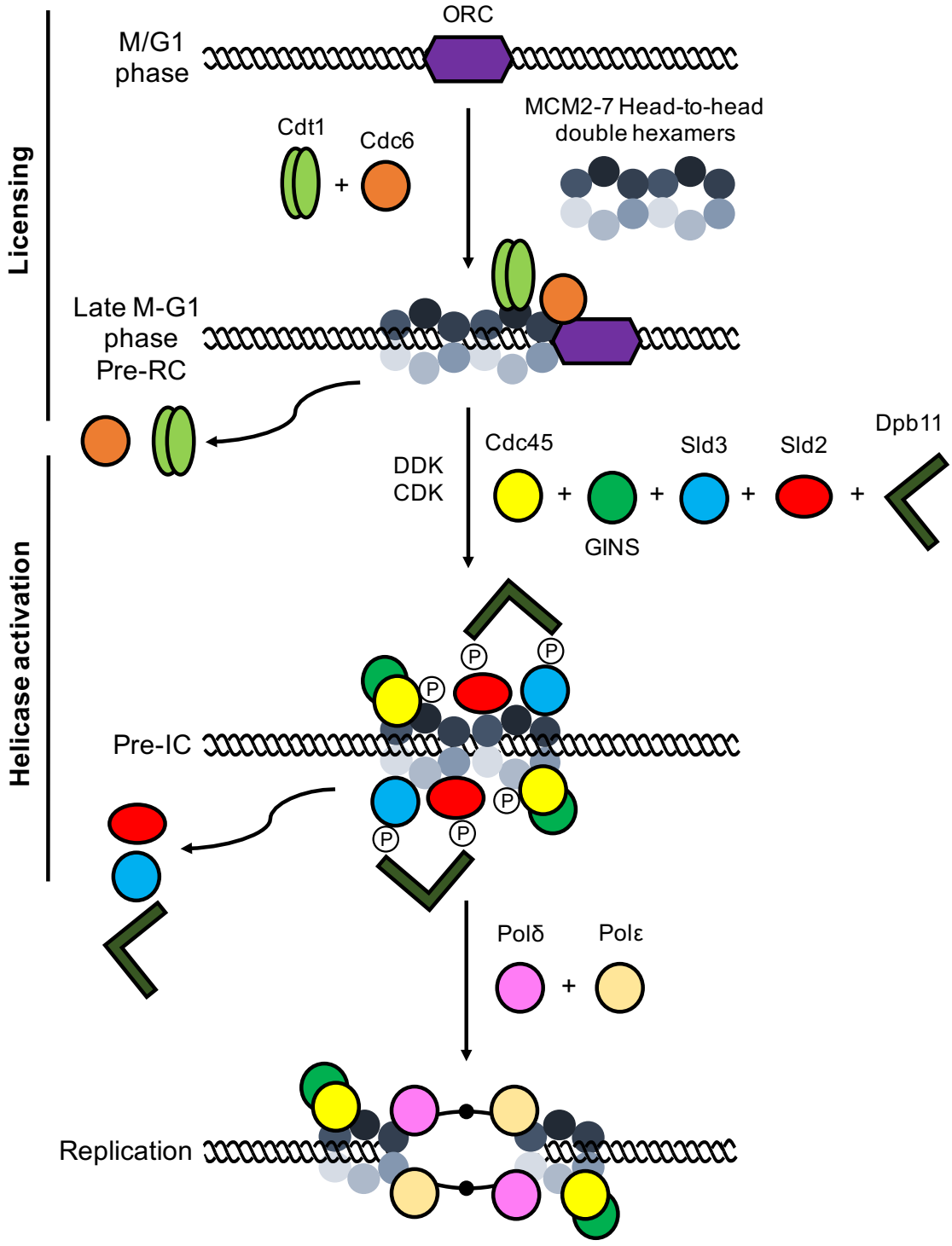

Figure 1.13: Initiation of DNA replication in *S. cerevisiae*.
Replication origins are licensed in the late M and G1 phases and are activated throughout the S phase by the actions of the kinases CDK and DDK. Factors such as Mcm10 and Sld7 have been left out for the purpose of simplicity. For more details, see text. Figure adapted from (Zegerman, 2015).

1.2.2.3 DNA Replication Elongation

Once the double helix is unwound by a DNA helicase, DNA synthesis begins. Reannealing of the separated DNA strands is inhibited by a single-strand binding protein known as replication protein A (RPA). RPA has been identified in cellular processes such as DNA replication, checkpoint signalling, and DNA repair (Fanning et al., 2006). Initiation of strand synthesis is carried out by Polymerase α/primase, and elongation is carried out by Polymerase ε and Polymerase δ. Nucleotides can only be attached to a growing DNA strand at its 3' hydroxyl group; they cannot to be attached to the 5' phosphate at the other end. Therefore, the genome is replicated bidirectionally in a 5'-3' direction. Because the DNA strands are antiparallel, replication is a semi-discontinuous process (Alberts, 2002). Polymerase ε ensures that the leading strand is continuously replicated in the same direction as that of the movement of the replication fork, and Polymerase δ helps discontinuously replicate the lagging strand in the direction opposite to the direction of replication fork progression in short (~200 nucleotide long) DNA fragments known as Okazaki fragments (Alberts, 2002, Nick McElhinny et al., 2008, Miyabe et al., 2011). The polymerases need to be associated with the replisome and therefore loops are formed on the lagging strand due to the directionality of replication (Stillman, 2008). As mentioned above, the lagging strand is synthesized discontinuously as a series of RNA-DNA hybrids. The maturation of these Okazaki fragments involves the removal of the RNA primer (and perhaps some DNA), wherein Polymerase δ displaces a short flap when it arrives at the 5'-end of the preceding Okazaki fragment. This short flap is recognized and cleaved by flap endonuclease *h*Fen1 (*sc*Rad27 and *sp*Rad2) and the helicase/endonuclease Dna2, and then the Okazaki fragments are ligated by DNA ligase I (Burgers, 2009).

Polymerase α/primase first begins replication of the leading strand by copying a short stretch of the DNA template into RNA (10 nucleotides) (primase activity) and a stretch of DNA (20 nucleotides) (polymerase activity). This is repeated on the lagging strand for the initiation of formation of each Okazaki fragment (Hubscher, 2009). Therefore, Polymerase α/primase exhibits both primase and DNA polymerase activities. RPA molecules are also displaced by Polymerase

α/primase as they move along the DNA. Next, the clamp loader RFC (replication factor C) binds to the primer template junction, which can recruit a sliding clamp known as PCNA (proliferating cell nuclear antigen) around the DNA at the end of the primer. PCNA, loaded by RFC, creates a closed ring around the DNA template strand and can move freely along it; it also plays various roles in DNA replication and repair. DNA polymerases (Pol ε or δ) are recruited to the sliding clamp and elongate the new DNA strand, while PCNA inhibits the falling off of polymerases from the template DNA (Moldovan et al., 2007). Replicative polymerases are indispensable for cell viability, but interestingly the catalytic domain of polymerases ε is required for normal replication but is not essential for viability in yeast (Dua et al., 1999, Kesti et al., 1999, Feng and D'Urso, 2001, Ohya et al., 2002).

In addition to these enzymes, multiple accessory factors are required for efficient DNA replication as well as for other crucial processes such as establishment of cohesion between sister chromatids and checkpoint signalling. In the next section, I will introduce the roles of these factors in DNA replication.

1.2.3 Functions of Replisome Components in DNA Replication

In 2006, Gambus et al. isolated the CMG helicase from the extracts of S phase yeast cells and performed mass spectrometric analysis to detect a particular set of associated components known as the replisome progression complex (RPC) (Gambus et al., 2006). The RPC consists of the trimeric complex of regulatory factors including the checkpoint mediator Mrc1; Tof1, Csm3, and Ctf4 that are known to bind DNA polymerase α; the histone chaperone FACT; and the type I topoisomerase Top1. ChIP analysis has indicated that the components of the RPC migrates with replication forks (Aparicio et al., 1997, Kanemaki et al., 2003, Katou et al., 2003, Osborn and Elledge, 2003, Takayama et al., 2003, Calzada et al., 2005, Gambus et al., 2006, Foltman et al., 2013). Additional factors such as DNA polymerase α (Gambus et al., 2009), DNA polymerase ε (De Piccoli et al., 2012, Sengupta et al., 2013), and the E3 ubiquitin ligase known as SCF^{Dia2}

also interact with the RPC (Figure 1.14) (Morohashi et al., 2009).

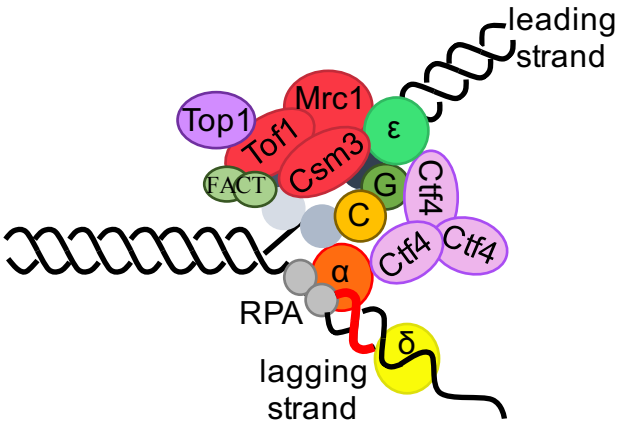

Figure 1.14: The eukaryotic replisome complex coordinates DNA replication.
In budding yeast, the RPC binds around the CMG helicase at replication forks during DNA replication. The RPC is linked to Pol ε and Pol α at the forks, but it does not appear to link to Pol δ. For more details, see text. Factors such as Ctf18-RFC, Chl1, and Dia2 have been left out for the purpose of simplicity. Figure adapted from (Bell and Labib, 2016).

One of the reasons for RPC assembly might be to link the MCM2-7 helicase to other replisome factors such as DNA polymerases. The Dpb2 subunit of Polymerase ε interacts directly with the Psf1 subunit of GINS, and this particular interaction has a key function in the formation of the Cdc45-MCM-GINS helicase during chromosome replication initiation and in linking Polymerase ε and the replisome at DNA replication forks (Sengupta et al., 2013). Zhu et al. (2007) showed that the interaction between Mcm10 and Ctf4 is important for the recruitment of Polymerase α to the chromatin during the initiation of chromosome replication in extracts of *Xenopus* eggs (Zhu et al., 2007). Ctf4 interacts directly with both the CMG complex and Polymerase α; therefore, it is required for the linkage of the CMG complex to the lagging-strand primase (Polymerase α) (Gambus et al., 2009). However, unlike Polymerase ε and Polymerase α, Polymerase δ does not appear to be linked to the CMG helicase. Therefore, unlike the synthesis of the leading strand by Polymerase ε, the synthesis of the lagging strand by Polymerase δ seems to be uncoupled from the CMG helicase action (reviewed by Bell and Labib, 2016).

1.2.3.1 Mrc1

*sc*Mrc1 (*sp*Mrc1 and *h*Claspin) (mediator of the replication checkpoint) has functions both at the replication fork and at the S phase checkpoint. Although Mrc1 is not crucial for viability, it exists at unperturbed DNA replication forks. Mrc1 is recruited onto replication origins at the same time as DNA polymerases in every cell cycle, where it interacts with other components in a complex around the DNA helicase (Alcasabas et al., 2001, Katou et al., 2003). Lou et al. (2008) have shown that Mrc1 physically interacts with Polymerase ε (Lou et al., 2008); it has also been shown to interact with the Mcm6 subunit of the CMG helicase (Komata et al., 2009). However, it is still unclear as to whether Mrc1 directly alters the role of either component. Additionally, Mrc1 also acts as a mediator of the DNA replication checkpoint at defective DNA replication forks. Replication forks move very slowly when cells are treated with hydroxyurea (HU), a drug that depletes deoxyribonucleotide (dNTPs); in such cases, Mrc1 is hyperphosphorylated by upstream checkpoint kinases, which leads to the activation of the downstream checkpoint kinase Rad53 (will be discussed further in section 1.3.2.1) (Alcasabas et al., 2001, Osborn and Elledge, 2003). However, in *mrc1Δ* cells under nucleotide depletion, replication fork proteins seem to progress farther along the chromatin, whereas the progression of DNA synthesis halts; this indicates that the replication apparatus is uncoupled from the site of DNA synthesis. Furthermore, this uncoupling causes extensive exposure of ssDNA at the replication fork and subsequent activation of DNA damage checkpoints. As a result, Mrc1 acts in a pausing complex to maintain replisome integrity in response to exogenous stresses (Katou et al., 2003), but not at protein-DNA barriers (Calzada et al., 2005, Hodgson et al., 2007) (will be explained in more detail in section 1.2.3.2).

Osborn and Elledge (2003) identified that *mrc1AQ*, a mutant in which all of the possible Mec1 S/TQ phosphorylation sites have been changed to non-phosphorylatable AQ, is defective in full Rad53 activation but is competent in DNA replication, which suggests that the functions of Mrc1 in replication and checkpoint regulation are independent of each other. In the absence of exogenous damaging agents, cells lacking Mrc1 experience extensive replication

fork damage, which results in constitutive Rad53 phosphorylation, and this defect is independent of the checkpoint regulation function of Mrc1 (Alcasabas et al., 2001, Osborn and Elledge, 2003). High levels of gross chromosomal rearrangements (GCRs) are observed in *mrc1Δ* cells (Putnam et al., 2009).

Moreover, *mrc1Δ* cells are also defective in the establishment of sister chromatid cohesion (SCC) (Xu et al., 2004). SCC is normally established during DNA replication in the S phase and ensures that sister chromosomes are held together until they are separated equally during mitosis (Uhlmann and Nasmyth, 1998).

1.2.3.2 Tof1/Csm3

*sc*Tof1 (*sp*Swi1 and *h*Timeless) (topoisomerase I-interacting factor 1) and *sc*Csm3 (*sp*Swi3 and *h*Tipin) (chromosome segregation in meiosis 3) interact with each other both physically and functionally. Tof1 and Csm3 form a heterodimeric complex, and the deletion of either of these proteins results in a similar phenotype. This heterodimeric complex associates with chromatin as well as other factors of the replisome, such as (MCM) DNA helicase subunits, DNA Polymerases δ, and ε, RPA and other replisome factors (Unsal-Kacmaz et al., 2007, Chou and Elledge, 2006, Gotter et al., 2007, Mayer et al., 2004, Noguchi et al., 2004, Errico et al., 2007, Gambus et al., 2006, Katou et al., 2003). The Tof1-Csm3 complex also interacts with the CMG complex and DNA polymerases to couple DNA unwinding and DNA synthesis (Katou et al., 2003, Errico et al., 2007, Cho et al., 2013). Tof1 has also been shown to interact with topoisomerase I, both in yeast two-hybrid assay and *in vitro* (Park and Sternglanz, 1999). Several studies have also revealed the roles of the Tof1-Csm3 complex in SCC, DNA replication checkpoints, pausing/stalling of replication fork progression, normal DNA replication, and replication at hard-to-replicate genomic regions. The complex interacts with replication origins at the onset of the S phase and travels with the replisome during DNA replication in both yeast and human cells (Katou et al., 2003, Noguchi et al., 2004, Leman et al., 2010). Yeast genetic studies have also shown that both Tof1 and Csm3 are required in the establishment of SCC during DNA replication (Mayer et al., 2004, Warren et al., 2004).

Two parallel checkpoint pathways exist in *S. cerevisiae*; one is an S phase-specific pathway and the other is a cell cycle-wide pathway dependent on Rad9. Both pathways are dependent on the central kinase Mec1 for their function. A Rad9-mutant strain is not as sensitive as a Mec1-deficient cell to DNA damage by methyl methanesulphonate (MMS) treatment. In 2001, Foss performed synthetic lethal screening in budding yeast to identify new genes in the S phase-specific checkpoint pathway and found that *tof1Δ* cells were highly sensitive to MMS in combination with a *rad9Δ* cells, equivalent to the sensitivity of a *mec1* mutant strain. Furthermore, cells lacking Tof1 have been shown to be sensitive to other S phase-stressing agents such as HU and UV light (UV), which indicate that Tof1 is required for the S phase-specific checkpoint pathway (Foss, 2001). Further findings of Foss (2001) revealed that cells lacking both Rad9 and Tof1 prevent phosphorylation and activation of Rad53 in response to HU but not in the absence of either Rad9 or Tof1, and this role has been shown to be conserved in *S. pombe* and metazoans (reviewed by Leman and Noguchi, 2012). Thus, the Tof1/Csm3 complex has been proposed to play a role in mediating checkpoint signalling in response to replication stress (Foss, 2001).

One of the roles of the S phase checkpoint is to prevent the firing of late replication origins in response to replication stress. In budding yeast, Rad53-dependent phosphorylation of Dbf4 leads to late origin firing inhibition after DNA damage (explained in the next section) (Zegerman and Diffley, 2010). As mentioned earlier, Dbf4 interacts with the Cdc7 kinase to form the DDK complex, which is required for the initiation of DNA replication. In addition, the DDK complex plays a role throughout the S phase in the firing of origins (Zou and Stillman, 2000). Interestingly, several findings suggest that DDK is required for Tof1 function. First, in fission yeast, Swi1/Swi3 functionally associates with the Hsk1-Dfp1 complex, the fission yeast ortholog of the DDK complex, as shown in the two-hybrid system and by co-immunoprecipitation experiments (Matsumoto et al., 2005). Cells lacking Hsk1 are sensitive to S phase-stressing agents such as HU and MMS, and this mutant also shows defects in arresting S phase progression in response to MMS exposure. These effects are epistatic with Swi1 and Swi3 mutations, thereby suggesting that the interaction of DDK with the Swi1/Swi3 complex inhibits origin activation in response to DNA damage.

However, the role of Swi1 and Swi3 in origin inhibition needs to be identified mechanistically (Matsumoto et al., 2005, Shimmoto et al., 2009, Sommariva et al., 2005). Second, in budding yeast, co-immunoprecipitation experiments have shown that Tof1/Csm3 also form a complex with DDK (Murakami and Keeney, 2014). In addition, recent data have shown that when DDK is inactivated *in vivo*, Tof1 is no longer bound to the chromatin fractions (Bastia et al., 2016). *In vitro*, DDK has been found to phosphorylate Mcm2-7 and/or CMG, which is required for the recruitment of phosphorylated Tof1/Csm3 (but not the dephosphorylated form) at the replisome. However, it has not been determined yet whether this interaction causes the phosphorylation of Tof1 by DDK (Bastia et al., 2016).

Similar to what is observed in *mrc1Δ* cells, the migration of the replication fork along the chromatin in *tof1Δ* cells seems to be faster than the progression of DNA synthesis upon HU treatment. This result suggests that the replication apparatus is uncoupled from the site of DNA synthesis in *tof1Δ* cells. This uncoupling leads to extensive exposure of ssDNA at the replication fork and subsequent activation of DNA damage checkpoints (Katou et al., 2003), presumably through Rad9 (Foss, 2001, Alcasabas et al., 2001). Katou et al. (2003) further showed that Rad9 is loaded onto replicated regions in both *mrc1* and *tof1* mutants but not in wild-type cells, which leads to DNA damage checkpoint activation. As a result, it appears that Tof1 as well as Mrc1 acts in a pausing complex to maintain replisome integrity in response to exogenous stresses by inhibiting the uncoupling of the replication machinery from DNA synthesis (Katou et al., 2003). Tof1, Csm3, and Mrc1 appear to be recruited onto DNA independently of each other. Tof1/Csm3 have also been reported to be required for the association of Mrc1 to the replication fork complex. However, Mrc1 is not required for the binding of Tof1/Csm3 to chromatin (Bando et al., 2009, Uzunova et al., 2014). Further, the simultaneous loss of Mrc1 and Tof1 results in a more severe growth defect; these cells are also more sensitive to HU than to either of the single mutants, which indicates that Mrc1 and Tof1 are not part of the same replication checkpoint cascade (Katou et al., 2003).

The rate of fork progression has to be maintained at a high level during DNA replication (~1.5 kb per minute in yeast cells), and the forks need to overcome

numerous obstacles as they move from each origin to the point of termination. In addition to disrupting chromatin and displacing histones, forks have to bypass many sites such as centromeres and transfer RNA (tRNA) promoters, where non-nucleosomal proteins bind very tightly to DNA; cope with supercoils in the unwound template ahead of the fork, which are formed by the action of the replicative helicase; and deal with any DNA damage or unusual structures that can be formed in the parental DNA (reviewed by Bell and Labib, 2016). DNA unwinding occurs due to the action of the CMG helicase, but the rate of progression of CMG is influenced by other replisome factors. Polymerase ε, via its Dpb2 subunit, stimulates CMG activity *in vitro*, which has been observed in both yeast and human proteins; therefore, the rate of progression of CMG is particularly influenced by the physical interaction of CMG with Polymerase ε (Georgescu et al., 2014, Kang et al., 2012, Langston et al., 2014). Several studies have also shown that reduction in the deoxyribonucleotide (dNTP) levels slows the rate of progression of the DNA helicase as well as DNA synthesis; therefore, the whole replisome moves slowly under such conditions (Aparicio et al., 1997, Kanemaki et al., 2003, Katou et al., 2003, Takayama et al., 2003). The rate of fork progression can also be influenced by other replisome factors. Chromosome replication proceeds more slowly in the absence of Mrc1 in budding yeast, and this is because the rate of DNA replication fork progression is reduced to about half the normal rate (Szyjka et al., 2005, Tourriere et al., 2005, Hodgson et al., 2007). However, the effect of Mrc1 on the rate of fork progression does not depend on its role in checkpoint signalling, as *mrc1AQ* (the checkpoint-deficient mutant) progresses normally through the S phase. The rate of fork progression is also reduced in the absence of Tof1 and Csm3, similar to that observed in *mrc1Δ* cells (Tourriere et al., 2005), but the effect is milder (Hodgson et al., 2007). Taken together, these data indicate that Tof1/Csm3 and Mrc1 proteins are required for efficient replisome progression, where they act by stabilizing replication fork structures and replisome factors during DNA replication throughout the genome.

Several studies have revealed that cells lacking Timeless, the mammalian Tof1 homolog, show some increase in Chk1 phosphorylation in the absence of exogenous genotoxic agents (Unsal-Kacmaz et al., 2007, Yoshizawa-Sugata and

Masai, 2007, Smith et al., 2009). As a result, although the Timeless-Tipin heterodimeric complex is required for Chk1 activation in response to replication stress, its absence leads to some checkpoint activation in the absence of exogenous replication stress. In fission yeast, the deletion of *swi1* leads to replication fork collapse close to the rDNA replication pausing site, in which recombination structures such as Holliday junctions are formed; this structure has been detected by two-dimensional gel electrophoresis (2D gel) of chromosomal DNA. This formation of Holliday junction structures acts as a marker of replication fork collapse and rearrangement, which is an indication of a DNA repair process. Taken together, these data indicate that Swi1 inhibits replication fork collapse (Noguchi et al., 2003, Noguchi et al., 2004). Similar phenomena have also been observed in Timeless-depleted mouse cells, where high levels of DNA damage lead to high levels of sister chromatid exchange, which is an indication of a DNA repair process that uses sister chromatids for homologous recombination (Urtishak et al., 2009). Deletion of Timeless or Tipin from human cells leads to histone H2AX phosphorylation (γH2AX), a marker of DSB formation, (Chou and Elledge, 2006, Urtishak et al., 2009) which is indicative of DNA damage even in the absence of genotoxic agents. High levels of GCRs are also observed in cells lacking Tof1 (Putnam et al., 2009). Together, these results suggest that Timeless-Tipin play an essential role in preventing DNA damage at replication forks and are therefore required for maintaining genome integrity during unperturbed DNA replication.

Several studies using two-dimensional DNA gels and ChIP have shown that during the normal process of chromosome replication, replication forks pause transiently at a number of places around the genome where non-nucleosomal proteins are bound very tightly to DNA, such as the centromeres (Greenfeder and Newlon, 1992), tRNA promoters (Deshpande and Newlon, 1996, Ivessa et al., 2003), ribosomal DNA (rDNA) (Brewer and Fangman, 1988, Linskens and Huberman, 1988, Calzada et al., 2005), silent origins of replication (Wang 2001) and telomeres (Makovets et al., 2004). Some barriers such as centromeres can pause the progression of forks that arrive from either direction (Greenfeder and Newlon 1992). Others such as tRNA promoters (Deshpande and Newlon 1996; Ivessa 2003) or rDNA act unidirectionally (Brewer and Fangman 1988; Linskens

and Huberman 1988). Ivessa et al. (2003) showed that the size of the pause at the tRNA does not increase with an increase in the size of the transcribed region, which suggests that the transcription complex rather than transcription itself leads to fork pausing, i.e. pausing of a fork appears to occur when the fork encounters tightly bound protein-DNA complexes at the tRNA promoter (Ivessa et al., 2003). Calzada et al. (2005) found that when a eukaryotic DNA replication fork pauses at a protein-DNA barrier, the replisome does not disassemble. In this case, similar to the replisome that is retained at HU-stalled forks, the intact replisome is maintained at the paused fork (Calzada et al., 2005). Interestingly, pausing at protein-DNA barriers depends on the Tof1-Csm3 complex (Calzada et al., 2005, Tourriere et al., 2005, Mohanty et al., 2006, Hodgson et al., 2007), which interacts with the CMG helicase as part of the RPC (Gambus et al., 2006), but does not require Mrc1 (Calzada et al., 2005, Szyjka et al., 2005, Tourriere et al., 2005, Mohanty et al., 2006, Hodgson et al., 2007). Similarly, pausing at protein-DNA barriers depends on the Swi1-Swi3 complex in fission yeast (Dalgaard and Klar, 2000, Krings and Bastia, 2004). Thus, Tof1-Csm3 and Mrc1 are functionally different, at least in the context of a paused DNA replication fork. Further findings of Calzada et al. (2005) showed that Rad53 and Mec1 in budding yeast are not essential for replisome pausing; therefore, Tof1-Csm3–dependent fork pausing is independent of checkpoints. Before the protein-DNA barrier is removed and the replication restarts its progression, pausing might allow other replisome components to help remove the barriers. However, the molecular mechanism and the importance of pausing at protein-DNA barriers is not yet clear. Increased levels of genome instability have been observed in cells lacking Tof1 or Csm3, but it is not clear as to whether this is because of deficient pausing of replication forks or due to other roles of Tof1-Csm3 (reviewed by Bell and Labib, 2016).

1.2.3.3 Ctf4

*sc*Ctf4 (*sp*Mcl1 and *h*And1) is not important for viability in budding yeast. However, *ctf4Δ* cells show a high rate of genome instability, are defective in establishing cohesion between sister chromatids, and delay their cell cycle progression (Kouprina et al., 1992, Miles and Formosa, 1992, Hanna et al., 2001). It is important to note that budding yeast cells can remain viable in the

absence of any two of the RPC components, but lack of both Mrc1 and Ctf4 is lethal (Warren et al., 2004). However, this lethality is not due to the role of Mrc1 in checkpoint activation, as cells with the *mrc1-AQ* allele, which are competent in replication but defective in checkpoint activation (Osborn and Elledge, 2003), remain viable when it is combined with *ctf4Δ* (Gambus et al., 2009). Gambus et al. (2009) also showed that cells deficient in both Mrc1 and Ctf4 undergo chronic checkpoint activation during chromosome replication and do not complete the cell cycle. Furthermore, the ability of Ctf4 to link MCM helicase through the GINS complex to DNA polymerase α is highly important for the preservation of genome stability in cells lacking Mrc1, which binds DNA polymerase ε (Gambus et al., 2009).

1.2.3.4 Ctf18

*Sc*Ctf18 (*sp*Ctf18 and *h*Ctf18) is part of a RFC^{Ctf18} complex. It associates with Rfc2, Rfc3, Rfc4, and Rfc5. RFC^{Ctf18} also interacts with two more subunits, Dcc1 and Ctf8. RFC^{Ctf18} interacts physically and genetically with replication fork components and is not essential for viability. *ctf18Δ* cells show defects in cohesion establishment (Mayer et al., 2001, Hanna et al., 2001). Ctf18 contributes to loading PCNA *in vivo* and has also been shown to unload PCNA from DNA *in vitro* (Bylund and Burgers, 2005, Lengronne et al., 2006, Bermudez et al., 2003). RFC^{Ctf18} is also involved in S phase checkpoint activation. Cells lacking Ctf18 are hypersensitive to the replication inhibitor HU, and the DNA damaging agent MMS (Bellaoui et al., 2003). Kubota et al. (2011) identified that *ctf18Δ* and *rad9Δ* double mutants are defective in Rad53 phosphorylation in response to DNA replication stress, which indicates that Ctf18, like Mrc1, is required for DNA replication checkpoint activation (Kubota et al., 2011).

1.2.3.5 Chl1

*sc*Chl1 (*sp*Chl1 and *h*ChlR1) is a DNA helicase (Gerring et al., 1990) and its deletion leads to SCC defects in yeast and humans (Farina et al., 2008, Mayer et al., 2004, Skibbens, 2004, Parish et al., 2006). Mutations in human ChlR1 lead to a cohesinopathy-related disease known as Warsaw breakage syndrome (van

der Lelij et al., 2010). Samora (2016) showed that Ctf4 recruits the Chl1 helicase to the replication forks and that Chl1 appears to link the replisome with cohesion. The author further found that the Chl1 helicase promotes replication fork progression under conditions of dNTP depletion, but not under unchallenged conditions and that this role is not dependent on its interaction with Ctf4. In contrast, the function of Chl1 in sister chromatid cohesion is dependent on its interaction with Ctf4 but not on its helicase activity. However, it is not clear as to how Chl1 mechanistically contributes to cohesion establishment (Samora et al., 2016).

1.2.3.6 Dpb3/Pol32

Polymerase ε and Polymerase δ include several subunits encoded by different genes. Yeast Polymerase ε is composed of four subunits and is crucial for chromosomal DNA replication. These subunits are encoded by *POL2*, *DPB2*, *DPB3,* and *DPB4* in budding yeast. The genes essential for cell viability are *POL2* and *DPB2,* and cells with either of these genes deleted show cell cycle arrest and inhibition of DNA replication. However, the *scDPB3* (*spDPB3* and *hP17*) and *DPB4* genes are non-essential, and mutations in either of these two genes result in defects in nucleotide incorporation (Chilkova et al., 2003, Araki et al., 1991b, Araki et al., 1991a, Ohya et al., 2000). Homologs of these proteins have also been identified in human cells (Li et al., 2000). Budding yeast DNA Polymerase δ consists of three subunits, the catalytic subunit Pol3 and the Pol31 subunit, both of which are essential for viability, and a third small accessory subunit, Pol32 (Burgers and Gerik, 1998). Fission yeast DNA polymerase δ is composed of four subunits, the catalytic subunit Pol3, and three small accessory subunits Cdc1, Cdc27 (budding yeast Pol31 and Pol32 respectively), and Cdm1 (Zuo et al., 1997). Orthologs of these four yeast proteins in mammals are known as p125, p50, p66, and p12, respectively (Liu et al., 2000a). Cells lacking Pol32 are viable in budding yeast; however, the ortholog Cdc27 is essential for growth in fission yeast. The basic roles of Pol32 are to increase Polymerase δ complex activity during replication and to repair DNA. *pol32Δ* cells show defects in replication with frequent stalls and are also sensitive to HU exposure, ultraviolet (UV) irradiation, and MMS treatment (Haracska et al., 2001, Huang et al., 2002, Hanna et al.,

2007).

1.2.3.7 Dia2

At the end of chromosome replication, the replication forks converge, and the replisomes must disassemble. To do this, an essential F-box protein known as *sc*Dia2 (*sp*Pof3 and *h* unclear) is needed to disassemble the CMG helicase (Maric et al., 2014). Maric et al. (2014) further identified that Mcm7, the subunit of CMG, is ubiquitylated by the action of the E3 ligase SCF^{Dia2} as part of the disassembly process. SCF^{Dia2}, through the tetratricopeptide-repeat domain located at the amino-terminal, interacts with Mrc1 and Ctf4 and couples itself to the RPC (Morohashi et al., 2009). It turns out that this tethering mechanism enhances the efficiency of ubiquitylation of the Mcm7 and the disassembly at the end of chromosome replication both *in vitro* and *in vivo* (Maculins et al., 2015). Interestingly, it has also been shown that Dia2 is required to restart replication after MMS-induced DNA damage (Fong et al., 2013).

1.3 Cause and Consequences of Perturbed DNA Replication

Cell growth, DNA replication, chromatin condensation, chromosome segregation, and cell division have to be accurately accomplished and tightly controlled in order to generate viable daughter cells. In 1989, Hartwell and Weinert identified checkpoint mechanisms that ensure that a certain process is initiated only after the previous one has been successfully completed and terminated (Hartwell and Weinert, 1989). Several checkpoint genes that delay the onset of mitosis during DNA replication arrest have been recognized (Weinert et al., 1994, Friedel et al., 2009, Allen et al., 1994). Thus, checkpoint factors preserve the order of events and contribute to the maintenance of genome stability (Harper and Elledge, 2007). The loss of genome stability has harmful consequences such as cell death (Haering and Nasmyth, 2003). In this section, I will first introduce the nature of DNA lesions, which lead to a checkpoint response. Next, I will explain the mechanism of S phase checkpoint response and then describe how cells down-regulate the checkpoint signal to restart the cell cycle after the damage has been removed or repaired. Finally, I will briefly explain the repair of DSBs.

1.3.1 Impediments to Replication Progression

The progression of the replisome can be impeded by different factors during DNA replication. Impediments can be either endogenous, such as proteins bound to DNA or secondary DNA structures, or exogenous, such as genotoxic drugs. The progression of either the helicase or the polymerase can be prevented by these barriers, and in both cases, the linkage between the helicase and the polymerase can be broken, thereby forcing the replisome to stop DNA synthesis (Cortez, 2005, Zegerman and Diffley, 2009).

1.3.1.1 Natural Impediments to Replication Fork Progression

In budding yeast, many DNA structures that inhibit the progression of DNA

replication have been characterized. Such barriers are located at centromeres, tRNA sites, replication origins, rDNA repeats, Ty long-terminal repeats (LTR), G-quadruplexes, and the *HMR* and *HML* heterochromatic loci (Roeder and Fink, 1980, Deshpande and Newlon, 1996, Argueso et al., 2008, Greenfeder and Newlon, 1992, London et al., 2008, Anand et al., 2012, Szilard et al., 2010). However, natural fork pausing does not lead to checkpoint responses, and as explained in the previous section, the Tof1-Csm3 complex is associated with all replication forks and leads to stable fork pausing for instance when a replication fork encounters barriers such as tRNA genes or the rDNA locus (Tourriere et al., 2005, Hodgson et al., 2007).

1.3.1.2 Genotoxic Drugs Causing Replication Fork Stalling

Many genotoxic drugs that are used frequently lead to fork stalling and slow down S phase progression. For example, hydroxyurea (HU) inhibits the action of ribonucleotide reductase (RNR) by decreasing the amount of the reactive tyrosyl radical in the active centre of the enzyme (Eklund et al., 2001). Once replication is initiated, nucleotide levels are rapidly reduced if the action of RNR is prevented, and this causes stalling of the fork, as dNTPs are not available to continue DNA synthesis. As a result, the helicase uncouples from the polymerase and forms ssDNA, which leads to checkpoint activation. One of the checkpoint responses is to upregulate nucleotide production, which counteracts the action of HU and allows cells to replicate at a 10- to 20-fold reduced speed (Poli et al., 2012).

The alkylating agent, methyl methanesulphonate (MMS), is the second example, which forms bulky lesions by alkylating DNA. Convergence of the replication fork with the alkylated DNA leads to checkpoint activation during S phase (Tercero et al., 2003).

1.3.1.3 Repair Following DNA Damage Caused by Impeding Replication Fork Progression

DNA damage tolerance mechanisms have evolved to allow forks to replicate past damaged DNA, e.g. following MMS treatment. However, there are different kinds of DNA lesions that can inhibit the progression of the replication fork, such as damaged DNA bases or damage to the DNA backbone. Prolonged stalling of replication forks may cause a collapse of the replication machinery, which can lead to the formation of DSBs and GCRs or even to a permanent cell-cycle arrest and cell death. Two main pathways mediate replication past DNA lesions: DNA translesion synthesis (TLS) and template switching. TLS is an error-prone mechanism, but template switching works via an HR-dependent pathway and shows high fidelity. Thus, it is essential for the cell to maintain a balance between these two mechanisms in order to keep mutation events rare. Budding yeast contains different translesion polymerases, which replicate damaged DNA. Translesion polymerases are tolerant of distortions in the DNA helix, which allows them to recognize damaged nucleotides. These polymerases can accommodate either an incorrect or a correct nucleotide opposite to the lesion making the process more error-prone than that with replicative polymerases (Moldovan et al., 2007, Sale et al., 2009, Sale et al., 2012, Sale, 2013). Translesion DNA polymerases in yeast are also recruited when RPA-coated ssDNA accumulates at defective replication forks. The accumulation of RPA-coated ssDNA at defective replication forks leads to ubiquitination of the clamp loader PCNA by the conserved Rad18-Rad6 proteins, which causes polymerase switches. Therefore, translesion DNA polymerases are recruited due to the changed affinity of PCNA for translesion polymerases. Once the damage is repaired or removed, TLS polymerases are replaced by replicative polymerases (Figure 1.17I) (Kannouche et al., 2004, Moldovan et al., 2007).

1.3.2 The S Phase Checkpoint

Checkpoint pathways in the S phase function to protect cells from problems during chromosome replication. The following paragraphs focus on the molecular mechanism of these checkpoints in budding yeast. An overview of the homologous counterparts of some of the most important proteins involved in the checkpoint is shown in Table 1.4.

Table 1.4: Conserved checkpoint proteins and their functions.

S. cerevisiae	***S. pombe***	***H. sapiens***	**Function**
Mec1-Ddc2	Rad3-Rad26	ATR-ATRIP	checkpoint signalling kinase
Tel1	Tel1	ATM	checkpoint signalling kinase
Rad24-RFC	Rad17-RFC	RAD17-RFC	RFC-like complex, 9-1-1 clamp loader
Ddc1-Rad17-Mec3	Rad9-Rad1-Hus1	RAD9-RAD1-HUS1	9-1-1 complex, DNA damage checkpoint clamp, Mec1 activation
Dpb11	Cut5/Rad4	TOPBP1	Mec1 ATR activation
Dna2	Dna2	DNA2	Mec1 activation in S phase
Mre11-Rad50-Xrs2	Mre11-Rad50- Nbs1	MRE11-RAD50-NBS1	MRX/MRN complex, DSB resection, Tel1/ATM recruitment
Mrc1	Mrc1	Claspin	fork-associated, checkpoint mediator
Rad9	Crb2	53BP1,BRCA1	checkpoint mediator
Rad53	Cds1	CHK2	effector kinase
Chk1	Chk1	CHK1	effector kinase

1.3.2.1 Checkpoint Activation

Two main protein kinases are involved in response to DNA damage checkpoints: *sc*Mec1 (Mitosis Entry Checkpoint 1) (*sp*Rad3 and *h*ATR) and *sc*Tel1 (telomere maintenance 1) (*sp*Tel1 and *h*ATM) (Friedel et al., 2009). Both are phosphoinositide 3-kinase (PI3K)-related kinases (PIKKs), and they have high sequence homology with each other and can phosphorylate an overlapping set

of substrates (Kim et al., 1999, Chan et al., 1999, Cortez et al., 1999, Sweeney et al., 2005). Mec1 is also active during normal DNA replication in budding yeast, controls the initiation of DNA replication without inhibiting cell cycle progression and controls dNTP levels (Zhao et al., 2001, Randell et al., 2010). Furthermore, in the absence of exogenous damage, Mec1 is required to inhibit chromosome breakage at fragile sites where replication forks frequently slow down (Cha and Kleckner, 2002). In addition, Mec1 is essential for cell viability and is hyper-activated in response to many different forms of DNA damage, such as stalled replication fork, DSBs and nucleotide damage; in contrast, the lack of Tel1 is not lethal in budding yeast and Tel1 is activated primarily by DSBs. In mammalian cells, the deletion of either ATR or ATM causes an increased risk of developing cancer (Cimprich and Cortez, 2008, Morrow et al., 1995).

Fork stalling due to DNA lesions or nucleotide depletion induced by exogenous genotoxic agents often results in the formation of a significant amount of ssDNA. This is either due to the uncoupling of the helicase and the polymerase, or of the leading and the lagging strand polymerases, or due to resection at DSBs (Branzei and Foiani, 2007, Aguilera and Gomez-Gonzalez, 2008, Segurado and Tercero, 2009). The Mre11-Rad50-Xrs2 complex recruits and activates Tel1 at DSBs, which then facilitates resection. Resection results in the formation of ssDNA and a ds-ssDNA junction (Jazayeri et al., 2006, Shiotani and Zou, 2009, Costanzo et al., 2001, Myers and Cortez, 2006). At stalled replication forks as well as at resected DSBs, ssDNA is bound by the ssDNA-binding protein, RPA (Alani et al., 1992), and RPA-coated ssDNA recruits Mec1 and Ddc2 (an important cofactor of the Mec1 kinase) (Zou and Elledge, 2003, Ball et al., 2005).

The ds-ssDNA junctions are identified by the Rad24-RFC complex, which recruits the 9-1-1 checkpoint clamp (Ddc1, Rad17, and Mec3 in *S. cerevisiae*). Along with these structures, RPA can then activate Mec1. Thus, after complex recruitment, Mec1 phosphorylates Ddc1, which then recruits Dpb11, leading to the induction of Mec1 kinase activity (reviewed by Hustedt et al., 2013). Kumar and Burgers (2013) also found that Dna2, a conserved nuclease-helicase that has a crucial role in Okazaki fragment maturation, also activates Mec1 in the S phase (Kumar and Burgers, 2013). Thus, after the localization of Mec1 and Tel1, they are

activated by DNA damage-sensing proteins.

Next, one of the two kinases transduces the signal through the mediator proteins, Mrc1, Tof1, Csm3 and *sc*Rad9 (*sp*Crb2 and *h*BRCA1, 53BP1), to the effector kinases, *sc*Rad53 (*sp*Cds1 and *h*Chk2) and *sc*Chk1 (*sp*Chk1 and *h*Chk1) (Sanchez et al., 1999, Sanchez et al., 1996, Pellicioli et al., 1999, Alcasabas et al., 2001, Foss, 2001), which leads to the transient recruitment of the effector kinases to the site of DNA damage; these are then released after activation (Gilbert, 2001, Katou et al., 2003). This process allows the transfer of the checkpoint response to a range of effector proteins (Gardner et al., 1999). It is important to note that Mrc1, in comparison to Tof1/Csm3, appears to be the main mediator of the replication checkpoint; in fact, Tof1 only has an indirect function in this process (Tourriere et al., 2005). Presumably, Tof1 is required for Mrc1 recruitment at replication forks (Katou et al., 2003).

Mec1 and Rad53 are also needed to slow the rate of progression of DNA synthesis when yeast cells are treated with MMS with continued activation of repair and checkpoint pathways, which suggests that Mec1 and Rad53 are central to an S phase checkpoint response that controls chromosome replication in response to DNA damage in budding yeast (Paulovich and Hartwell, 1995, Labib and De Piccoli, 2011). However, so far, the targets of Mec1 and Chk1 in replication fork stabilization remain unknown (Figure 1.15).

Rad9 is phosphorylated by Mec1/Tel1 in response to DNA damage and is needed for efficient Rad53 activation (Emili, 1998). However, Rad9 has only a small role or no role to play in the replication checkpoint triggered by HU-arrested forks (Weinert et al., 1994, Weinert and Hartwell, 1988). It has been predicted that phosphorylated Rad9 increases Rad53 concentration, leading to efficient Rad53 autophosphorylation and activation (Gilbert, 2001, Ma et al., 2006). Thereafter, studies have also indicated that Mec1/Tel1 also directly phosphorylates Rad53 and therefore are required for Rad53 activation (Sweeney et al., 2005, Ma et al., 2006).

As mentioned in the previous section, Mrc1 is a mediator protein for Rad53

activation during replication stress. Mrc1 appears to recruit Rad53 to stalled forks to promote Rad53-Mec1 interaction (Alcasabas et al., 2001, Osborn and Elledge, 2003, Tanaka and Russell, 2001, Chen and Zhou, 2009). Mrc1 is phosphorylated by Mec1, and a mutant in which all Mrc1 [S/T]Q sites are mutated to AQ shows a defect only in checkpoint signalling, but not in replisome progression (Alcasabas et al., 2001, Osborn and Elledge, 2003). Mrc1 also seems to activate the replication checkpoint in response to replication stress; however, the lack of Mrc1 can be compensated for by Rad9 (Alcasabas et al., 2001), which suggests that in cells lacking Mrc1, Rad9 accumulates at stalled replication forks in the presence of HU (Katou et al., 2003). This is indicative of the fact that cells lacking Mrc1 form DSBs or damaged structures, which activates Rad9-dependent Rad53 (Hustedt et al., 2013).

In addition to transducing the signal to the effector kinases, Mec1 and Tel1 also phosphorylate proteins bound at the site of damage, such as the serine residue S129 on histone H2A in budding yeast, which is the homolog of the histone variant H2AX in mammals, forming γH2AX. Therefore, phosphorylated H2A has become an important marker for DNA damage in budding yeast and mammals (Figure 1.17IIa) (Downs et al., 2000).

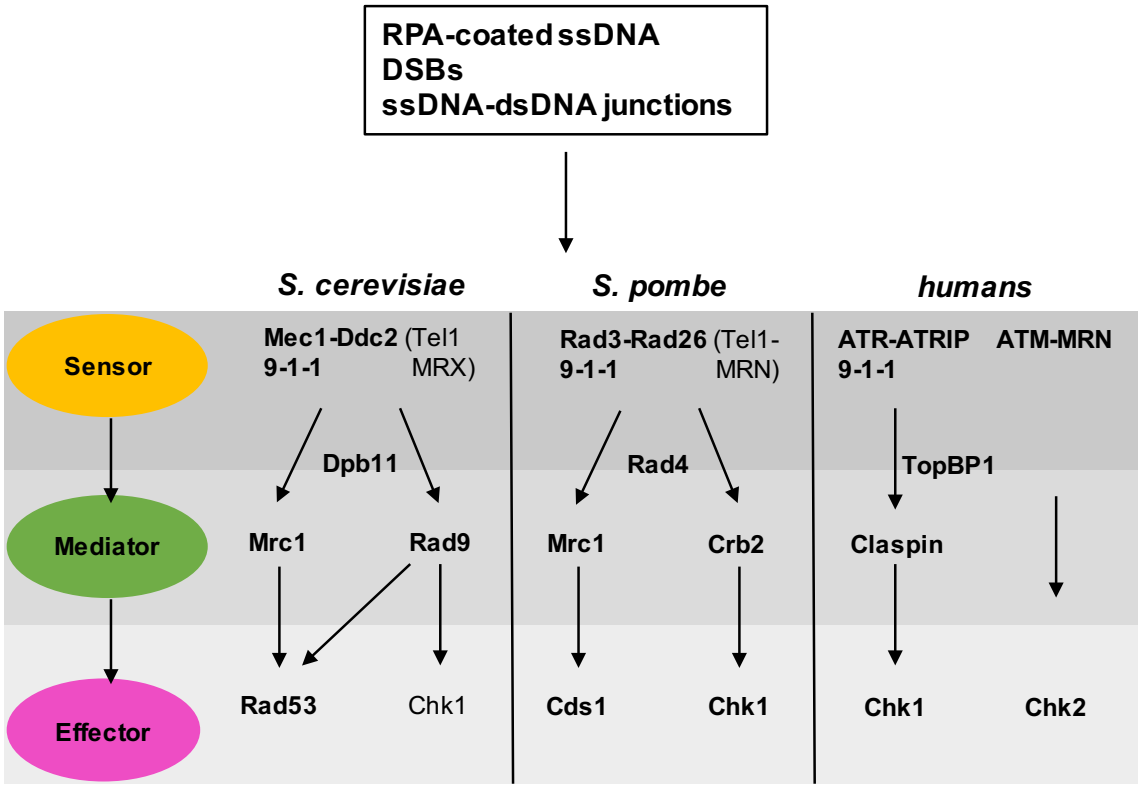

Figure 1.15: A general overview of checkpoint signalling.
Factors involved in DNA damage and replication checkpoints in humans, *S. pombe,* and *S. cerevisiae* are indicated. The main factors are shown in bold. In response to DNA damage or replication stress, RPA-coated ssDNA, dsDNA-ssDNA junctions and DSBs can be exposed. The checkpoint sensors identify these substrates, which, through mediators, activate effector kinases via phosphorylation events. The effector kinases transfer the signal to their target proteins and initiate the full checkpoint response.

1.3.2.2 Targets of the S Phase Checkpoint

The phosphorylation of Rad53 by Mec1 and the subsequent autophosphorylation results in various distinct responses including inhibition of origin firing, dNTP pool regulation, transcriptional response, fork stabilization and mitotic delay (Figure 1.17II).

1.3.2.2.1 Inhibition of Origin Firing

The Rad53 checkpoint kinase prevents the firing of later origins of replication in response to defects in DNA synthesis at forks from early origins, thus allowing the cell to avoid making more defective forks. In budding yeast, the treatment of

cells with HU or MMS impedes the activation of late and dormant origins, a process that is dependent on Mec1 and Rad53 (Paulovich and Hartwell, 1995, Santocanale et al., 1999, Santocanale and Diffley, 1998, Shirahige et al., 1998). Several studies have also revealed that activated Rad53 inhibits the firing of late origins through inhibitory phosphorylation of the two replication proteins, Sld3 and Dbf4. Therefore, cells that have Sld3 and Dbf4 but lack Rad53 phosphorylation sites can activate late origin firing in the presence of genotoxic drugs. The phosphorylation of Sld3 inhibits its interaction with the replication proteins, Dpb11 and Cdc45; the mechanism of inhibition of Dbf4 is currently unknown (Zegerman and Diffley, 2010, Duch et al., 2011, Lopez-Mosqueda et al., 2010). Thus, all origins are not fired at the time point of checkpoint activation; i.e. the firing of late and dormant origins is prevented through the above-described mechanism, which results in a decrease in the rate of S phase progression (Figure 1.17IIb) (Zegerman and Diffley, 2010).

1.3.2.2.2 dNTP Pool Regulation: an Essential Function for Cell Viability

A reduction in dNTP levels slows fork progression and induces chromosome instability. In budding yeast, one of the crucial roles of Mec1 and Rad53 is the generation of dNTPs to counteract the endogenous levels of DNA damage during the S phase. *MEC1* and *RAD53* genes are essential for cell viability even in the absence of exogenous sources of replication stress or DNA damage. Cells lacking these essential genes become viable when the ribonucleotide reductase inhibitor, Sml1, is inactivated or when other mechanisms to increase the level of dNTPs are activated (Zhao et al., 2001, Desany et al., 1998, Zhao et al., 1998). Rad53 phosphorylates the Rad53-related kinase, Dun1, which then phosphorylates Sml1 and Dif1; this in turn leads to their degradation in response to DNA damage and replication defects. Sml1 is also degraded in each round of the cell cycle when the cells enter the S phase. It should also be noted that the Mec1-Rad53-Dun1 pathway is crucial for the degradation of Sml1 in response to checkpoint activation; however, in the normal cell cycle, Rad53 and particularly Dun1 are less important for the downregulation of Sml1 (Figure 1.17IIc)

(Nordlund and Reichard, 2006, Zhao and Rothstein, 2002, Lee et al., 2008, Zhao et al., 2001, Zhao et al., 1998).

1.3.2.2.3 Transcriptional Response

Another process that is regulated by the S phase checkpoint is transcription. Activation of the DNA replication checkpoint results in replication fork stalling and therefore changes the transcription of a large number of genes. In such cases, specific pathways activate the transcription of genes that have essential roles in maintaining cell viability during DNA replication stress. For instance, Dun1 phosphorylates and inhibits the transcriptional repressor, Crt1, which leads to the upregulation of many genes involved in DNA repair and ribonucleotide biosynthesis (Huang et al., 1998). Indeed, the main function of Dun1 and the Dun1-dependent transcriptional response is to increase nucleotide levels. Similarly, along with Crt1, Rad53 phosphorylates the Swi6 subunits of the transcriptional activators, SBF and MBF, which leads to the upregulation of many repair and replication factors and genes essential for the G1/S transition (Figure 1.17IIc) (Zegerman and Diffley, 2009).

1.3.2.2.4 Fork Stabilization

One of the essential responses of the S phase checkpoint is to stabilize stalled forks to ensure their ability to restart after the replication block in budding yeast as well as in human cells (Figure 1.17IId), (Smith-Roe et al., 2013, Syljuasen et al., 2005). The completion of DNA replication in this situation depends on the checkpoint kinases, Mec1 and Rad53, as cells without these kinases cannot recover from a replication block and are arrested in the S phase. Stalled forks that cannot recover eventually collapse. Rad53 appears to inhibit this process in two distinct ways. First, replisome factors such as RPA, Mcm2-7, or polymerases are directly phosphorylated by Rad53; however, it is not clear as to how this contributes to fork stability (Hustedt et al., 2013, Zegerman and Diffley, 2009). Second, Rad53 also regulates the activities of nucleases such as the exonuclease Exo1; i.e. a major role of Rad53 is to downregulate Exo1 at arrested forks. This inhibits the creation of aberrant structures such as reversed forks,

which are also known as the “chicken foot” structure, at the replication fork. Indeed, the deletion of the nuclease Exo1 rescues the sensitivity of *rad53* mutants to the S phase-damaging agent, MMS, thus indicating that the inhibition of Exo1 by Rad53 promotes survival during replication stress (Segurado and Diffley, 2008). Thus, the role of a replication checkpoint is to maintain the stable association of replication polymerases at stalled forks and to inhibit the creation of reversed forks under replication stress (Hustedt et al., 2013).

1.3.2.2.5 Mitotic Delay

Another essential response of the S phase checkpoint is mitotic delay. In budding yeast, several processes that impede cells at the metaphase–anaphase transition or in the G2/M phase upon DNA damage and replicative stress have been identified (Figure 1.16; Figure 1.17IIe).

Several different pathways are activated by the S phase checkpoint and cause the stabilization of the securin Pds1. First, Rad53 inhibits the interaction between the APC/C activator, Cdc20, and Pds1, which is needed for Pds1 degradation. If this interaction fails to occur, it leads to the arrest of the cells at the metaphase-anaphase transition. Unfortunately, the molecular details of this inhibition are unclear so far. Furthermore, securin has been shown to inhibit separase (Esp1 in budding yeast), which is a protein responsible for cleaving cohesins. Cohesins are required to hold sister chromatids together and their stabilization prevents the metaphase-anaphase transition, i.e. the segregation of chromosomes (Harrison and Haber, 2006). In addition to Rad53, the kinase Chk1 is also a substrate of Mec1 and has been shown to stabilize Pds1 directly (Harrison and Haber, 2006, Liu et al., 2000b, Sanchez et al., 1999). Pds1 is also regulated by the spindle assembly checkpoint (SAC). Mec1 and Tel1 phosphorylate the SAC proteins, Mad1, Mad2, Mad3, Bub1, and Bub3, which leads to their activation; as a result, Cdc20 is inhibited (Kim and Burke, 2008). Thus, this pathway indicates another mechanism that ensures Pds1 stabilization in the presence of replication stress.

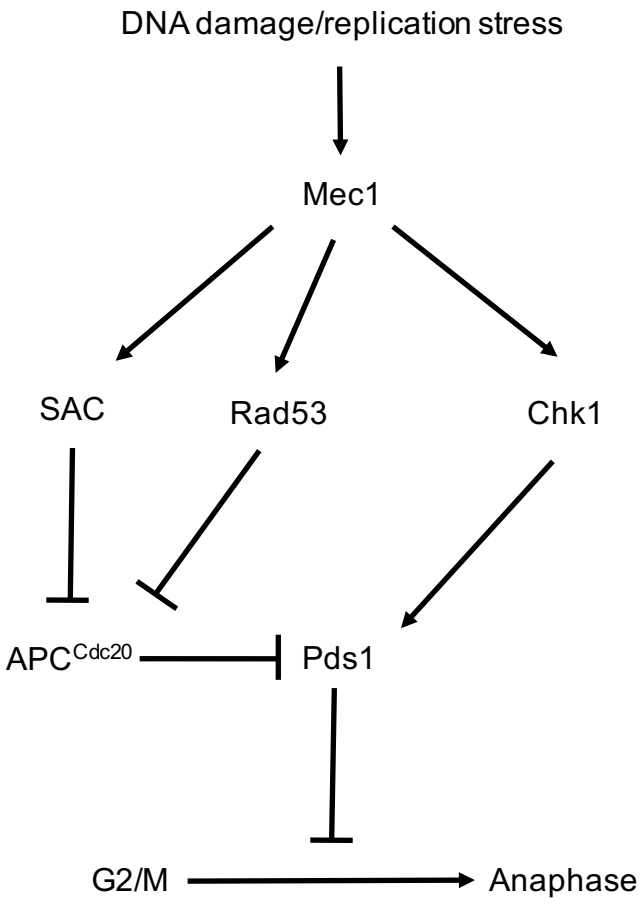

Figure 1.16: Mechanisms of mitotic delay upon DNA damage or replication stress.
DNA damage or replication stress leads to Mec1 activation. Mechanisms involving the stabilisation of Pds1 result in cell arrest at the metaphase–anaphase transition.

Finally, the checkpoint has to be inactivated in a process known as recovery in order to continue the cell cycle after the repair of DNA damage or the removal of other impediments to the fork. In budding yeast, recovery from the checkpoint is associated with de-phosphorylation and hence inactivation of Rad53 (Hustedt et al., 2013).

I

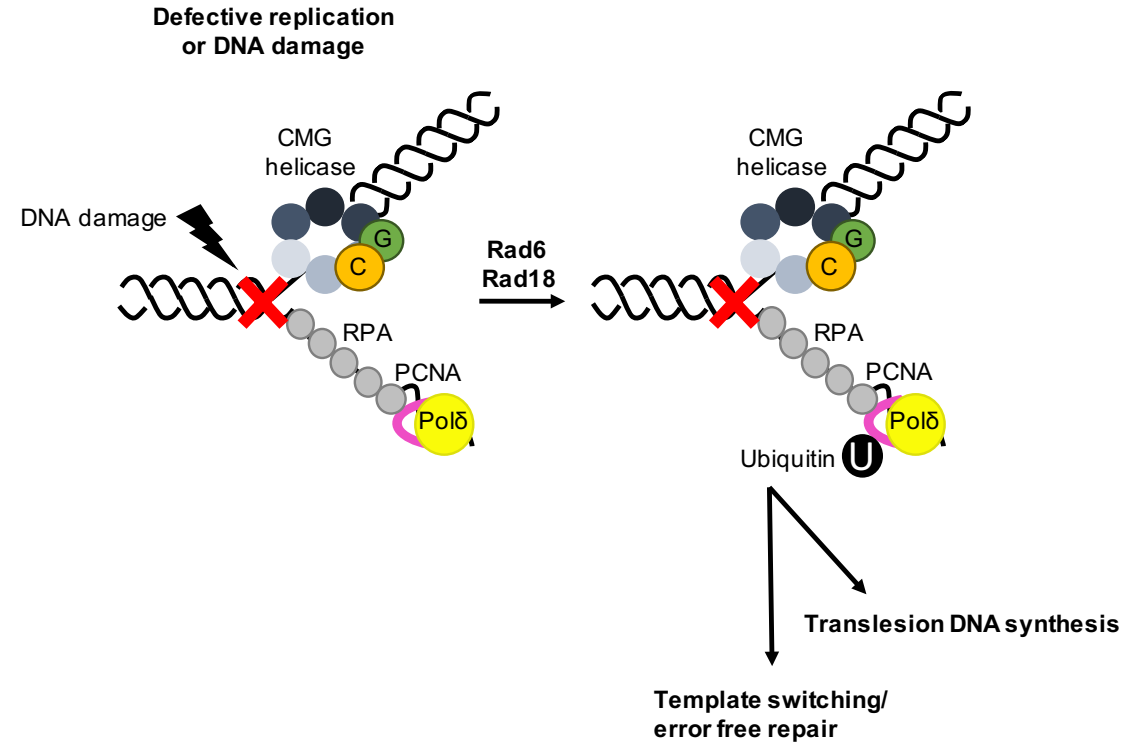
Defective replication
or DNA damage
CMG
helicase
DNA damage
G
C
RPA
PCNA
Polδ
Rad6
Rad18
CMG
helicase
G
C
RPA
PCNA
Polδ
Ubiquitin
U
Translesion DNA synthesis
Template switching/
error free repair

II

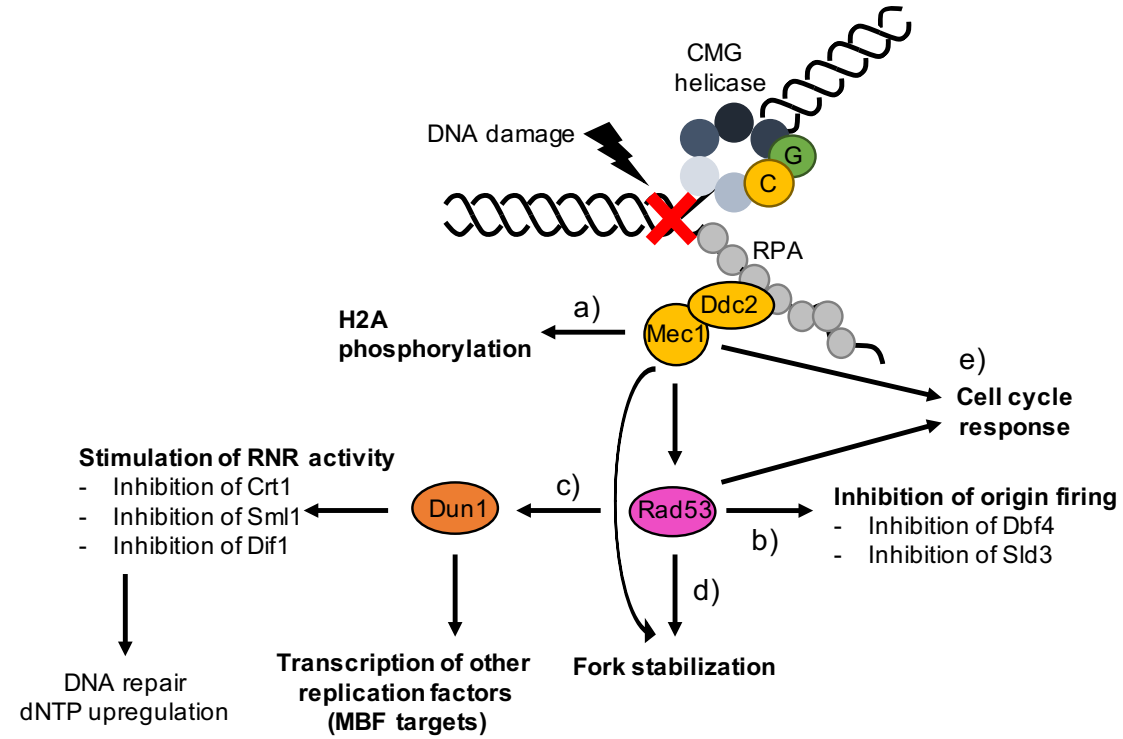
CMG
helicase
DNA damage
G
C
RPA
Ddc2
Mec1
a)
H2A
phosphorylation
e)
Cell cycle
response
Stimulation of RNR activity
- Inhibition of Crt1
- Inhibition of Sml1
- Inhibition of Dif1
Dun1
c)
Rad53
b)
Inhibition of origin firing
- Inhibition of Dbf4
- Inhibition of Sld3
d)
DNA repair
dNTP upregulation
Transcription of other
replication factors
(MBF targets)
Fork stabilization

Figure 1.17: Replication defects lead to ssDNA exposure at forks and therefore cause accumulation of RPA.
I) This causes ubiquitylation of PCNA, which can activate translesion DNA synthesis as well as an error-free repair pathway. **II**) Accumulation of RPA also leads to the S phase checkpoint activation and triggers a pathway involving the central kinases, Mec1 and Rad53. Amongst several responses, Mec1 (together with Tel1, not shown) phosphorylates the core histone H2A to form γH2A (**a**). Rad53 inhibits Sld3 and Dbf4 in order to prevent the firing of late origins (**b**), induces the upregulation of many genes involved in DNA repair, nucleotide biosynthesis, and cell cycle regulation (**c**), stabilizes forks (**d**), and induces cell cycle responses by various mechanisms as explained in the text (**e**). Figure adapted from (Bell and Labib, 2016).

1.3.3 Repair of DNA DSBs

DSBs can occur in numerous ways during replication, such as when the replication machinery is dissociated at a stalled fork, which leads to fork collapse and the formation of a one-ended DSB. Two main pathways facilitate the repair of DSBs: non-homologous end joining (NHEJ) and homologous recombination (HR). NHEJ operates through the actions of the Ku proteins, in which the proteins are required to protect the ends of the DSB and recruit the DNA-PK catalytic subunit to generate the heterotrimeric DNA-PK holoenzyme. The final ligation is mediated by the Lig4-Lif1 complex. In this pathway, the two ends formed by the DSB are simply religated; hence, this process is more error-prone, because the ends are sometimes processed before the ligation, which results in the addition or loss of nucleotides (Aylon and Kupiec, 2004, Abbas et al., 2013). In HR, the homologous sister chromatid is used as a template to repair the damaged DNA; therefore, HR is much less error prone. HR begins by the resection of 5' ends and therefore forms 3' overhangs. The protein RPA coats the formed ssDNA, and RPA is subsequently replaced by Rad51. The Rad51-coated ssDNA tail is known as the Rad51 nucleoprotein filament, which invades the undamaged sister chromatid while looking for sequence homology. After the invasion, the filament pairs with the complementary strand, the opposite strand of the DNA duplex is displaced to generate a single-stranded displacement loop known as a D-loop, and DNA polymerase extends the invading end using the sister chromatid as a template. A Holliday junction is created, and depending on how it is resolved, HR leads to either non-crossover events (preferred during the repair of DSBs) or crossover events. In non-crossover events, DNA repair enzymes extend the 3' end of the invading strand on the homologous template, but the invading strand eventually dissociates and returns to the chromatid from which it came and acts as template for the repair of the other broken strand. In crossover events (common during meiosis), the chromosomal information is exchanged (Abbas et al., 2013, Aylon and Kupiec, 2004). NHEJ tends to take place in the G1 phase, although it is active during the rest of the cell cycle. However, HR operates in the late-S and G2 phases of the cell cycle, as a sister chromatid template has to be available for this pathway (Abbas et al., 2013).

1.4 DNA Replication/DNA Catenane Formation

Topological stress is a serious problem caused by the double helical nature of the DNA; therefore, it is crucial to remove the topological problem of separating the two DNA strands in order to allow duplication and segregation of the genetic code to the daughter cells. Two steps are involved in this process: first, the hydrogen bonds between the two strands need to be disrupted, which is carried out by enzymes known as DNA helicases (reviewed by Lohman, 1993). Second, all the topological links between the two strands have to be eliminated, and this is carried out by DNA topoisomerases (reviewed by Wang, 1996). This indicates that DNA helicases and topoisomerases are both essential for the swivel mechanism for DNA replication; This was suggested for the first time by Cairns (Cairns, 1963). The topological constraint observed in most studies so far are relevant in both prokaryotic and eukaryotic systems. Although replication in eukaryotes is more complicated, the same topological effects will take place (Bates and Maxwell, 2005). As explained in section 1.2.2, DNA replication is divided into three steps: initiation, elongation and termination. In the next section, I will describe the effect of topological changes in each of these steps of DNA replication.

1.4.1 Replication Initiation

Replication initiation requires negatively supercoiled DNA, which is the responsibility of DNA gyrase in bacteria (Smelkova and Marians, 2001). The same phenomena were also observed in yeast autonomously replicating sequences (ARS), in which the efficiency of DNA unwinding is maximum when the DNA is negatively supercoiled (Umek and Kowalski, 1988). It appears that DNA topoisomerases are not involved directly in the initiation of DNA replication, but their presence might be essential to maintain the DNA in a negatively supercoiled state prior to initiation (Bates and Maxwell, 2005).

1.4.2 Replication Elongation: Removing DNA Linkages during DNA Replication through the Relaxation of Positive Supercoiling

As replication proceeds, twisting tension builds up in front of the fork due to the action of helicases, which leads to the formation of positive supercoils ahead of the elongating replication fork. If left unresolved, this tension will ultimately stop DNA replication (Brill et al., 1987, Bermejo et al., 2007). Two pathways can be used to resolve the single-stranded intertwines in the parental DNA.

In *E. coli,* DNA gyrase has been shown to be required for preserving the negative supercoiled state of the chromosome (Champoux, 2001). DNA gyrase functions ahead of the replication fork and removes positive supercoils by directly converting positive supercoils into negative supercoils (Levine et al., 1998, Wang, 2002). However, this enzyme cannot decatenate replicated DNA molecules (Zechiedrich and Cozzarelli, 1995). Positive supercoils generated ahead of the fork in *E. coli* can also be resolved directly by the action of topo IV, particularly when gyrase is not active (Khodursky et al., 2000). In eukaryotes, positive supercoils generated ahead of the fork can be resolved either by type IB DNA topoisomerases (e.g. Top1 in budding yeast) or by type II enzymes (e.g. Top2 in yeast) (Figure 1.18A) (Postow et al., 2001a, Wang, 2002).

In the second pathway suggested by Champoux and Been, the positive supercoils formed ahead of the fork by the action of helicase may diffuse to behind the fork due to the rotation of the fork to cause intertwining of the daughter duplexes. These intertwinings generated by fork rotation are known as ‘pre-catenanes’. Therefore, as a result of fork rotation, the tension ahead of the fork is resolved and results in DNA pre-catenation behind the fork. The pre-catenane nodes, if not resolved, will lead to a physical link between the sister chromatids, which will inhibit their accurate segregation during mitosis (Champoux and Been, 1980, Wang, 2002, Postow et al., 2004). As explained earlier, the resolution of DNA catenanes formed by fork rotation requires the decatenation activity of type II topoisomerases (Figure 1.18B), which will be explained in further detail in the

following sections.

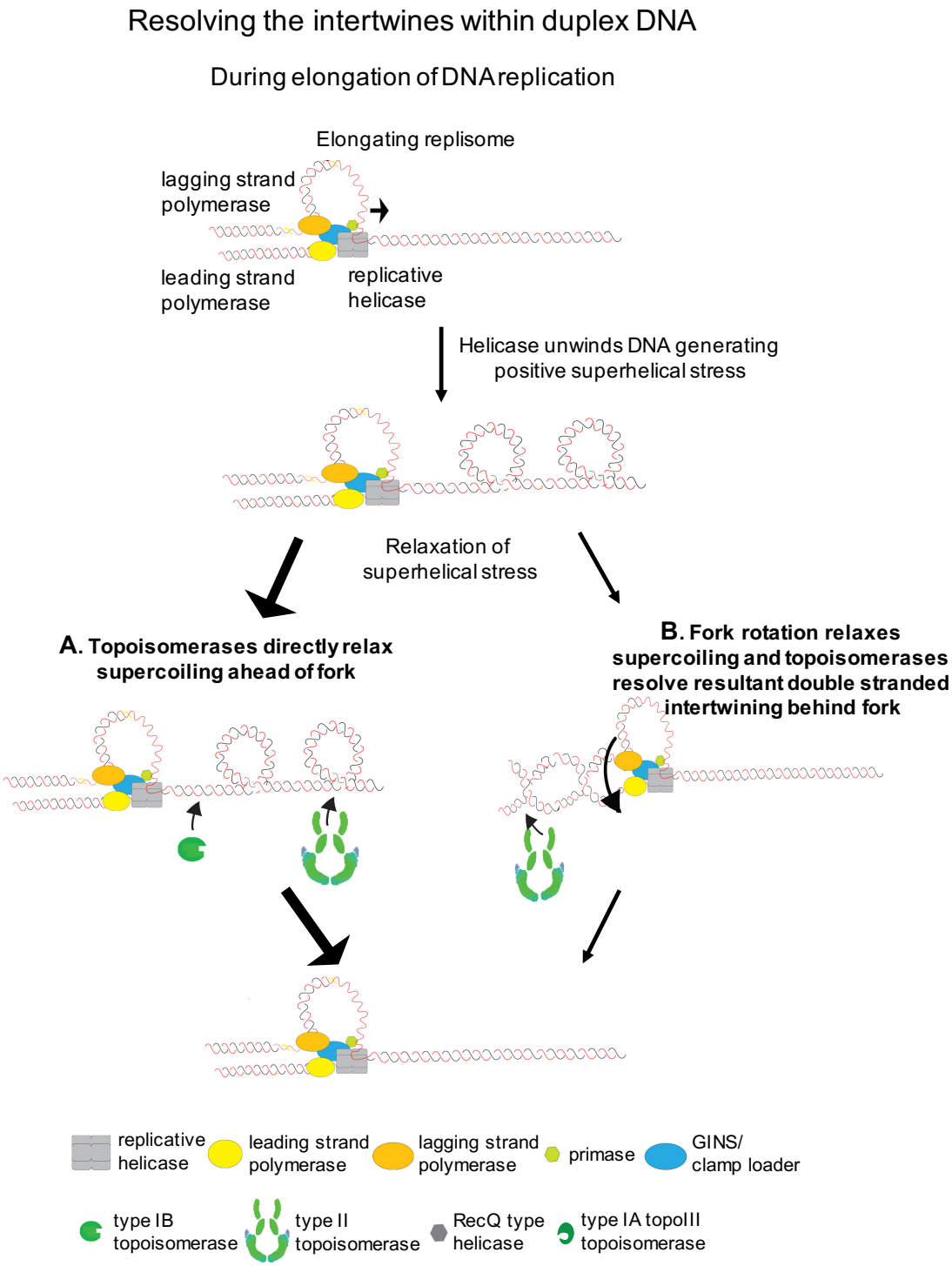

Figure 1.18: Model of topological stress generation and relaxation during elongation of DNA replication.
A) First model for the topology of a replicating chromosome. During DNA replication, the action of helicase on DNA forms positive superhelical stress on the DNA. This leads to the formation of positive supercoils in front of the fork. This tension is normally resolved by the action of either a type IB topoisomerase (e.g. eukaryotic topoisomerase I) or a type II topoisomerase (e.g. eukaryotic topoisomerase II). **B**) Second model for the topology of a replicating chromosome. During DNA replication, the superhelical tension generated ahead of the fork is relaxed by rotation of the fork to form catenated DNA sister chromatid intertwines behind the fork. It is crucial that type II topoisomerases resolve all DNA catenation before cell division is completed. Figure taken from (Baxter, 2015).

1.4.3 Replication Termination

Two pathways exist to resolve the linkages between the DNA duplex during DNA replication: 1. direct relaxation of positive supercoiling by topoisomerases and 2. fork rotation and decatenation of the pre-catenated intertwines generated. The preference for which pathway is used during DNA replication is not clear, except during the termination phase of DNA replication. Sundin and Varshavsky used culture conditions for SV40 to prevent decatenation activity and showed that sister chromatid intertwines appear during termination of replication (Sundin and Varshavsky, 1980, Sundin and Varshavsky, 1981). This is consistent with the idea that as replication forks converge at replication termination, the length of the unreplicated DNA continues to become shorter, until finally, there is little room for containing the positive supercoils formed in front of the fork and for their removal by topoisomerases (Figure 1.19). A solution to this issue is the effective conversion of positive superhelical tension in front of the fork to positive superhelical tension behind the fork. To do this, the replication fork needs to be rotated in order to generate dsDNA sister chromatid intertwines in the newly replicated DNA behind the fork. However, as mentioned above, these intertwinings or ‘pre-catenanes’ will become proper catenanes if they are not removed before the completion of DNA replication (Figure 1.19) (Sundin and Varshavsky, 1980, Sundin and Varshavsky, 1981, Postow et al., 2001a).

DNA catenation can be resolved by type I or type II topoisomerases. However, overwhelmingly, it appears that type II topoisomerase are required in resolving

DNA catenanes *in vivo*. In *E. coli*, topo IV is the primary enzyme required to remove dsDNA pre-catenanes produced in the newly replicated DNA by fork rotation (Zechiedrich and Cozzarelli, 1995, Hiasa and Marians, 1996, Crisona et al., 2000). When *E. coli* is depleted of topo IV, DNA catenanes accumulate on a plasmid (Zechiedrich and Cozzarelli, 1995); this is consistent with the findings of Sundin and Varshavsky (Sundin and Varshavsky, 1980, Sundin and Varshavsky, 1981). Potentially, type IA enzymes such as topo III can also resolve pre-catenanes behind the fork before the ligation of Okazaki fragments. To do this, topo III has to act near or at the point of nascent DNA synthesis, where there is a single-stranded template DNA available for it to bind to. Thus, topoisomerase III in *E. coli* can decatenate replication products, but only when at least one of the products has a single-stranded break (Nurse et al., 2003, Perez-Cheeks et al., 2012).

In eukaryotes, type II topoisomerases are essential for resolving the intertwines generated by fork rotation (Holm et al., 1985, Lucas et al., 2001, Baxter and Diffley, 2008). For instance, a study on plasmid replication in *Xenopus* cell extracts showed that the inhibition of type II topoisomerases during plasmid replication causes the accumulation of highly linked replication intermediates; therefore, Top II is required for resolving daughter chromosomes during DNA replication (Lucas et al., 2001). In budding yeast, inactivation of topoisomerase II causes the accumulation of catenanes of a closed-circular plasmid, which suggests that this enzyme is crucial for chromosome segregation after the termination of replication, similar to that observed in SV40 or *E. coli* (Baxter and Diffley, 2008). Further findings also indicate that Top II is also required during mitosis in *S. pombe*, further supporting the fact that the enzyme plays a role in chromosome segregation (Bates and Maxwell, 2005). Failure to resolve all DNA catenanes between sister chromatids leads to chromosome bridging, nondisjunction, and aneuploidy (Baxter, 2015).

Generation of DNA catenations at the termination of DNA replication

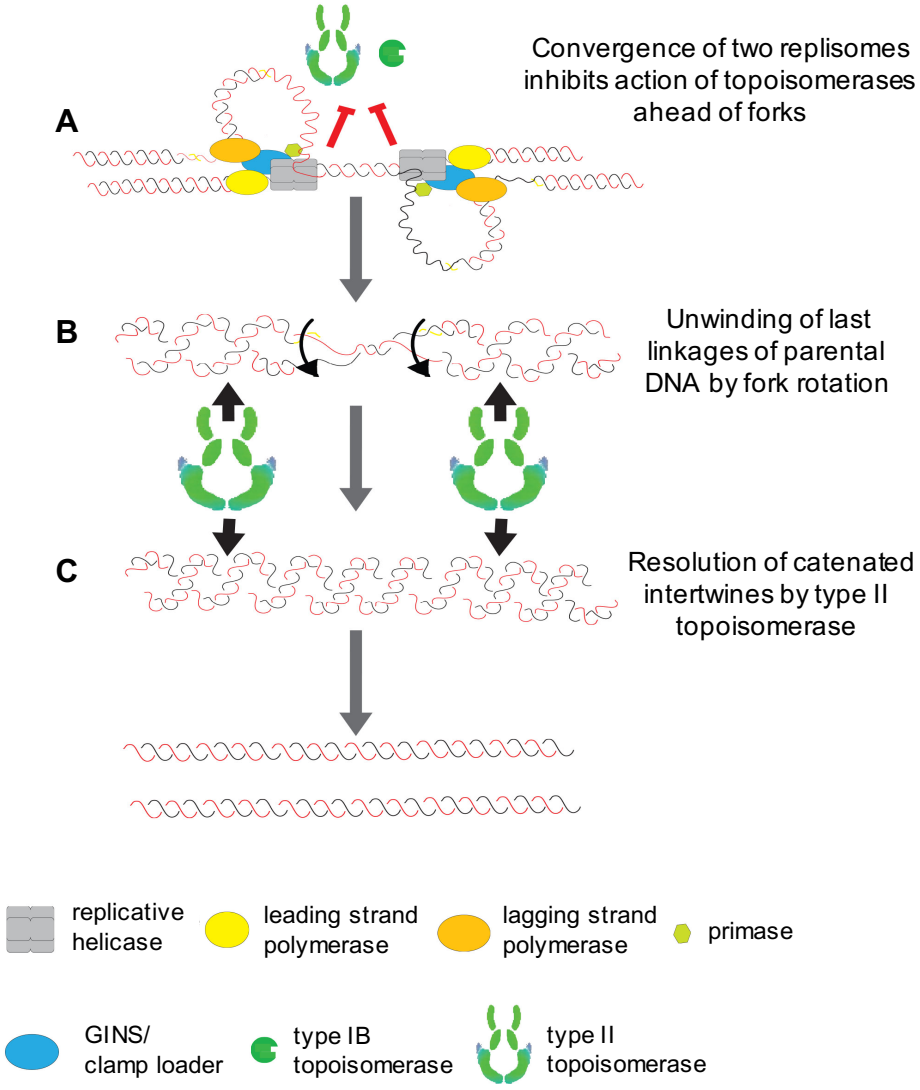

Figure 1.19: Generation of DNA catenanes at the termination of replication. At the termination of replication, converging replication forks (**A**) cause the intertwining of daughter molecules and the creation of pre-catenanes (**B**). Upon completion of DNA replication, catenated DNA molecules are formed (circles) (**C**). Figure taken from (Baxter, 2015).

1.4.4 Sterical Impediments to Replication Increase Topological Stress and Fork Rotation

There is a lot of evidence indicating that topological stress can also occur in the DNA template during transcription events, like in DNA replication. During transcription, the DNA template has to be pulled apart in order for the RNA polymerase holoenzyme to access the coding strand and produce nascent transcripts. DNA unwinding by a transcribing polymerase forms positive supercoiling ahead and negative supercoiling behind the transcription bubble. This model is known as the twin supercoiled domain model (Figure 1.20A) (Liu and Wang, 1987). In this case, it is important for DNA topoisomerases to be able to resolve the formed torsional stress, failing which the transcription can be inhibited due to the accumulation of positive helical stress ahead of the RNA polymerase. Studies in budding yeast have shown that topoisomerases are more active at highly expressed genes such as rRNA genes (Brill et al., 1987) and at long genes (Joshi et al., 2012). This suggests that more topological stress is created at genes that need the action of topoisomerases to relax the formed stress. RNA transcription is potentially one of the most important obstacles for DNA replication. In this case, as the replication machinery approaches the transcription bubble, topological stress seems to build up between the converging replication and transcription sites. The predicted reason for the increased topological stress is that, analogous to the termination of DNA replication, the function of topoisomerases is limited between the converging replication and transcription machineries; therefore, fork rotation and DNA pre-catenation remain potentially the sole pathways to facilitate DNA unwinding (Figure 1.20B) (Keszthelyi et al., 2016). We know that DNA catenation caused by fork rotation cannot be directly observed on endogenous chromosomes, unlike in plasmids. However, surprisingly, Jeppsson et al. (2014) used chromatin immunoprecipitation (ChIP) analysis and identified that, in the absence of Top2, SMC5/6 (marker of double-stranded intertwining *in vivo*) in eukaryotes is enriched at sites of converging genes, i.e. when the occurrence of DNA replication is through transcription sites (Jeppsson et al., 2014). These data suggest that increase in fork rotation at these sites is because of the collisions between the

head-on replication and transcription machineries. Thus, fork rotation and DNA catenation appear to be context dependent in situations where the action of topoisomerases ahead of the fork is inhibited. Wherever fork rotation is required, it is crucial that every catenane formed between the sister chromatids is resolved to allow faithful segregation of chromosomes into the daughter cells.

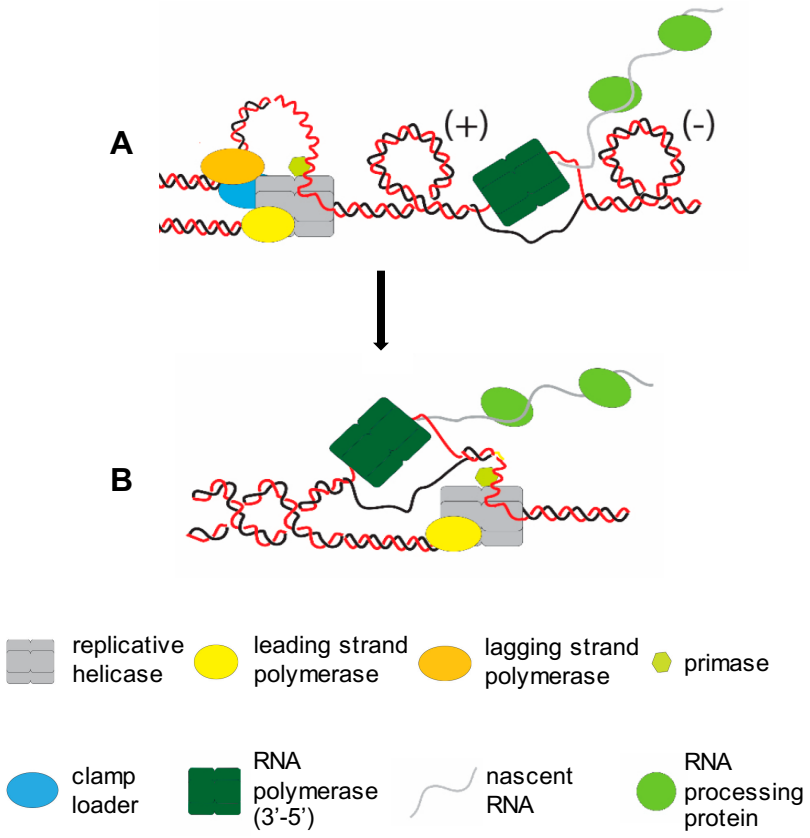

Figure 1.20: Hypothetical model for the generation of DNA catenanes when the DNA replication machinery converges at the transcription bubble.
At the head-on replication and transcription sites, converging replication and transcription machineries may potentially cause the intertwining of daughter molecules and create pre-catenanes. Figure taken from (Keszthelyi et al., 2016).

A study in budding yeast revealed that overexpression of inactive topoisomerase II during DNA replication enhances the frequency of fork rotation and DNA catenation on a plasmid substrate (Baxter and Diffley, 2008). Although all decatenation activity had been prevented, the presence of inactive topoisomerase in the cell (that can bind to but not break DNA) somehow increased fork rotation. One possible explanation for the increased fork rotation is that the DNA-bound inactive topoisomerase inhibits the binding of other active

topoisomerases ahead of the fork, which increases the frequency of fork rotation and DNA catenation on replicated plasmids. This is consistent with the mechanism observed at termination (Baxter and Diffley, 2008) and suggests that protein-DNA complexes might also induce topological barriers, which can be overcome by fork rotation.

1.4.5 Effect of Replisome Structure on DNA Catenation

It has been predicted that *in vivo* fork rotation and DNA catenation is more frequent in cases of a minimal replisome (Figure 1.21A), Whereas the eukaryotic replisome holoenzyme consists of many non-core proteins associated with it, such as the cohesion- establishment machinery, the ctf4 trimer, the replication fork protection complex and histone deposition proteins. Therefore, in this case, the frequency of fork rotation and DNA catenation is expected to be low *in vivo* (Figure 1.21B). The resistance to rotation is also expected to be higher in eukaryotes than in prokaryotes (reviewed by Baxter, 2015). Therefore, *in vivo*, except under particular chromosomal contexts such as termination of DNA replication or potentially at head-on DNA replication-transcription collisions where DNA catenation is more favourable, the preferential pathway for removing the topological stress during DNA replication is likely to involve the action of topoisomerases ahead of the fork instead of for fork rotation and DNA catenation (Baxter, 2015, Keszthelyi et al., 2016).

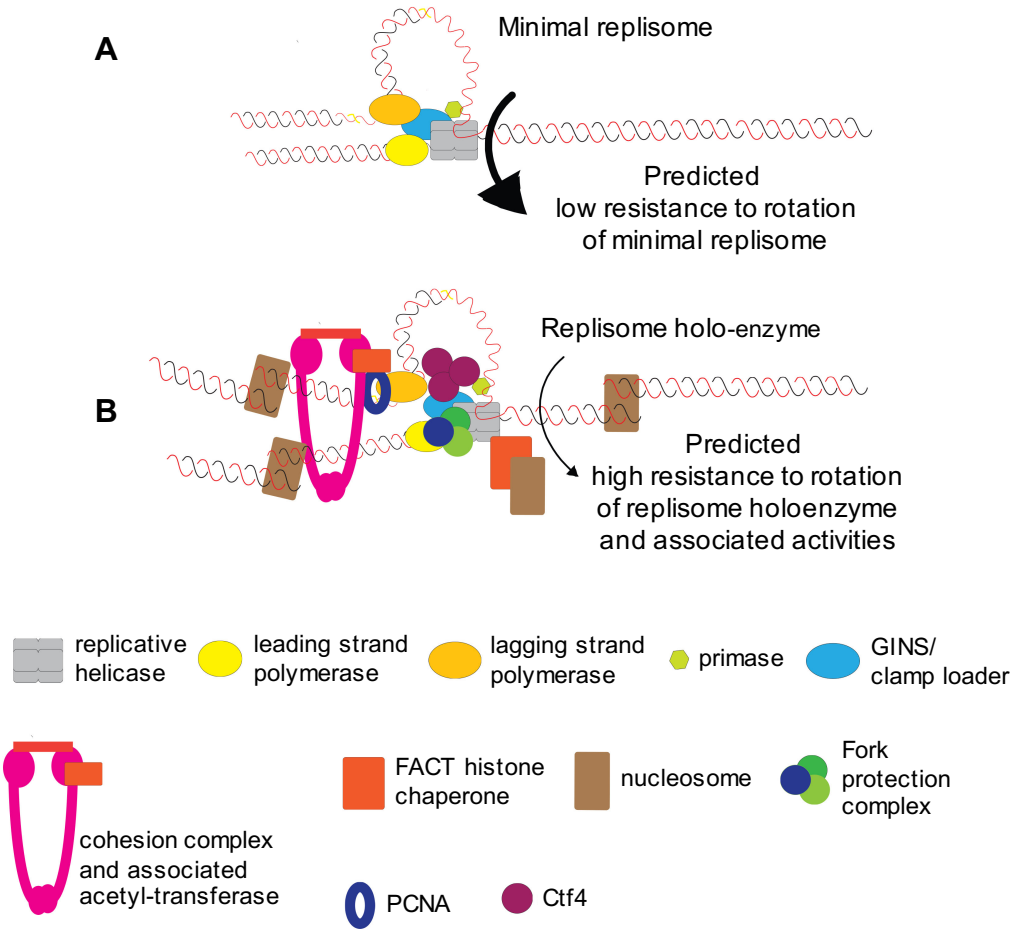

Figure 1.21: Resistance to rotation is likely to increase with increasing complexity of the holo-replisome complex.
This figure was taken from (Baxter, 2015).

1.5 Work Presented in this Thesis

The double-helical nature of the DNA generates a special set of problems for processes that require strand unwinding, such as replication. Therefore, it is crucial that the two strands of the template DNA double helix are entirely unwound and that all of the intertwining between the strands is removed. This DNA unwinding forms positive supercoils ahead of the replication fork, which have to be removed by the direct action of topoisomerases on the overwound region ahead of the fork or need to be transferred to behind the fork due to the rotation of the fork to cause intertwining of the daughter duplexes. Moreover, these intertwinings have to be completely unlinked (decatenated) for chromosome segregation by the action of type II topoisomerases (Baxter, 2015, Brill et al., 1987, Bermejo et al., 2007, Champoux and Been, 1980, Bermejo et al., 2012). In certain contexts, such as during termination, the ability of topoisomerases to function ahead of the replication fork is limited. Therefore, the topological stress created ahead of the fork is transferred to behind the fork by fork rotation, which creates pre-catenanes that become catenated daughter DNA molecules upon the completion of replication. These catenations also need to be resolved by type II topoisomerases (Sundin and Varshavsky, 1980, Sundin and Varshavsky, 1981). Moreover, *in vitro* studies have indicated that fork rotation seems to be a frequent event during replication elongation, which helps ongoing replication and results in extensive pre-catenation behind the elongating forks (Hiasa et al., 1994, Lucas et al., 2001, Peter et al., 1998). Such pre-catenation potentially braids the newly replicated DNA. The eukaryotic replisome holoenzyme, unlike viral replisomes and replication complexes established in *in vitro* systems, consists of many proteins whose activities appear to facilitate replication and coordinate DNA synthesis with other processes such as Okazaki fragment maturation, cohesion establishment, and chromatin assembly. So far, it remains elusive whether these activities happening in the wake of the fork are inhibited by pre-catenation.

In this thesis, I have directly assessed fork rotation and DNA pre-catenation in budding yeast. In the first part, Chapter 3, I investigated when pre-catenation occurs during DNA replication. In Chapter 4, I aimed to examine the architectural

replisome factors that could be important in determining how often the replisome rotates. Therefore, I studied how the deletion of replisome-associated factors alters fork rotation under topological stress. In the fifth chapter, I assessed the phenotype observed in the absence of *MRC1* in further detail and then investigated if the phenotype observed is associated with the replication function of *MRC1* or with its checkpoint function. Interestingly, in the fourth chapter, I found that some of the architectural replisome factors appear to influence fork rotation during elongation and that these factors are associated with both full replication and checkpoint signalling following replication stress. Therefore, in Chapter 6, I investigated the influence of checkpoint activation and checkpoint kinases on fork rotation on plasmid replicons. Furthermore, since the deletion of all these factors leads to DNA damage in the S phase, in the seventh chapter, I examined how the regulation of fork rotation could be important for genome stability.

Chapter 2

Materials and Methods

2.1 Methods for Yeast Experiments

2.1.1 Yeast Media

Yeast was grown in autoclaved YP medium supplemented with 2% glucose (YPD) unless otherwise stated (Table 2.1). To select for the marker genes *URA3*, *TRP1*, *HIS3* or *LEU2*, minimal medium or synthetic complete medium lacking the relevant amino acid was used (Table 2.1). Yeast cells were also grown on media containing 100 µg/ml nourseothricin, 300 µg/ml hygromycin B, or 200 µg/ml geneticin G418 to select for strains carrying the respective resistance gene. For long-term storage, a saturated culture was mixed with 15% glycerol and stored at -80°C. For short-term storage, the yeast cells were kept on a plate at 4°C. A list of the media used in this study is shown in Table 2.1.

Table 2.1: Yeast media used in this study.

Media	Composition
YPDA	2% peptone (Melford), 1% yeast extract (Melford), 2% agar. Glucose (Fisher Scientific) was filter-sterilised and added after autoclaving to a final concentration of 2%. Adenine sulphate (Formedium) was also added at a final concentration of 0.8%. For liquid medium (YP), the agar was left out.
YPRGA	2% peptone, 1% yeast extract. Raffinose (Sigma) and galactose (Sigma-Aldrich) were filter-sterilised and added to a final concentration of 2%. Adenine sulphate was also added at a final concentration of 0.8%.
Synthetic complete media (per 0.5 L)	400 ml of autoclaved ddH_2O containing 50 ml of 10X Yeast Nitrogen Base (YNB) (Melford) without amino acids and 0.96 g yeast synthetic drop-out medium supplements without the relevant amino acid (Sigma). Glucose was added to a final concentration of 2%.
Minimal medium (per 0.5 L)	400 ml of autoclaved ddH_2O containing 2% agar, 50 ml of 10X Yeast Nitrogen Base (YNB) without amino acids, and the following ingredients as required: 4 ml adenine sulphate 5 mg/ml, 10 ml uracil 2 mg/ml, 4 ml leucine 10 mg/ml, 10 ml tryptophan 2 mg/ml, 2 ml histidine 10 mg/ml. Glucose was

	added to a final concentration of 2%. For liquid medium, the agar was left out.
Amino acid stock	5 mg/ml adenine sulphate, 2 mg/ml uracil, 10 mg/ml histidine, 10 mg/ml leucine, 2 mg/ml tryptophan in Milli-Q water. Filter-sterilized.
RSM medium (per 0.5 L)	400 ml of 8.0 g agar, 0.4 g glucose, 6.0 g of potassium acetate, and 1.0 g of yeast extract in autoclaved ddH_2O, 10 ml of sterile filtered amino acid stock was added.
YPD NAT (Nourseothricin - Jena Bioscience, AB-102L)	YPD containing NAT at a final concentration of 100 µg/ml.
YPD G418 (Geneticin Disulphate - Melford, G0175)	YPD containing G418 at a final concentration of 200 µg/ml.
YPD Hygromycin B (Invitrogen)	YPD containing hygromycin B at a final concentration of 300 µg/ml.
Doxycycline (Sigma)	Made up to 50 mg/ml freshly in ddH_2O.

2.1.2 Yeast Strains

The yeast strains used in this study are based on W303 *ade2-1 his3-11 leu2-3 trp1-1 ura3-1 can1-100* and are listed in Table 2.2.

Table 2.2: Yeast strains used in this study.

Strain	Relevant genotype	Source
JB1	*MATa ade2-1 his3-11 leu2-3 trp1-1 ura3-1 can1-100*	JB lab
JB2	*MATα ade2-1 his3-11 leu2-3 trp1-1 ura3-1 can1-100*	JB lab
JB8	*MATa ade2-1 his3-11 leu2-3 trp1-1 ura3-1 can1-100* *UBR1::GAL1-10-Ubiquitin-M-LacI fragment-Myc-UBR1 (HIS3)* *leu2-3::pCM244 (CMVp-tetR'-SSN6, LEU2) x3* *top2-td TOP2 5' upstream -100 to -1 replaced with kanMX-tTA (tetR-VP16) - tetO2 - Ub - DHFRts - Myc - linker*	JB lab
JB11	*MATa ade2-1 his3-11 leu2-3 trp1-1 ura3-1 can1-100* *UBR1::GAL1-10-Ubiquitin-M-LacI fragment-Myc-UBR1 (HIS3)* *leu2-3::pCM244 (CMVp-tetR'-SSN6, LEU2) x3*	JB lab
JB13	*MATa ade2-1 his3-11 leu2-3 trp1-1 ura3-1 can1-100* *UBR1::GAL1-10-Ubiquitin-M-LacI fragment-Myc-UBR1 (HIS3)* *leu2-3::pCM244 (CMVp-tetR'-SSN6, LEU2) x3* *top2-td TOP2 5' upstream -100 to -1 replaced with kanMX-tTA (tetR-VP16) - tetO2 - Ub - DHFRts - Myc – linker* *pRS316*	JB lab
JB275	*MATa his4-539 lys2-801 ura3-52* *top2-4* *pRS316*	JB lab
JB379	*MATa ade2-1 his3-11 leu2-3 trp1-1 ura3-1 can1-100* *UBR1::GAL1-10-Ubiquitin-M-LacI fragment-Myc-UBR1 (HIS3)* *leu2-3::pCM244 (CMVp-tetR'-SSN6, LEU2) x3* *top2-td TOP2 5' upstream -100 to -1 replaced with kanMX-tTA (tetR-VP16) - tetO2 - Ub - DHFRts - Myc - linker* *tof1Δ::hphNT1*	JB lab
JB381	*MATa ade2-1 his3-11 leu2-3 trp1-1 ura3-1 can1-100* *UBR1::GAL1-10-Ubiquitin-M-LacI fragment-Myc-UBR1 (HIS3)* *leu2-3::pCM244 (CMVp-tetR'-SSN6, LEU2) x3*	JB lab

	tof1Δ::hphNT1	
JB393	*MATa ade2-1 ura3-1 his3-11,15 trp1-1 leu2-3,112 can1-100* *UBR1::GAL1-10-Ubiquitin-M-LacI fragment-Myc-UBR1 (HIS3)* *leu2-3::pCM244 (CMVp-tetR'-SSN6, LEU2) x3* *mrc1Δ::URA3*	JB lab
JB395	*MATa ade2-1 ura3-1 his3-11,15 trp1-1 leu2-3,112 can1-100* *UBR1::GAL1-10-Ubiquitin-M-LacI fragment-Myc-UBR1 (HIS3)* *leu2-3::pCM244 (CMVp-tetR'-SSN6, LEU2) x3* *top2-td TOP2 5' upstream -100 to -1 replaced with kanMX-tTA (tetR-VP16) - tetO2 - Ub - DHFRts - Myc - linker* *mrc1Δ::URA3*	JB lab
JB479	*MATa his4-539 lys2-801 ura3-52* *top2-4*	JB lab
JB484	*MATa his4-539 lys2-801 ura3-52* *top2-4* *3x tRNA-pRS316*	JB lab
JB578	*MATa his4-539 lys2-801 ura3-52* *top2-4* *pRS426*	JB lab
JB617	*MATa his4-539 lys2-801 ura3-52* *top2-4 mrc1Δ::natNT2* *pRS426*	This study
JB618	*MATa his4-539 lys2-801 ura3-52* *top2-4 mrc1Δ::natNT2* *pRS316*	This study
JB619	*MATa his4-539 lys2-801 ura3-52* *top2-4 mrc1Δ::natNT2* *tRNA-pRS316*	This study
JB625	*MATa ade2-1 ura3-1 his3-11,15 trp1-1 leu2-3,112 can1-100* *UBR1::GAL1-10-Ubiquitin-M-LacI fragment-Myc-UBR1 (HIS3)* *leu2-3::pCM244 (CMVp-tetR'-SSN6, LEU2) x3* *top2-td TOP2 5' upstream -100 to -1 replaced with kanMX-tTA (tetR-VP16) - tetO2 - Ub - DHFRts - Myc - linker* *tof1Δ::hphNT1* *pRS316*	This study
JB631	*MATa his4-539 lys2-801 ura3-52*	This study

	top2-4 csm3Δ::natNT2 *pRS316*	
JB637	*MATa his4-539 lys2-801 ura3-52* *top2-4 ctf4Δ::natNT2* *pRS316*	This study
JB638	*MATa his4-539 lys2-801 ura3-52* *top2-4 ctf4Δ::natNT2* *tRNA-pRS316*	This study
JB664	*MATa his4-539 lys2-801 ura3-52* *top2-4 ctf18Δ::natNT2* *pRS316*	This study
JB665	*MATa his4-539 lys2-801 ura3-52* *top2-4 ctf18Δ::natNT2* *tRNA-pRS316*	This study
JB672	*MATa his4-539 lys2-801 ura3-52* *top2-4 chl1Δ::natNT2* *pRS316*	This study
JB674	*MATa his4-539 lys2-801 ura3-52* *top2-4 chl1Δ::natNT2* *tRNA-pRS316*	This study
JB680	*MATa his4-539 lys2-801 ura3-52* *top2-4 sml1Δ::natNT2* *pRS316*	This study
JB682	*MATa his4-539 lys2-801 ura3-52* *top2-4 sml1Δ::natNT2* *tRNA-pRS316*	This study
JB726	*MATa ade2-1 his3-11 leu2-3 trp1-1 ura3-1 can1-100* *UBR1::GAL1-10-Ubiquitin-M-LacI fragment-Myc-UBR1 (HIS3)* *leu2-3::pCM244 (CMVp-tetR'-SSN6, LEU2) x3* *top2-td TOP2 5' upstream -100 to -1 replaced with kanMX-tTA* *(tetR-VP16) - tetO2 - Ub - DHFRts - Myc - linker* *rad9Δ::natNT2 tof1Δ::hphNT1*	This study
JB760	*MATa his4-539 lys2-801 ura3-52* *top2-4 sml1Δ::natNT2 mec1Δ::hphNT1* *pRS316*	This study
JB762	*MATa his4-539 lys2-801 ura3-52*	This study

	top2-4 sml1Δ::natNT2 mec1Δ::hphNT1 *tRNA-pRS316*	
JB766	*MATa his4-539 lys2-801 ura3-52* *top2-4 sml1Δ::natNT2 rad53Δ::hphNT1* *pRS316*	This study
JB768	*MATa his4-539 lys2-801 ura3-52* *top2-4 sml1Δ::natNT2 rad53Δ::hphNT1* *tRNA-pRS316*	This study
JB774	*MATa ade2-1 his3-11 leu2-3 trp1-1 ura3-1 can1-100* *UBR1::GAL1-10-Ubiquitin-M-LacI fragment-Myc-UBR1 (HIS3)* *leu2-3::pCM244 (CMVp-tetR'-SSN6, LEU2) x3* *top2-td TOP2 5' upstream -100 to -1 replaced with kanMX-tTA (tetR-VP16) - tetO2 - Ub - DHFRts - Myc - linker* *trp1-1::TRP1 pFA6 GAL1 HATOP2Y-F (7M-6)* *pRS316*	JB lab
JB778	*MATa ade2-1 his3-11 leu2-3 trp1-1 ura3-1 can1-100* *UBR1::GAL1-10-Ubiquitin-M-LacI fragment-Myc-UBR1 (HIS3)* *leu2-3::pCM244 (CMVp-tetR'-SSN6, LEU2) x3* *top2-td TOP2 5' upstream -100 to -1 replaced with kanMX-tTA (tetR-VP16) - tetO2 - Ub - DHFRts - Myc - linker* *trp1-1::TRP1 pFA6 GAL1 HATOP2Y-F (7M-6)* *mrc1Δ::natNT2* *pRS316*	This study
JB813	*MATa ade2-1 his3-11 leu2-3 trp1-1 ura3-1 can1-100* *top2-4*	JB lab
JB898	*MATa his4-539 lys2-801 ura3-52* *top2-4 dpb3Δ::natNT2* *pRS316*	JB lab
JB902	*MATa his4-539 lys2-801 ura3-52* *top2-4 dpb3Δ::natNT2* *tRNA-pRS316*	JB lab
JB904	*MATa his4-539 lys2-801 ura3-52* *top2-4 pol32Δ::natNT2* *pRS316*	JB lab
JB908	*MATa his4-539 lys2-801 ura3-52* *top2-4 pol32Δ::natNT2*	JB lab

	tRNA-pRS316	
JB916	*MATa ade- ura- his+* *leu2-3::pCM244 (CMVp-tetR'-SSN6, LEU2) x3* *top2-4 sgs1Δ::TRP1 top3Δ::hphNT1* *pRS316*	JB lab
JB951	*MATa ade2-1 his3-11 leu2-3 trp1-1 ura3-1 can1-100* *UBR1::GAL1-10-Ubiquitin-M-LacI fragment-Myc-UBR1 (HIS3)* *leu2-3::pCM244 (CMVp-tetR'-SSN6, LEU2) x3* *top2-td TOP2 5' upstream -100 to -1 replaced with kanMX-tTA (tetR-VP16) - tetO2 - Ub - DHFRts - Myc - linker* *dpb3Δ::natNT2*	JB lab
JB977	*MATa ade2-1 his3-11 leu2-3 trp1-1 ura3-1 can1-100* *UBR1::GAL1-10-Ubiquitin-M-LacI fragment-Myc-UBR1 (HIS3)* *leu2-3::pCM244 (CMVp-tetR'-SSN6, LEU2) x3* *pol32Δ::natNT2*	JB lab
JB1025	*MATa his4-539 lys2-801 ura3-52* *top2-4 tof1Δ::hphNT1* *pRS316*	This study
JB1026	*MATa his4-539 lys2-801 ura3-52* *top2-4 tof1Δ::hphNT1* *tRNA-pRS316*	This study
JB1027	*MATa his4-539 lys2-801 ura3-52* *top2-4 tof1Δ::hphNT1* *pRS426*	This study
JB1128	*MATa his4-539 lys2-801 ura3-52* *top2-4 dia2Δ::hphNT1* *pRS316*	This study
JB1129	*MATa his4-539 lys2-801 ura3-52* *top2-4 dia2Δ::hphNT1* *tRNA-pRS316*	This study
JB1135	*MATa ade2-1 his3-11 leu2-3 ura3-1* *top2-4 tof1Δ::hphNT1 mrc1Δ::natNT2* *pRS316*	This study
JB1136	*MATa ade2-1 his3-11 leu2-3 ura3-1* *top2-4 tof1Δ::hphNT1 mrc1Δ::natNT2* *tRNA-pRS316*	This study

JB1146	*MATa his4-539 lys2-801 ura3-52* *top2-4* *8kb pRS316*	This study
JB1162	*MATa ade2-1 his3-11 leu2-3 trp1-1 ura3-1 can1-100* *ho::hisG or LYS2, ura3, leu2::hisG, his4x, mec1D::LEU2,* *arg4N::mec1-40-KanMX4 ts* *UBR1::GAL1-10-Ubiquitin-M-LacI fragment-Myc-UBR1 (HIS3)* *leu2-3::pCM244 (CMVp-tetR'-SSN6, LEU2) x3* *top2-td TOP2 5' upstream -100 to -1 replaced with kanMX-tTA* *(tetR-VP16) - tetO2 - Ub - DHFRts - Myc - linker* *tel1Δ::natNT2 tof1Δ::hphNT1*	This study
JB1165	*MATa ade2-1 his3-11 leu2-3 trp1-1 ura3-1 can1-100* *UBR1::GAL1-10-Ubiquitin-M-LacI fragment-Myc-UBR1 (HIS3)* *leu2-3::pCM244 (CMVp-tetR'-SSN6, LEU2) x3* *top2-td TOP2 5' upstream -100 to -1 replaced with kanMX-tTA* *(tetR-VP16) - tetO2 - Ub - DHFRts - Myc - linker* *rad9Δ::natNT2 tof1Δ::hphNT1 tel1Δ::natNT2*	This study
JB1169	*MATa ade2-1 his3-11 leu2-3 trp1-1 ura3-1 can1-100* *UBR1::GAL1-10-Ubiquitin-M-LacI fragment-Myc-UBR1 (HIS3)* *leu2-3::pCM244 (CMVp-tetR'-SSN6, LEU2) x3* *top2-td TOP2 5' upstream -100 to -1 replaced with kanMX-tTA* *(tetR-VP16) - tetO2 - Ub - DHFRts - Myc - linker* *tel1Δ::natNT2 tof1Δ::hphNT1*	This study
JB1177	*MATa ade2-1 his3-11 leu2-3,112 trp1-1 ura3-1 can1-100* *top2-4 mrc1Δ::natNT2* *tRNA-pRS316 mrc1-AQ residues*	This study
JB1178	*MATa ade2-1 his3-11 leu2-3,112 trp1-1 ura3-1 can1-100* *top2-4 mrc1Δ::natNT2* *tRNA-pRS316 MRC1 cloned*	This study
JB1212	*MATa his4-539 lys2-801 ura3-52* *top2-4 sml1Δ::natNT2 mec1Δ::hphNT1 tel1Δ::kanMX6* *pRS316*	This study
JB1213	*MATa his4-539 lys2-801 ura3-52* *top2-4 sml1Δ::natNT2 mec1Δ::hphNT1 tel1Δ::kanMX6* *tRNA-pRS316*	This study

JB1236	*MATa ade2-1 ura3-1 his3-11, 15 trp1-1 leu2-3, 112 can1-100 top2-4 DBF4-13myc::kanMX6 pRS316*	This study
JB1237	*MATa ade2-1 ura3-1 his3-11, 15 trp1-1 leu2-3, 112 can1-100 top2-4 DBF4-13myc::kanMX6 tRNA-pRS316*	This study
JB1239	*MATa ade2-1 ura3-1 his3-11, 15 trp1-1 leu2-3, 112 can1-100 top2-4 mcm5-bob1::HIS3 tRNA-pRS316*	This study
JB1243	*MATa ade2-1 ura3-1 his3-11, 15 trp1-1 leu2-3, 112 can1-100 top2-4 cdc7Δ::LEU2 mcm5-bob1::HIS3 tRNA-pRS316*	This study
JB1378	*MATa ade2-1 his3-11 leu2-3 trp1-1 ura3-1 can1-100 UBR1::GAL1-10-Ubiquitin-M-LacI fragment-Myc-UBR1 (HIS3) leu2-3::pCM244 (CMVp-tetR'-SSN6, LEU2) x3 dpb3Δ::natNT2*	JB lab

- To generate strains 1236, 1237, 1239 and 1243, *DBF4-myc::kanMX6 mcm5-bob1::HIS3 cdc7Δ::LEU2* cells obtained from the Zegerman lab (Gurdon Institute, University of Cambridge) were crossed with the *top2-4* strain.
- To generate strain 1162, *mec1D::LEU2 arg4N::mec1-40-KanMX4 ts* cells obtained from the Cha lab (Cha and Kleckner, 2002) were crossed with the *top2-td* strain.

2.1.3 Mating and Tetrad Dissection

To obtain strains containing a new combination of genes, the relevant *MATα* strain was crossed with the relevant *MATa* strain by plating a thin layer of each strain together on YPD and incubating them for at least 24–48 h to create a diploid strain. The diploids were selected using the singer tetrad dissector (Singer MSM400). Single colonies of the diploid cells were then grown on rich sporulation medium (RSM) plates at 25°C for at least 3 days. Once sporulated, the tetrads were dissected and genotyped using selection plates to identify the desired genetic markers. PCR genotyping was also used where necessary.

A tip-full of sporulated cells was transferred to a clean tube containing 250 µl of water and then incubated with 1 µl of Zymolyase T-20 at a concentration of 10 mg/ml (120493-1 AMS Biotech) for 5–10 min at room temperature to digest the asci. The cells were then spun down (2500 rpm for 1 min), and the pellet was collected and re-suspended in 250 µl water. Next, 10 µl of the cell suspension was pipetted onto a YPD plate in the top right corner with the plate placed at an incline to encourage vertical spreading of the cells. The plate was then left to dry before the tetrads were dissected using the singer tetrad dissector (Singer MSM400).

2.1.4 Gene Disruption

The gene knockout strains were established by homology-mediated recombination using the primers and plasmids (pFA6a–natNT2, pFA6a–hphNT1, pFA6a–kanMX6, and pYM22) designed by (Janke et al., 2004, Bahler et al., 1998). The *S. cerevisiae* strain was transformed using the high efficiency LiOAc/TE method (Knop et al., 1999), and the successful transformants were then selected using antibiotic resistance. Correct integrations were also checked by PCR. The oligonucleotides used in this study are listed in Table 2.3. The numbers of the oligonucleotides listed below refer to the collections in the JB lab (SS – Stephanie Schalbetter, SM – Sahar Mansoubi) unless stated otherwise.

Table 2.3: Oligonucleotides used in this study.

Primer number	Sequence
SM – 1	CTAAGGAAGTTCGTTATTCGCTTTTGAACTTATCACCAAATATTTTAG TGCGTACGCTGCAGGTCGAC
SM – 2	AAGACAGCTTCTGGAGTTCAATCAACTTCTTCGGAAAAGATAAAAAA CCAATCGATGAATTCGAGCTCG
SM – 3	ATAAGGGCATGAATGAAGAACGAA
SM – 4	CGACGCGTCATGAAGAGATAGA
SM – 5	AAATAATTGAGAAGGGCAAGAAGTGACGTAAATATACTAGACGTACT ATTCGTACGCTGCAGGTCGAC
SM – 6	TGAACAGGTATCAAATAATTGTCTCTTGCGTATATATATTTTACATTTT TATCGATGAATTCGAGCTCG
SM – 7	TTATTATCGTCGCATTCAAAGA
SM – 8	CCAACGGGACAGCAACCT
SM – 12	ACCCAAAAGAGTAGAAAACCAGGCTAAAAACAGTCACACTAGTCCAA AAAATGCGTACGCTGCAGGTCGAC
SM – 13	TTACTATAATATATAGTAGTAATCACAGTATACACGTAAACGTATTCC TTTTAATCGATGAATTCGAGCTCG
SM – 14	CCTAATGTGTACACTATTTGACCCAAAAGGTGGATGTAAGGTCAGGG ATCATGCGTACGCTGCAGGTCGAC
SM – 15	CATATACAAGTATGCTTCTTAAGAGAGACTGCGTATATATCTTACGTC ATTTAATCGATGAATTCGAGCTCG
SM – 16	CGTAACCACAGAGTTGAGGTA
SM – 17	CGAGATGATTTGAATGATTATGGT
SM – 19	CGATATACCAGGAAAGGACACT
SM – 20	GCTCTTCGGGGTTCCATTTAT
SM – 22	AGTGACGCGTAAAATTGGCAGAA
SM – 23	ATAGTACCCGGAAGGCATAAGACG
SM – 24	CAAAAGGCCGCTGAACTACGAG
SM – 25	CGCCGGAGAAAAGCACCTG
SM – 26	CCGCGGTCGCCATTTTG
SM – 27	GATTGCGGACGCTCTGTTTTGT
SM – 28	CTGGACAACAAGAACGACATACACCGCGTAAAGGCCCACAAGACTG CATGCGTACGCTGCAGGTCGAC
SM – 29	TTAGATCAAGAGGAAGTTCGTCTGTTGCCGAAAATGGTGGAAAGTC GTTAATCGATGAATTCGAGCTCG

SM – 30	AAGAGAGAATAGTGAGAAAAGATAGTGTTACACAACATCAACTAAAA ATGCGTACGCTGCAGGTCGAC
SM – 31	TTCTCTCTTAAAAAGGGGCAGCATTTTCTATGGGTATTTGTCCTTGGT TAATCGATGAATTCGAGCTCG
SM – 33	CGAGTCATGTAATTAGTTATGTCA
SM – 34	GCAGCGTAATCTGGAACGTCA
SM – 35	GCACCATCATCCACAGCAGT
SM – 36	TAGCCATGTCGTATAAATTTATTACCAAGAACAAAAAATACACCCCGA TGCGTACGCTGCAGGTCGAC
SM – 37	TAAGAATTTTCCGAAGGATACTGCATTATCATCAGTGATTTATTAATC TAATCGATGAATTCGAGCTCG
SM – 38	CGGTCTTGGTAACACTAGCTT
SM – 39	CGACAATTTCATGAACAATTCAGA
SM – 52	GCACCAGCCGTACAATATGCA
SM – 53	GCTCAGAATTTACGGGCACGA
SM – 54	GCGTCAATCGTATGTGAATGCT
SM – 55	GCTCGCAGGTCTGCAGCGA
SM – 67	GGATGATGCCTTGCATGCTTT
SM – 68	GGTCTCGTCAACGAAACTTCT
SM – 69	GCTTCAGAAGATTCTAAAAGGGA
SM – 70	CCGAATAAAAGTAAAGACCCAAAA
SM – 71	CGCCATTAATCTGGGCCATTA
SM – 72	GCTAGAACTAAGTGATGATGAT
SM – 73	CGACCACTTCAAAAACAGTAAA
SM – 74	AACGCCATAGAAAAGAGCATAGTGAGAAAATCTTCAACATCAGGGCT ATGCGTACGCTGCAGGTCGAC
SM – 75	TTAATCGTCCCTTTCTATCAATTATGAGTTTATATATTTTTATAATTTCA ATCGATGAATTCGAGCTCG
SS – 86	CCAACCACGTCGTAGAGCA
SS – 88	CGTATATCCATTGCAGCTGCT
SS – 127	ATGGGGATGTATGGGCTAAATG
SS – 128	GGGCGCCGGGCACCTCTGG
SS – 131	GCTGGCTCTGCACCTTGGTGA
SS – 133	GCTTTGCTCGACGCCTTAGCCA
SS – 158	ACATTAACTAACAACCAGAAATAGGCTTTAGTTAACTCAATCGGTAAT TACGTACGCTGCAGGTCGAC
SS – 159	ATACATTACATCACAATTAGTAATGGAAAGTGTTTGGAAAAAAAAGAA

	GAATCGATGAATTCGAGCTCG
SS – 160	CCTGCCCCAACAGATAAAAACAAGCAAGGGTCAACCGTGTTGCAAA AAAACGTACGCTGCAGGTCGAC
SS – 161	TATAACATATTGCATCGAATAGTAATTACATAGCAATAATAGCAACAA CAATCGATGAATTCGAGCTCG
SS – 166	CACCAGCCGTACAATATGCATATTTTGACA
SS – 176	GCACGAATGAAAGAGTACCGACAAGCAT
SS – 217	GCGTGTGGGAGGATGTTCTTAGACT
SS – 218	GAGTGCAGTTCTGATTAAACACGCGAGGA
SS – 225	CCAGAATACCCAGGCGTCCTCTCTGA

2.1.5 Yeast Transformation

S. cerevisiae cells were grown in 50 ml YPD to a concentration of 1 x 10^7 cells/ml mid-log phase. The cells were then pelleted by centrifugation at 3000 rpm for 5 min and washed in 20 ml ddH_2O before being pelleted again and transferred to microcentrifuge tubes after resuspension in 1 ml ddH_2O. The cells were then again centrifuged at 6000 rpm for 1 min and washed in 1 ml LiOAc-TE (0.1 M LiOAc, 1X TE (pH 7.5)) and then again pelleted and re-suspended in 250 µl LiOAc-TE. For each transformation, 5 µl of denatured salmon sperm DNA (10 mg/ml) (15632-011 UltraPure™ Salmon Sperm DNA Solution, Life technologies), 1–5 µl of plasmid DNA (1 µg) or PCR fragment (up to 10 µg) and 300 µl of 40% PEG_{3350} (polyethylene glycol) in LiOAc-TE (200 µl 1 M LiOAc, 200 µl 10X TE, 1.6 ml 40% PEG) was added to 50 µl of cell solution and mixed thoroughly. Next, the cells were agitated at 25°C for 45 min, followed by the addition of 40 µl dimethyl sulphoxide (DMSO, D/4121/PB08, Fisher scientific) before the cells were heat-shocked for 15 min at 42°C. The cells were then kept on ice for 2 min and centrifuged at 6000 rpm for 1 min and re-suspended in 500 µl YPD medium, followed by incubation for 1 h at 25°C. Next, the cells were re-suspended in 200 µl 1X TE, and 100 µl of the cell suspension was plated on the appropriate minimal medium for plasmid transformation. For integration of antibiotic markers such as G418, hygromycin B or NAT, the cells were grown in YPD medium for 4 h before plating. The plates were incubated at 25°C for 2–4 days until colonies had formed. Centrifugation steps were carried out at low speed for 1 min.

2.1.6 Spot Test

The cells in the mid-log growth phase were subjected to 10-fold serial dilutions to reduce the concentration from ~10^8 cells/ml to ~10^3 cells/ml in YP liquid medium (with 2% carbon source and 0.1% ampicillin). Next, 5 µl of each of the 6 dilutions was spotted onto YPD plates. The YPD plates contained either no doxycycline (control) or the indicated doses of doxycycline. The plates were then incubated at 25°C for 1–2 days.

2.1.7 Genomic DNA Extraction from Yeast Cells

The yeast cells were re-suspended in 200 µl lysis buffer (50 mM Tris-HCl (pH 8.0), 100 mM NaCl, 10 mM EDTA, 1% SDS) and the cell wall was removed by incubation with 40 units lyticase (Sigma, L2524) and 5 µl 2-mercaptoethanol (Sigma Aldrich, 63689) at 37°C for 5 min. DNA was then extracted using 500 µl phenol/chloroform/iso-amylalcohol (25:24:1-Sigma) and mixed on an Eppendorf rotator for 2 min. The aqueous layer was then collected using phase lock tubes (5 prime, 2302800). DNA was then precipitated with 2 volumes of 100% ethanol and washed with 70% ethanol before being re-solubilized in 50 µl 10 mM Tris (pH 8.0).

2.1.8 Liquid Culture and Synchronisation

For the plasmid catenation assays, yeast cells were grown in synthetic complete media lacking the relevant amino acid supplemented with 2% glucose at 25°C until they reached the mid-log phase and then transferred to YP media supplemented with 2% glucose and 0.8% adenine for 1 h before being arrested. To synchronise yeast cells in the G1 phase, alpha factor peptide (GenScript custom synthesis) was added at a concentration of 10 µg/ml for 150 min. The arrest was confirmed by microscopic analysis by counting the ratio of the budded and non-budded cells (>90% non-budded). The cells were then incubated at 37°C for an additional hour to inactivate Top2 (*top2-4*). In order to release the cells from G1 arrest, they were washed three times in YPDA and then re-suspended into YPDA medium. To synchronise cells in G2/M phase, nocodazole (Sigma, M1404) at a concentration of 10 µg/ml was added 30 min after release.

To assess the budding index, the yeast cells were collected at specific time points (80 min) after release and sonicated; the budded cells were then counted using a microscope (>90% budded). Samples were then collected at 90 min after release, pelleted, and frozen on dry ice.

For the time course experiment with Top2-td, the cells were grown at 25°C in YP medium supplemented with 2% raffinose and 0.8% adenine until they reached the mid-log phase, after which they were arrested in the G1 phase using 10 µg/ml alpha factor. When 90% of the cells were in G1 (100 min), galactose was added to the culture medium (2%) followed by addition of 50 µg/ml doxycycline 30 min later. Forty-five minutes after the addition of galactose, temperature was shifted to 37°C and the cells were incubated for 1 h. The cells were then released from the arrest by transferring them to YP medium supplemented with 2% raffinose, 2% galactose, 0.8% adenine and 50 µg/ml doxycycline. A FACS sample was collected at the time of re-suspension of the cells in the first wash (of three) (Time 0), and the rest of the samples were collected at the time points indicated in the results chapter.

2.1.9 Cytology and FACS Analysis

I collected 0.5 ml of 1 x 10^7 cells/ml of the yeast cell culture, spun it down, and re-suspended it in 0.5 ml 70% ethanol. For cytology, the fixed cells were spread onto a glass slide and the DNA was stained with Fluoroshield with DAPI (4,6-diamidino-2-phenylindole) Sigma F6057 before examination on an EVOS fl microscope. For flow-cytometric analysis, the cells were re-suspended in 1 ml 50 mM Tris (pH 8.0) containing 5 µl of 10 mg/ml RNaseA (Fisher Bio reagents, DNase-Free). The samples were incubated overnight at 37°C and pelleted by centrifugation. The pellet was then re-suspended in 0.5 ml ddH_2O containing 5 mg/ml pepsin freshly dissolved in 55 mM HCl and then incubated for 30 min at 37°C. The cells were then collected by centrifugation and washed once in 1 ml 50 mM Tris (pH 8.0) and finally re-suspended in 0.5 ml 50 mM Tris (pH 8.0) containing 10 µl of 0.5 mg/ml propidium iodide (Sigma). The samples were then sonicated using a micro-tip ultrasonic processor at 20% amplitude for 10 s. Next, 100 µl of the cell suspension was transferred to 1 ml of 50 mM Tris (pH 8.0). The

samples were then analysed using a Calibur FACS machine with the CellQuest software.

2.1.10 Preparation of Trichloroacetic Acid (TCA) Whole Cell Extract

5 ml of 2 x 10^7 cells/ml of yeast culture were collected by centrifugation and re-suspended in 200 µl of 20% trichloroacetic acid (TCA). After adding 200 µl of glass beads, the cells were lysed in a ryboliser (FastPrep24, MP) machine for 1 min at a speed of 6.5 m/s. The tube was then punctured with a hot needle and placed into a clean tube, followed by centrifugation of the sample for 5 min at 4000 rpm at 4°C. To ensure the collection of the whole cell lysate, 600 µl of 5% TCA was added to the beads and the mixture was spun again for 5 min at 4000 rpm at 4°C in the same collection tube. The supernatant was then discarded and the protein pellet was re-suspended in 200 µl of 1X TCA sample buffer, boiled for 5 min and centrifuged at maximum speed for 5 min. The samples were then stored at -20°C or 10–15 µl of the sample was loaded on a polyacrylamide gel.

4X SDS Sample Buffer:

250 mM	Tris-base (pH 6.8)
20%	Glycerol
0.004 g/ml (w/v)	Bromophenol blue
0.08 g/ml (w/v)	SDS

1X TCA Sample Buffer:

1 volume	4X SDS sample buffer
1 volume	1 M Tris (pH 8)
2 volume	ddH2O
2.5%	β-mercaptoethanol

2.2 Methods for Bacterial Experiments

2.2.1 Bacterial Media, Growth and Strains

Luria-Bertani (LB) medium (10 g/l tryptone, 5 g/l yeast extract, 5 g/l sodium chloride) was used for the liquid cultures of *E. coli* at 37°C with shaking at around 180 rpm. LB medium containing 10 g/l agar was used to grow the bacteria on plates. To select for bacteria containing a resistance marker, LB medium was supplemented with 100 µg/ml ampicillin. Chemically competent DH5α bacteria were used for the transformation and amplification of shuttle vectors.

2.2.2 Bacterial Transformation

50 µl of competent bacteria was thawed on ice, and 50 ng plasmid DNA was added and mixed by gentle pipetting. The mixture was incubated on ice for 30 min, after which the bacteria were heat-shocked at 42°C for 1 min and chilled on ice for 2 min. Next, 1 ml of LB medium was added and the bacteria were incubated for 1 h at 37°C before plating on LB plates containing 100 µg/ml ampicillin and grown overnight at 37°C.

2.3 DNA Methods

2.3.1 Plasmids

Table 2.4: Plasmids used in this study.

Plasmid	Description	Selective marker	Source
pRS426	Yeast episomal plasmid.	URA3	(Christianson et al., 1992)
pRS316	Yeast centromere plasmid.	URA3	(Sikorski and Hieter, 1989)
8kb pRS316	pRS316 containing 3-kb bacterial sequence.	URA3	(Schalbetter et al., 2015)
tRNApRS316	3tRNA fragment cloned into the SmaI site of pRS316.	URA3	(Schalbetter et al., 2015)
mrc1 AQ	mrc1 AQ residues.	LEU2	(Osborn and Elledge, 2003)
MRC1	MRC1 cloned.	LEU2	(Osborn and Elledge, 2003)

2.3.2 Nucleic Acid Quantification

DNA was quantified by spectrophotometry using a ND-1000 NanoDrop Spectrophotometer (Thermo Scientific), and the absorbance was measured at a wavelength of 260 nm.

2.3.3 Polymerase Chain Reaction (PCR)

Two types of DNA polymerases, Taq and KOD, were used for the two different PCRs. Taq DNA polymerase (Thermo Fisher) was used to amplify DNA fragments without high fidelity, and KOD hot start DNA polymerase (Novagen) was used to amplify fragments that were used for the construction of yeast strains. Conditions for the Taq DNA polymerase PCR were as follows: 94°C for 2 min, 1 cycle; denaturation at 94°C for 20 s, annealing at 55°C for 30 s, extension at 72°C for 1 min/1 kb, 29 cycles; 72°C for 5 min, 1 cycle. Conditions for the KOD hot start DNA polymerase PCR were as follows: 95°C for 2 min, 1 cycle; denaturation at 95°C for 20 s, annealing at 55°C for 10 s, extension at 70°C for 2 min, 29 cycles; 70°C for 10 min, 1 cycle. The PCR products were visualized using agarose gel electrophoresis and purified using the QIAquick PCR purification kit (Qiagen).

2.3.4 Agarose Gel Electrophoresis

DNA was resolved on 1% agarose (Fisher Scientific) gels made in 0.5X TBE [54 g of Tris base, 27.5 g of boric acid, 20 ml of 0.5 M EDTA (ethylenediaminetetraacetic acid) in 1 l of ddH_2O] containing 0.5 µg/ml ethidium bromide. The samples were prepared with 6X loading buffer (Thermo Scientific; R0611), and the DNA samples were resolved alongside a 1 kb DNA ladder (Bioline; HyperLadder 1 kb) to estimate their sizes. The electrophoresis apparatus was operated at 80–100 V for around 30 min in TBE buffer. DNA bands were visualized with a UV illuminator (Syngene InGenious Gel Analysis System) and the images were analysed using GeneSnap (Syngene).

2.3.5 Plasmid Extraction from *E. coli* Cells (Miniprep)

E. coli cells were grown overnight in 5 ml LB medium with ampicillin (100 µg/ml) at 37°C before being pelleted and re-suspended in 250 µl P1 buffer (50 mM Tris-HCl (pH 8), 10 mM EDTA, 100 µg/ml RNaseA, QIAGEN Qiaprep®). Next, 250 µl of buffer P2 (200 mM NaOH, 1% SDS) and 350 µl of buffer N3 (4.2 M Gu-HCl, 0.9 M potassium acetate (pH 4.8)) was added and the samples were mixed by inverting the tube 4–6 times. The samples were then spun at 13,000 rpm for 10 min, and the supernatants were applied to QIAprep spin columns. The samples were then spun for 30–60 s and the flow-through discarded. The QIAprep column was washed with 750 µl buffer PE (10 mM Tris-HCl (pH 7.5), 80% ethanol) and eluted into 30–50 µl buffer EB (10 mM Tris-HCl (pH 8.5)) or water.

2.3.6 Sanger Sequencing and Sequence Analysis

Sequencing of plasmid DNA was performed by Source Bioscience Sequencing (Nottingham, UK). The sequence was analysed using Seqman program and Seqbuilder.

2.4 Preparative and Analytical Biochemistry

2.4.1 Plasmid Catenation Assay

2.4.1.1 Genomic DNA Extraction

DNA was purified for resolution and nonradioactive southern blotting. To begin with, the frozen pellets were re-suspended in 400 µl lysis buffer, and the rest of the protocol was carried out as described in section 2.1.7. Finally, DNA was re-solubilized in 120 µl 10 mM Tris (pH 8.0).

2.4.1.2 Two-Dimensional DNA Gel Electrophoresis

For catenation in the 2D gels, the DNA was nicked with Nb.BsmI (NEB) according to the manufacturer's instructions. Next, 30 µl samples were made up to 90 µl with 1X digestion buffer and 2.5 µl of Nb.BsmI for the corresponding plasmids. The samples were then incubated for 2 h at 65°C. In order to precipitate the DNA, 10 µl of 3 M sodium acetate (pH 5.2) was added, followed by the addition of 200 µl 100% ethanol. The tubes were inverted to mix the contents and placed at -20°C for 30 min. The samples were then centrifuged for 30 min at 13000 rpm and incubated in 70% ethanol for 2 min. The samples were then spun down for 15 min, the ethanol was removed and they were left to dry before being dissolved in 50 µl 10 mM Tris (pH 8.0).

Nicked catenanes were separated in the first dimension on a 0.4% agarose (MegaSieve; Flowgen) gel in 250 ml 1X TBE (54 g of Tris base, 27.5 g of boric acid, 20 ml of 0.5 M EDTA in 1 l of ddH_2O) without adding ethidium bromide. Next, 6X loading dye was added to the samples and they were loaded on the gel, with each of them flanked by an empty lane; 5 µl of a size marker was also loaded. The gel was run at 30 V for 13–24 h at room temperature with 1X TBE as the running buffer. For the second dimension, the marker lane from the first dimension was cut out and stained with ethidium bromide and the position of the 3 kb and 14 kb bands was measured using a ruler. The respective lanes were then excised and embedded into a 0.8-1.2% (depending on plasmid size)

agarose (MegaSieve; Flowgen) gel and run at 45–120 V in 250 ml 1X TBE in the cold room (Table 2.5).

Table 2.5: Second dimension running conditions for different plasmids.

Plasmid	Plasmid size	Agarose concentration	Voltage	Running time
pRS426	5,726 bp	1%	100 V	16 h
pRS316	4,887 bp	1.2%	120 V	16 h
8kb pRS316	7,936 bp	0.8%	45 V	24 h
tRNApRS316	6,060 bp	1%	100 V	16 h

2.4.1.3 Southern Blot

The next day, the gel was depurinated with 0.125 M HCl for 10 min with agitation and rinsed with water, which was followed by 45 min of incubation in denaturing solution (0.5 M NaOH, 1.5 M NaCl) with agitation. The gel was finally neutralized in neutralization buffer (0.5 M Tris-HCl, 1.5 M NaCl (pH 7.5)) for 45 min with agitation. The DNA was transferred onto a positively charged nylon transfer membrane (Hybond N+, Amersham Biosciences) by capillary action in 20X SCC (1 l: 175.3 g NaCl, 88.2 g Sodium citrate (pH 7.0)) and left overnight. The blot was ultraviolet-crosslinked by the auto-crosslinking function of the UV Stratalinker 1800 (Stratagene) and was incubated in 5X SSC for at least 3 h. Plasmids in this study were detected by probing with DNA amplified from the sequences of pRS316 including the URA3 sequences. The PCR product was labelled using the Fluorescein High Prime labelling system (Roche) following the manufacturer's instructions and incubated for 2 h at 37°C. The membrane was first incubated in blocking solution [5X SSC, 5% Dextran Sulphate (Sigma), 0.2% iBlock (Applied Biosystems), 0.1% SDS] at 60°C for 1 h before the probe was added and left overnight to allow hybridization. The blots were washed twice in 1X SSC with 0.1% SDS, followed by 2 washes with 0.5X SSC and 0.1% SDS. The membrane was then blocked in AB buffer (100 mM Tris-HCl, 150 mM NaCl (pH 7.5)) plus 1% skimmed milk powder for 1 h before incubating it in AB buffer plus 0.5% milk powder and alkaline phosphatase Anti-fluorescein-AP Fab fragments (Roche) for 1 h. The membrane was then washed 3 times with AB buffer plus 0.2% Tween

20 (Sigma). CDP-Star substrate (Amersham detection agent, GE Healthcare) was then added to the membrane to allow visualization of the DNA. Non-saturating exposures of the blot were acquired using ImageQuant LAS 4000 (GE Healthcare), and densitometry analysis was carried out using ImageQuant TL software. Overexposed images were taken to clearly identify the CatAn = 1 signal, which was often weak in non-saturating exposures.

2.4.2 SDS-PAGE and Immunoblotting (IB)

Appropriate amounts of resolving and stacking polyacrylamide (ProtoGel 30%, 37.5:1 Acrylamide to Bisacrylamide) solutions were made as described by (Sambrook et al., 1989) and the gels were prepared. The table below shows the compositions of separating gels of 6% and 8% for a volume of 10 ml.

Table 2.6: Western blot gel mix.

	6%	**8%**
H2O (ml)	5.3	4.6
30% Acrylamide mix (ml)	2.0	2.7
1.5M Tris (pH 8.8) (ml)	2.5	2.5
10% SDS (ml)	0.1	0.1
10% APS (ml)	0.1	0.1
TEMED (ml)	0.008	0.006

Table 2.7 shows the composition of the stacking gel for a volume of 5 ml.

Table 2.7: Western blot stacking gel mix.

	Stacking gel (5ml)
H2O (ml)	3.4
30% Acrylamide mix (ml)	0.83
1M Tris (pH 6.8) (ml)	0.63
10% SDS (ml)	0.05
10% APS (ml)	0.05
TEMED (ml)	0.005

Protein samples prepared by TCA extraction were separated by SDS-PAGE (Sodium Dodecyl Sulphate Polyacrylamide Gel Electrophoresis) using a BIORAD Mini-PROTEAN TetraCell system. The protein samples were run through the stacking gel at 80 V and through the separating gel at 120 V using 1X running buffer (0.025 M Tris base, 0.25 M Glycine, 0.1% SDS). PageRuler Plus Prestained Protein Ladder (Thermo Scientific, 26619) was used as a size reference. Subsequently, the gels were transferred onto a nitrocellulose membrane (Amersham™ Protran® Premium Western blotting membranes GE10600004) over 2 h at room temperature in 1X transfer buffer (20 mM Tris, 20% Methanol, 750 mM Glycine) using the XCell SureLock™ Mini-Cell Electrophoresis System. The nitrocellulose membranes were initially assessed for protein content using Ponceau-S protein stain solution (0.2% Ponceau S, 3% Trichloro acetic acid) before being washed with PBS-T [Phosphate buffered saline (137 mM NaCl, 2.7 mM KCl, 10 mM Na2HPO4, 1.76 mM KH2PO4) containing 0.1% Tween 20 Sigma P1379]. The membranes were then blocked with 5% milk powder (Marvel dried skimmed milk) in PBS-T for at least 1 h with rotation at room temperature or overnight at 4°C under agitation. The primary antibody was added at a dilution factor as listed below (section 2.4.2.1) in PBS-T containing 5% milk, and the membrane was incubated for 2 h at room temperature or overnight at 4°C under agitation. The membranes were then washed in PBS-T containing 5% milk for 30 min at room temperature, changing the solution three times. The secondary antibody was added at a dilution factor as listed below (section 2.4.2.2) in PBS-T containing 5% milk, and the membranes were incubated for 1 h at room temperature under agitation. The membranes were then washed in PBS-T for 30 min, changing the solution three times, and the bound antibody was detected using Plus-ECL Western Lightning (Perkin Elmer, NEL104001EA) and exposed to Amersham hyperfilm (28900837). The film was developed with a Protec photon imaging system. Alternatively, the ECL reaction was imaged on an Image Quant LAS 4000 luminescence image analyser.

2.4.2.1 Primary Antibodies Used in Western Blots

Anti-HA antibody (12CA5 mouse monoclonal $IgG_{2b}\kappa$. Roche, Fisher scientific 10026563) was used at 1:4000 concentration, **Anti-PGK1 antibody** (mouse monoclonal, Invitrogen, 459250) was used at 1: 50,000 concentration and **Anti-Top2 antibody** (rabbit polyclonal, *TopoGEN, Inc*. Cat# 2014, Anti-yeast topo II, 250 µL (serum), Lot 010193bcu) was used at 1:1000 concentration.

2.4.2.2 Secondary Antibodies Used in Western Blots

Anti-Rabbit antibody (goat**,** P0448 Dako) was used at 1:5000 concentration and **Anti-Mouse antibody** (rabbit, P0260 Dako) was used at 1:5000 concentration.

2.4.3 Chromatin Immunoprecipitation-Sequencing (ChIP-Seq)

2.4.3.1 ChIP

50 ml cultures of 1.5–4.0 x 10^7 cells/ml were cross-linked using 1.35 ml 37% formaldehyde for 45 min. The cells were then centrifuged at 3000 rpm for 2 min at 4°C and re-suspended in 10 ml cold PBS, and the wash was repeated. After a third round of centrifugation, only 8 ml of PBS was discarded and the remaining 2 ml was used to re-suspend the cells. The cells were then pelleted again and frozen at -80°C. Next, the cells were re-suspended in 500 µl SDS buffer (1% SDS, 10 mM EDTA, 50 mM Tris HCl (pH 8.0), one protease inhibitor tablet (Roche)). Next, I added 200 µl glass beads, and the cells were ribolysed at 4°C (4X 1 min, 3 min on ice in between). The bottoms of the tubes were pierced with needles and the contents were transferred to a 15-ml falcon tube, and the cells were centrifuged at 2000 rpm for 30 s. The supernatant was transferred to Covaris tubes (520130) and sonicated for 20 min with 30 s on/off cycles (Duty Cycle 10%, Peak Incident Power 75 Watts, Cycles per Burst 200, Bath Temperature 7°C) using the Covaris M220 system. The sonicated samples were then centrifuged for 20 min at 14000 rpm at 4°C, and the supernatant was collected and the pellet was discarded. Next, 4.5 ml of cold IP buffer (0.1% SDS,

1.1% Triton-X-100, 1.2 mM EDTA, 16.7 mM Tris HCl (pH 8.0), 167 mM NaCl, one protease inhibitor tablet) was added. 1ml was transferred to each of the new tubes and 8 µl of γH2A antibody was added to each tube. The remainder of the sample was kept as input. The samples with the antibody were then placed on a rotating wheel at 4°C overnight. Next, 30 µl of a 50/50 mix of A/G dynabeads (Sigma) washed in IP buffer was added and the cells were incubated at room temperature on the wheel for 90 min. The beads were then washed on the wheel for 3 min with 1 ml TSE-150 buffer (1% Triton-X-100, 0.1% SDS, 2 mM EDTA, 20 mM Tris HCl (pH 8.0), 150 mM NaCl), for 3 min with 1 ml TSE-500 (1% Triton-X-100, 0.1% SDS, 2 mM EDTA, 20 mM Tris HCl (pH 8.0), 500 mM NaCl), for 3 min with 1 ml LiCl buffer (0.25 M LiCl, 1% NP-40, 1% deoxycholate, 1 mM EDTA, 10 mM Tris HCl (pH 8.0)) and for 3 min with 1 ml of TE (pH 8.0). Next, 200 µl of Elution buffer (1% SDS, 0.1 M NaHCO3) was added and the cells were left on the wheel for 3 min at room temperature. The supernatant was then transferred to a new tube and 20% 5 M NaCl was added, followed by incubation at 95°C for 15 min to reverse the crosslinking of the proteins from the DNA. Next, 10 µl DNase-free RNase was added (0.5 mg/ml, Roche), followed by incubation for 30 min at 37°C. All the samples were purified using the Qiagen PCR purification kit by adding 1 ml PB buffer to start. The DNA was then eluted in 40 µl of ddH_2O. 50 µl of the input DNA was reverse crosslinked, RNase was added and DNA was purified as for the other samples. Sequencing libraries were prepared as described in section 2.4.3.2.

2.4.3.2 ChIP-Seq Library Preparation

To adjust for the low concentration of DNA, a modified protocol (Ford, 2015) was used to prepare ChIP-Seq libraries using the TruSeq Kit from Illumina. To end DNA repair, the entire DNA obtained from the ChIP was mixed with 10X NEB T4 DNA ligase buffer, 2 µl of 10 mM dNTPs and 0.5 µl of End Repair Enzyme Mix (NEB) in a total volume of 50 µl. The mixture was then incubated for 30 min at 20°C. To purify the obtained product, 35 µl of AMPure XP beads (Beckman Coulter) and 65 µl of 30% PEG_{3350}/1.25 M NaCl was added, followed by incubation at room temperature for 10 min. The mixture was then placed on a magnetic rack for 5 min, and the supernatant was removed, washed twice with

80% ethanol, left to dry, and eluted with 17 µl of ddH_2O. To add A bases to the 3′ ends, the eluted DNA was mixed with 2 µl of 10X NEB buffer 2, 1 µl of 4 mM dATP and 0.5 µl of Klenow 3′ to 5′exo (-) at 5 U/µl (NEB) in a total volume of 20 µl, followed by incubation for 30 min at 37°C. To ligate adapters to the DNA fragments, the A-tailed DNA was mixed with 25 µl of 2X quick ligase buffer (NEB), 1 µl of diluted adapter 1:250 (Illumina TruSeq), 2.5 µl of ddH_2O and 1.5 µl of quick ligase at 2000 U/µl (NEB), mixed gently, and incubated for 20 min at room temperature; then, 5 µl of 0.5 M EDTA (pH 8.0) was added. Next, I added 0.9 volume of AMPure beads, mixed the mixture gently and incubated it for 10 min at room temperature. The mixture was then placed on a magnetic rack for 5 min, and the supernatant was removed, washed twice with 80% ethanol, left to dry and eluted with 20 µl of ddH_2O. To PCR-amplify the library, the eluted DNA was mixed with 1 µl of TruSeq PCR primer cocktail and 20 µl of 2X Kapa HiFi HotStart Ready Mix in a total volume of 40 µl. The PCR program included 10 s of denaturation at 98°C, 30 s of annealing at 60°C and 30 s of elongation at 72°C. To remove fragments longer than 370 bp, 0.7 volume of AMPure beads was added, and the mixture was incubated for 5 min and placed on a magnetic rack for 5 min; the supernatant was then transferred to a new tube. To recover all the DNA from the supernatant, 0.75 volumes of beads and 0.75 volumes of PEG 30%/1.25 M NaCl was added, the previously described steps were carried out and the DNA was eluted in 40 µl. To recover fragments smaller than 250 bp, 0.8 volumes of beads were added, the same steps were carried out and the DNA was eluted in 15 µl of EB (Qiagen). To check the quality of the DNA, 1 µl was used to measure the concentration using the High Sensitivity Qubit kit (Invitrogen), and 1 µl was run on the Bioanalyser (Agilent Technologies).

2.4.3.3 Bioinformatics Analysis

Bioinformatics analysis was performed in collaboration with the Zegerman lab (Gurdon Institute, University of Cambridge).

2.4.3.4 Antibody Used in ChIP

I used 8 µl of **Anti-Histone H2A (phospho S129) antibody** (rabbit, Abcam AB15083).

Chapter 3

Measuring Fork Rotation

All the data presented in this chapter have been published in Schalbetter et al. (2015) (Schalbetter et al., 2015).

3.1 Objective

In this thesis, my objective was to assess fork rotation and DNA pre-catenation during DNA replication *in vivo* in budding yeast. My initial aim in this chapter was to examine the accuracy of the primary method used in this project. Second, I wanted to discover when fork rotation and DNA pre-catenation occurs during DNA replication, i.e. to determine whether the extent of fork rotation and pre-catenation during DNA replication is dependent on the size of the replicons or whether it occurs under certain chromosomal contexts.

3.2 Approach

To study fork rotation *in vivo*, I performed a plasmid DNA catenation assay in *S. cerevisiae* by adapting a method initially used to study supercoiling on plasmids (Martinez-Robles et al., 2009, Baxter et al., 2011). Budding yeast can stably propagate small plasmids that contain origin sequences, and their segregation dynamics is similar to those of endogenous chromosomes. Hence, any topological characteristics indicated in the plasmids could be observed as analogous to the state of the endogenous chromosomes *in vivo*. To prevent plasmid loss, the plasmids also contained a selective marker and the cells were grown in selective media.

The small size of these plasmids (5–8kb) means that they can be resolved on agarose gels, which allows us to probe and visualize structural changes that occur upon their catenation. The advantages of using this assay is that the plasmids can maintain all their topological characteristics when they are extracted from the cell because they are topologically closed. However, this assay cannot be carried out on genomic DNA as it is linear and therefore the extraction leads to loss of topological characteristics that were maintained while the DNA was within the cell. Genomic DNA is also long, which makes purification difficult.

In this experiment, I used single origin plasmids that included a centromere pause

site (pRS316), no known pause site (pRS426) or multiple pausing sites containing three tRNA genes and a centromere (tRNApRS316). Moreover, I used the 8-kb pRS316 in which 3 kb of DNA was ligated into 5-kb pRS316; this increased the size of the replicon by 60%. All these plasmids also contained the *URA3* gene as a selection marker and therefore were transformed into *top2-4* cells deleted for the genes in question, followed by selection of the transformants on -ura medium. The plasmids used in this study are shown in Figure 3.1.

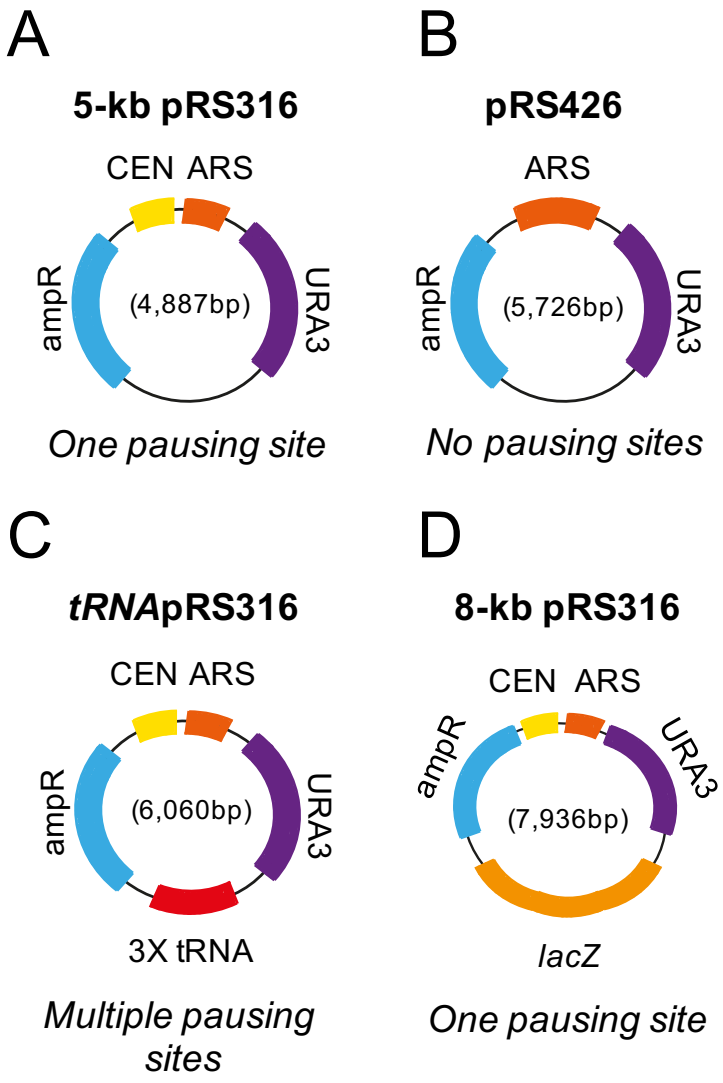

Figure 3.1: Plasmids used in this study.
A) 5-kb pRS316 containing a centromere pause site. **B**) pRS426 with no known pause site. **C**) tRNApRS316 containing three tRNA genes and a centromere. **D**) 8-kb pRS316 containing a centromere pause site and a 3-kb additional bacterial sequence.

If the activity of budding yeast type II topoisomerase, Top2, is conditionally depleted before DNA replication, the DNA pre-catenanes generated through fork rotation are not resolved, which leads to the accumulation of a catenated replicated plasmid (Baxter and Diffley, 2008, Baxter et al., 2011). In my experiments, I assessed the extent of DNA catenation on the aforementioned plasmids using two-dimensional (2D) agarose gel electrophoresis. This assay allowed us to directly quantitate the number of DNA catenanes and therefore the extent of fork rotation that leads to pre-catenane formation.

As described in Figure 3.2, to deplete the activity of topoisomerase II conditionally from cells, particularly during DNA replication, an exponentially growing *top2-4* yeast strain was synchronized (Holm et al., 1985) in the G1 phase by addition of the mating pheromone alpha factor. Following arrest in G1, the cells were switched to the restrictive temperature (37°C) for 1 h to deplete the activity of Top2 and then released from the alpha factor block into the cell cycle in the presence of the microtubule-depolymerizing drug, nocodazole. In the presence of nocodazole, the cells entered mitosis but were arrested at the spindle checkpoint because they could not form the spindle and bi-orient the chromosomes correctly on the metaphase plate, which led to their arrest in the prometaphase. Finally, the cells were collected 90 min after release. Thus, this protocol allowed plasmid replication and generation of catenated sister chromatids. This defined preparation protocol ensured as much consistency as possible between repeats and between different yeast strains, as the cells were at the same stage of the cell cycle and under the same external conditions when fork rotation was assayed. The cell cycle arrest in all the experiments was confirmed based on the budding index determined using a microscopic analysis, which involved counting the ratio of the budded and non-budded cells (i.e. >90% non-budded for G1 arrest or >90% budded cells for G2 arrest) or by analysis of the DNA content using fluorescence-activated cell sorting (FACS). As an example, FACS analysis of *top2-4* pRS316 is shown in Figure 3.3.

For analysis, the DNA was purified following replication in the absence of Top2. As shown in Figure 3.2A, supercoiled and monomeric plasmid (CCCm) that appeared before the S phase was converted into a catenated plasmid dimer

(CatC) 40 min after release from G1 arrest (corresponding with the onset of the S phase). “CatC” is used to refer to dimers present in the cell until a ‘pre-anaphase’ state. Figure 3.4 A and B represent the varying monomer and dimer species as well as the different kind of catenanes that could be converted into each other by single or double nicking. Both CCCm and CatC are negatively supercoiled (Baxter and Diffley, 2008) and therefore cannot be resolved on the gel properly; the plasmids had to be nicked using a site-specific nuclease to remove any supercoiling from the replicated plasmids. The entire distribution of the relaxed and catenated plasmids (referred to as CatAn, where *n* = number of catenated linkages) was subsequently resolved by 2D gel electrophoresis and detected by Southern blotting using a Fluorescein-labelled probe specific to *URA3*. Therefore, the plasmids in this study were detected by probing with DNA amplified from the sequences of pRS316 including the *URA3* sequences. Using a non-radioactive method, nucleotides tagged with fluorescein were introduced into the probe. Detection was then carried out with a highly specific anti-fluorescein antibody conjugated to alkaline phosphatase (AP). Fluorescein-labelled DNA, like radiolabelled probes, is stable under standard hybridization conditions. Finally, chemiluminescent detection was carried out using CDP-star to visualize DNA in a Southern blot.

The signals of the plasmid forms were then quantified by densitometry. Relative intensities of all the signals related to regions 1 to 27 were calculated and corrected for local background. Moreover, the relative amounts of all the signals in the arc containing regions 1 to 20 and 21 and above were quantified and corrected for local background. Next, the median of the entire distribution was calculated by relating signals in regions 1 to 20 to the total signal of the large region 1–20, and the position along the arc where 50% of the total signal (total signal in regions 1 to 20 and 21 and above) had accumulated was identified; the average of at least two experiments was taken for quantification. The exact number of replicates for each experiment has also been displayed in Tables 3.1. A schematic overview of the experimental procedures is shown in Figure 3.2.

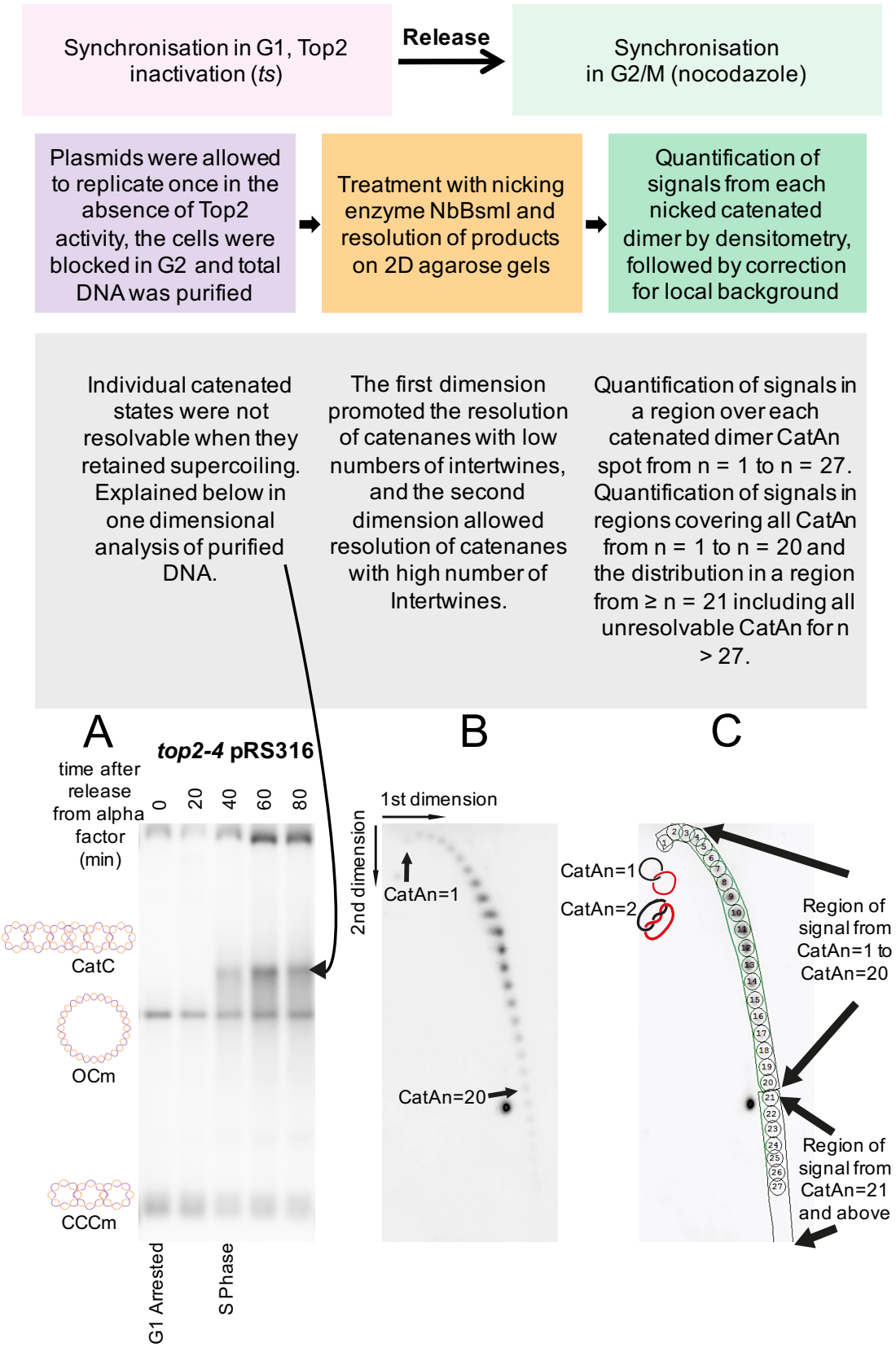
Synchronisation in G1, Top2 inactivation (ts)
Release
Synchronisation in G2/M (nocodazole)
Plasmids were allowed to replicate once in the absence of Top2 activity, the cells were blocked in G2 and total DNA was purified
Treatment with nicking enzyme NbBsmI and resolution of products on 2D agarose gels
Quantification of signals from each nicked catenated dimer by densitometry, followed by correction for local background
Individual catenated states were not resolvable when they retained supercoiling. Explained below in one dimensional analysis of purified DNA.
The first dimension promoted the resolution of catenanes with low numbers of intertwines, and the second dimension allowed resolution of catenanes with high number of Intertwines.
Quantification of signals in a region over each catenated dimer CatAn spot from n = 1 to n = 27. Quantification of signals in regions covering all CatAn from n = 1 to n = 20 and the distribution in a region from ≥ n = 21 including all unresolvable CatAn for n > 27.
A
top2-4 pRS316
time after release from alpha factor (min)
0
20
40
60
80
CatC
OCm
CCCm
G1 Arrested
S Phase
B
1st dimension
2nd dimension
CatAn=1
CatAn=20
C
CatAn=1
CatAn=2
Region of signal from CatAn=1 to CatAn=20
Region of signal from CatAn=21 and above

Figure 3.2: Quantification of fork rotation during DNA replication.
A) Both pre-catenanes and catenanes produced during DNA replication were decatenated by Top2 in wild-type cells. Thus, to assess how often fork rotation and pre-catenation take place during replication on a plasmid replicon, the cells containing the plasmid were synchronously released from G1 block in the absence of Top2 activity and allowed to accumulate in G2 by adding nocodazole (+NOCODAZOLE) to the culture before cell collection (note that catenated dimers appeared following replication at 40 min after G1 release). The DNA was then purified; however, at this point, all the catenated products (CatC) were negatively supercoiled because of nucleosome deposition in the sister chromatids. Thus, this supercoiling of deproteinized plasmids was not properly resolvable on the gel (the mobilities of CCCm – covalently closed circular monomer / supercoiled monomer, OCm – open circular monomer and CatC – covalently closed catenated dimers are indicated). Hence, an additional step was required to resolve each catenated state. **B**) To do so, the purified DNA was nicked with a site-specific nicking enzyme to remove supercoiling while retaining the catenated nodes. Agarose gel electrophoresis in two separate dimensions was carried out to resolve both low- and high-catenated states. Next, Southern blotting was performed, followed by probing with pRS316 sequences. **C**) Densitometry was then used to calculate the relative intensities of each state in two ways. Initially, the signal in equally sized regions centred on each catenated signal state was quantified on states 1–27 and correction for local background was performed. The relative intensity was then expressed as a percentage of the total signal in all regions. With regard to the second measurement, the signal from the arc related to states 1–20 was compared to that related to states 21 and above. To do so, the regions were drawn around all states 1–20 and from the remainder of the arc relating to states 21 and above; then, each set of states was expressed as a percentage of the sum of both. The advantage of this measurement is that the signal from each unresolvable catenated state that formed detectable signal could be quantified.

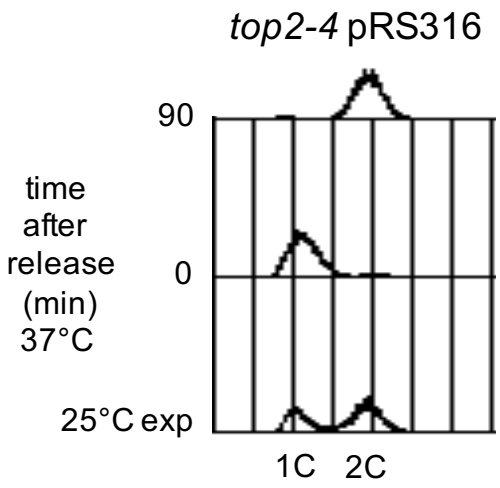

Figure 3.3: Representative FACS data showing the progression of *top2-4* pRS316 through the block and release protocol.
'exp' = exponentially growing population. '0 min' time point was taken just prior to release from G1 block. '90 min' time point was taken when cells reached G2/M, as assessed by the budding index.

A

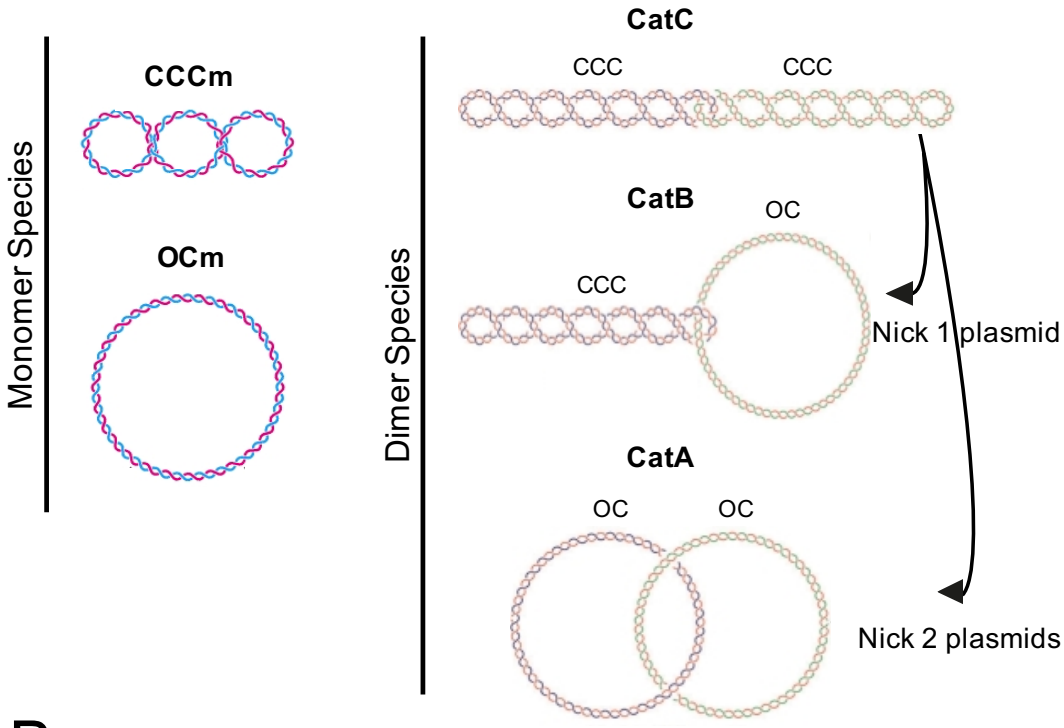
Monomer Species
CCCm
OCm
Dimer Species
CatC
CCC
CCC
CatB
OC
CCC
Nick 1 plasmid
CatA
OC
OC
Nick 2 plasmids

B

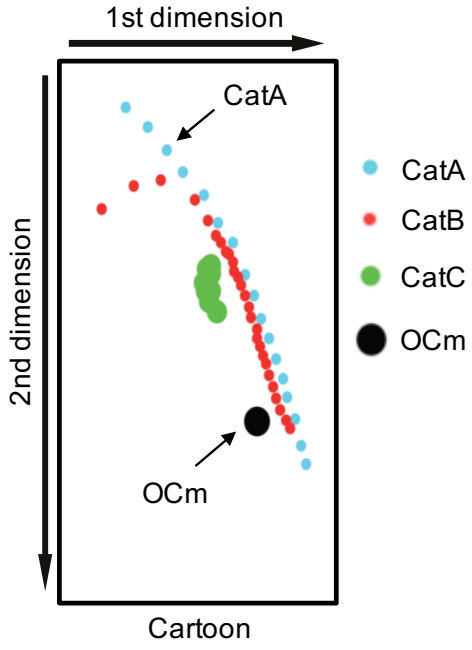
1st dimension
2nd dimension
CatA
OCm
Cartoon
CatA
CatB
CatC
OCm

Figure 3.4: Different forms of topoisomers.
A) Covalently closed circular monomer or supercoiled monomer = CCCm; open circular monomer = OCm. Covalently closed catenated dimers or CatC could be converted to CatB, where one ring was nicked and the other was covalently closed and supercoiled, and to CatA, where two rings were nicked. Only one catenated node is shown for diametric purposes. Figure adapted from (Berg et al., 2002, Martinez-Robles et al., 2009). **B**) Autoradiogram of 2D gel where CatAs are shown in blue, CatBs in red and CatCs in green. Figure taken from (Baxter et al., 2011).

3.3 Analysis of DNA Catenation as a Direct Assessment of Fork Rotation

The work conducted in the lab using this assay revealed that a normal distribution of catenated states with a median of 13 was introduced in the 5-kb yeast ARS/CEN episomal plasmid pRS316 during one round of replication. The tail of the distribution was also analysed and showed that 14% of the population was highly catenated (i.e. with plasmids including more than 20 catenations (CatAn>20)) (Figure 3.5A).

First, I confirmed that the number of DNA catenanes observed in this assay was directly related to the number of fork rotation events that occurred during the replication of the plasmid. One way that the number of DNA catenanes may not be directly related to fork rotation is if there is a pathway distinct from Top2 that can resolve pre-catenanes. Bacterial topoisomerase III has been shown *in vitro* to carry out elongation by removing pre-catenanes behind the fork before the ligation of Okazaki fragments. To do this, Topo III functions near or at the point of nascent DNA synthesis, where there is a single-stranded template DNA available for it to bind to, as already explained in Chapter 1. Thus, topoisomerase III in *E. coli* can decatenate replication products, but only when at least one of the products has a single-stranded break (Hiasa et al., 1994). To determine whether yeast Top3 can also resolve replication products behind the fork, I examined the DNA catenation of the plasmid pRS316 in cells lacking both Top2 and Top3 in *sgs1Δ* background. SGS1 was deleted in this strain to allow relatively normal levels of proliferation of the cells. However, no change in DNA catenation of pRS316 was observed in cells lacking both Top2 and Top3 in comparison with

that in cells lacking Top2 alone (median *n* = 12; 17% of plasmids had >20 catenations) (Figure 3.5B). This result suggested that yeast Top3 does not decatenate replication products in this context.

Next, I examined if the *top2-4* mutation left residual topoisomerase II activity in the cells. If residual *top2-4* activity was present in the cells, this would reduce the number of DNA catenanes relative to the number of pre-catenanes formed. To test this, I used cells containing pRS316, inactivated Top2 (*top2-4*) in G1 and released them into nocodazole, collecting a sample immediately after DNA replication (50 min post-G1 release) and one hour later (110 min post-G1 release). As shown in Figures 3.5 C and D, the plasmids 50 min and 110 min post-G1 both have a median number of catenanes *n* = 12, with 11% and 12% of plasmids with >20 catenations, respectively. If residual Top2 activity was present, the number of DNA catenanes at 110 min could be expected to be lower than that at 50 min. However, the data indicated that there was no residual Top2 decatenation activity in this assay. It was therefore concluded that our DNA catenation assay could efficiently measure fork rotation and pre-catenation of the replicons. Table 3.1 represents the summary of the results of the DNA catenation quantification experiments.

A

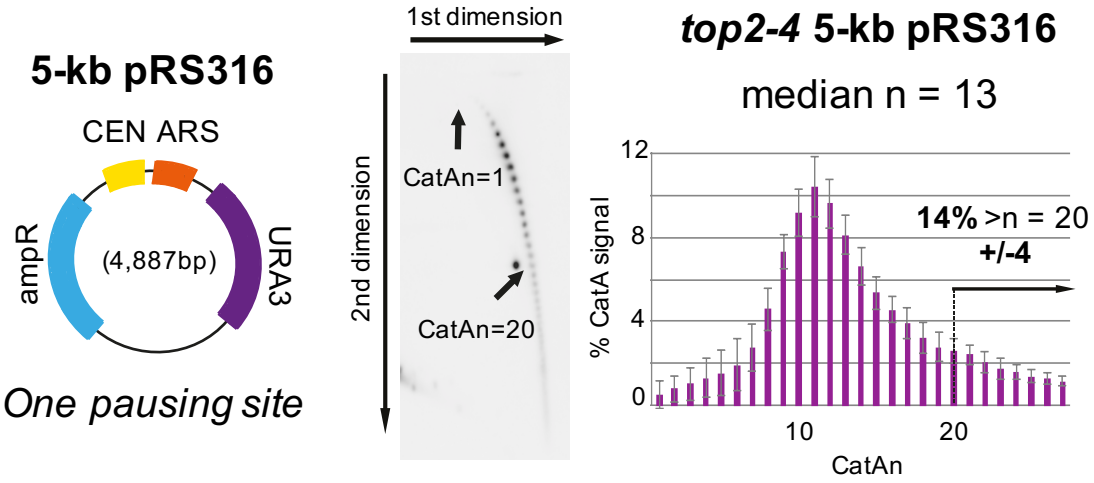
5-kb pRS316
CEN ARS
ampR
URA3
(4,887bp)
One pausing site
1st dimension
2nd dimension
CatAn=1
CatAn=20
top2-4 5-kb pRS316
median n = 13
% CatA signal
14% >n = 20
+/-4
CatAn

B

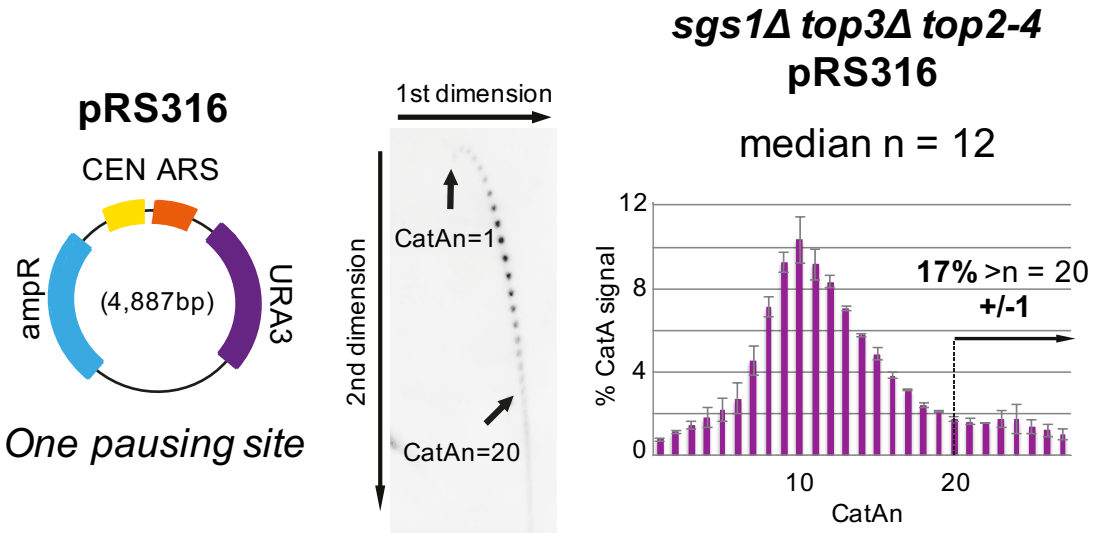
pRS316
CEN ARS
ampR
URA3
(4,887bp)
One pausing site
1st dimension
2nd dimension
CatAn=1
CatAn=20
sgs1Δ top3Δ top2-4
pRS316
median n = 12
% CatA signal
17% >n = 20
+/-1
CatAn

C

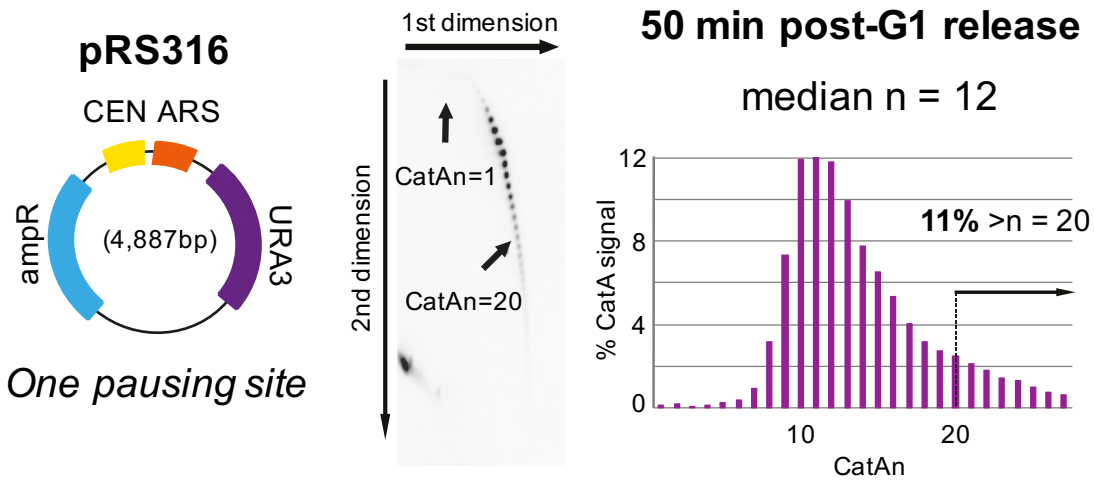
pRS316
CEN ARS
ampR
URA3
(4,887bp)
One pausing site
1st dimension
2nd dimension
CatAn=1
CatAn=20
top2-4 pRS316
50 min post-G1 release
median n = 12
% CatA signal
11% >n = 20
CatAn

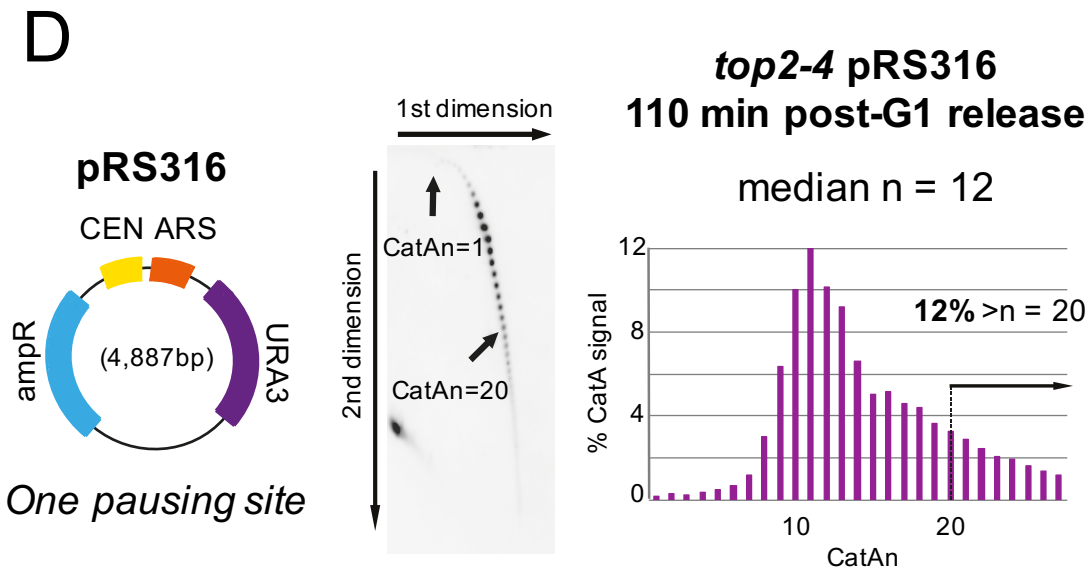

Figure 3.5: Analysis of DNA catenation provides a direct assessment of fork rotation and pre-catenation on these replicons.
A) Cells containing the *top2-4* allele and plasmid pRS316 (indicated in the cartoon) were examined for DNA catenation following one round of DNA replication in the absence of Top2 activity. **B**) Depletion of *TOP3* activity did not change the level of DNA catenation in the catenated plasmids. DNA catenation of plasmid pRS316 in *sgs1Δ top3Δ top2-4* cells was analysed and SGS1 was deleted in this strain to allow relatively normal levels of proliferation of the cells. **C**) and **D**) There was no residual decatenation activity in *top2-4* cells retained under restrictive conditions. Analysis of DNA catenation of plasmid pRS316 in *top2-4* cells isolated either 50 or 110 min after release from alpha factor arrest. Representative autoradiograms are indicated; the top arrow shows electrophoresis in the first dimension, and the side arrow shows electrophoresis in the second dimension. Histograms indicate the relative intensity of catenanes containing 1–27 catenated links (CatAn), along with the median of the whole distribution and percentage of catenanes from plasmids with >20 catenanes. Arrows show the mobility of plasmids containing 1 (*n* = 1) and 20 catenanes (*n* = 20). Error bars or values are average deviation. See Figure 3.2 for full explanation. Light blue, *ampR* gene; purple, *URA3* gene; other colours are as shown.

3.4 Analysis of DNA Catenation at Stable Protein-DNA Complexes

In this section, at first, my objective was to address whether increasing the size of a replicon would cause high levels of fork rotation and pre-catenation during replication elongation. If more DNA catenanes would be observed in the larger plasmid, it would suggest that fork rotation was occurring with detectable frequency during elongation through the additional DNA length. To do so, I compared the 8-kb pRS316 plasmid with the previously analysed 5-kb pRS316 (i.e. I increased the size of the replicon by 60%). As shown in Figure 3.6A, I found no difference in the distribution of DNA catenation (median *n* = 12; 14% of plasmids had >20 catenations). Thus, I found that an increase in the size of the plasmid replicon *in vivo* did not dramatically change the overall level of DNA catenation. This data suggested that the primary determinant of the extension of fork rotation and pre-catenation during DNA replication was not the elongation distance. Instead, based on the previous findings, fork rotation and pre-catenation formation appeared to be context-dependent to allow ongoing replication, for instance at termination of DNA replication (Sundin and Varshavsky, 1980, Sundin and Varshavsky, 1981).

Next, the hypothesis was that replication through stable protein-DNA complexes that are known to pause ongoing replication, such as tRNA genes and centromeres in plasmid replicons (Ivessa et al., 2003), would increase fork rotation and pre-catenation during replication elongation by a mechanism similar to that thought to occur at termination. In this model, as the replisome converges at a stable protein-DNA complex, the access of topoisomerases ahead of the fork is limited between the converging replisome and the complex, thereby causing fork rotation and DNA pre-catenation at these hard-to-replicate and fragile loci in order to allow ongoing replication; this is consistent with the mechanism that occurs at termination (Figure 3.6B). To test whether the presence of stable protein-DNA complexes cause high levels of fork rotation, studies conducted by Stephanie Schalbetter in the lab were carried out using similarly sized plasmids including pRS426 (no centromere) and tRNApRS316 (centromere and 3tRNAs).

The results for these plasmids were then compared with those for pRS316 (centromere). As shown in Figure 3.6C, a slight reduction in fork rotation and DNA pre-catenation was observed in plasmid pRS426 compared with that in plasmid pRS316 (median *n* = 12; 8% of plasmids had >20 catenations). A significant increase in fork rotation was detected during DNA replication of the tRNApRS316 plasmid with a median *n* = 16 and with 28% of the population having >20 catenations (Figure 3.6D). Thus, elevated levels of fork rotation and DNA catenation were observed through tRNAs and potentially centromeres during DNA replication, and this DNA catenation was more than the catenation that occurs at termination. We therefore concluded that under certain chromosomal contexts such as termination or in the presence of stable protein-DNA complexes, fork rotation and DNA catenation is favourable for ongoing DNA replication. Table 3.1 represents the summary of the results of the DNA catenation quantification experiments.

A

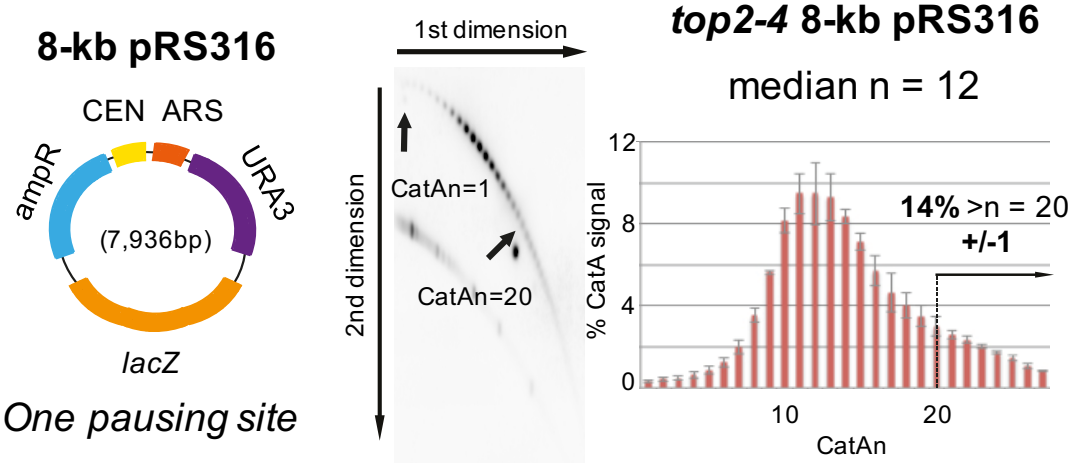

B

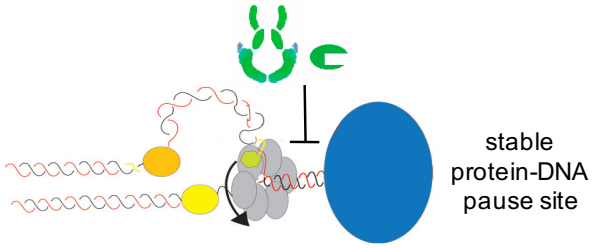

topoisomerase exclusion between replisome and stable protein-DNA pause site triggers fork rotation

C

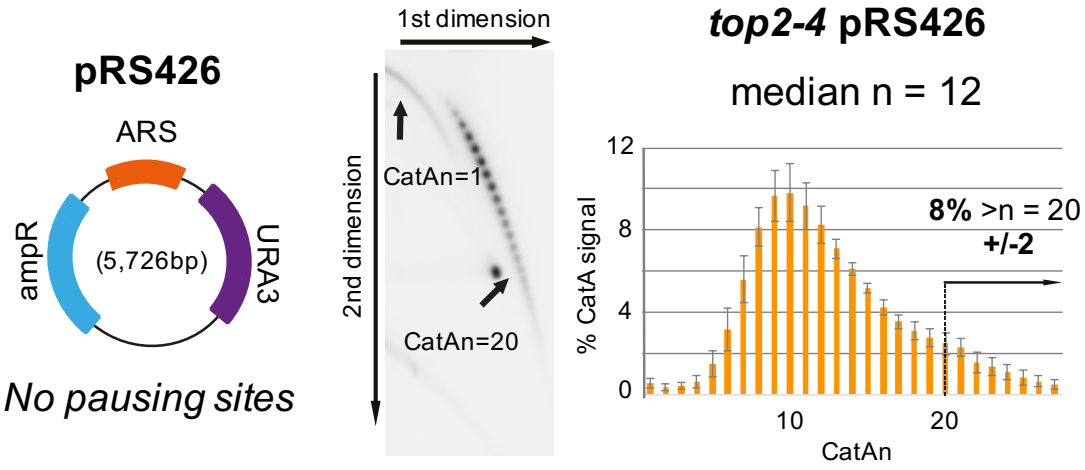

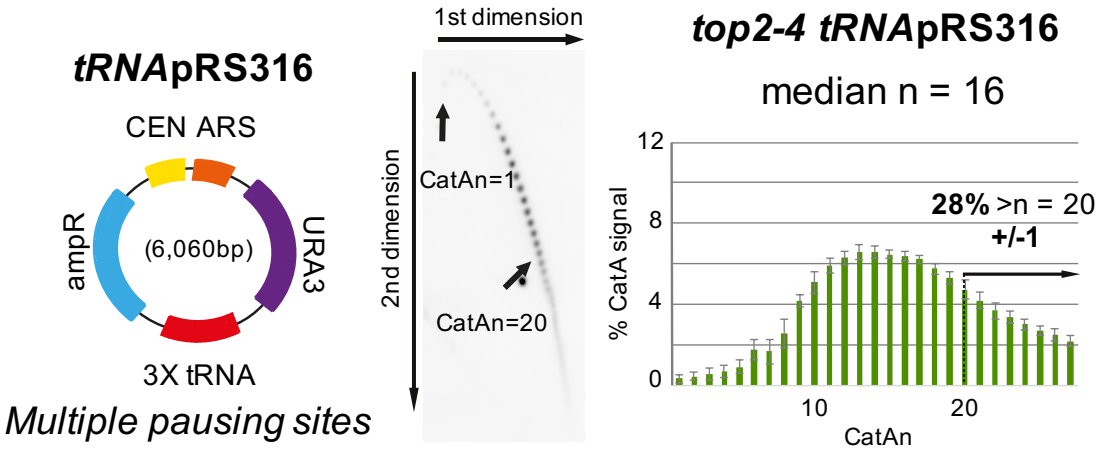

Figure 3.6: The occurrence of fork rotation and DNA catenation upon replication through stable protein-DNA pause sites.
A) Cells containing the *top2-4* allele and plasmid pRS316 containing a 3-kb additional bacterial sequence was examined for DNA catenation following one round of DNA replication in the absence of Top2 activity. **B**) Model for topoisomerase exclusion in the presence of a stable protein-DNA complex. As the replisome approaches a stable protein-DNA complex, the access of topoisomerases to relax helical tension in the final few turns is limited. Thus, fork rotation is the only pathway for DNA unwinding in this case. **C**) and **D**) Cells containing the *top2-4* allele and plasmids pRS426 and tRNApRS316 (CEN and 3x tRNA gene) (the plasmids are indicated in the cartoons) were examined for DNA catenation following one round of DNA replication in the absence of Top2 activity. Representative autoradiograms are indicated; the top arrow shows electrophoresis in the first dimension, and the side arrow shows electrophoresis in the second dimension. Histograms indicate the relative intensity of catenanes containing 1–27 catenated links (CatAn), along with the median of the whole distribution and percentage of catenanes from plasmids with >20 catenanes. Arrows show the mobility of plasmids containing 1 (*n* = 1) and 20 catenanes (*n* = 20). Error bars or values are average deviation. See Figure 3.2 for full explanation. Light blue, *ampR* gene; purple, *URA3* gene; other colours are as shown.

Table 3.1: Summary of the results of DNA catenation quantification experiments in this chapter.

Strains	Plasmid size, bp	Number of replicates	Median CatAn	% >20
***top2-4* 5-kb pRS316**	4,887	5	13	14 ± 4
***sgs1Δ top3Δ top2-4* pRS316**	4,887	2	12	17 ± 1
***top2-4* pRS316 (50 min post-G1 release)**	4,887	1	12	11
***top2-4* pRS316 (110 min post-G1 release)**	4,887	1	12	12
***top2-4* 8-kb pRS316**	7,936	3	12	14 ± 1
***top2-4* pRS426**	5,726	5	12	8 ± 2
***top2-4 tRNA*pRS316**	6,060	3	16	28 ± 1

3.5 Conclusions

In this chapter, I examined whether the plasmid DNA catenation assay allowed a direct assessment of the fork rotation event that occurred during the replication of the plasmid. From the experiments, I concluded that our DNA catenation assay allowed direct examination of fork rotation and pre-catenation of the replicons. This conclusion is based on the experiments that show that *TOP3* deletion from yeast cells does not lead to higher levels of DNA catenation. This suggests that, in contrast to bacterial Topo III, which can resolve DNA pre-catenation (Hiasa and Marians, 1994), Top3 in yeast does not resolve DNA pre-catenation during DNA replication. In addition, the *top2-4* mutant used to prevent decatenation of plasmids does not appear to have any residual activity under the restrictive conditions.

Using this assay, I showed that the extent of fork rotation and DNA pre-catenation during DNA replication does not depend on the elongation distance. It can be argued that fork rotation does not generally occur during replication elongation. Instead, the extent of fork rotation and pre-catenation during DNA replication appears to be context-dependent, for instance at termination of DNA replication or at stable protein-DNA complexes, to allow ongoing replication. In these contexts, it is possible that the action of topoisomerases ahead of the fork is restricted; therefore, fork rotation remains the sole pathway for DNA unwinding and for allowing ongoing replication (Figure 3.6B).

Chapter 4

Influence of Replisome Components on Fork Rotation

Some of the data presented in this chapter have been published in Schalbetter et al. (2015) (Schalbetter et al., 2015).

4.1 Objective

It appears that fork rotation does not generally occur during elongation, but instead, it is restricted to regions where topoisomerase may be prevented from acting ahead of the fork (section 3.4). This could be due to the conformation of the replisome, which actively prevents fork rotation during elongation except where fork rotation is necessary. Therefore, the presence of known architectural replisome factors could be important in determining how often the replisome rotates. In this chapter, I aimed to examine if changes in replisome structure alter the frequency of fork rotation. To this end, I directly assessed fork rotation and pre-catenation in budding yeast using circular plasmids in different genetic backgrounds *in vivo*.

4.2 Approach

For this chapter, I deleted the genes encoding factors that are associated with replisome stability. To begin with, I created *tof1Δ, csm3Δ*, *mrc1Δ*, *ctf4Δ*, *chl1Δ*, *ctf18Δ*, and *dia2Δ* alleles in *top2-4* cells as described in section 2.1.4. To generate *DBF4-myc, mcm5-bob1* and *cdc7Δ mcm5-bob1* in *top2-4* cells, *DBF4-myc mcm5-bob1 cdc7Δ* cells obtained from the Zegerman lab (Gurdon Institute, University of Cambridge) were crossed with the *top2-4* strain as described in Materials and Methods (section 2.1.3). The remaining strains used in this chapter had already been created and were stored in the JB lab collection box as mentioned in Table 2.1. Here, to examine fork rotation *in vivo*, I performed a plasmid DNA catenation assay as previously described in Chapter 3 (Figure 3.2) for use with yeast episomal plasmids.

4.3 Effect of Architectural Replisome Factors on Fork Rotation during Replication of Plasmid pRS316

To begin with, I determined how the deletion of *TOF1*, *CSM3*, *MRC1*, and *CTF4* alters fork rotation during the replication of plasmid pRS316. As stated in the Introduction section (Chapter 1), Tof1, Csm3 and Mrc1 are thought to be important in linking leading strand DNA synthesis to the CMG complex (see section 1.2.3.1 and 1.2.3.2), whereas Ctf4 is thought to be required for linking lagging strand DNA synthesis to the CMG complex (see section 1.2.3.3).

Replication forks have been shown to pause transiently at several places in the genome during the normal process of chromosome replication, where non-nucleosomal proteins are bound very tightly to DNA, for instance at centromeres (Greenfeder and Newlon, 1992) and tRNA promoters (Deshpande and Newlon, 1996, Ivessa et al., 2003). Moreover, interestingly, pausing appears to be reduced in the absence of the *Timeless* homolog, *TOF1*, at stable protein-DNA complexes, which suggests that pausing at protein-DNA barriers relies on Tof1 (Calzada et al., 2005, Tourriere et al., 2005, Mohanty et al., 2006, Hodgson et al., 2007). Studies conducted in our lab also revealed that fork rotation and DNA pre-catenation are induced at such protein-DNA complexes, in particular at tRNAs and potentially centromeres, during replication elongation (Chapter 3; section 3.4). Therefore, I wanted to analyse whether Tof1 that influences fork pausing would also change fork rotation and DNA pre-catenation during the replication of plasmid pRS316. To test this hypothesis, I used the *in vivo* plasmid catenation assay (Figure 3.2) to measure fork rotation and surprisingly found that the number of DNA catenanes was dramatically increased in the absence of Tof1 with a median of more than 20 and with 89% of the distribution containing >20 catenanes compared to that observed during the replication of *top2-4* pRS316 (median n = 13; 14% of plasmids had >20 catenations) (Figure 4.1A and 3.5A). This result indicated that Tof1 inhibits fork rotation and DNA pre-catenation during DNA replication on this replicon.

We know that Tof1 and Csm3 associate with each other, both physically and

functionally, and thus form an essential heterodimeric complex in which the deletion of either one results in a similar phenotype (Leman and Noguchi, 2012). Therefore, for my next experiment, I used the *csm3Δ top2-4* pRS316 strain. Interestingly, I also observed excessive fork rotation and pre-catenation in the *csm3Δ* cells with a median of more than 20 and 89% of the distribution containing >20 catenanes (Figure 4.1B). These data suggested that the Timeless/Tipin homologs, Tof1/Csm3, restrict fork rotation during DNA replication of plasmid pRS316.

Claspin/Mrc1 and AND1/Ctf4 have been shown to interact with Tof1 and Csm3 in the replisome (Katou et al., 2003, Errico et al., 2009). Hence, I aimed to determine whether Mrc1 and Ctf4 also increase fork rotation similar to Tof1 and Csm3. The median in *mrc1Δ* cells was *n* = 12 with 10% of the plasmid population having >20 catenations; further, in the *ctf4Δ* cells, the median was *n* = 12 with 17% of the plasmid population having >20 catenations. Thus, no excessive fork rotation could be detected on plasmid pRS316 in the *mrc1Δ* and *ctf4Δ* cells (Figure 4.1 C and D). The results so far indicated that Tof1 and Csm3, but not Mrc1 and Ctf4, which are required for fork pausing, also inhibit fork rotation.

A

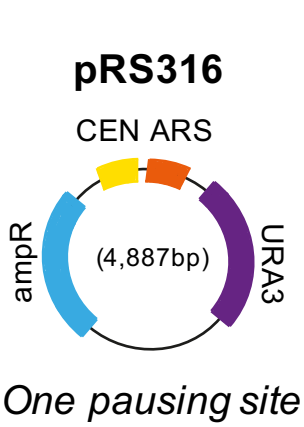
pRS316
CEN ARS
ampR
(4,887bp)
URA3
One pausing site

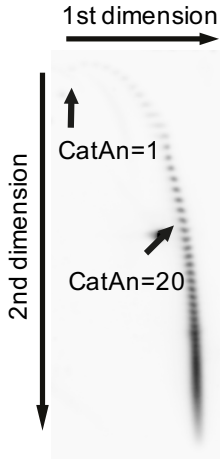
1st dimension
2nd dimension
CatAn=1
CatAn=20

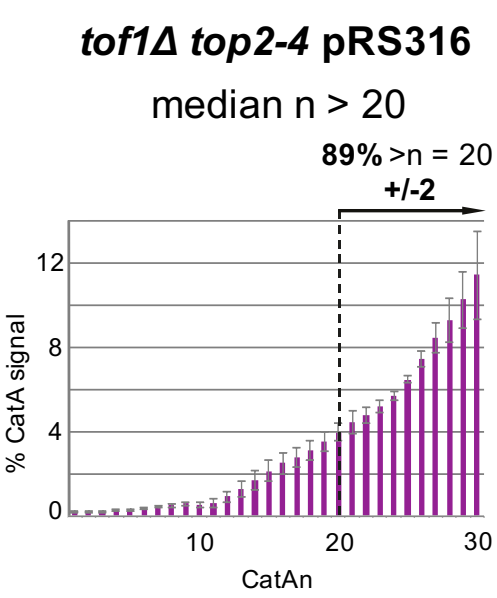
tof1Δ top2-4 pRS316
median n > 20
89% >n = 20
+/-2
% CatA signal
CatAn
0
4
8
12
10
20
30

B

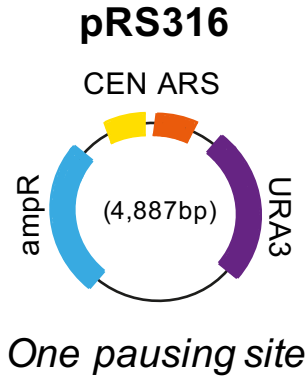
pRS316
CEN ARS
ampR
(4,887bp)
URA3
One pausing site

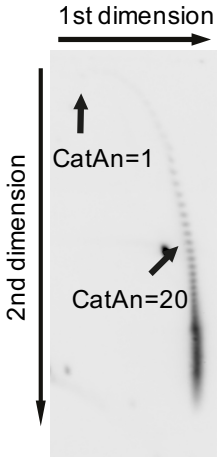
1st dimension
2nd dimension
CatAn=1
CatAn=20

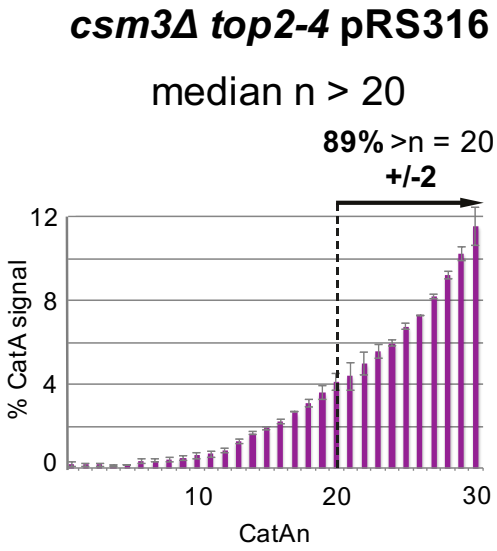
csm3Δ top2-4 pRS316
median n > 20
89% >n = 20
+/-2
% CatA signal
CatAn
0
4
8
12
10
20
30

C

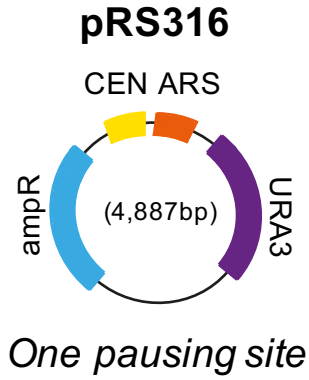
pRS316
CEN ARS
ampR
(4,887bp)
URA3
One pausing site

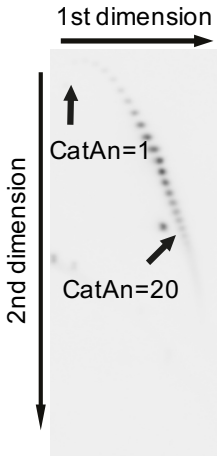
1st dimension
2nd dimension
CatAn=1
CatAn=20

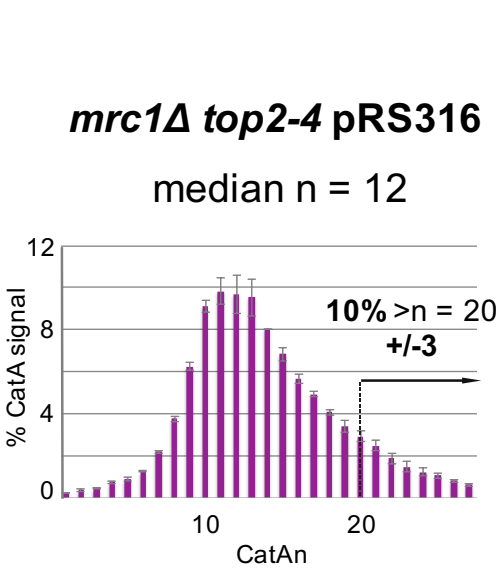
mrc1Δ top2-4 pRS316
median n = 12
10% >n = 20
+/-3
% CatA signal
CatAn
0
4
8
12
10
20

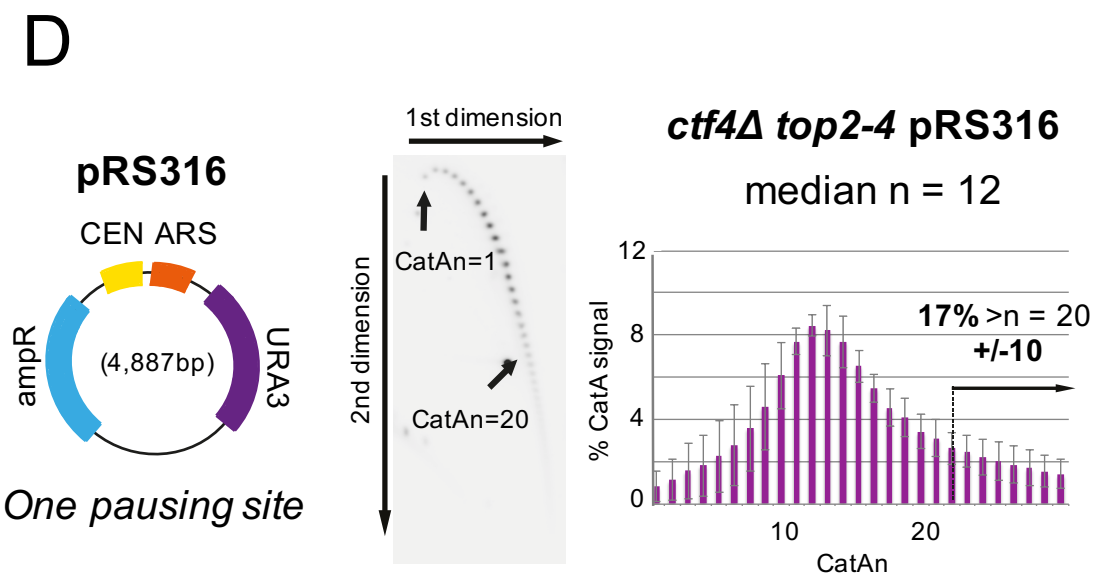

Figure 4.1: Yeast *Timeless* and *Tipin* homologs, *TOF1* and *CSM3*, restrict fork rotation and DNA catenation.
Analysis of DNA catenation of plasmid pRS316 (indicated in the cartoon) in *top2-4* cells and the different deletion alleles (**A**) *tof1Δ*, (**B**) *csm3Δ*, (**C**) *mrc1Δ* and (**D**) *ctf4Δ* was carried out as explained in Figure 3.2. Representative autoradiograms are indicated; the top arrow shows electrophoresis in the first dimension, and the side arrow shows electrophoresis in the second dimension. Histograms indicate the relative intensity of catenanes containing 1–27 catenated links (CatAn), along with the median of the whole distribution and percentage of catenanes from plasmids with >20 catenanes. Arrows show the mobility of plasmids containing 1 (n = 1) and 20 catenanes (n = 20). Error bars or values are average deviation. See Figure 3.2 for full explanation. Light blue, *ampR* gene; purple, *URA3* gene; other colours are as shown.

Potentially, the link between Tof1/Csm3 and fork rotation may not be due to its role in replisome stability. It is also known that loss of these genes causes a sister chromatid cohesion (SCC) defect (Mayer et al., 2004, Warren et al., 2004). Therefore, I wondered if the excessive fork rotation in cells lacking Tof1 and Csm3 could be due to defects in cohesion establishment. Hence, I decided to determine the effects of two more replication fork components: a DNA helicase, ChlR1/Chl1, and the PCNA loading factor, Ctf18/Ctf18. Deletion of both factors is known to lead to SCC defects (Mayer et al., 2001, Mayer et al., 2004). However, deletion of neither *CHL1* (median n = 12; 11% of plasmids had >20 catenations) nor *CTF18* alone (median n = 11; 8% of plasmids had >20 catenations) increased fork rotation during replication of the plasmid pRS316 (Figure 4.2 A and B). I therefore concluded that among all the examined factors,

Tof1/Csm3 are two unique replisome components that restrict fork rotation and DNA pre-catenation during DNA replication.

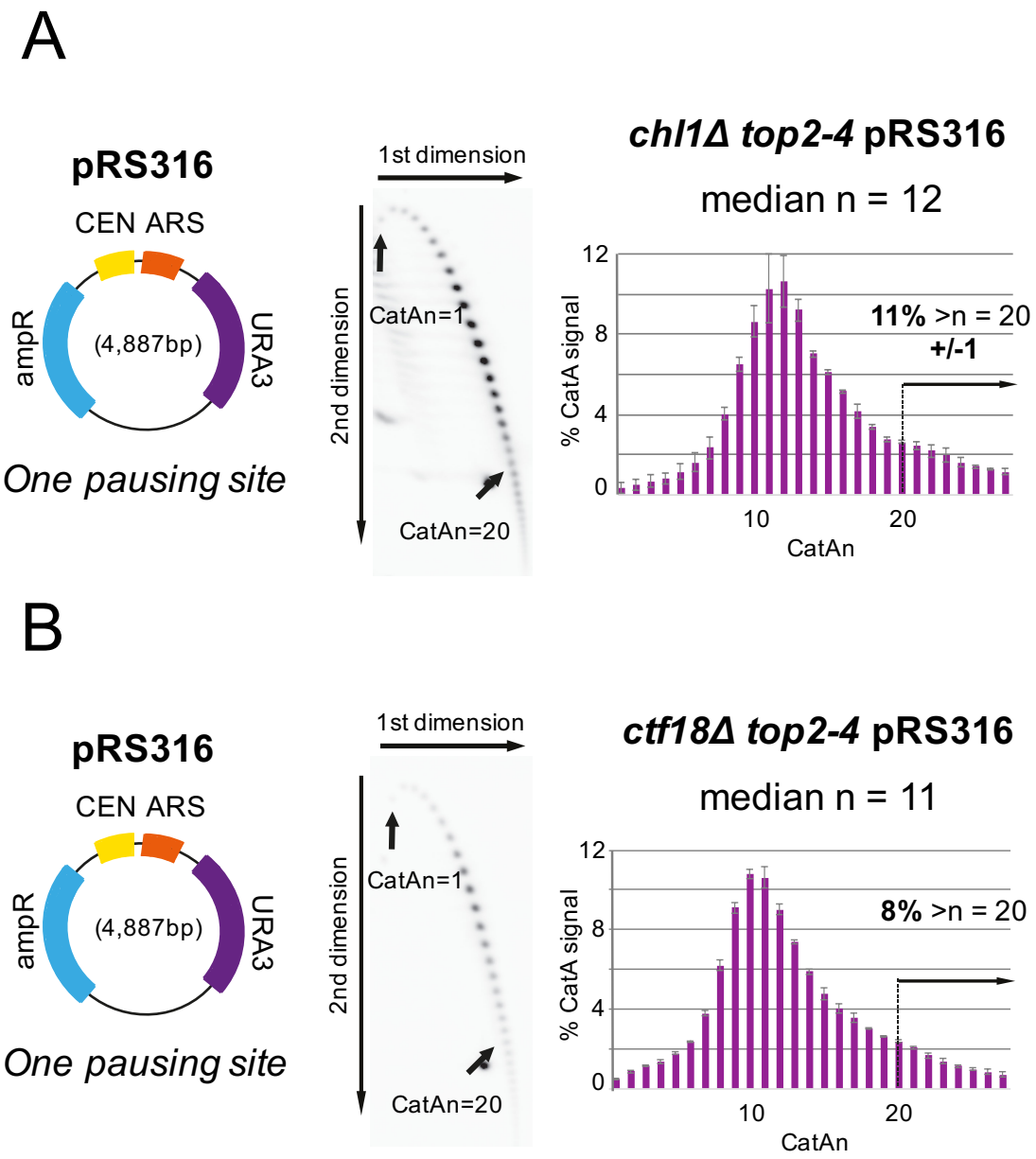

Figure 4.2: Neither Chl1 nor Ctf18 alters fork rotation during DNA replication.
Analysis of DNA catenation of plasmid pRS316 (indicated in the cartoon) in (**A**) *chl1Δ top2-4* and (**B**) *ctf18Δ top2-4* cells was carried out as explained in Figure 3.2. Representative autoradiograms are indicated; the top arrow shows electrophoresis in the first dimension, and the side arrow shows electrophoresis in the second dimension. Histograms indicate the relative intensity of catenanes containing 1–27 catenated links (CatAn), along with the median of the whole distribution and percentage of catenanes from plasmids with >20 catenanes. Arrows show the mobility of plasmids containing 1 (*n* = 1) and 20 catenanes (*n* = 20). Error bars or values are average deviation. See Figure 3.2 for full

explanation. Light blue, *ampR* gene; purple, *URA3* gene; other colours are as shown.

Next, I investigated another replication fork factor known as SCF^{Dia2}. Dia2, an essential F-box protein, is required to disassemble the CMG helicase at the end of chromosome replication when the two replication forks converge through the ubiquitination of Mcm7 (a subunit of CMG) (Maric et al., 2014). I wanted to test if changes in replisome configuration alter fork rotation during replication of plasmid pRS316. Dia2 has also been proposed to be required for replication restart after MMS-induced DNA damage (Fong et al., 2013). Therefore, it could be important for replisome stability at sites of fork rotation, i.e. fork rotation might occur at a higher frequency if the replisome is not stable in the absence of *DIA2*. However, I found that fork rotation showed no significant change in the *dia2Δ* cells (median *n* = 13; 16% of plasmids had >20 catenations) (Figure 4.3), which indicated that Dia2 has no function in altering fork rotation during DNA replication, unlike Tof1 and Csm3.

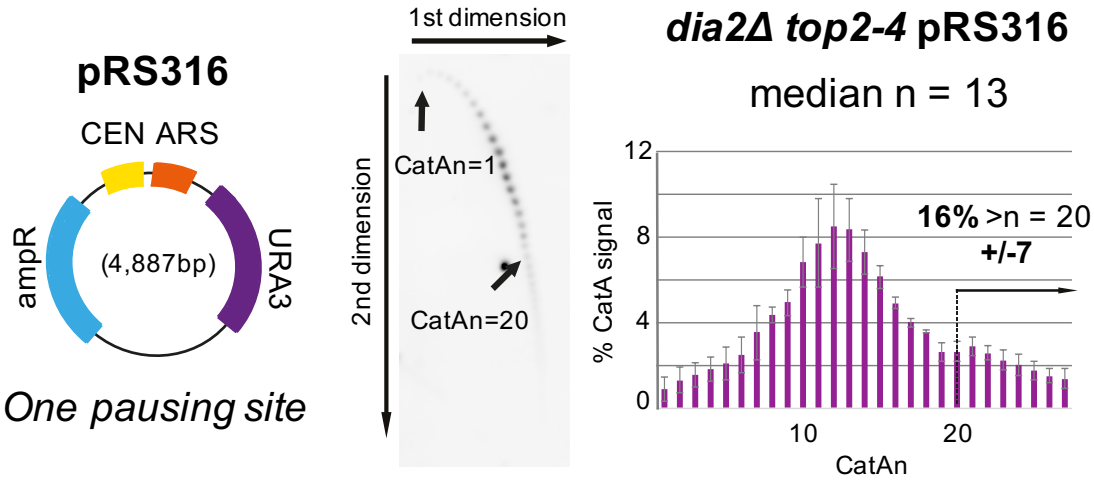

Figure 4.3: Deletion of *DIA2* does not alter fork rotation during DNA replication.
Analysis of DNA catenation of plasmid pRS316 (indicated in the cartoon) in *dia2Δ top2-4* cells was carried out as explained in Figure 3.2. Representative autoradiograms are indicated; the top arrow shows electrophoresis in the first dimension, and the side arrow shows electrophoresis in the second dimension. Histograms indicate the relative intensity of catenanes containing 1–27 catenated links (CatAn), along with the median of the whole distribution and percentage of catenanes from plasmids with >20 catenanes. Arrows show the mobility of plasmids containing 1 (*n* = 1) and 20 catenanes (*n* = 20). Error bars or values are average deviation. See Figure 3.2 for full explanation. Light blue, *ampR* gene;

purple, *URA3* gene; other colours are as shown.

Previously, Tourriere et al. (2005) showed that the rate of fork progression decreases in the absence of Tof1 and Csm3 (Tourriere et al., 2005). Therefore, I hypothesized that high levels of fork rotation in the absence of Tof1 and Csm3 would be caused due to slower elongation, which could lead to fork rotation. To confirm this hypothesis, I examined the effect of deletion of p17/Dpb3, which is a non-essential subunit of Polymerase ε, on fork rotation during DNA replication of plasmid pRS316. Interestingly, studies conducted in our lab revealed slow rates of DNA replication in *dpb3Δ* cells (Figure 4.4D). However, no increase in fork rotation was observed during the replication of plasmid pRS316 (median *n* = 12; 11% of plasmids had >20 catenations) (Figure 4.4A). Additionally, to further test my hypothesis, *top2-4* pRS316 cells were synchronized in the G1 phase and released into the S phase in the presence of 200 mM HU and then collected 90 min after release. In the presence of HU, replication forks move very slowly due to lowering dNTP levels (Figure 4.4D). However, excessive fork rotation could not be observed in the cells treated with HU (median *n* = 11; 8% of plasmids had >20 catenations) (Figure 4.4B). I therefore concluded that slowing down replication either by *DPB3* deletion or by HU treatment does not affect fork rotation on plasmid pRS316.

Next, I also checked if reducing Polymerase δ activity affected fork rotation. p66/Pol32 is a non-essential subunit of Polymerase δ and its depletion appears to reduce Polymerase δ complex activity during replication (Gerik et al., 1998). I examined the levels of fork rotation in *pol32Δ* cells during the replication of plasmid pRS316. In contrast to *dpb3Δ* cells, *pol32Δ* cells did not show low rates of DNA replication (Figure 4.4D). Surprisingly, I noticed a consistent reduction in the level of fork rotation in *pol32Δ top2-4* pRS316 (median *n* = 10; 6% of plasmids had >20 catenations) in comparison with that in wild-type cells (Figure 4.4C). To confirm this data, I also conducted an additional experiment using a different plasmid, the details of which can be found in section 4.5.

A

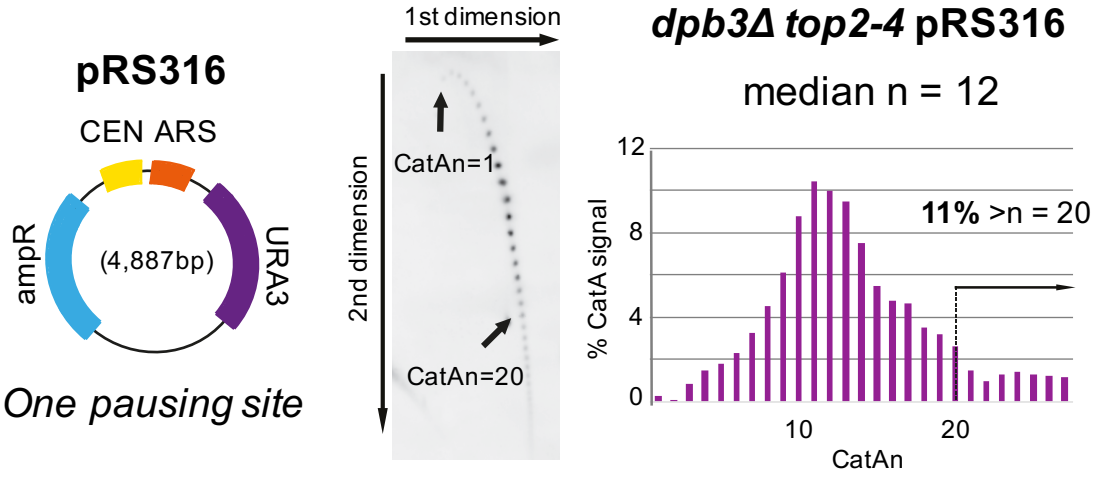
pRS316
CEN ARS
ampR
URA3
(4,887bp)
One pausing site
1st dimension
2nd dimension
CatAn=1
CatAn=20
dpb3Δ top2-4 pRS316
median n = 12
11% >n = 20
% CatA signal
CatAn
0
4
8
12
10
20

B

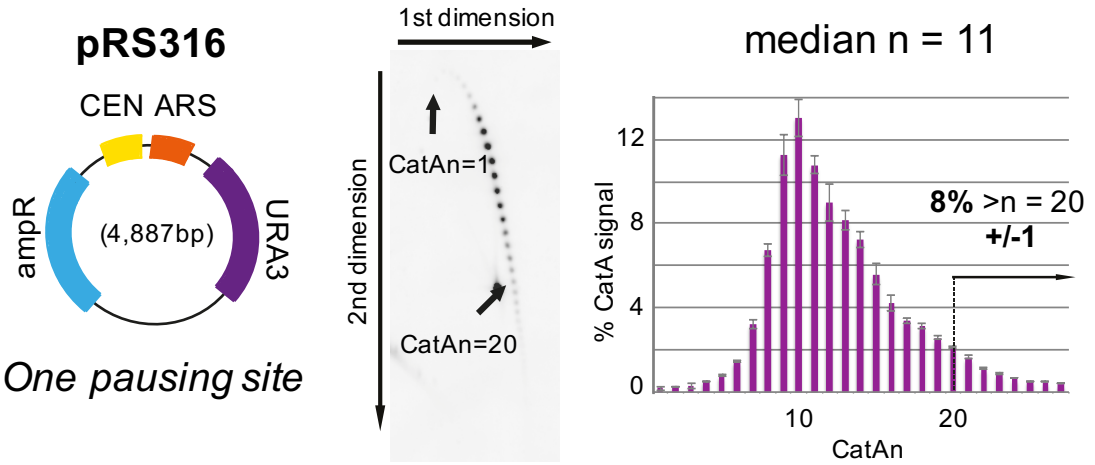
pRS316
CEN ARS
ampR
URA3
(4,887bp)
One pausing site
1st dimension
2nd dimension
CatAn=1
CatAn=20
top2-4 pRS316
plus 200 mM HU
median n = 11
8% >n = 20
+/-1
% CatA signal
CatAn
0
4
8
12
10
20

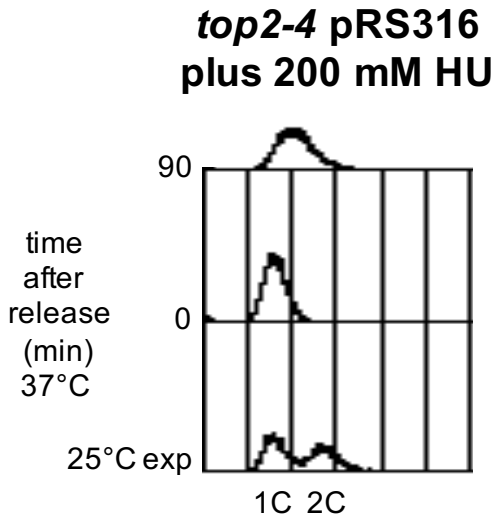
top2-4 pRS316
plus 200 mM HU
time
after
release
(min)
37°C
90
0
25°C exp
1C 2C

C

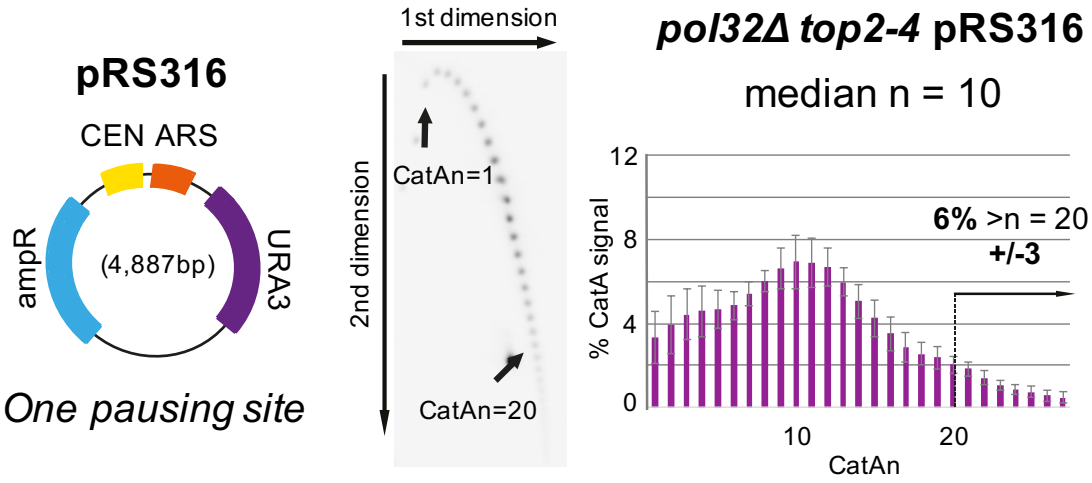
pRS316
CEN ARS
ampR
URA3
(4,887bp)
One pausing site
1st dimension
2nd dimension
CatAn=1
CatAn=20
pol32Δ top2-4 pRS316
median n = 10
% CatA signal
12
8
4
0
6% >n = 20
+/-3
10
20
CatAn

D

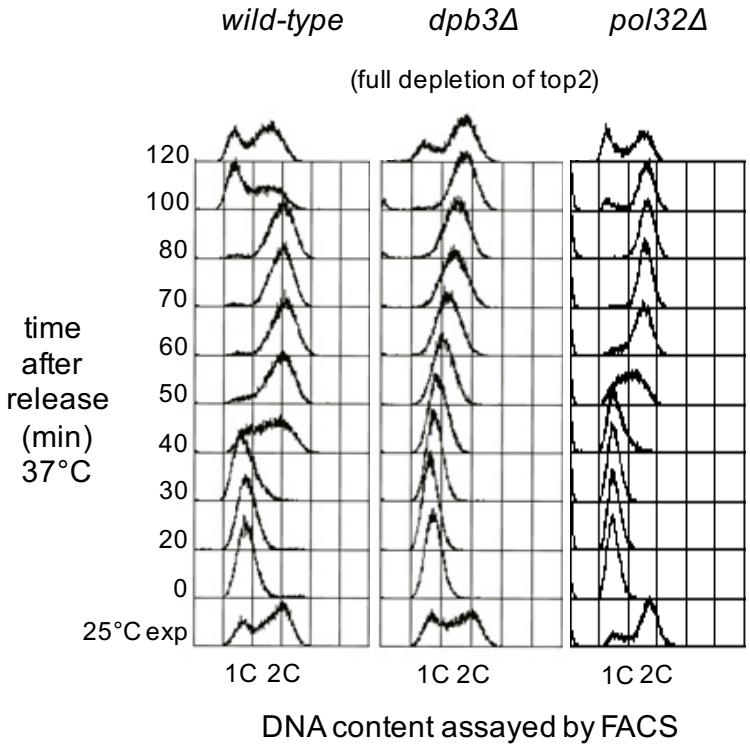
wild-type
dpb3Δ
pol32Δ
(full depletion of top2)
time after release (min) 37°C
120
100
80
70
60
50
40
30
20
0
25°C exp
1C 2C
1C 2C
1C 2C
DNA content assayed by FACS

Figure 4.4: No excessive fork rotation and DNA catenation is detected when the rate of fork progression is low. Loss of *POL32* function leads to decreased fork rotation.
Analysis of DNA catenation of plasmid pRS316 (indicated in the cartoon) in (**A**) *dbp3Δ top2-4* and (**C**) *pol32Δ top2-4* was carried out as explained in Figure 3.2. (**B**) Analysis of DNA catenation of plasmid pRS316 in *top2-4* cells released from alpha factor arrest into 200 mM hydroxyurea (HU). The cells were collected 90 min after release, and the extracted DNA was analysed as described in Figure 3.2. FACS for DNA content is also depicted. Representative autoradiograms are indicated; the top arrow shows electrophoresis in the first dimension, and the side arrow shows electrophoresis in the second dimension. Histograms indicate the relative intensity of catenanes containing 1–27 catenated links (CatAn), along with the median of the whole distribution and percentage of catenanes from plasmids with >20 catenanes. Arrows show the mobility of plasmids containing 1 (n = 1) and 20 catenanes (n = 20). Error bars or values are average deviation. See Figure 3.2 for full explanation. Light blue, *ampR* gene; purple, *URA3* gene; other colours are as shown. (**D**) FACS data showing the progression of wild-type, *dpb3Δ* and *pol32Δ* cells through the cell cycle. Exponentially growing cells were arrested in G1 using alpha factor mating pheromone and placed under restrictive conditions (the conditions of *top2-td* deletion will be explained in detail in Chapter 7) before being released synchronously into the cell cycle. Cell samples for FACS analysis were taken just before release (0 min) and every 10 and 20 min after for 120 min.

Budding yeast Dbf4-dependent kinase (DDK) is an essential gene that interacts with the Cdc7 kinase to form the DDK complex. This complex is required for the initiation of DNA replication as well as throughout S phase in the firing of origins (Zou and Stillman, 2000). In addition, it is known that Swi1 and Swi3 in fission yeast (Tof1 and Csm3 homolog) functionally interact with the Hsk1-Dfp1 complex (Cdc7-Dbf4 homolog) (see section 1.2.3.2) (Matsumoto et al., 2005). Therefore, Cdc7-Dbf4 activity could be important for Tof1 function throughout replication elongation. Hence, I wondered if Dbf4 alters fork rotation during DNA replication of plasmid pRS316 in budding yeast, potentially acting through Tof1. Deletion of *DBF4* is lethal; therefore, to test this idea, I initially used *DBF4-myc* (tagged at the C terminus) in which the *myc* tag appears to reduce Dbf4 function at the centromeres (Natsume et al., 2013). However, no excessive fork rotation could be detected in *DBF4-myc top2-4* pRS316 (median n = 12; 10% of plasmids had >20 catenations) (Figure 4.5).

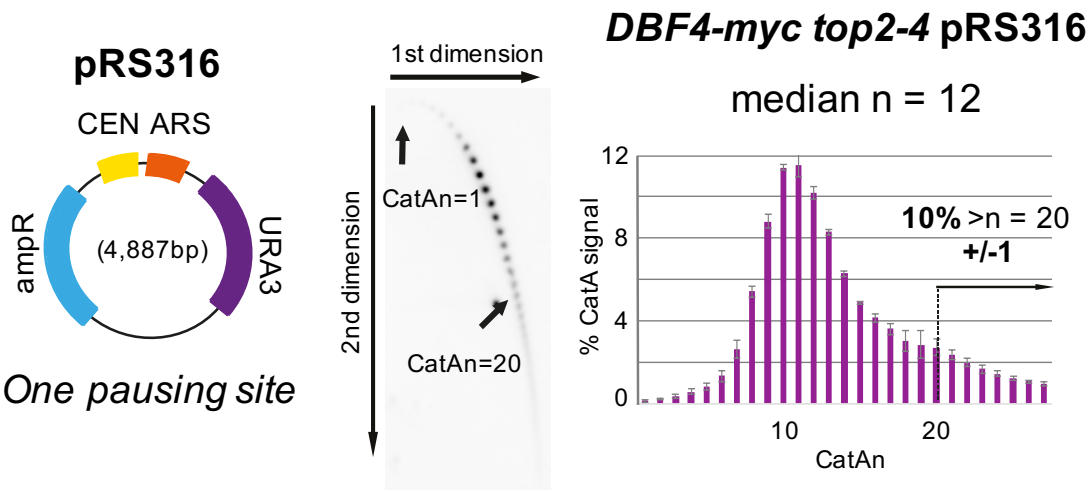

Figure 4.5: *DBF4-myc* does not alter fork rotation during DNA replication. Analysis of DNA catenation of plasmid pRS316 (indicated in the cartoon) in *DBF4-myc top2-4* cells was carried out as explained in Figure 3.2. Representative autoradiograms are indicated; the top arrow shows electrophoresis in the first dimension, and the side arrow shows electrophoresis in the second dimension. Histograms indicate the relative intensity of catenanes containing 1–27 catenated links (CatAn), along with the median of the whole distribution and percentage of catenanes from plasmids with >20 catenanes. Arrows show the mobility of plasmids containing 1 (*n* = 1) and 20 catenanes (*n* = 20). Error bars or values are average deviation. See Figure 3.2 for full explanation. Light blue, *ampR* gene; purple, *URA3* gene; other colours are as shown.

Table 4.1 represents the summary of the DNA catenation quantification experiments in plasmid pRS316.

Table 4.1: Summary of the results of DNA catenation quantification experiments in plasmid pRS316.

Strain plus (pRS316)	Plasmid size, bp	Number of replicates	Median CatAn	% >20
top2-4	4,887	5	13	14 ± 4
tof1Δ top2-4	4,887	2	>20	89 ± 2
csm3Δ top2-4	4,887	2	>20	89 ± 2
mrc1Δ top2-4	4,887	2	12	10 ± 3
ctf4Δ top2-4	4,887	2	12	17 ± 10
chl1Δ top2-4	4,887	2	12	11 ± 1
ctf18Δ top2-4	4,887	2	11	8
dia2Δ top2-4	4,887	2	13	16 ± 7
dpb3Δ top2-4	4,887	1	12	11
top2-4 **plus 200 mM HU**	4,887	2	11	8 ± 1
pol32Δ top2-4	4,887	5	10	6 ± 3
DBF4-myc top2-4	4,887	2	12	10 ± 1

4.4 Effect of Architectural Replisome Factors on Fork Rotation during Replication of Plasmid pRS426

Tof1/Csm3 are associated with stable fork pausing at sites that impede DNA replication (Hodgson et al., 2007). The pRS316 plasmid used in the first set of experiments contained one pause site. Therefore, it could be particularly affected by deletion of *TOF1* or *CSM3*. Hence, I decided to assess the effects of deleting *TOF1* and *MRC1* on the plasmid without pause sites (pRS426) on fork rotation and compared them with the observations for *top2-4* pRS426. I found that fork rotation was more highly catenated in the *tof1Δ* cells during the replication of plasmid pRS426 (median n > 20; 93% of plasmids had >20 catenations) compared to that observed during the replication of *top2-4* pRS426 (median n = 12; 8% of plasmids had >20 catenations) (Figure 4.6A and 3.6C). However, the levels of fork rotation after deletion of *MRC1* during the replication of plasmid pRS426 remained the same as that for *top2-4* pRS426 (median n = 12; 8% of plasmids had >20 catenations) (Figure 4.6B). I therefore concluded that Tof1/Csm3 do not require pause sites on the plasmid to inhibit excessive fork rotation. Table 4.2 displays the summary of the results of the DNA catenation quantification experiments in plasmid pRS426.

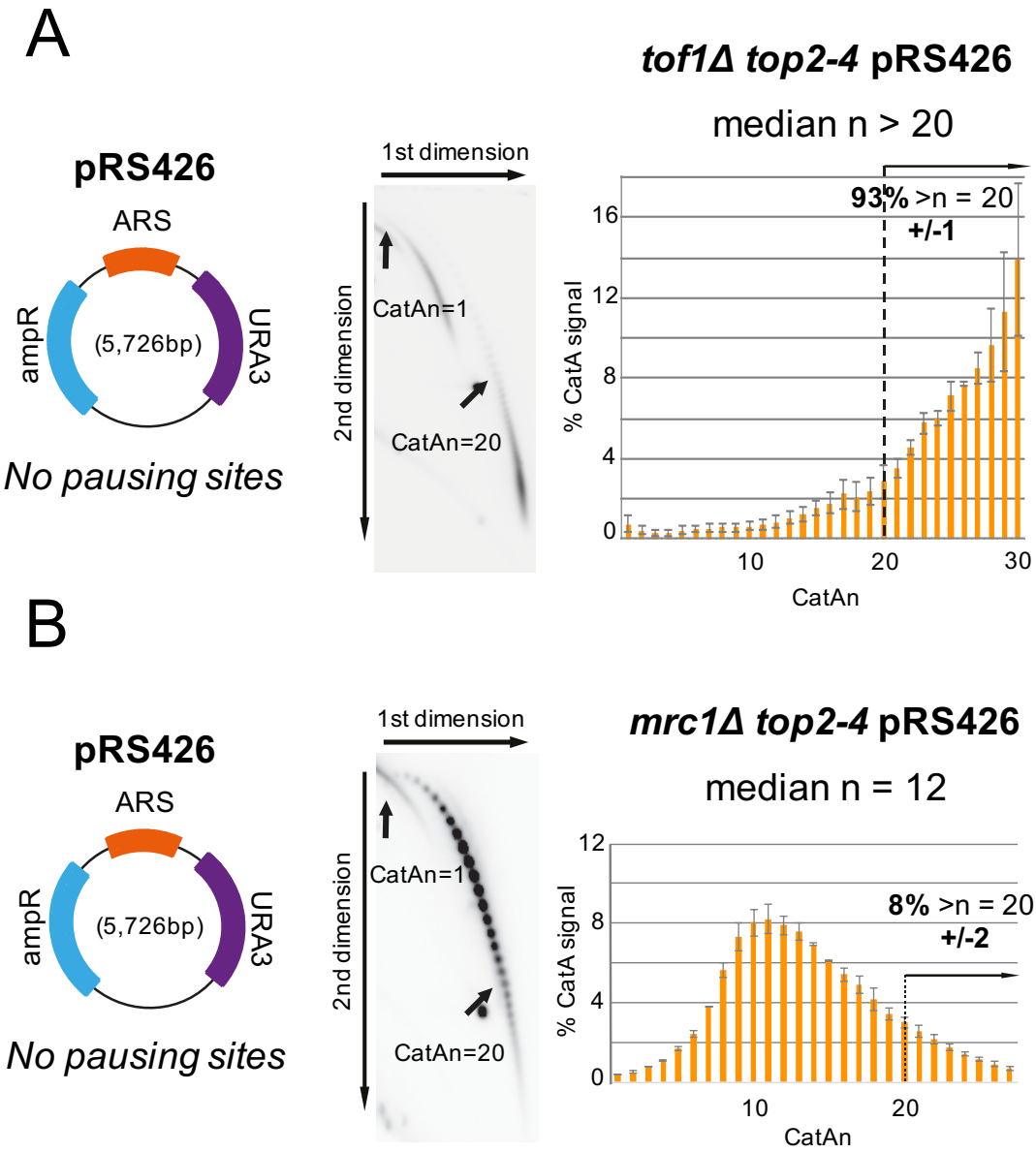

Figure 4.6: Frequency of fork rotation and pre-catenation increases generally in the *tof1Δ* cells, irrespective of the number of pause sites. Plasmid pRS426 (indicated in the cartoon) in (**A**) *tof1Δ top2-4* and (**B**) *mrc1Δ top2-4* cells were cultured and collected, DNA was prepared, and DNA catenation analysis was carried out as described in Figure 3.2. Representative autoradiograms are indicated; the top arrow shows electrophoresis in the first dimension, and the side arrow shows electrophoresis in the second dimension. Histograms indicate the relative intensity of catenanes containing 1–27 catenated links (CatAn), along with the median of the whole distribution and percentage of catenanes from plasmids with >20 catenanes. Arrows show the mobility of plasmids containing 1 (*n* = 1) and 20 catenanes (*n* = 20). Error bars or values are average deviation. See Figure 3.2 for full explanation. Light blue, *ampR* gene; purple, *URA3* gene; other colours are as shown.

Table 4.2: Summary of the results of the DNA catenation quantification experiments in plasmid pRS426.

Strain plus (pRS426)	Plasmid size, bp	Number of replicates	Median CatAn	% >20
top2-4	5,726	5	12	8 ± 2
tof1Δ top2-4	5,726	2	>20	93 ± 1
mrc1Δ top2-4	5,726	2	12	8 ± 2

4.5 Effect of Architectural Replisome Factors on Fork Rotation during Replication of Plasmid tRNApRS316

As described in Chapter 3, relatively high levels of fork rotation and pre-catenation were detected in the plasmid containing multiple pause sites i.e. tRNApRS316 with median *n* = 16 and with 28% of the population having >20 catenations (Figure 3.6D). In the initial screening of factors that may affect fork rotation, I observed clear increases in fork rotation following deletion of *TOF1*/*CSM3*. In order to determine if the addition of multiple tRNA genes to the plasmid would lead to other factors affecting fork rotation, I set out to identify how often fork rotation would take place if the number of pausing sites in the plasmid in different genetic backgrounds was increased.

To this end, I first tested the levels of fork rotation in cells deleted for *TOF1* to investigate the possible change in fork rotation observed in *tof1Δ* cells during DNA replication of plasmid tRNApRS316. As expected, the *tof1Δ* cells showed a considerable increase in catenation compared to *top2-4* tRNApRS316 cells, with median *n* > 20 and 95% of the population having >20 catenations (Figure 3.6D and 4.7A), in which (as also described in the previous section) the levels of fork rotation in the *tof1Δ* cells was independent of the number of difficult-to-replicate loci on the plasmids. Therefore, I concluded that Tof1 generally and actively inhibits fork rotation and pre-catenation during DNA replication.

I next assessed the effects of deleting *MRC1* on fork rotation during DNA replication of plasmid tRNApRS316. As shown in Figure 4.1C and 4.6B, a slight but consistent reduction in fork rotation and DNA pre-catenation was observed in plasmid pRS316 in the *mrc1Δ* cells. In *mrc1Δ top2-4* tRNApRS316 cells, the median was 13 with 19% of the plasmid being highly catenated (decrease from 28% to 19%, Figure 4.7B). This was in contrast with the DNA catenation for plasmid tRNApRS316 in wild-type cells as well as my previous observation that the levels of fork rotation in *mrc1Δ top2-4* pRS426 was the same as that for *top2-4* pRS426. This result was indicative of the possibility that Mrc1 promotes fork rotation during the replication of plasmid tRNApRS316. The confirmation of this

data was further carried out in different genetic backgrounds and will be explained in detail in the next chapter.

I then aimed to determine how often fork rotation was occurring in the *ctf4Δ*, *chl1Δ*, *ctf18Δ*, *dia2Δ* and *dpb3Δ* cells during replication of plasmid tRNApRS316. However, no clear increase or decrease in the levels of DNA catenanes formed on the plasmid could be observed in any of these mutants. The median and distribution of the genes in question were as follows: *ctf4Δ top2-4* tRNApRS316 (median *n* = 15; 25% of plasmids had >20 catenations); *chl1Δ top2-4* tRNApRS316 (median *n* = 15; 23% of plasmids had >20 catenations); *ctf18Δ top2-4* tRNApRS316 (median *n* = 15; 29% of plasmids had >20 catenations); *dia2Δ top2-4* tRNApRS316 (median *n* = 17; 32% of plasmids had >20 catenations) and *dpb3Δ top2-4* tRNApRS316 (median *n* = 16; 32% of plasmids had >20 catenations) (Figure 4.7 C, D, E, F and G). Thus, the experiments so far suggested that in budding yeast, Ctf4, Chl1, Ctf18, Dia2 and Dpb3 do not inhibit fork rotation and DNA pre-catenation during DNA replication. However, interestingly, Mrc1 seemed to promote fork rotation during DNA replication at tRNAs and potentially at centromeres.

As shown and discussed in Figure 4.4C, I also observed a reduction in the number of DNA catenanes in *pol32Δ top2-4* pRS316. To confirm the result, I repeated the experiment with the tRNApRS316 plasmid. A clear decrease in the number of DNA catenanes was also detected in *pol32Δ top2-4* tRNApRS316 with median *n* = 13 and with 18% of the population having >20 catenations (decrease from 28% to 18%, Figure 4.7H). This result suggested that loss of *POL32* function lead to decreased fork rotation and DNA pre-catenation during DNA replication of these replicons.

As mentioned earlier, Swi1 and Swi3 (Tof1 and Csm3 homologs) functionally associate with the Hsk1-Dfp1 complex (Cdc7-Dbf4 homolog) in fission yeast (Matsumoto et al., 2005). Although no excessive fork rotation was detected in *DBF4-myc* with the pR316 plasmid, I wanted to check whether the addition of tRNA genes to the plasmid made them more susceptible to Cdc7-Dbf4 function. Cells with *DBF4-myc* did not show a clear change in the extent of fork rotation in

the tRNApRS316 plasmid compared to the wild-type cells. In these cells, the median was 15 with 23% of the population having >20 catenations (Figure 4.7I). Next, to examine if potentially stronger loss of *CDC7* function caused changes in fork rotation, I assessed fork rotation in the *cdc7Δ mcm5-bob1 top2-4* tRNApRS316 strain. Deletion of *CDC7* is lethal; however, this lethality can be suppressed by the *mcm5-bob1* (Mcm5-P83L) mutation, i.e. a mutant allele of *MCM5* known as *bob1* can bypass the lethality of *CDC7* (Hardy et al., 1997). I found that *cdc7Δ mcm5-bob1 top2-4* showed an increase in fork rotation during DNA replication of the tRNApRS316 plasmid with median *n* = 18 and with 38% of the population having >20 catenations compared to the wild-type (increase from 28% to 38%, Figure 4.7K). Interestingly, an obvious reduction in the number of DNA catenanes was observed in *mcm5-bob1 top2-4* tRNApRS316 with median *n* = 13 and with 16% of the population having >20 catenations (decrease from 28% to 16%, Figure 4.7J). Together, these data suggested that Cdc7 potentially inhibits fork rotation during DNA replication, which implied that Cdc7 might be associated with Tof1 functionally in budding yeast as well as in fission yeast. Since the presence of *mcm5-bob1* reduces fork rotation when wild-type levels of *CDC7* are present, it appears that *mcm5-bob1* may partially neutralize the *CDC7* phenotype in a manner that reduces the level of fork rotation observed. Thus, in the future, it is essential to confirm this result using different methods to eliminate Cdc7 activity in a manner that would still allow origin firing. Table 4.3 represents the summary of the results of the DNA catenation quantification experiments in plasmid tRNApRS316.

A

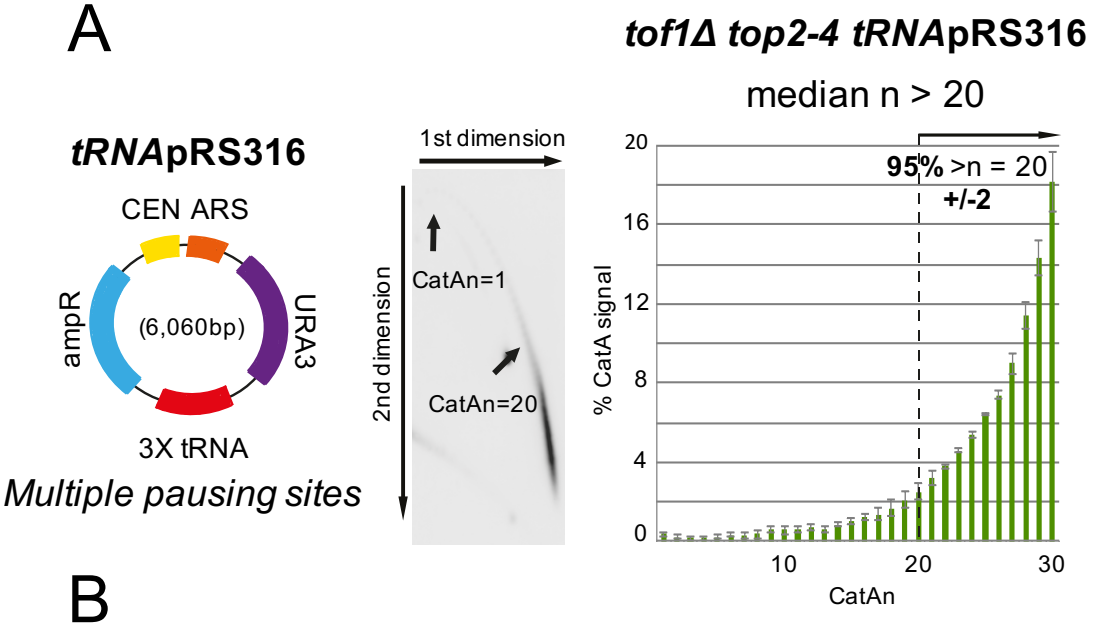
tRNApRS316
CEN ARS
ampR
URA3
(6,060bp)
3X tRNA
Multiple pausing sites
1st dimension
2nd dimension
CatAn=1
CatAn=20
tof1Δ top2-4 tRNApRS316
median n > 20
95% >n = 20
+/-2
% CatA signal
CatAn

B

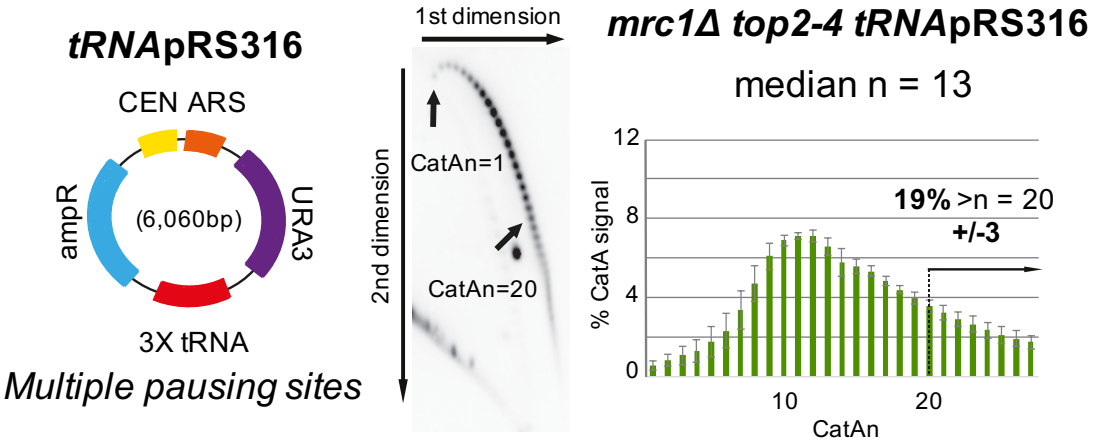
tRNApRS316
CEN ARS
ampR
URA3
(6,060bp)
3X tRNA
Multiple pausing sites
1st dimension
2nd dimension
CatAn=1
CatAn=20
mrc1Δ top2-4 tRNApRS316
median n = 13
19% >n = 20
+/-3
% CatA signal
CatAn

C

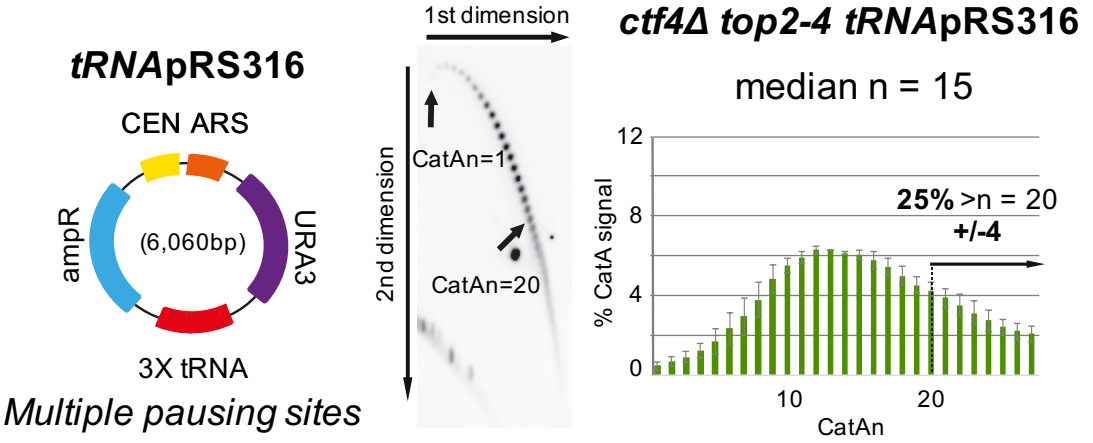
tRNApRS316
CEN ARS
ampR
URA3
(6,060bp)
3X tRNA
Multiple pausing sites
1st dimension
2nd dimension
CatAn=1
CatAn=20
ctf4Δ top2-4 tRNApRS316
median n = 15
25% >n = 20
+/-4
% CatA signal
CatAn

D

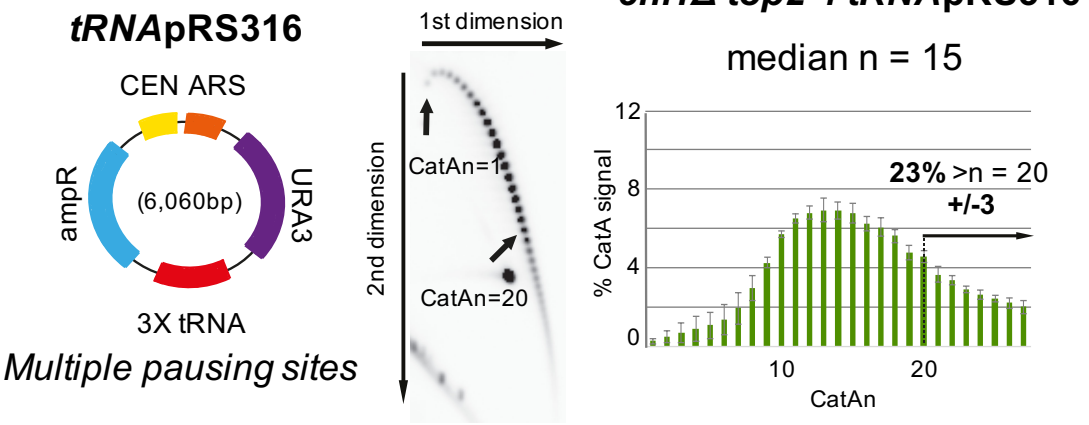
tRNApRS316
CEN ARS
ampR
URA3
(6,060bp)
3X tRNA
Multiple pausing sites
1st dimension
2nd dimension
CatAn=1
CatAn=20
chl1Δ top2-4 tRNApRS316
median n = 15
% CatA signal
23% >n = 20
+/-3
CatAn

E

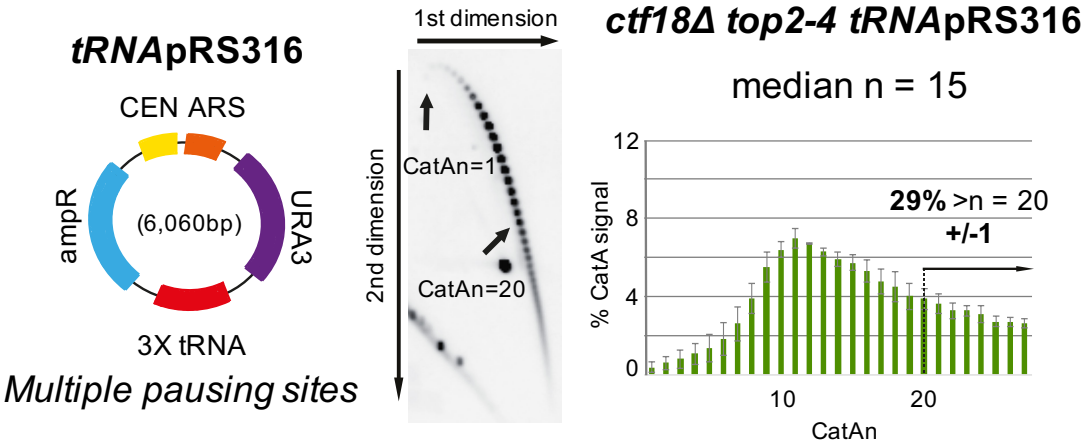
tRNApRS316
CEN ARS
ampR
URA3
(6,060bp)
3X tRNA
Multiple pausing sites
1st dimension
2nd dimension
CatAn=1
CatAn=20
ctf18Δ top2-4 tRNApRS316
median n = 15
% CatA signal
29% >n = 20
+/-1
CatAn

F

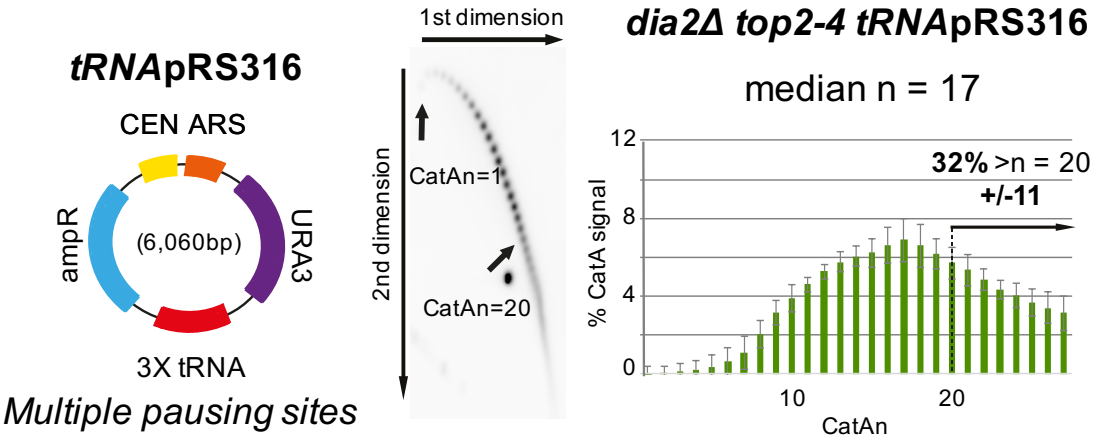
tRNApRS316
CEN ARS
ampR
URA3
(6,060bp)
3X tRNA
Multiple pausing sites
1st dimension
2nd dimension
CatAn=1
CatAn=20
dia2Δ top2-4 tRNApRS316
median n = 17
% CatA signal
32% >n = 20
+/-11
CatAn

G

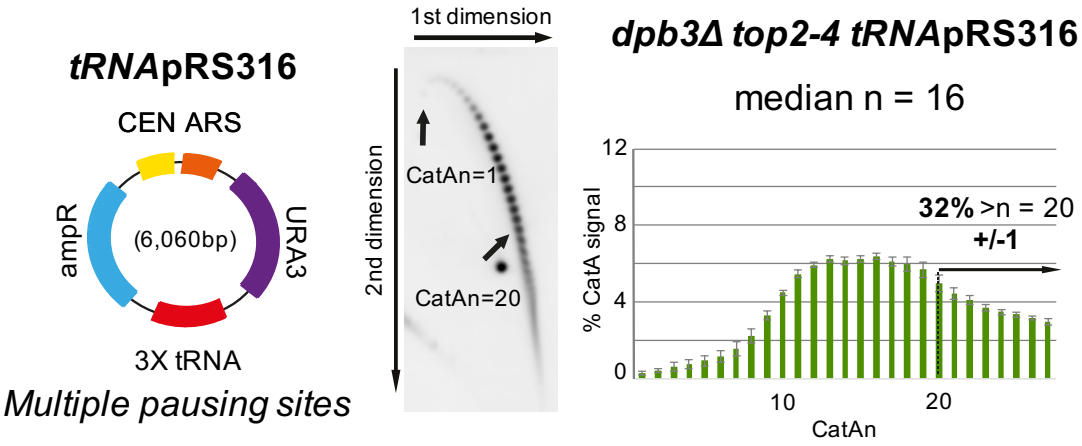
tRNApRS316
CEN ARS
ampR
URA3
(6,060bp)
3X tRNA
Multiple pausing sites
1st dimension
2nd dimension
CatAn=1
CatAn=20
dpb3Δ top2-4 tRNApRS316
median n = 16
32% >n = 20
+/-1
% CatA signal
CatAn

H

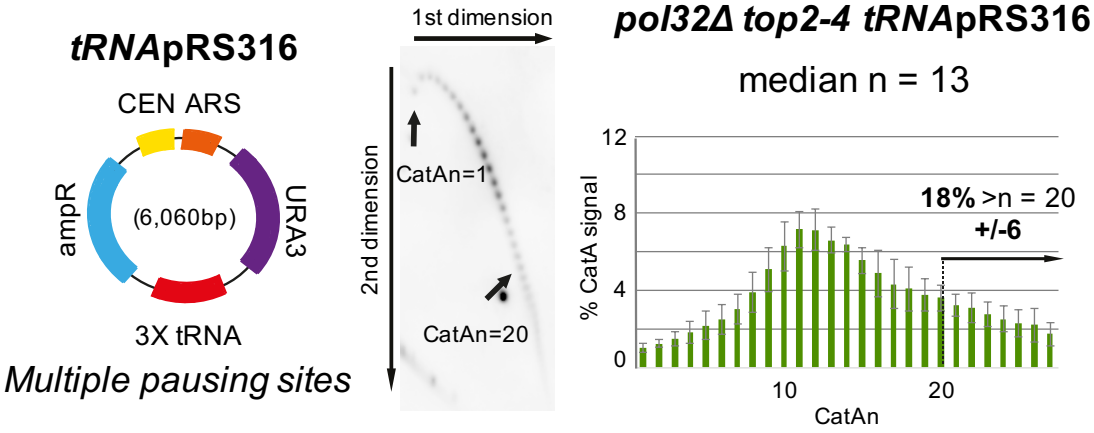
tRNApRS316
CEN ARS
ampR
URA3
(6,060bp)
3X tRNA
Multiple pausing sites
1st dimension
2nd dimension
CatAn=1
CatAn=20
pol32Δ top2-4 tRNApRS316
median n = 13
18% >n = 20
+/-6
% CatA signal
CatAn

I

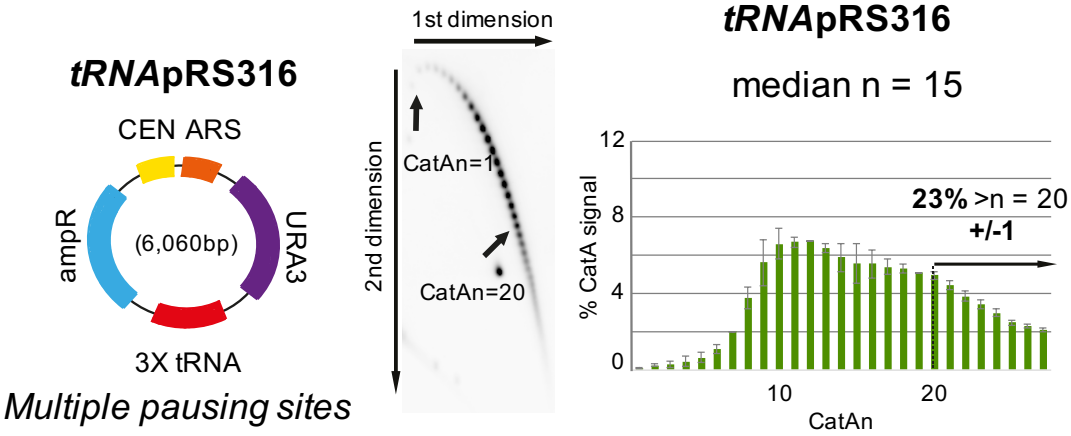
tRNApRS316
CEN ARS
ampR
URA3
(6,060bp)
3X tRNA
Multiple pausing sites
1st dimension
2nd dimension
CatAn=1
CatAn=20
DBF4-myc top2-4
tRNApRS316
median n = 15
23% >n = 20
+/-1
% CatA signal
CatAn

J

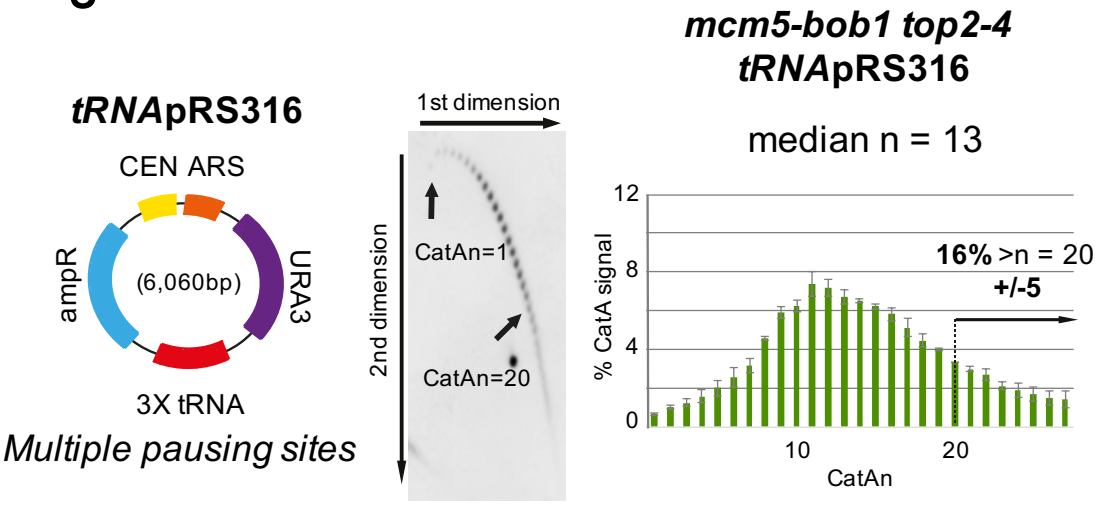
tRNApRS316
CEN ARS
ampR
URA3
(6,060bp)
3X tRNA
Multiple pausing sites
1st dimension
2nd dimension
CatAn=1
CatAn=20
mcm5-bob1 top2-4
tRNApRS316
median n = 13
16% >n = 20
+/-5
% CatA signal
CatAn
0
4
8
12
10
20

K

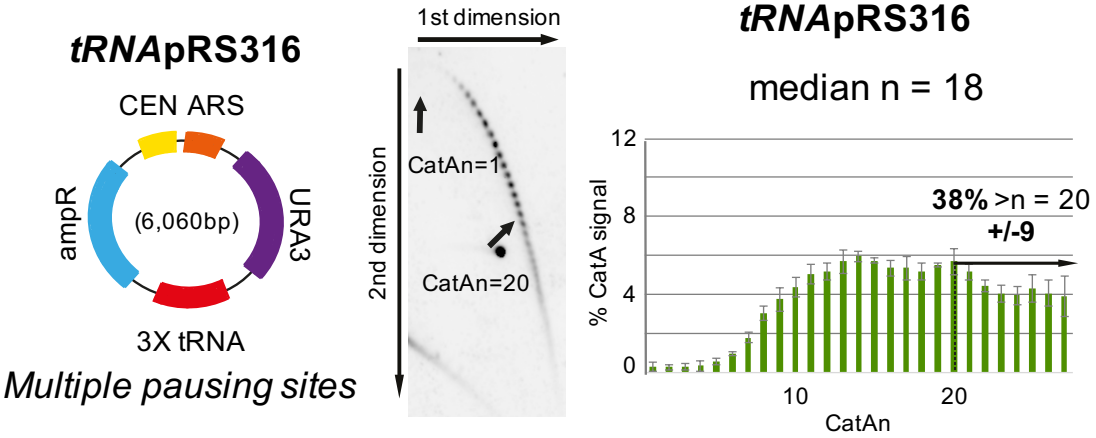
tRNApRS316
CEN ARS
ampR
URA3
(6,060bp)
3X tRNA
Multiple pausing sites
1st dimension
2nd dimension
CatAn=1
CatAn=20
cdc7Δ mcm5-bob1 top2-4
tRNApRS316
median n = 18
38% >n = 20
+/-9
% CatA signal
CatAn
0
4
8
12
10
20

Figure 4.7: Frequency of fork rotation and pre-catenation in different genetic backgrounds in plasmid tRNApRS316.
Frequency of fork rotation and pre-catenation was increased in *tof1Δ* cells, irrespective of the number of pause sites. Loss of *MRC1* and *POL32* function lead to decreased fork rotation and DNA pre-catenation. Deletion of *CDC7* in the *mcm5-bob1* background seemed to promote fork rotation, but this increase appeared modest compared with that in the *tof1Δ* cells.
DNA catenation analysis of plasmid tRNApRS316 (indicated in the cartoon) in *top2-4* cells and the different deletion alleles (**A**) *tof1Δ*, (**B**) *mrc1Δ*, (**C**) *ctf4Δ*, (**D**) *chl1Δ*, (**E**) *ctf18Δ*, (**F**) *dia2Δ*, (**G**) *dbp3Δ*, (**H**) *pol32Δ,* (**I**) *DBF4-myc*, (**J**) *mcm5-bob1* and (**K**) *cdc7Δ mcm5-bob1* was carried out as described in Figure 3.2. Representative autoradiograms are indicated; the top arrow shows electrophoresis in the first dimension, and the side arrow shows electrophoresis in the second dimension. Histograms indicate the relative intensity of catenanes containing 1–27 catenated links (CatAn), along with the median of the whole distribution and percentage of catenanes from plasmids with >20 catenanes. Arrows show the mobility of plasmids containing 1 (*n* = 1) and 20 catenanes (*n* = 20). Error bars or values are average deviation. See Figure 3.2 for full explanation. Light blue, *ampR* gene; purple, *URA3* gene; other colours are as shown.

Table 4.3: Summary of the results of the DNA catenation quantification experiments in plasmid tRNApRS316.

Strain plus (*tRNA*pRS316)	Plasmid size, bp	Number of replicates	Median CatAn	% >20
top2-4	6,060	3	16	28 ± 1
tof1Δ top2-4	6,060	2	>20	95 ± 2
mrc1Δ top2-4	6,060	4	13	19 ± 3
ctf4Δ top2-4	6,060	2	15	25 ± 4
chl1Δ top2-4	6,060	3	15	23 ± 3
ctf18Δ top2-4	6,060	2	15	29 ± 1
dia2Δ top2-4	6,060	3	17	32 ± 11
dpb3Δ top2-4	6,060	4	16	32 ± 1
pol32Δ top2-4	6,060	4	13	18 ± 6
dbf4-myc top2-4	6,060	2	15	23 ± 1
mcm5-bob1 top2-4	6,060	2	13	16 ± 5
cdc7Δ mcm5-bob1 top2-4	6,060	4	18	38 ± 9

4.6 Conclusions

Our data indicated that, in yeast, the occurrence of fork rotation is less frequent during DNA replication, unless in certain chromosomal contexts. Hence, it was predicted that either the levels of DNA topoisomerases are generally sufficient *in vivo* ahead of the fork during normal DNA replication to prevent the accumulation of torsional stress, or the structure of the replisome is resistant to rotation and thus fork rotation only occurs in certain chromosomal contexts. I therefore decided to investigate the architectural replisome components that could be crucial in determining how often the replisome rotates. I found that the evolutionary conserved Timeless/Tipin factors, Tof1/Csm3, restrict fork rotation during DNA replication in budding yeast. It is currently elusive as to how Tof1/Csm3 mechanistically inhibit fork rotation. However, based on a previous study by Hodgson et al. (2007) that indicated that Tof1/Csm3, but not Mrc1, are essential for the replisome to pause at stable protein-DNA sites (Hodgson et al., 2007), I believe that fork rotation and pausing might be linked. Potentially, in wild-type cells, Tof1/Csm3 restrict fork rotation and hence DNA unwinding at difficult-to-replicate loci, which leads to fork pausing. In the absence of Tof1/Csm3, excessive fork rotation leads to DNA unwinding; thus, no pausing at such sites seemed to occur. I then wondered whether mechanistically the function of Tof1/Csm3 in inhibiting fork rotation could be due to either of the following two reasons. The first is that the replisome structure could be disrupted in the absence of Timeless/Tipin orthologues, which could potentially lead to excessive fork rotation compared to that in the wild-type, because Timeless/Tipin proteins have been shown to be involved in coordinating the actions of the helicase and the leading strand polymerase; in their absence, this cooperation seems to be disrupted (Errico et al., 2009, Bando et al., 2009, Cho et al., 2013). This explanation would suggest that the presence of Tof1/Csm3 typically maintains the replisome structure in a conformation that is resistant to rotation. An alternative explanation for the role of Tof1/Csm3 in preventing fork rotation could be that Tof1 actively recruits type IB topoisomerase to the fork to relax supercoiling, which is based on the fact that Tof1 has been shown to interact with eukaryotic topoisomerase I, both in yeast two-hybrid assay and *in vitro* (Park and Sternglanz, 1999). Therefore, this interaction might lead to the resolution of

topological stress by topoisomerase I at the fork and therefore prevent excessive fork rotation. Taken together, our data indicate that the torsional stress ahead of the fork is relaxed by DNA topoisomerases as well as the replication machinery involving Tof1/Csm3 at least in budding yeast. This suggests that fork rotation only occurs where it is required, such as at termination or at stable protein-DNA complexes or wherever the activity of topoisomerases is limited, and that fork rotation in these cases is the only pathway to unwind DNA.

Furthermore, I showed that *cdc7Δ mcm5-bob1* might potentially increase fork rotation during replication in plasmids containing multiple pause sites; however, a substantial decrease in *mcm5-bob1* was also observed. One explanation for this could be that the number of DNA catenanes in *cdc7Δ* cells might be partially neutralized by *mcm5-bob1*; therefore, in the future, it is crucial to examine the effects of elimination of Cdc7 activity in a manner that would still allow origin firing. As mentioned in the first chapter of this thesis (see section 1.2.3.2), studies in fission and budding yeasts have revealed that DDK interacts with Tof1/Csm3 (Matsumoto et al., 2005, Murakami and Keeney, 2014). Furthermore, *in vivo*, Tof1 is released from the chromatin fractions when DDK is inactivated (Bastia et al., 2016). *In vitro*, phosphorylation of Mcm2-7 and CMG by DDK leads to the recruitment of phosphorylated Tof1 at the replisome. However, it remains unknown whether this interaction leads to the phosphorylation of Tof1 by DDK (Bastia et al., 2016). These data suggest that Cdc7 might phosphorylate Tof1 and that this phosphorylation increases the efficiency of Tof1 function in preventing fork rotation.

I also observed that *MRC1* deletion reduced fork rotation only on plasmids containing pause sites. However, this reduction was not detected at termination, i.e. on the plasmid without pause sites (pRS426). These results suggested that Mrc1 promotes only the fork rotation occurring during elongation but not that occurring at termination. Details about experiments conducted for further confirmation and discussion about Mrc1 are included in the next chapter.

I also found that excessive fork rotation observed in the absence of *TOF1* was not due to general fork slowing, as indicated by the frequency of fork rotation in

the absence of *DPB3* or in cells under HU treatment. However, a clear and consistent reduction in the levels of fork rotation was detected during DNA replication in the absence of the lagging strand DNA polymerase, *POL32*. Further discussion and explanation for why Pol32 may lead to a decrease in the frequency of fork rotation during DNA replication is included in Chapter 6.

Chapter 5

Investigating the Role of Mrc1 in Fork Rotation

5.1 Objective

Tof1, Csm3, and Mrc1 are the three proteins that form a complex and have been found to co-localize at both normal and stalled replication forks (see introduction; section 1.2.3.1 and 1.2.3.2) (Noguchi et al., 2004, Calzada et al., 2005, Nedelcheva et al., 2005). Our data indicate that Tof1/Csm3 generally restrict fork rotation during DNA replication. In contrast, Mrc1 appeared to promote fork rotation only at tRNAs and possibly at centromeres during replication elongation, but this promotion did not appear to affect the fork rotation occurring during termination. In this chapter, my initial aim was to confirm that Mrc1 deletion reduces the frequency of fork rotation. In addition, I examined if the phenotype observed is associated with the replication function of Mrc1 or with its checkpoint function.

5.2 Approach

In order to generate strains for use in these experiments, I created *tof1Δ mrc1Δ top2-4* cells, wherein the mutants were constructed by mating the 'a' and 'α' mating types of the existing strains as described in section 2.1.3 of the Materials and Methods. I also created *mrc1Δ top2-td GALTOP2Y-F* cells as described in section 2.1.4. Strain *top2-td GALTOP2Y-F* used in this chapter had already been created and was stored in the JB lab collection as mentioned in Table 2.1. In this chapter, to examine fork rotation *in vivo*, I again performed a plasmid DNA catenation assay as previously described in Chapter 3 (Figure 3.2) for use with yeast episomal plasmids.

5.3 Confirmation of the Effect of Mrc1 on Fork Rotation during DNA Replication

In the previous chapter, I found that Mrc1 promotes fork rotation during DNA replication on plasmids containing tRNAs and potentially centromeres. In order to further confirm this phenotype, I decided to evaluate this effect in a more extreme situation using the Top2Y-F strain established by Baxter and Diffley (2008). In the Top2Y-F strain, a catalytically inactive form of Top2 is expressed

from a galactose-inducible promoter in the *top2-td* background. To create this mutant, the authors changed the active site tyrosine at position 782 (which generates the transient phosphodiester bond with the DNA backbone) to phenylalanine (Top2Y-F), so that the mutant could bind to DNA but could not catalyse strand breakage (Morais Cabral et al., 1997, Liu and Wang, 1998, Baxter and Diffley, 2008). To generate the *top2-td* strain, Baxter and Diffley (2008) replaced the endogenous *TOP2* gene with a heat-inducible "degron" allele *top2-td* expressed from a doxycycline-repressible promoter to deplete wild-type Top2 protein from yeast cells (Baxter and Diffley, 2008). The authors showed that Top2 protein is conditionally depleted under the following restrictive conditions. The first condition is when the *TOP2* gene is placed under the control of the TetR/TetO-repressible promoter (Belli et al., 1998), which represses transcription when doxycycline is added to the culture. The second condition is when the cellular concentration of Ubr1 is highly increased in the presence of galactose. The target protein is tagged with a degron moiety (*top2-td*) and when the degron moiety is accessible, the high levels of E3 ligase leads to an increase in polyubiquitination of the degron moiety, resulting in the degradation of the target protein by the proteasome. Finally, the degron system is temperature-sensitive and therefore shifting the culture to the restrictive temperature of 37°C leads to unfolding of the degron moiety attached to the protein of interest, thus exposing internal lysine sites and promoting its polyubiquitination and protein degradation via the proteasome (Baxter and Diffley, 2008). Hence, the restrictive conditions under which the tet-degron system is used include the addition of doxycycline, galactose, and an increase in temperature from 25°C to 37°C.

To assess the number of DNA catenanes in the *top2-td GALTOP2Y-F* strain containing the pRS316 plasmid, the cells were arrested in the G1 phase by the alpha factor mating pheromone and then the Top2-td protein was degraded by shifting the culture to the restrictive conditions for 1 h. The cells were then released from the alpha factor arrest under the restrictive conditions explained above into the cell cycle in the presence of nocodazole and collected 90 min after release. I then purified and nicked the DNA as described in Figure 3.2. As shown in Figure 5.1A, DNA catenanes with a median of more than 20 were introduced in *top2-td GALTOP2Y-F* cells containing the pRS316 plasmid with 64% of the

distribution containing >20 catenanes, as predicted from the earlier analysis of one dimensional gels (Baxter and Diffley, 2008). I then wondered if knocking out MRC1 in the *top2-td GALTOP2Y-F* strain containing pRS316 would change the levels of catenated plasmid. Surprisingly, I observed a significant reduction in the frequency of fork rotation and pre-catenation in *mrc1Δ top2-td GALTOP2Y-F* with a median of 13 and with 22% of the distribution containing >20 catenanes (Figure 5.1 B). I confirmed that this change was not due to changes in TOP2Y-F expression in this background, since the proteins levels of expressed TOP2Y-F were the same in the wild-type and *mrc1Δ* cells (Figure 5.1 C). These results indicated that the Claspin homolog, Mrc1, facilitates the fork rotation occurring in the *top2-td GALTOP2Y-F* strain.

Next, to further show this phenotype, I decided to knock out both Tof1 and Mrc1 in *top2-4* background cells. As expected, the simultaneous loss of Mrc1 and Tof1 resulted in a more severe growth defect; I used the approach represented in Figure 3.2 and surprisingly observed that the number of DNA catenanes was decreased in *mrc1Δ tof1Δ top2-4* containing pRS316 plasmid. The median was still in excess of 20; however, 54% of the distribution contained >20 catenanes (decrease from 89% to 54%, Figure 5.1D). The same phenotype was also detected using the tRNApRS316 plasmid in the same background cells; the median was still in excess of 20 and 66% of plasmids had >20 catenations (decrease from 95% to 66%, Figure 5.1E). I therefore concluded that MRC1 promotes fork rotation and DNA pre-catenation during DNA replication under conditions that normally lead to frequent fork rotation. Table 5.1 represents the summary of the DNA catenation quantification experiments.

A

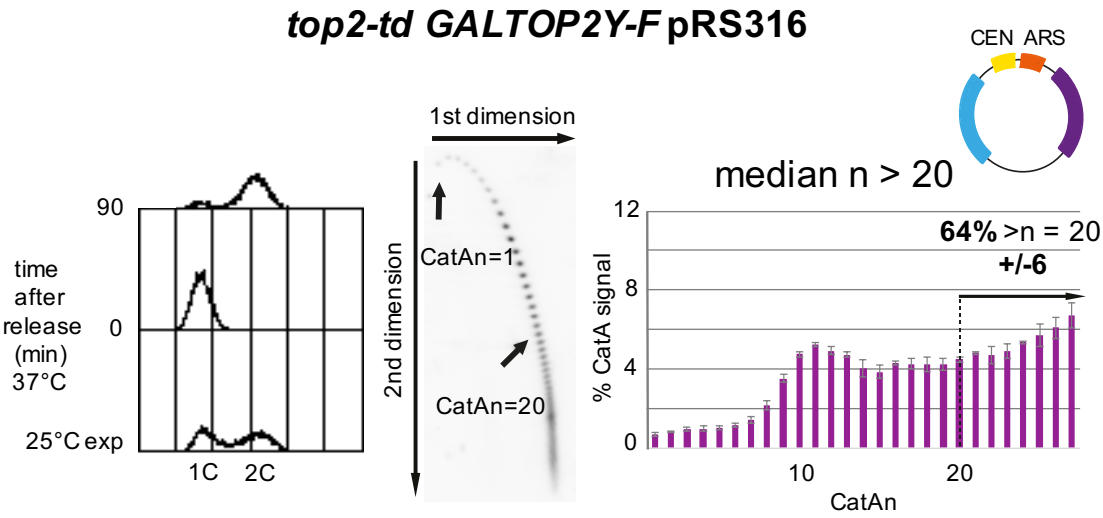
top2-td GALTOP2Y-F pRS316
CEN ARS
1st dimension
2nd dimension
CatAn=1
CatAn=20
time after release (min) 37°C
90
0
25°C exp
1C 2C
median n > 20
64% >n = 20
+/-6
% CatA signal
12
8
4
0
10
20
CatAn

B

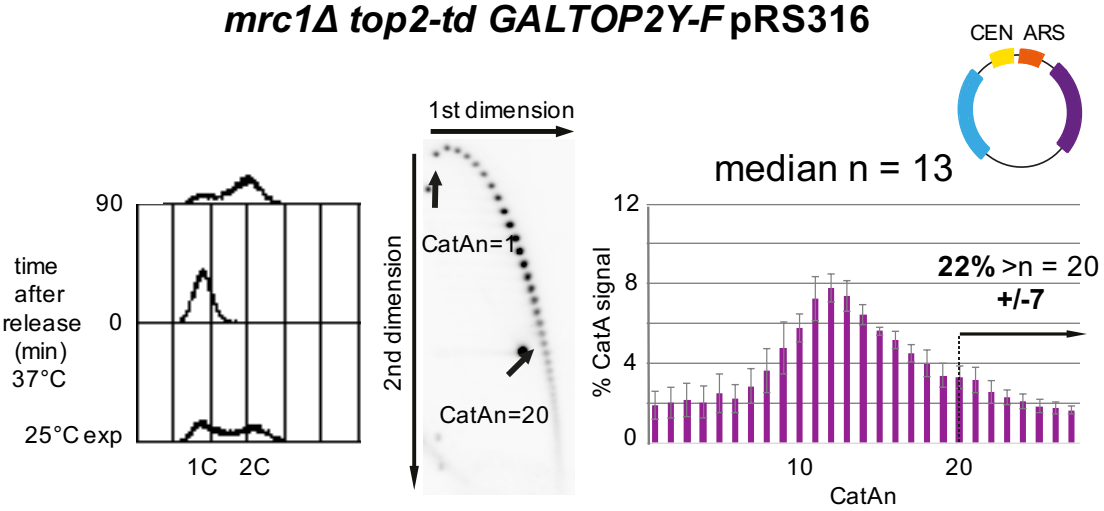
mrc1Δ top2-td GALTOP2Y-F pRS316
CEN ARS
1st dimension
2nd dimension
CatAn=1
CatAn=20
time after release (min) 37°C
90
0
25°C exp
1C 2C
median n = 13
22% >n = 20
+/-7
% CatA signal
12
8
4
0
10
20
CatAn

C

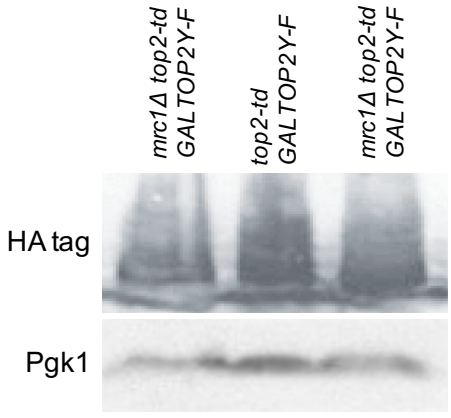
mrc1Δ top2-td GALTOP2Y-F
top2-td GALTOP2Y-F
mrc1Δ top2-td GALTOP2Y-F
HA tag
Pgk1

D

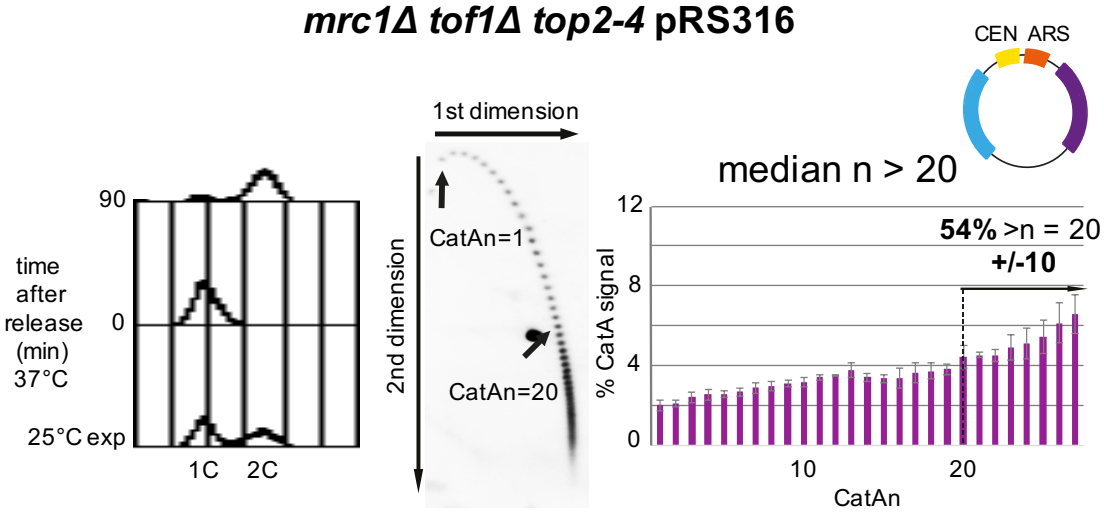
mrc1Δ tof1Δ top2-4 pRS316
CEN ARS
1st dimension
median n > 20
time after release (min) 37°C
90
0
25°C exp
1C 2C
2nd dimension
CatAn=1
CatAn=20
% CatA signal
12
8
4
0
54% >n = 20
+/-10
10
20
CatAn

E

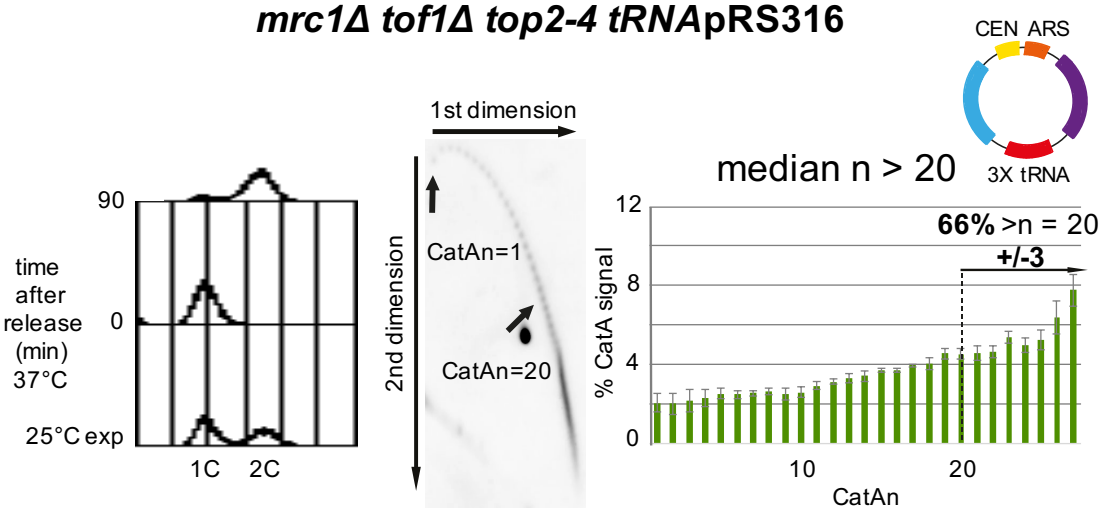
mrc1Δ tof1Δ top2-4 tRNApRS316
CEN ARS
3X tRNA
1st dimension
median n > 20
time after release (min) 37°C
90
0
25°C exp
1C 2C
2nd dimension
CatAn=1
CatAn=20
% CatA signal
12
8
4
0
66% >n = 20
+/-3
10
20
CatAn

Figure 5.1: The yeast *Claspin* homolog, *MRC1*, promotes fork rotation and DNA pre-catenation.
Analysis of DNA catenation of plasmid pRS316 in (**A**) *top2-td GALTO2Y-F* (**B**) *mrc1Δ top2-td GALTOP2Y-F* (**D**) *mrc1Δ tof1Δ top2-4* and plasmid tRNApRS316 in (**E**) *mrc1Δ tof1Δ top2-4* cells was carried out as explained in Figure 3.2. FACS for DNA content is also depicted. Representative autoradiograms are indicated; the top arrow shows electrophoresis in the first dimension, and the side arrow shows electrophoresis in the second dimension. Histograms indicate the relative intensity of catenanes containing 1–27 catenated links (CatAn), along with the median of the whole distribution and percentage of catenanes from plasmids with >20 catenanes. Arrows show the mobility of plasmids containing 1 (*n* = 1) and 20 catenanes (*n* = 20). Error bars or values are average deviation. See Figure 3.2 for full explanation. Light blue, *ampR* gene; purple, *URA3* gene; other colours are as shown. (**C**) Western blot analysis of exogenously expressed Top2 (HA tag) in *top2-td GALTOP2Y-F* and *mrc1Δ top2-td GALTOP2Y-F* cells. Samples were prepared for western blot analysis using whole-cell TCA extraction (as described in section 2.1.10). Western blot was carried out as described in section 2.4.2, and the samples were run on a 6% polyacrylamide gel. Pgk1 western blot of the same lanes is shown for loading comparison.

5.4 Potential Action of Checkpoint through Mrc1 Phosphorylation

As mentioned in Chapter 1, in budding yeast, Mrc1 performs two functions. First, Mrc1 acts as a non-essential component of the replisome and is required for normal DNA replication (Katou et al., 2003, Osborn and Elledge, 2003). Second, at the S phase checkpoint in budding yeast, Mrc1 is hyperphosphorylated by upstream checkpoint kinases, which leads to the activation of the downstream checkpoint kinase, Rad53 (Alcasabas et al., 2001, Osborn and Elledge, 2003). *mrc1-AQ* is a mutant in which all the possible Mec1 S/TQ phosphorylation sites have been mutated to non-phosphorylatable AQ. This allele shows a defect only in checkpoint signalling to activate Rad53, but not in replisome progression; this has been measured by DNA content analysis, which have shown that the rate of replication fork progression is almost normal (Alcasabas et al., 2001, Osborn and Elledge, 2003). The existence of *mrc1-AQ* indicates that the two functions of Mrc1, i.e. replication and checkpoint regulation, are independent of each other.

I also found that *MRC1* deletion reduces fork rotation on a plasmid with multiple pausing sites (tRNApRS316) and possibly on a plasmid with one pause site

(pRS316). I also further confirmed this phenotype in two different strains with high levels of fork rotation. I then aimed to determine whether the result obtained for Mrc1 is associated with the checkpoint role of Mrc1 or if it is replication dependent. To this end, I obtained two plasmids: *mrc1-AQ*, which is defective in full Rad53 activation but is competent in DNA replication, and wild-type *MRC1* (Osborn and Elledge, 2003). I also checked the sequences of both plasmids using primers indicated in Table 2.3 in the Materials and Methods section (primers numbers: 67-73), and I could successfully confirm that in *mrc1-AQ* 17 SQ and TQ motifs were changed to AQ throughout the molecule consistent with the *mrc1-AQ* plasmid in the study by Osborn and Elledge (Osborn and Elledge, 2003). I then introduced these two plasmids separately in the *mrc1Δ top2-4* strain containing a plasmid with multiple pause sites (tRNApRS316). Similar levels of fork rotation were detected in *mrc1-AQ* (median *n* = 15; 27% of plasmids had >20 catenations) (Figure 5.2A) compared to the wild-type *MRC1* (median *n* = 16; 32% of plasmids had >20 catenations) (Figure 5.2B). Therefore, these data suggested that the observed phenotype in *mrc1Δ* cells is not potentially dependent on the checkpoint function of Mrc1; instead, the sole dependency for the observed phenotype seems to be on the replication function of Mrc1 during replication elongation. Table 5.1 indicates the summary of the DNA catenation quantification experiments.

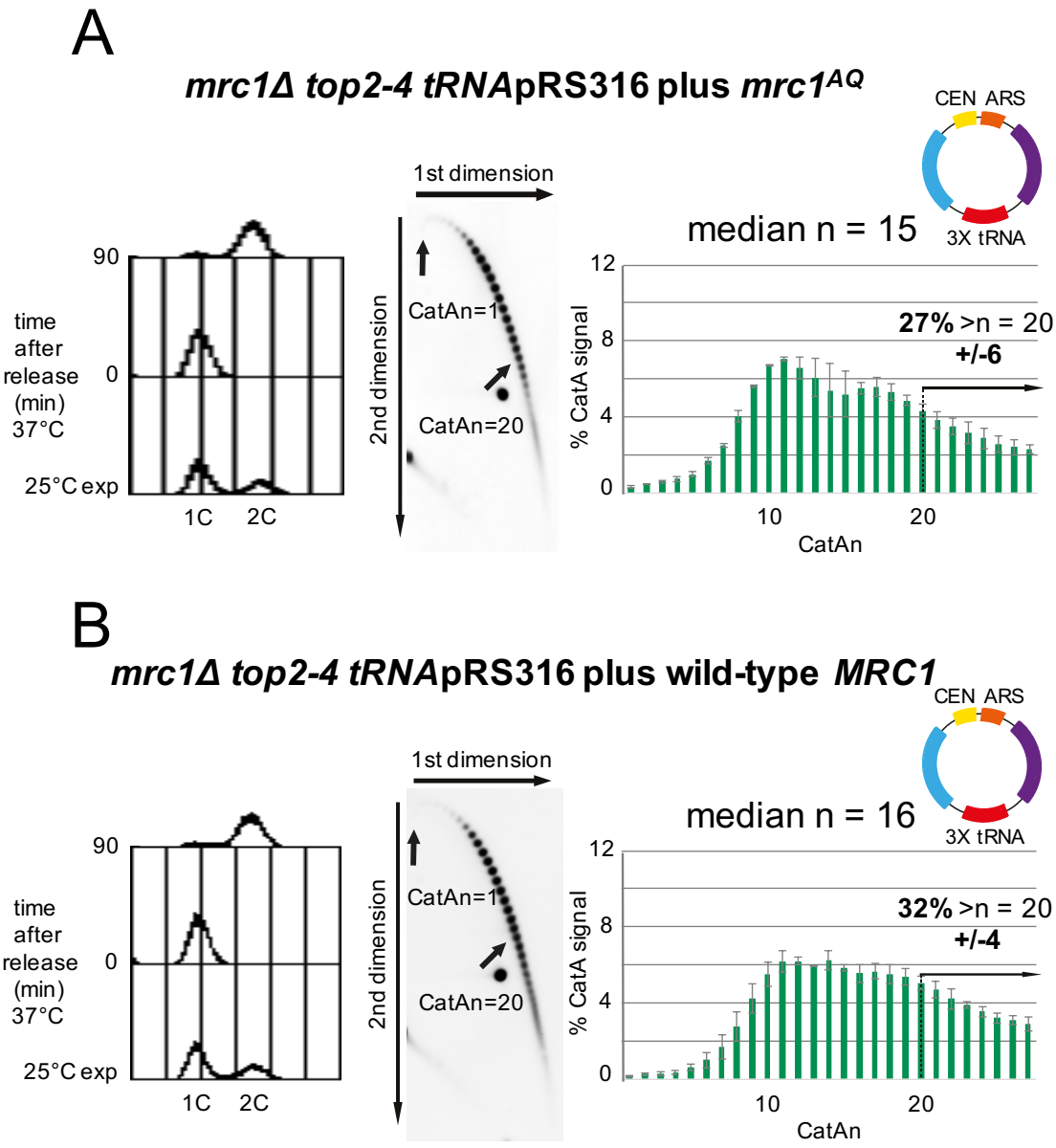

Figure 5.2: Low levels of fork rotation in *mrc1Δ* cells are not dependent on the checkpoint function of Mrc1.
DNA catenation analysis of plasmid tRNApRS316 in *mrc1Δ top2-4* containing (**A**) *mrc1-AQ* and (**B**) wild-type *MRC1* was carried out as described in Figure 3.2. FACS for DNA content is also depicted. Representative autoradiograms are indicated; the top arrow shows electrophoresis in the first dimension, and the side arrow shows electrophoresis in the second dimension. Histograms indicate the relative intensity of catenanes containing 1–27 catenated links (CatAn), along with the median of the whole distribution and percentage of catenanes from plasmids with >20 catenanes. Arrows show the mobility of plasmids containing 1 (n = 1) and 20 catenanes (n = 20). Error bars or values are average deviation. See Figure 3.2 for full explanation. Light blue, *ampR* gene; purple, *URA3* gene; other colours are as shown.

Table 5.1: Summary of the results of DNA catenation quantification experiments.

Strain	Plasmid name	Number of replicates	Median CatAn	% >20
top2-td GALTOP2Y-F	pRS316	3	>20	64 ± 6
mrc1Δ top2-td GALTOP2Y-F	pRS316	3	13	22 ± 7
mrc1Δ tof1Δ top2-4	pRS316	3	>20	54 ± 10
mrc1Δ tof1Δ top2-4	*tRNA*pRS316	3	>20	66 ± 3
mrc1Δ top2-4	*tRNA*pRS316 plus *mrc1*^{AQ}	3	15	27 ± 6
mrc1Δ top2-4	*tRNA*pRS316 plus *MRC1*	3	16	32 ± 4

5.5 Conclusions

Mrc1 interacts with replication forks and acts as a mediator of replication checkpoint. In fact, Mrc1 transduces signals from the “sensor” kinase, Mec1, to the “effector” kinase, Rad53, in response to replication stress (Alcasabas et al., 2001, Tanaka and Russell, 2001, Osborn and Elledge, 2003, Katou et al., 2003). Therefore, Mrc1 activates Rad53 through Mec1. In response to exogenous stresses such as HU, Mrc1 acts in a pausing complex that maintains replisome integrity (Katou et al., 2003). In addition, Mrc1 also plays a role during normal DNA synthesis in unperturbed cells. The rate of fork progression in these cells is slow throughout much or all of the genome, and, interestingly, this phenotype is not due to replication fork pausing at difficult-to-replicate loci such as tRNA genes (Szyjka et al., 2005).

Previously, I also showed that Mrc1 promotes fork rotation during DNA replication at tRNAs and possibly at centromeres. In this chapter, I confirmed that Mrc1 deletion reduces the frequency of fork rotation in cells of different genetic backgrounds with high levels of fork rotation, e.g. *tof1Δ top2-4* or *top2-td GALTOP2Y-F* background cells. Since *mrc1Δ* has no effect on plasmids without pause sites, it appears that Mrc1 promotes fork rotation during elongation at pause sites but not at termination. However, the reason why Mrc1 promotes fork rotation at pause sites but not during termination is currently unclear. One possible reason for deletion of *mrc1Δ* leading to apparently decreased fork rotation during elongation could be the increased amount of ssDNA generated in this mutant. In cells lacking Mrc1, the physical interaction between helicase and polymerase activities in the eukaryotic replisome may be disrupted at pause sites due to uncoupling, which leads to increased ssDNA formation in the newly replicated chromatids. This ssDNA might act as a substrate for Top3 decatenation and therefore lead to a decrease in the number of DNA catenanes. Although in Chapter 3 (section 3.3), I found that Top3 does not decatenate replication products, I believe that, under certain conditions where ssDNA is formed, Top3 might be activated. This could be the reason for why low levels of DNA catenation are observed during elongation in the absence of Mrc1. Further discussion about how Top3 might resolve DNA pre-catenation at certain places

is included in the next chapter. Furthermore, I did not find any change in fork rotation in *mrc1-AQ* cells in comparison with wild-type *MRC1* cells. Given that *mrc1-AQ* (the checkpoint-deficient mutant) shows a phenotype similar to wild-type *MRC1* cells throughout the S phase, our data are potentially consistent with the conclusion that the effect of Mrc1 on fork rotation is primarily due to the role of Mrc1 during DNA replication.

Chapter 6

Influence of Checkpoint Activation and Checkpoint Kinases on Fork Rotation

6.1 Objective

Through my experiments, I found that the architectural replisome factors, Tof1/Csm3 and Mrc1 influence fork rotation during elongation, which suggested that replisome stability affects fork rotation. Checkpoint activation following replication stress is also thought to stabilize the replisome when the fork is stalled. Therefore, in this chapter, I investigated the influence of checkpoint activation and checkpoint kinases on fork rotation in plasmid replicons.

6.2 Approach

To generate strains for these experiments, I made *sml1Δ*, *sml1Δ mec1Δ*, *sml1Δ mec1Δ tel1Δ*, and *sml1Δ rad53Δ* in *top2-4* cells as described in section 2.1.4 (Table 2.1). Here, to examine fork rotation *in vivo*, I performed a plasmid DNA catenation assay as previously described in Chapter 3 (Figure 3.2) for use with yeast episomal plasmids.

6.3 Activation of the Intra-S Phase Checkpoint using HU and MMS

Activation of either the intra-S checkpoint or DNA damage checkpoint leads to the activation of the checkpoint kinases Mec1 and Rad53. Both these active kinases are thought to target replisome components, thus potentially stabilizing the replisome (reviewed by Branzei and Foiani, 2006, Branzei and Foiani, 2010). In fact, checkpoint activation is crucial for maintaining the stability of stalled DNA replication forks, for example in response to hydroxyurea (HU) (Lopes et al., 2001), and therefore for inhibiting replisome disassembly (Cobb et al., 2003). The activation of both kinases, Mec1 and Rad53, is also essential for preserving the integrity of stalled DNA replication forks in response to methyl methanesulphonate (MMS) (Tercero and Diffley, 2001). Nonetheless, in undamaged cells, both these kinases are essential, which suggested that they constantly regulate replisome stability (Zhao et al., 1998, Zhao et al., 2001, Cha and Kleckner, 2002, Bastos de Oliveira et al., 2015). Therefore, these kinases could affect fork rotation by altering replisome stability and function.

To examine the effect of checkpoint activation on fork rotation, I first aimed to use HU treatment. HU causes fork stalling and thus strongly activates the checkpoint kinases. Specifically, it inhibits the activity of RNR and thus lowers cellular dNTP levels. This leads to the arrest of replication progression due to unavailability of dNTPs for continuing DNA synthesis (Poli et al., 2012). Thus, the helicase uncouples from the polymerase and generates a ssDNA, thereby causing checkpoint activation (Branzei and Foiani, 2005). Previously in my thesis, I found that HU treatment does not strongly affect fork rotation during the replication of plasmid pRS316 (Figure 4.4B). However, I decided to determine how often fork rotation would take place in cells under HU treatment if the number of pausing sites in the plasmid was increased. Thus, to examine fork rotation following HU treatment, *top2-4* cells containing the tRNApRS316 plasmid were synchronised in the G1 phase and released into the S phase in the presence of 200 mM HU to stall replication forks and to activate the S phase checkpoint. Interestingly, I found that, in these cells, the catenated state was 13 with 16% of the plasmid being highly catenated (decrease from 28% to 16%, Figure 6.1A), which suggested that checkpoint activation does change the frequency of fork rotation.

Next, I wondered whether checkpoint activation using MMS instead of HU would alter the levels of fork rotation on the tRNApRS316 plasmid. MMS causes the formation of lesions by alkylating DNA, which reduces replication fork progression and causes checkpoint activation (Tercero and Diffley, 2001). To test if MMS treatment would alter fork rotation on the tRNApRS316 plasmid, I repeated the experiment described in the previous paragraph, but this time, the cells were exposed to 0.033% MMS and nocodazole and were collected 90 min after release. I found that the cells treated with MMS showed a slight reduction in catenation compared to the *top2-4* tRNApRS316 cells, with median n = 14 and with 21% of the population having >20 catenations (decrease from 28% to 21%, Figure 6.1B). Together, these results suggested that checkpoint activation potentially reduces fork rotation during DNA replication on plasmids containing multiple pause sites. If the change in fork rotation were due to checkpoint activation, then the change would not be observed in cells without the checkpoint kinases, i.e. high levels of fork rotation would be detected in the absence of checkpoint kinases in response to replication stress. However, when I attempted

to analyse *sml1Δ mec1Δ top2-4* cells after HU treatment, I only isolated very small amounts of intact plasmid in these cells and therefore could not properly address the above question. In the next section, I will describe my analysis of these cells without HU treatment. Table 6.1 represents the summary of the results of the DNA catenation quantification experiments.

A

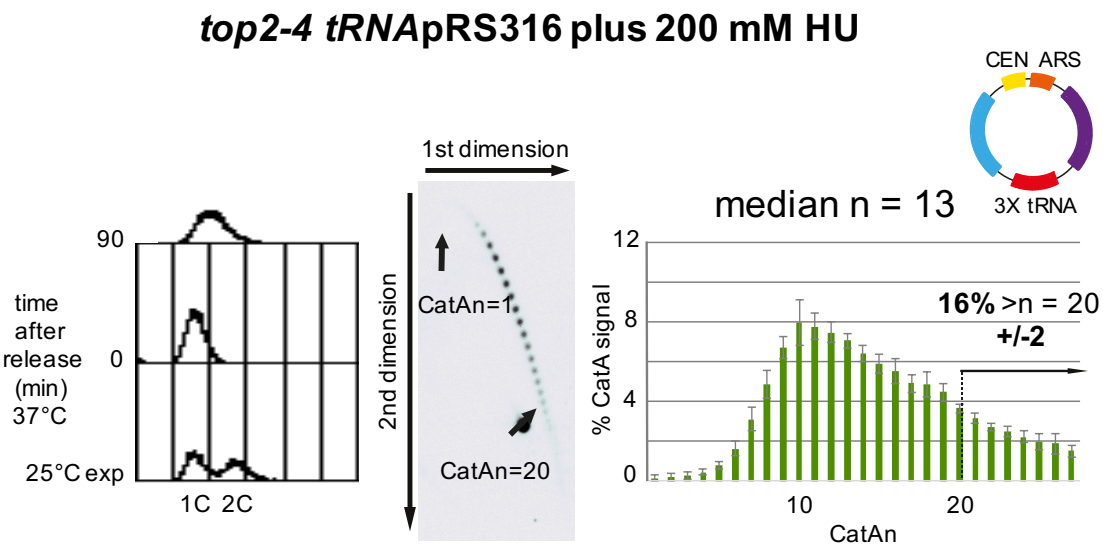

B

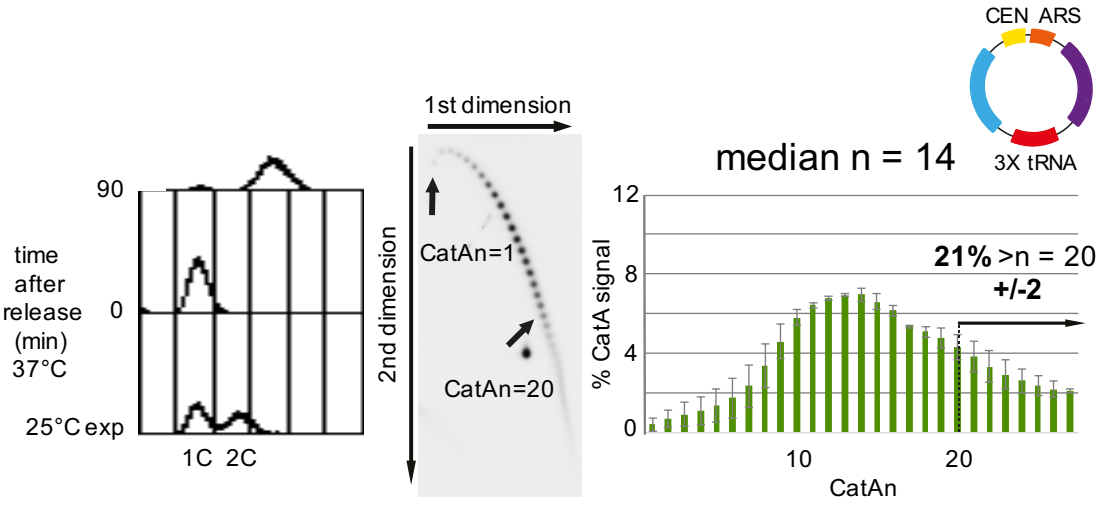

Figure 6.1: Reduction in the frequency of fork rotation in cells treated with HU; this reduction is milder in cells treated with MMS.
Analysis of DNA catenation of plasmid tRNApRS316 in *top2-4* cells released from alpha factor arrest into (**A**) 200 mM HU and (**B**) 0.033% MMS. The cells were collected 90 min after release, and the extracted DNA was analysed as described in Figure 3.2. FACS for DNA content is also depicted. Representative autoradiograms are indicated; the top arrow shows electrophoresis in the first dimension, and the side arrow shows electrophoresis in the second dimension. Histograms indicate the relative intensity of catenanes containing 1–27 catenated links (CatAn), along with the median of the whole distribution and the percentage of catenanes from plasmids with >20 catenanes. Arrows show the mobility of plasmids containing 1 (*n* = 1) and 20 catenanes (*n* = 20). Error bars or values indicate average deviation. See Figure 3.2 for full explanation. Light blue, *ampR* gene; purple, *URA3* gene; other colours are as shown.

6.4 Effect of Checkpoint Kinases on Fork Rotation during Replication of Plasmid pRS316

We know that the activities of Mec1 kinase and the related Tel1 kinase are typically associated with checkpoint signalling in response to replication stress and S phase DNA damage. Previously, Bastos de Oliveira et al. (2015) found that Mec1 is also activated during normal DNA replication. In their experiment, using a quantitative mass spectrometry approach (QMAPS), the authors showed that Mec1 phosphorylates several proteins during unperturbed DNA replication. Furthermore, Tel1 partially compensates for Mec1 function in the absence of Mec1, which indicated that there are sets of Mec1 substrates that can also be phosphorylated by Tel1. The authors also found that phosphorylation of Tof1 is dependent on Mec1 and Tel1 (Bastos de Oliveira et al., 2015), which suggested that Mec1/Tel1 activity may change fork rotation through Tof1 even in undamaged cells.

Since the upstream checkpoint kinase, yeast ATR homolog, Mec1, is thought to be primarily responsible for phosphorylating targets downstream of the checkpoint, I next aimed to determine if *MEC1* deletion would alter fork rotation during DNA replication in plasmid pRS316. Cells lacking Mec1 are only viable when the ribonucleotide reductase inhibitor, Sml1, is inactivated (Zhao et al., 1998). Therefore, in order to delete *MEC1*, I first had to delete *SML1* and test

whether the deletion of *SML1* changed the frequency of fork rotation on plasmid pRS316. However, no significant change in the levels of fork rotation was detected in *sml1Δ top2-4* pRS316 cells, with median *n* = 14 and with 19% of the plasmid population having >20 catenations (Figure 6.2A). Therefore, I then examined the frequency of fork rotation in the absence of both *SML1* and *MEC1* in *top2-4* background cells containing the pRS316 plasmid. However, no dramatic change in DNA catenation of pRS316 was observed in these cells (median *n* = 15; 23% of plasmids had >20 catenations) (Figure 6.2B). These results suggested that loss of Mec1 does not markedly alter the frequency of fork rotation. This could be because Tel1 might be compensating for the lack of Mec1. Therefore, I next tried to examine if *MEC1* and *TEL1* double mutants in *sml1Δ top2-4* background cells would show altered fork rotation under topological stress during DNA replication in plasmid pRS316. However, I found that the median and distribution in *sml1Δ mec1Δ tel1Δ top2-4* pRS316 was the same as that in *sml1Δ mec1Δ top2-4* pRS316 (median *n* = 15; 23% of plasmids had >20 catenations) (Figure 6.2C). This result indicated that the lack of both Mec1 and Tel1 does not alter the frequency of fork rotation and DNA pre-catenation during DNA replication on plasmid pRS316. Table 6.1 represents the summary of the DNA catenation quantification experiments.

A

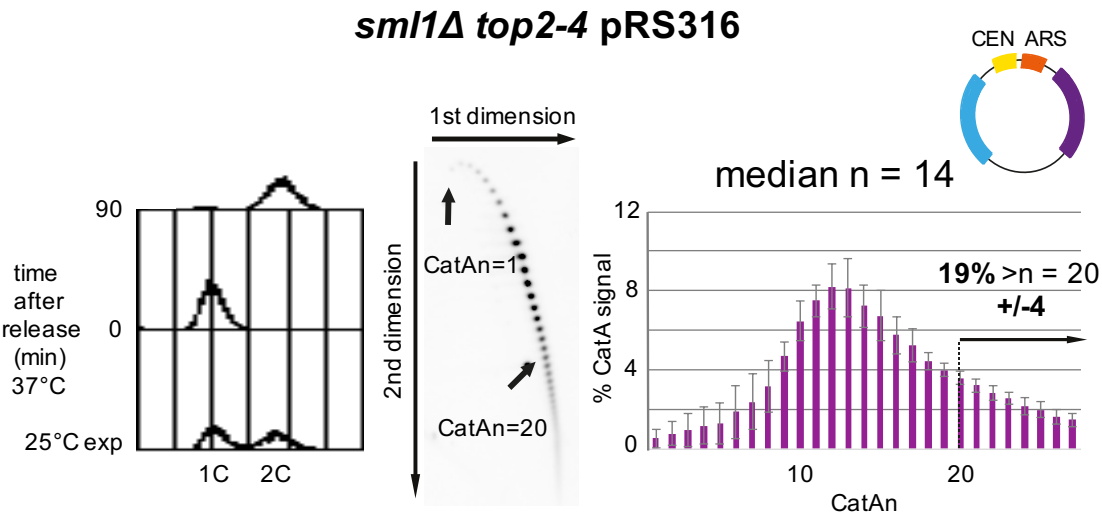
sml1Δ top2-4 pRS316
CEN ARS
1st dimension
median n = 14
time after release (min) 37°C
90
0
25°C exp
1C 2C
2nd dimension
CatAn=1
CatAn=20
% CatA signal
12
8
4
0
19% >n = 20
+/-4
10
20
CatAn

B

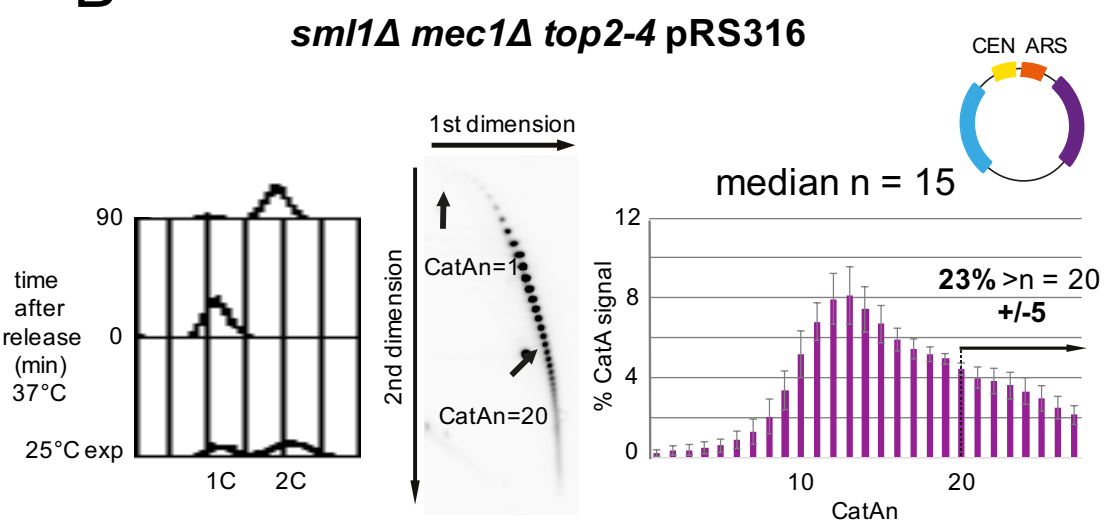
sml1Δ mec1Δ top2-4 pRS316
CEN ARS
1st dimension
median n = 15
time after release (min) 37°C
90
0
25°C exp
1C 2C
2nd dimension
CatAn=1
CatAn=20
% CatA signal
12
8
4
0
23% >n = 20
+/-5
10
20
CatAn

C

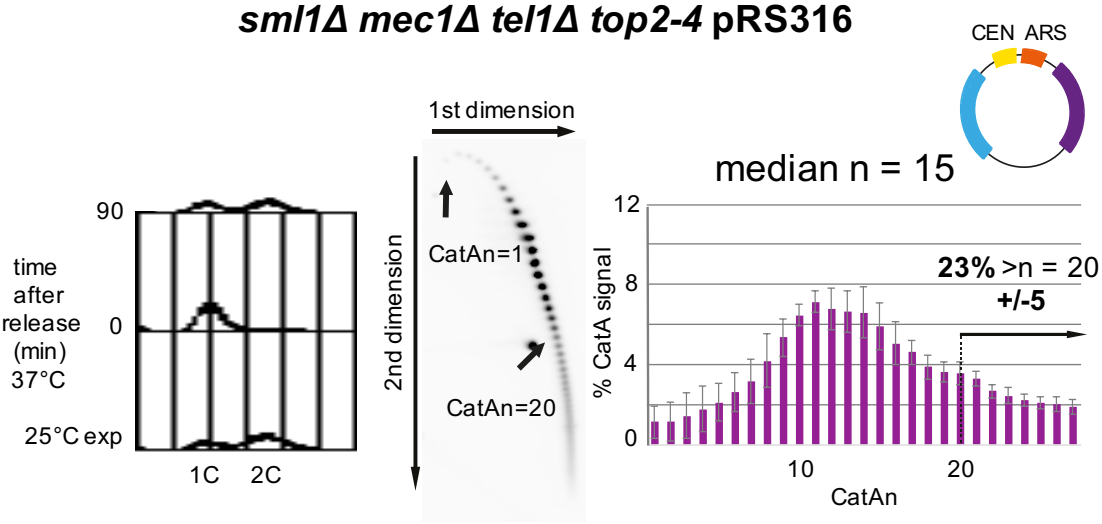
sml1Δ mec1Δ tel1Δ top2-4 pRS316
CEN ARS
1st dimension
median n = 15
time after release (min) 37°C
90
0
25°C exp
1C 2C
2nd dimension
CatAn=1
CatAn=20
% CatA signal
12
8
4
0
23% >n = 20
+/-5
10
20
CatAn

Figure 6.2: Frequency of fork rotation and DNA catenation is not significantly altered in *sml1Δ*, *sml1Δ mec1Δ* and *sml1Δ mec1Δ tel1Δ* cells. DNA catenation analysis of plasmid pRS316 in (**A**) *sml1Δ,* (**B**) *sml1Δ mec1Δ* and (**C**) *sml1Δ mec1Δ tel1Δ* cells in *top2-4* background was carried out as described in Figure 3.2. FACS for DNA content is also depicted. Representative autoradiograms are indicated; the top arrow shows electrophoresis in the first dimension, and the side arrow shows electrophoresis in the second dimension. Histograms indicate the relative intensity of catenanes containing 1–27 catenated links (CatAn), along with the median of the whole distribution and percentage of catenanes from plasmids with >20 catenanes. Arrows show the mobility of plasmids containing 1 (*n* = 1) and 20 catenanes (*n* = 20). Error bars or values indicate average deviation. See Figure 3.2 for full explanation. Light blue, *ampR* gene; purple, *URA3* gene; other colours are as shown.

6.5 Effect of Checkpoint Kinases on Fork Rotation during Replication of Plasmid tRNApRS316

In section 6.4, I showed that deletion of *MEC1/TEL1* did not affect fork rotation on plasmid pRS316. However, earlier, I had observed that the effect of *mrc1Δ* on fork rotation was much clearer on the tRNApRS316 plasmid than on the pRS316 plasmid. Thus, I wanted to determine how often fork rotation would take place if the number of pausing sites in the plasmid and therefore fork rotation during elongation in *sml1Δ*, *sml1Δ mec1Δ*, and *sml1Δ mec1Δ tel1Δ* cells was increased. To do this, I first tested the levels of fork rotation in cells with *SML1* deleted to investigate the possible change in fork rotation in *sml1Δ* cells during DNA replication of plasmid tRNApRS316. As expected, the *sml1Δ* cells showed similar results with regard to the number of catenations in comparison with *top2-4* tRNApRS316 cells, with median *n* = 16 and with 29% of the population having >20 catenations (Figure 6.3A). Therefore, I concluded that Sml1 alone does not alter the frequency of fork rotation and pre-catenation during DNA replication. I next wondered how often fork rotation was occurring in the *sml1Δ mec1Δ* and *sml1Δ mec1Δ tel1Δ* cells during replication of plasmid tRNApRS316. However, no clear increase or decrease in the frequency of DNA catenanes formed on the plasmid could be detected. The median and distribution of the genes in question were as follows: *sml1Δ mec1Δ top2-4* tRNApRS316 (median *n* = 16; 33% of plasmids had >20 catenations) and *sml1Δ mec1Δ tel1Δ top2-4* tRNApRS316 (median *n* = 17; 37% of plasmids had >20 catenations) (Figure 6.3 B and C).

Thus, my results indicated that neither Mec1 alone nor Mec1 and Tel1 together inhibit fork rotation during DNA replication, at least in unchallenged cells. Table 6.1 indicates the summary of the DNA catenation quantification experiments.

A

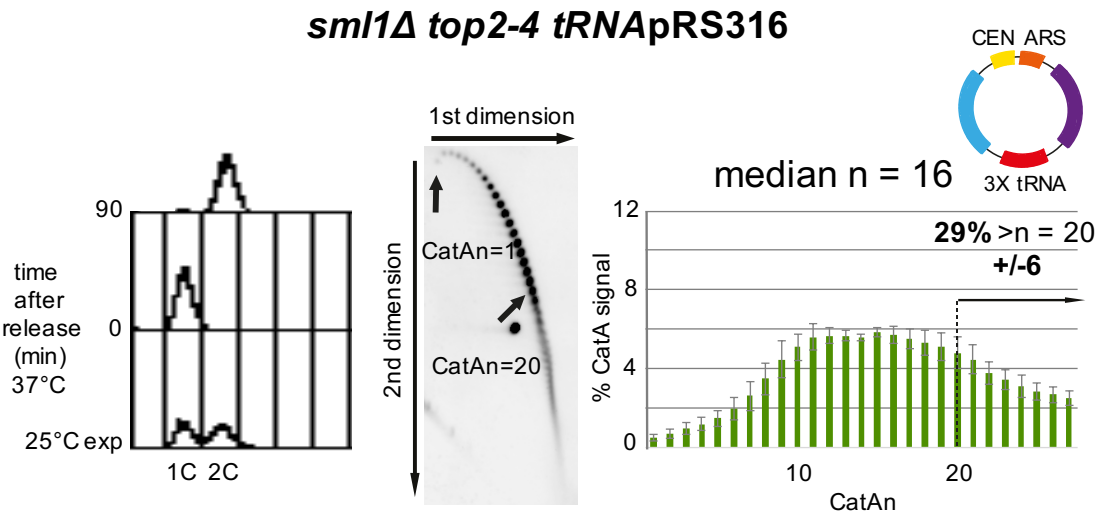
sml1Δ top2-4 tRNApRS316
CEN ARS
3X tRNA
1st dimension
2nd dimension
CatAn=1
CatAn=20
time after release (min) 37°C
25°C exp
90
0
1C 2C
median n = 16
29% >n = 20
+/-6
% CatA signal
12
8
4
0
10
20
CatAn

B

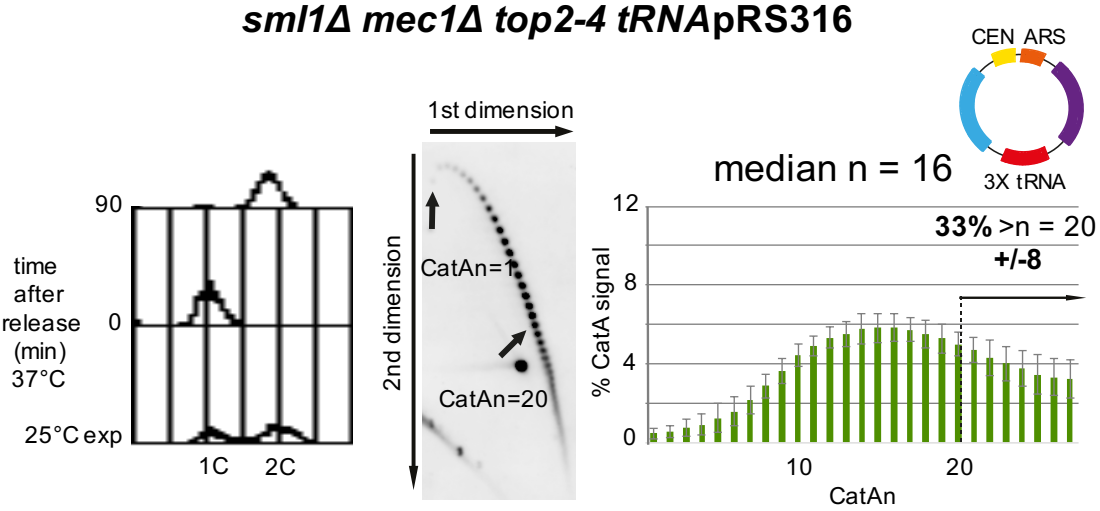
sml1Δ mec1Δ top2-4 tRNApRS316
CEN ARS
3X tRNA
1st dimension
2nd dimension
CatAn=1
CatAn=20
time after release (min) 37°C
25°C exp
90
0
1C 2C
median n = 16
33% >n = 20
+/-8
% CatA signal
12
8
4
0
10
20
CatAn

C

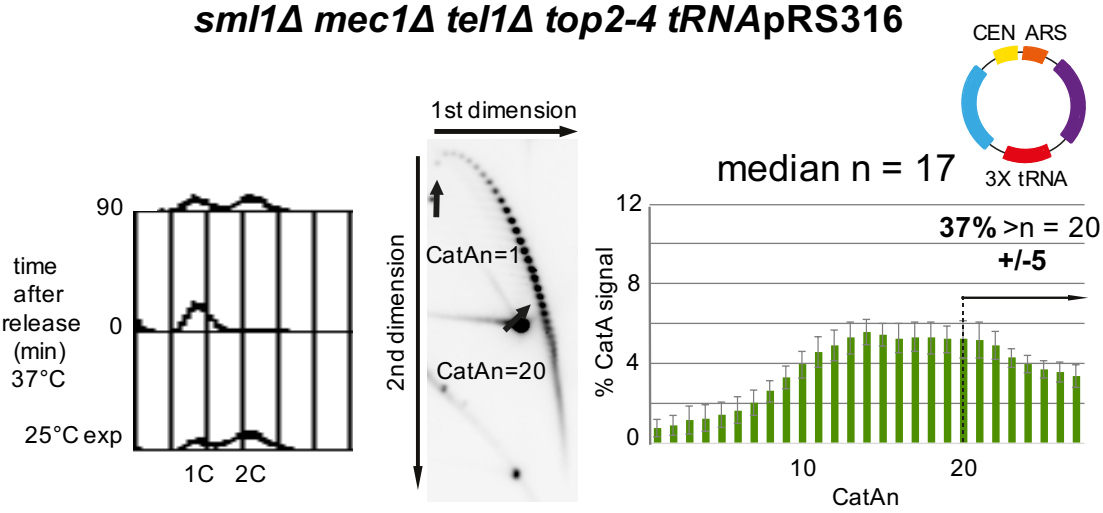
sml1Δ mec1Δ tel1Δ top2-4 tRNApRS316
CEN ARS
3X tRNA
1st dimension
2nd dimension
CatAn=1
CatAn=20
time after release (min) 37°C
25°C exp
90
0
1C 2C
median n = 17
37% >n = 20
+/-5
% CatA signal
12
8
4
0
10
20
CatAn

Figure 6.3: No excessive fork rotation and DNA catenation is detected in *sml1Δ*, *sml1Δ mec1Δ* and *sml1Δ mec1Δ tel1Δ* cells.
DNA catenation analysis of plasmid tRNApRS316 in *top2-4* cells in (**A**) *sml1Δ,* (**B**) *sml1Δ mec1Δ* and (**C**) *sml1Δ mec1Δ tel1Δ* was carried out as described in Figure 3.2. FACS for DNA content is also depicted. Representative autoradiograms are indicated; the top arrow shows electrophoresis in the first dimension, and the side arrow shows electrophoresis in the second dimension. Histograms indicate the relative intensity of catenanes containing 1–27 catenated links (CatAn), along with the median of the whole distribution and percentage of catenanes from plasmids with >20 catenanes. Arrows show the mobility of plasmids containing 1 (*n* = 1) and 20 catenanes (*n* = 20). Error bars or values indicate average deviation. See Figure 3.2 for full explanation. Light blue, *ampR* gene; purple, *URA3* gene; other colours are as shown.

6.6 Effect of Rad53 on Fork Rotation during Replication of Plasmids pRS316 and tRNApRS316

Mec1 kinase is activated in response to DNA damage or HU-induced replication stress, which, together with the activity of other checkpoint factors, leads to Rad53 activation (Pellicioli and Foiani, 2005). It is important to note that, in sharp contrast with Mec1, Rad53 has been found to phosphorylate very few targets during normal DNA replication (Bastos de Oliveira et al., 2015). However, Rad53 kinase is also required during normal DNA replication. Cells are not viable in the absence of Rad53, unless the RNR inhibitor *SML1* is also deleted (Zhao et al., 1998, Zhao et al., 2001). In this chapter, I found that cells lacking Mec1 alone or Mec1/Tel1 together in *sml1Δ top2-4* background cells do not show a strong change in the frequency of fork rotation. Therefore, I assumed that, in undamaged cells, Rad53, which functions downstream of Mec1, would not change the frequency of fork rotation. However, to confirm the data obtained regarding Mec1 and Mec1/Tel1, I decided to test the frequency of fork rotation in the absence of *RAD53* in *sml1Δ top2-4* background cells to check if there was another pathway for Rad53 reactivation. To this end, I examined the frequency of fork rotation in *sml1Δ rad53Δ top2-4* cells containing the pRS316 plasmid. As expected, no noticeable reduction or increase in the frequency of fork rotation could be detected (median *n* = 14; 18% of plasmids had >20 catenations) in comparison with that in the *sml1Δ top2-4* pRS316 and *top2-4* pRS316 strains (Figure 6.4A). Furthermore, I tested the levels of fork rotation in *sml1Δ rad53Δ*

top2-4 cells containing the tRNApRS316 plasmid and did not observe any clear change in the frequency of fork rotation (median *n* = 16; 30% of plasmids had >20 catenations) in comparison with that in the *sml1Δ top2-4* tRNApRS316 and *top2-4* tRNApRS316 cells (Figure 6.4B). These data indicated that checkpoint kinases do not affect the frequency of fork rotation in unchallenged cells. Table 6.1 indicates the summary of the DNA catenation quantification experiments.

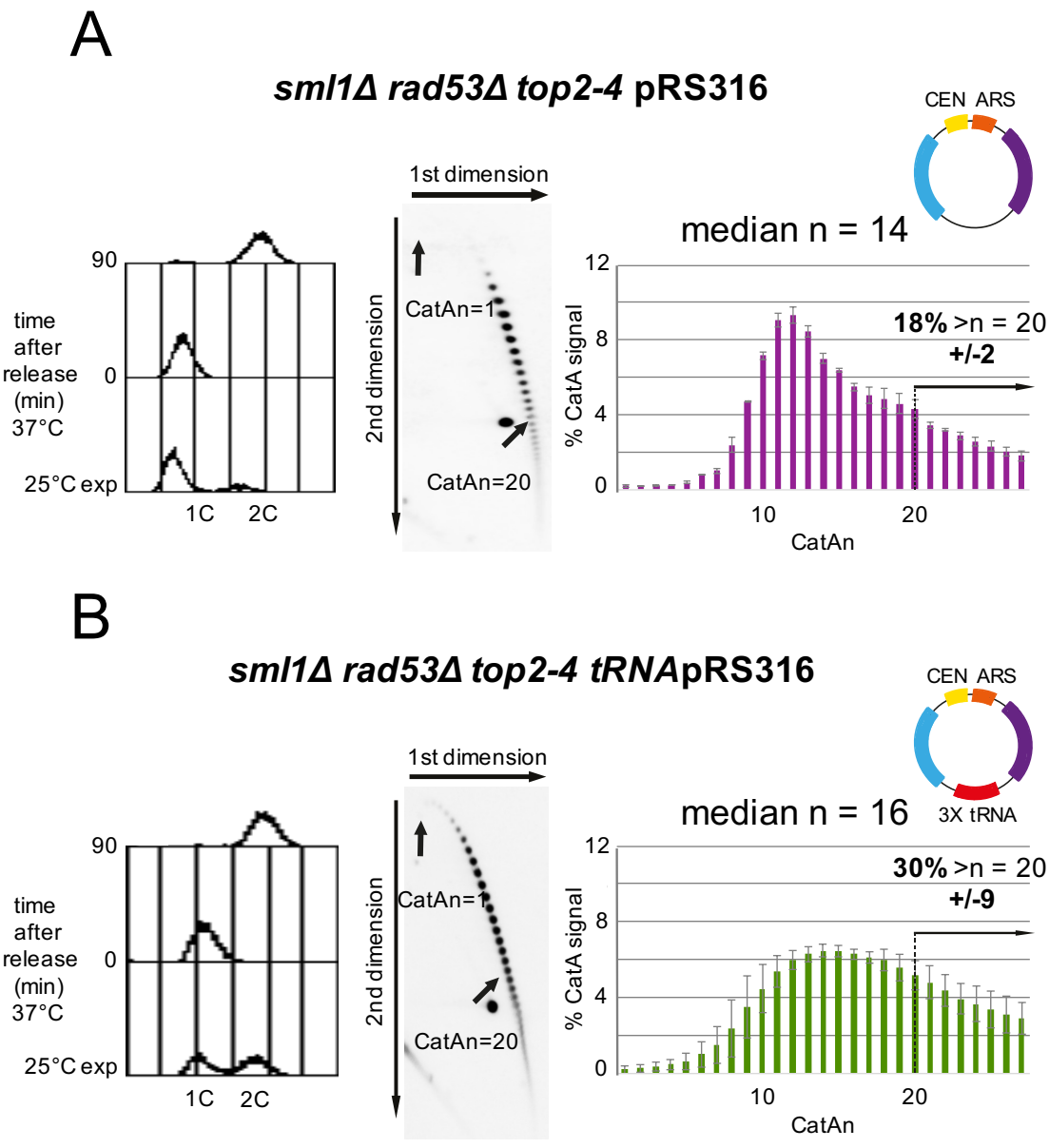

Figure 6.4: Deletion of *RAD53* does not alter fork rotation during DNA replication.
DNA catenation analysis of plasmids (**A**) pRS316 and (**B**) tRNApRS316 in *sml1Δ rad53Δ top2-4* cells was carried out as described in Figure 3.2. FACS for DNA content is also depicted. Representative autoradiograms are indicated; the top arrow shows electrophoresis in the first dimension, and the side arrow shows electrophoresis in the second dimension. Histograms indicate the relative intensity of catenanes containing 1–27 catenated links (CatAn), along with the median of the whole distribution and percentage of catenanes from plasmids with >20 catenanes. Arrows show the mobility of plasmids containing 1 (*n* = 1) and 20 catenanes (*n* = 20). Error bars or values indicate average deviation. See Figure 3.2 for full explanation. Light blue, *ampR* gene; purple, *URA3* gene; other colours are as shown.

Table 6.1: Summary of the results of DNA catenation quantification experiments.

Strain	Plasmid name	Number of replicates	Median CatAn	% >20
top2-4	*tRNA*pRS316	3	16	28 ± 1
***top2-4* plus 200 mM HU**	*tRNA*pRS316	4	13	16 ± 2
***top2-4* plus 0.033% MMS**	*tRNA*pRS316	2	14	21 ± 2
top2-4	pRS316	5	13	14 ± 4
sml1Δ top2-4	pRS316	4	14	19 ± 4
sml1Δ mec1Δ top2-4	pRS316	5	15	23 ± 5
sml1Δ mec1Δ tel1Δ top2-4	pRS316	6	15	23 ± 5
sml1Δ rad53Δ top2-4	pRS316	2	14	18 ± 2
sml1Δ top2-4	*tRNA*pRS316	6	16	29 ± 6
sml1Δ mec1Δ top2-4	*tRNA*pRS316	8	16	33 ± 8
sml1Δ mec1Δ tel1Δ top2-4	*tRNA*pRS316	6	17	37 ± 5
sml1Δ rad53Δ top2-4	*tRNA*pRS316	4	16	30 ± 9

6.7 Conclusions

Previously in my thesis, I found that Tof1/Csm3, Mrc1 and Pol32 influence fork rotation during replication elongation. As explained in the first chapter of this thesis, all these factors are required for maintaining genome integrity during unperturbed and perturbed DNA replication. In this chapter, I examined the influence of rapid checkpoint activation on fork rotation during DNA replication. Surprisingly, I found that when the replication fork progression is slowed by HU treatment, the frequency of fork rotation is reduced at tRNA genes. This result indicates that checkpoint activation potentially reduces fork rotation during DNA replication; therefore, high levels of fork rotation should be observed in the absence of checkpoint kinases in response to replication stress. Thus, the next experiment was to check if Mec1 alone or Mec1/Tel1 together were required for the reduction in fork rotation in HU-challenged cells. Although I attempted experiments to this end, I failed to answer this question due to the small amounts of intact plasmid isolated in these cells.

During DNA replication, replication forks can be exposed to many types of replicative stress, either endogenous or exogenous (see introduction; section 1.3.1). In response to replicative stress, sensor kinases are recruited to stalled replication forks, which leads to the phosphorylation of mediator proteins that then recruit effector kinases. These effector kinases are then phosphorylated by sensor kinases, which leads to the phosphorylation of specific target proteins. Eventually, this process leads to the stabilization of stalling replication forks. Therefore, the checkpoint kinase proteins, particularly Mec1 and Rad53, have been known to be required in budding yeast to stabilize the replisome in challenged cells (Gottifredi and Prives, 2005, Branzei and Foiani, 2006). In addition, these kinases also have been shown to be essential in budding yeast to stabilize the replisome in unchallenged cells (Zhao et al., 1998, Zhao et al., 2001, Cha and Kleckner, 2002). Thus, these kinases could influence fork rotation by changing replisome stability and function. In addition, Mec1/Tel1 have been shown to phosphorylate several targets during normal DNA replication, including Tof1, and this function of Mec1 is partially separated from Rad53 activation (Bastos de Oliveira et al., 2015). This suggests that Mec1/Tel1 activity may

change fork rotation through Tof1 in undamaged cells. However, I could not detect clear changes in the levels of fork rotation either in the absence of *MEC1* alone or in the absence of *MEC1* and *TEL1* together during DNA replication. To further confirm these results, I checked if the downstream checkpoint kinase, Rad53, which is required to stabilize the replisome, also alters the frequency of fork rotation. However, the levels of fork rotation did not change in the absence of Rad53. I therefore concluded that checkpoint kinases do not alter the frequency of fork rotation, at least in unchallenged cells.

In the previous chapters as well as in this chapter, I found that the frequency of fork rotation is reduced during DNA replication in the absence of *MRC1* and *POL32* and in cells under HU treatment on plasmid containing multiple pause sites. I further showed that, in the absence of Mrc1, this reduction is not due to the activation of checkpoint kinases. We know that yeast Top3, in the context of wild-type replisome, does not influence fork rotation (Figure 3.5B). However, one potential possibility is that Top3 is activated in the presence of ssDNA behind the fork, since type III enzyme requires single-stranded regions as a substrate (Harmon et al., 1999) and that it hence passes single-stranded regions through the double-stranded regions to resolve DNA pre-catenation. Therefore, Top3 might be activated in *mrc1Δ* cells or *pol32Δ* cells, which would lead to a decrease in the number of DNA pre-catenanes. The same hypothesis can also be applied to *top2-4* cells under HU treatment, in which ssDNA is created because of the uncoupling of the helicase and the polymerase or the leading and lagging strand polymerases in these cells (Branzei and Foiani, 2005). Thus, it seems that ssDNA appears in the leading strand in *mrc1Δ* cells and in the lagging strand in *pol32Δ* cells; finally, potentially, in both strands when replication fork progression is slowed under HU treatment, Top3 is activated and DNA decatenation occurs subsequently. More experiments need to be conducted in the future to assess this possibility.

Chapter 7

Investigating the Importance of Fork Rotation Regulation in Genome Stability

Some of the data presented in this chapter have been published in Schalbetter et al. (2015) (Schalbetter et al., 2015).

7.1 Objective

In Chapter 4, I showed that some of the architectural replisome factors appear to regulate fork rotation during elongation. As explained in section 1.2.3.2, several studies in different organisms have revealed elevated levels of DNA damage in the absence of exogenous genotoxic agents in cells lacking Timeless/Tipin, the Tof1/Csm3 homologs (Chou and Elledge, 2006, Leman and Noguchi, 2012). Furthermore, high levels of DNA damage were also observed in cells lacking Mrc1 in the absence of exogenous damaging agents, which leads to constitutive Rad53 phosphorylation, and this defect is not dependent on the checkpoint regulation function of Mrc1 (Alcasabas et al., 2001, Osborn and Elledge, 2003). Since deletion of all these factors lead to DNA damage, in this chapter, I examined whether regulating fork rotation was important for the maintenance of genomic stability. First, I investigated the influence of excessive fork rotation on endogenous chromosomes. I then decided to investigate whether unrestricted fork rotation and DNA pre-catenation during DNA replication would lead to checkpoint activation and elevated levels of DNA damage. I finally proceeded to use ChIP-Seq experiments to map the DNA damage arising after deregulation of fork rotation on a whole genome level.

7.2 Function of *TOF1* in Fork Rotation on Endogenous Chromosomes

In this chapter, I used the Top2-td strain made by Baxter and Diffley (2008) for all my experiments. Previous experiments conducted in our laboratory indicated that alpha factor block and release work better in the *top2-td* strain than in the *top2-4* strain, which was used in the previous chapters. As explained in Chapter 5 (section 5.3), this mutant strain cannot grow under the following restrictive conditions: first, when the *top2-td* promoter is suppressed by adding doxycycline; second, when the degron-specific E3 ubiquitin ligase, Ubr1, is increased by adding galactose; and third, when the temperature is shifted to 37°C (Baxter and

Diffley, 2008). For consistency, strains with a gene under the control of the tet-degron system were always compared with a strain containing both the GAL-UBR1 and TetR constructs (see Table 2.1) but no degron moiety or TetO promoter. This comparison strain is referred to as the wild-type. Importantly, the effects of *tof1Δ* on the pRS316 plasmid in the *top2-td* cells were the same as those previously observed in *tof1Δ top2-4* pRS316 cells (Figure 7.1).

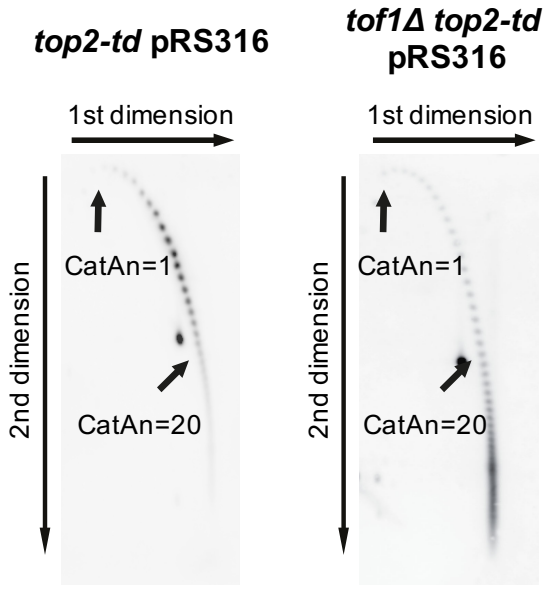

Figure 7.1: Frequency of fork rotation in *tof1Δ top2-td* pRS316 cells is higher than that in *top2-td* pRS316 cells, which is consistent with our previous observations (*tof1Δ top2-4*).

As was shown in the fourth chapter, loss of Tof1 function causes unrestricted fork rotation on the plasmid replicons. To test if unconstrained fork rotation also occurred on endogenous chromosomes in *tof1Δ* cells, I examined the cellular phenotype of the synthetic genetic interaction between Tof1 and partial loss of Top2 function. I conducted partial depleted spot tests, in which I used a temperature of 25°C and 12.5 µg/ml doxycycline to partially deplete the protein function of Top2. The wild-type, *top2-td*, *tof1Δ* and *tof1Δ top2-td* strains used in this chapter had already been created and existed in the JB lab collection box as mentioned in Table 2.1. The idea was that if excessive fork rotation was occurring in *tof1Δ* cells, they should be sensitive to partial loss of Top2 decatenation activity. As shown by the spot tests in Figure 7.2A, *tof1Δ* cells strongly synthetically interacted with partial loss of Top2 activity, which was induced by

the transcriptional repression of the *top2-td* allele. This result indicated that hyper-catenation in these cells is making them sensitive to partial loss of *TOP2* gene function.

To further test if excessive fork rotation was taking place on the endogenous chromosomes in *tof1Δ* cells, I assessed the extent of chromosome mis-segregation in cells lacking *TOF1* with partially depleted *TOP2* by FACS analysis and by cytological analysis of the dividing nuclei. Mis-segregation is an abnormal mitotic event, in which chromosomes are separated into daughter cells erroneously, which leads to failure in maintaining the correct number of chromosomes. Aneuploidy occurs as a consequence of chromosome mis-segregation. Aneuploidy is recognized by the appearance of peaks above the 2C and below the 1C of DNA. Previously, Baxter and Diffley (2008) showed that unresolved DNA catenation (full depletion of Top2) does not prevent cell-cycle progression, but results in aneuploidy following cell division in budding yeast (Figure 7.4A) and the appearance of distinctive “cut” type DNA structures are indicative of chromosome mis-segregation (Baxter and Diffley, 2008). Therefore, for my experiment, the idea was that if excessive fork rotation occurs in *tof1Δ* cells, aneuploidy would occur in these cells when the activity of Top2 is reduced to a level that is normally sufficient to allow chromosome segregation in one cell cycle. To test this prediction, exponentially growing cells were arrested in the G1 phase using alpha factor mating pheromone and were then subjected to semi-restrictive conditions (YPD + 12.5 µg/ml doxycycline at 37°C) to partially deplete Top2 function. The cells were then released synchronously to progress through the cell cycle under the above-mentioned conditions. Cell samples were then taken every 20 min for 160 min and processed for analysis of DNA content using FACS. Figure 7.2B shows that the partial depletion of *TOP2* function was just enough to segregate the endogenous chromosomes for one cell cycle in the *top2-td* cells. Moreover, in this degron strain, very few “cut” cells were cytologically detected (Figure 7.2C). Examples of cut cells are indicated in Figure 7.2C. The *tof1Δ* cells also showed a phenotype similar to that observed in *top2-td* cells, both in FACS and in cytological analysis for the “cut” and divided nuclei (Figure 7.2 B and C). However, massive mis-segregation of endogenous chromosomes and aneuploidy was interestingly observed in *tof1Δ* cells under partial loss of Top2

function (Figure 7.2B). Thus, this dosage of Top2 was not enough to prevent observable aneuploidy in the absence of Tof1. Furthermore, in this strain, “cut” cells were frequently detected in mitosis (Figure 7.2C). Hence, the phenotype obtained under partial loss of Top2 function in the *tof1Δ top2-td* strain resembled that obtained under full Top2 depletion in the *top2-td* strain (Baxter and Diffley, 2008). Based on these findings, I concluded that deletion of *TOF1* leads to excessive fork rotation on endogenous chromosomes. To confirm if Top2 was successfully partially depleted in this experiment, I analysed the conditional expression and depletion of endogenous *TOP2* mutant allele under permissive and semi-restrictive conditions using western blot (Figure 7.2D) and confirmed that the semi-restrictive conditions reduced the level of Top2 protein.

Potentially, the “cut” phenotype occurs as a result of general fork stalling and collapse. To determine if the aneuploidy and “cut” phenotype observed in the *tof1Δ top2-td* strain was not due to general destabilization of the replisome, which would result in frequent fork arrest and collapse, I repeated the same set of experiments described above in *mrc1Δ* cells under partial depletion of Top2 activity. Previously, Katou et al. (2003) showed that *mrc1Δ* cells show destabilization of the replisome in response to replication stress, which is similar to the effect of Tof1 (Katou et al., 2003). In contrast, in our analysis, excessive fork rotation was not observed in the mutant (Figure 4.1C). Again, I first tested the cellular phenotype of the synthetic genetic interaction between Mrc1 and partial loss of Top2 function. In this set of experiments, I used wild-type, *top2-td*, *mrc1Δ* and *mrc1Δ top2-td* strains that had already been created and existed in the JB lab collection box as mentioned in Table 2.1. I also included the *tof1Δ* and *tof1Δ top2-td* strains as a control alongside with this set of strains in the spot test. The result of the spot test revealed that synthetic genetic interaction between *mrc1Δ* and partial loss of Top2 function is not as strong as that in *tof1Δ top2-td* cells (Figure 7.3A), which indicated that the aneuploidy observed in *tof1Δ top2-td* cells might not be due to the same general destabilization of the replisome that occurs in *mrc1Δ* cells. To further examine the idea that the synthetic interaction between *TOF1* and *TOP2* is different from the less severe synthetic interaction between *MRC1* and *TOP2*, I examined the extent of chromosome mis-segregation in cells lacking *MRC1* and with partially depleted *TOP2* by FACS

analysis and by cytological analysis of dividing nuclei. As shown in Figure 7.3B, mis-segregation and aneuploidy was barely detectable in the *mrc1Δ* cells under partial loss of Top2, unlike the effect observed for *TOF1*. In addition, the number of “cut” cells did not show much increase in the *mrc1Δ* cells under partially depleted Top2 in comparison with that observed in the *tof1Δ* cells (Figure 7.3C). Taken together, these data suggested that the aneuploidy and mis-segregation observed in the *tof1Δ* cells was due to unrestricted fork rotation and excessive DNA pre-catenation on endogenous chromosomes and that it was not associated with the general destabilization of the replisome function that occurs in *mrc1Δ/tof1Δ* cells.

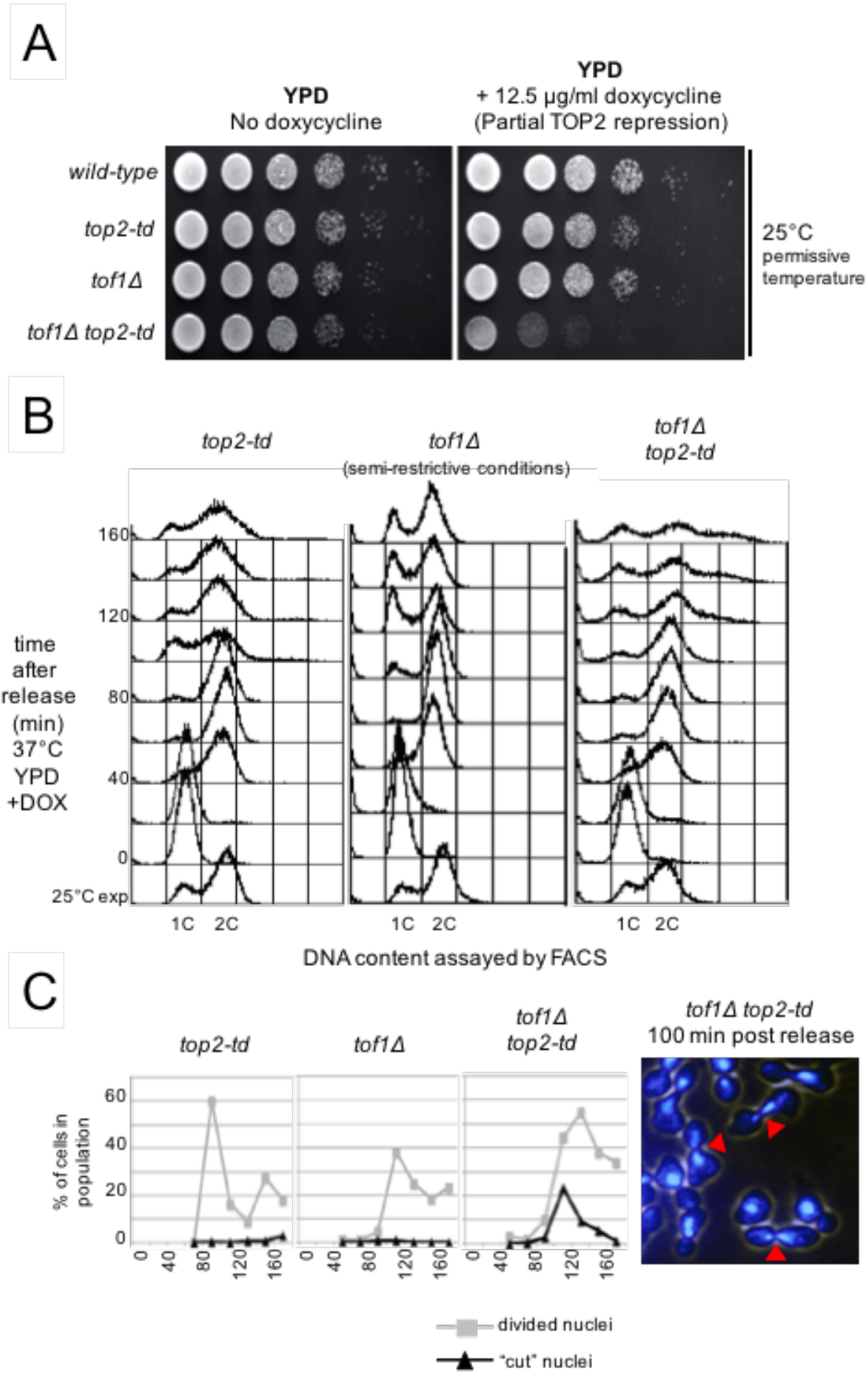
A
YPD
No doxycycline
YPD
+ 12.5 µg/ml doxycycline
(Partial TOP2 repression)
wild-type
top2-td
tof1Δ
tof1Δ top2-td
25°C
permissive
temperature
B
top2-td
tof1Δ
(semi-restrictive conditions)
tof1Δ
top2-td
time
after
release
(min)
37°C
YPD
+DOX
160
120
80
40
0
25°C exp
1C 2C
1C 2C
1C 2C
DNA content assayed by FACS
C
top2-td
tof1Δ
tof1Δ
top2-td
tof1Δ top2-td
100 min post release
% of cells in
population
60
40
20
0
0 40 80 120 160
0 40 80 120 160
0 40 80 120 160
divided nuclei
"cut" nuclei

D

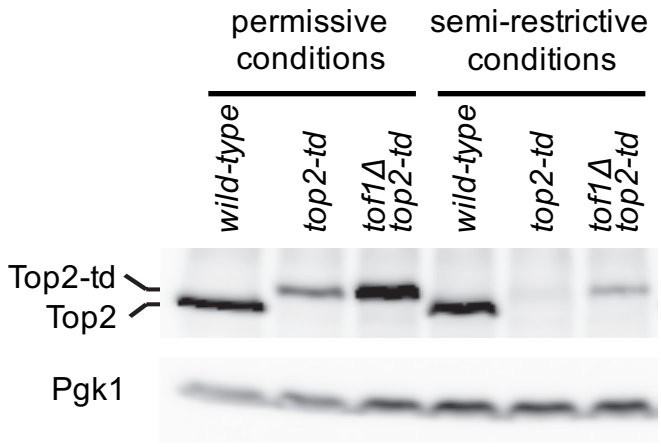

Figure 7.2: Deletion of *TOF1* leads to excessive fork rotation on endogenous chromosomes.
A) Spot tests indicating cell viability of wild-type, *top2-td*, *tof1Δ* and *tof1Δ top2-td* strains under the permissive and semi-restrictive conditions. Ten-fold serial dilutions of exponentially growing cells were plated onto YPD solid media with or without 12.5 µg/ml doxycycline (partial transcriptional repression of Top2) and incubated at 25°C for 48 h. **B**) Deletion of *TOF1* leads to aneuploidy following partial depletion of Top2 activity. FACS data shows the progression of *top2-td*, *tof1Δ* and *tof1Δ top2-td* strains through the cell cycle. Exponentially growing cells were synchronised in G1 using alpha factor mating pheromone and subjected to semi-restrictive conditions (YPD, 37°C, and 12.5 µg/ml doxycycline) before being released from G1 to progress through the cell cycle. Cell samples for FACS analysis of chromosome missegregation were taken at the mid-log phase (25°C exponential; exp) before alpha factor release (0 min) and every 20 min after, for 160 min. **C**) Deletion of *TOF1* leads to an increase in "cut" mitosis under partial depletion of Top2. Cell samples were taken for cytological analysis for "cut" and divided nuclei at the indicated time points. Examples of cut cells (arrowheads) are shown [DAPI-stained DNA (blue) is indicated over a light image of cells 100 min after release]. **D**) Western blot analysis indicating the partial degradation of Top2. Exponentially growing cells of the wild-type, *top2-td* and *tof1Δ top2-td* strains were placed under permissive (YPD, 25°C) and semi-restrictive (YPD, 37°C, and 12.5 µg/ml doxycycline) conditions for 2 h. Samples were prepared for western blot analysis using whole-cell TCA extraction (as described in section 2.1.9). Western blot was carried out as described in section 2.4.1, and the samples were run on an 8% polyacrylamide gel. Pgk1 western blot of the same lanes is indicated for loading comparison.

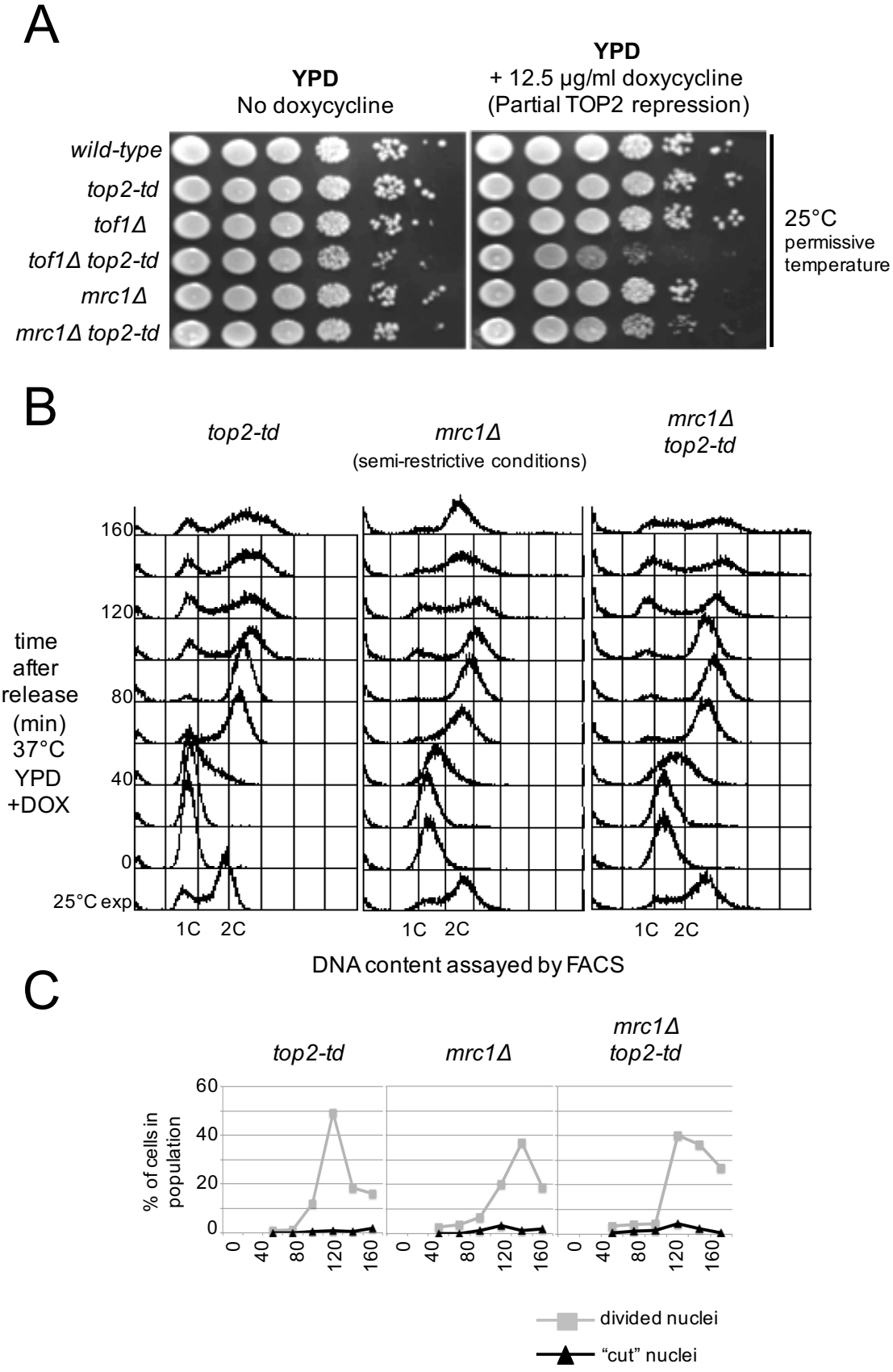
A
YPD
No doxycycline
YPD
+ 12.5 µg/ml doxycycline
(Partial TOP2 repression)
wild-type
top2-td
tof1Δ
tof1Δ top2-td
mrc1Δ
mrc1Δ top2-td
25°C
permissive
temperature
B
top2-td
mrc1Δ
(semi-restrictive conditions)
mrc1Δ
top2-td
time
after
release
(min)
37°C
YPD
+DOX
160
120
80
40
0
25°C exp
1C 2C
1C 2C
1C 2C
DNA content assayed by FACS
C
top2-td
mrc1Δ
mrc1Δ
top2-td
% of cells in
population
60
40
20
0
0 40 80 120 160
divided nuclei
"cut" nuclei

Figure 7.3: Deletion of *MRC1* does not lead to excessive DNA pre-catenation of endogenous chromosomes.
A) Spot tests showing the cell viability of wild-type, *top2-td*, *tof1Δ*, *tof1Δ top2-td*, *mrc1Δ* and *mrc1Δ top2-td* strains under the permissive and semi-restrictive conditions. Ten-fold serial dilutions of exponentially growing cells were plated onto YPD solid media with or without 12.5 µg/ml doxycycline (partial transcriptional repression of Top2), followed by incubation at 25°C for 48 h. **B**) Deletion of *MRC1* did not cause chromosomal aneuploidy following partial depletion of Top2 activity. FACS data indicates the progression of the *top2-td*, *mrc1Δ* and *mrc1Δ top2-td* strains through the cell cycle. Exponentially growing cells were synchronised in G1 using alpha factor mating pheromone and subjected to semi-restrictive conditions (YPD, 37°, and 12.5 µg/ml doxycycline) before being released from G1 to progress through the cell cycle. Cell samples for FACS analysis of chromosome missegregation were taken at the mid-log phase (25°C exponential; exp) before alpha factor release (0 min) and every 20 min after, for 160 min. **C**) Deletion of *MRC1* did not cause an increase in "cut" mitosis under partial depletion of Top2. Cell samples were taken for cytological analysis for cut and divided nuclei at the indicated time points.

7.3 Function of *TOF1* When Top2 Is Fully Depleted

The results of our plasmid analysis described in Chapter 4 showed that fork rotation is actively restricted during DNA replication through the cellular action of Tof1/Csm3. This leads to the question: why is fork rotation so actively restricted by Tof1/Csm3? Since cells with Tof1/Csm3 deletion are viable, it appears that there is sufficient Top2 activity in the cells to cope with the much higher levels of DNA pre-catenation. However, several studies in other organisms have indicated that cells lacking Timeless/Tipin, the Tof1/Csm3 homologs, show high levels of DNA damage in the absence of exogenous genotoxic agents (Chou and Elledge, 2006, Leman and Noguchi, 2012). High levels of gross chromosomal rearrangements have also been detected in cells lacking Tof1 (Putnam et al., 2009). These reports indicate that the function of Timeless-Tipin is to prevent DNA damage at replication forks; therefore, Timeless-Tipin is required for maintaining genome integrity during unperturbed DNA replication. It is possible that the observed phenotypes, i.e. constitutive DNA damage and genome instability, in cells lacking Tof1/Timeless are due to excessive fork rotation and pre-catenation during DNA replication. The hypothesis is that if the fork rotates too much, the DNA pre-catenanes that accumulate behind the fork might inhibit essential functions behind the fork, such as cohesion establishment or lagging

strand DNA synthesis. Problems in these processes could lead to the genomic instability phenotype in cells lacking *TOF1* and *CSM3*. I therefore predicted that if genome instability phenotypes in cells lacking *TOF1* were caused by excessive fork rotation, then, under full Top2 depletion, such genome instability phenotypes would increase, as Top2 would be no longer present to potentially remove the pre-catenanes formed following fork rotation.

To address this hypothesis, cell cycle progression and genome stability was examined in wild-type, *top2-td, tof1Δ* and *tof1Δ top2-td* cells. Wild-type, *top2-td* and *tof1Δ* strains were used as controls. Exponentially growing cells were blocked in G1, shifted to restrictive conditions (YP + 2% raffinose + 2% galactose; 37°C + 25 µg/ml doxycycline) to fully deplete the activity of Top2. The cells were then released under the same restrictive conditions. Cell samples were taken every 20 min for 160 min after release and processed for analysis by FACS. As shown in Figure 7.2B, a slight delay in anaphase onset could be detected in the *tof1Δ* cells under partial depletion of Top2. The same cells, under full depletion of Top2, showed a stable G2/M block in the cell cycle (Figure 7.4A). These cells began to exit G1 40 min after release from alpha-factor; almost all cells had reached G2/M by 80 min but then could not enter mitosis, thus arresting cells in G2/M with a single nucleus, as indicated by the accumulation of cells with 2C DNA content (Figure 7.4B). Hence, I found that *tof1Δ top2-td* results in a cell cycle arrest but the same effect cannot be seen in *top2-td* and *tof1Δ* cells. In fact, in this experiment, wild-type, *top2-td* and *tof1Δ* cells began to exit G1 40 min after release from alpha-factor, with almost all cells having reached G2/M by 80 min. By 120 min, a large subset of cells had continued back through the cell cycle to G1, but as mentioned earlier, *top2-td* was unable to properly segregate chromosomes during mitosis, which lead to lethal DNA damage (Figure 7.4) (Baxter and Diffley, 2008). These data suggest that defects in the newly replicated chromatids that are formed in *tof1Δ top2-td* cells trigger cell cycle checkpoints that prevent mitosis.

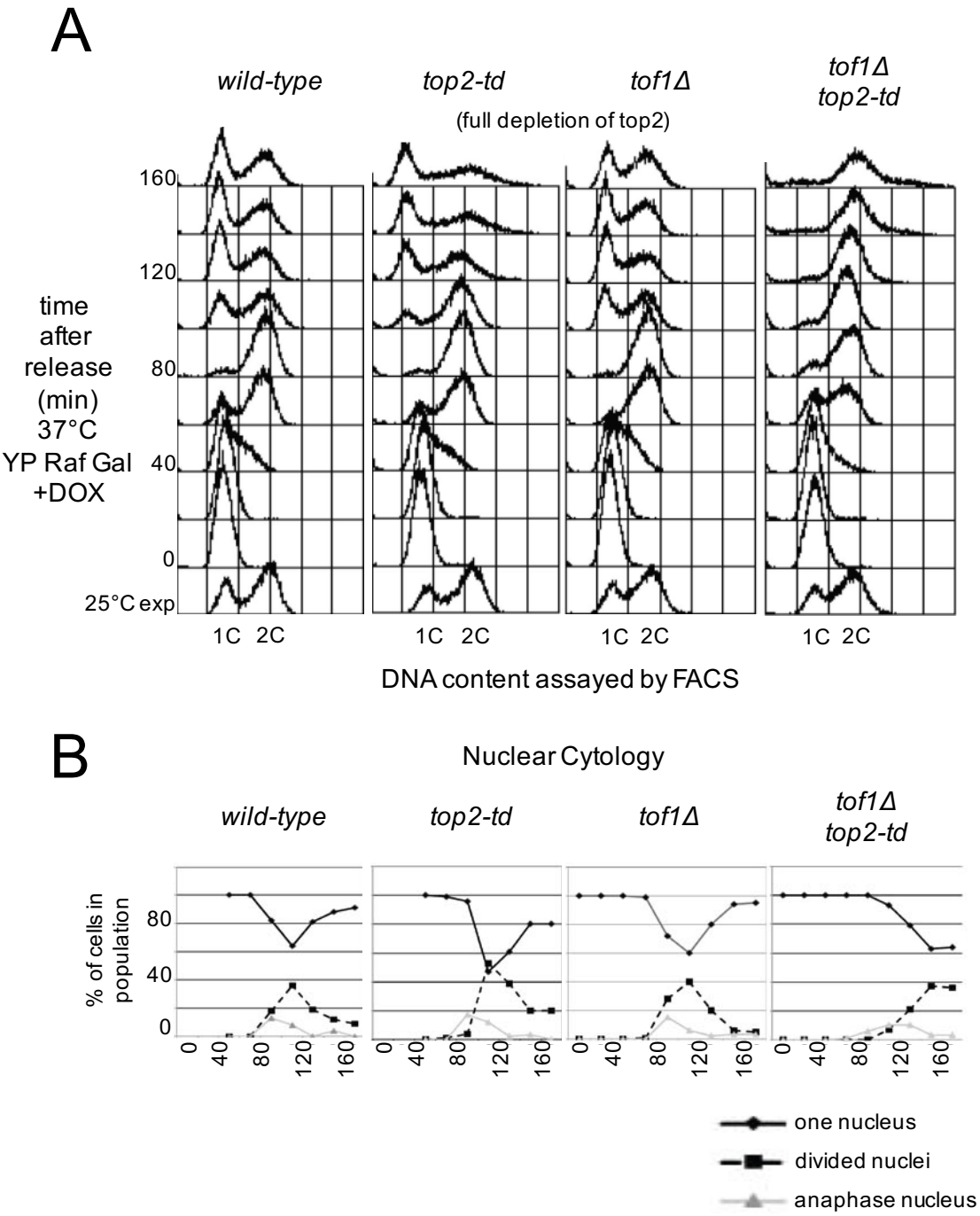

Figure 7.4: *tof1Δ top2-td* cells are arrested in G2/M with a single nucleus. **A**) FACS data shows the progression of the wild-type, *top2-td*, *tof1Δ* and *tof1Δ top2-td* strains through the cell cycle. Exponentially growing cells were synchronised in G1 using alpha factor mating pheromone and subjected to restrictive conditions (YP + 2% raffinose + 2% galactose; 37°C + 25 µg/ml doxycycline) before being released from G1 to progress through the cell cycle. Cell samples for FACS analysis of DNA content were taken at the mid-log phase (25°C exponential; exp) before alpha factor release (0 min) and every 20 min after, for 160 min. **B**) Cell samples were taken for cytological analysis of single and divided nuclei at the indicated time points. The percentages of single (circles) and divided nuclei (squares) and anaphase nuclei (triangles) are indicated.

7.4 Effects of Excessive Fork Rotation in Newly Replicated Chromatids

After obtaining the previous observation about G2/M arrest in *tof1Δ top2-td* cells, studies in the lab conducted by Stephanie Schalbetter (Figure 7.5) were aimed at determining whether excessive fork rotation and DNA pre-catenation during replication would lead to high levels of constitutive DNA damage. As I explained in the first chapter of this thesis, Downs et al. (2000) showed that Mec1 and Tel1 phosphorylate the serine residue S129 on histone H2A in budding yeast, forming H2AS129P (Downs et al., 2000). In fact, phosphorylated H2A is recognized as a marker of DNA damage in both budding yeast and mammals. We also know that deletion of Timeless in human cells results in histone H2AX phosphorylation in the absence of genotoxic agents, which is indicative of DNA damage (Chou and Elledge, 2006). To determine whether the highest levels of constitutive DNA damage would be detected in newly replicated chromatids in *tof1Δ top2-td* cells, the wild-type, *top2-td*, *tof1Δ* and *tof1Δ top2-td* strains were synchronously released from G1 block under restrictive conditions to deplete Top2 activity and allowed to accumulate in G2/M by adding nocodazole to the culture. Nocodazole was added to prevent detection of damage formed during mitosis. As shown in Figure 7.5A, high levels of DNA damage could be detected in the *tof1Δ* cells both in the S phase and in post-replicative whole cell extracts. Less damage was observed in the *top2-td* cells than in the *tof1Δ* cells; however, elevated levels of H2AS129P were detected in the post-replicative *tof1Δ top2-td* cells. This data indicated that unrestricted fork rotation and DNA pre-catenation during DNA replication result in the highest levels of DNA damage in *tof1Δ top2-td* cells.

Consistent with this, further experiments in the lab also indicated that the DNA damage checkpoint effector kinase, Rad53, was present at the highest levels in *tof1Δ top2-td* cells, as determined using the in-blot kinase assay. The Rad53 levels in the *tof1Δ* or the *top2-td* cells were not as high as those in the *tof1Δ top2-td* cells. Therefore, I concluded that the DNA damage checkpoint is active as a result of unrestricted fork rotation and DNA pre-catenation in the *tof1Δ top2-td* cells during DNA replication. As in the previous experiment, cells were treated

with nocodazole to prevent detection of damage occurring during mitosis (Figure 7.5B).

Next, to check if post-replication repair (PRR) is active following excessive fork rotation and DNA pre-catenation, Stephanie Schalbetter examined post-replicative protein extracts and found that the clamp loader PCNA is highly mono-ubiquitylated in *tof1Δ top2-td* cells (Figure 7.5C). This data indicated that excessive fork rotation and DNA pre-catenation during DNA replication lead to the activation of PRR. This observation indicated two possibilities: either an abnormal sister chromatid structure was created or gaps were formed in the newly replicated sister chromatids, either of which had result in PRR activation.

Together, these data indicated that high levels of constitutive DNA damage appeared in newly replicated chromatids as a consequence of both excessive fork rotation and DNA pre-catenation during DNA replication, which lead to the activation of the DNA damage checkpoint and extensive DNA repair.

A

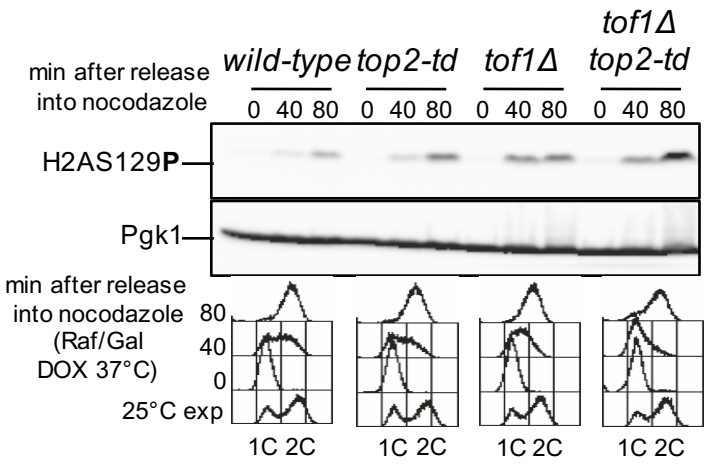
wild-type
top2-td
tof1Δ
tof1Δ top2-td
min after release into nocodazole
0 40 80 0 40 80 0 40 80 0 40 80
H2AS129P
Pgk1
min after release into nocodazole (Raf/Gal DOX 37°C)
80
40
0
25°C exp
1C 2C
1C 2C
1C 2C
1C 2C

B

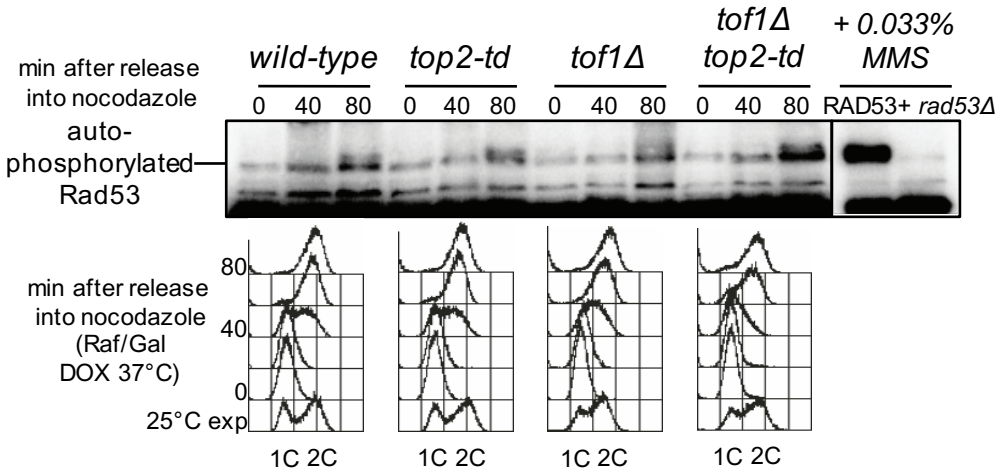
wild-type
top2-td
tof1Δ
tof1Δ top2-td
+ 0.033% MMS
min after release into nocodazole
0 40 80 0 40 80 0 40 80 0 40 80
RAD53+ rad53Δ
auto-phosphorylated Rad53
min after release into nocodazole (Raf/Gal DOX 37°C)
80
40
0
25°C exp
1C 2C
1C 2C
1C 2C
1C 2C

C

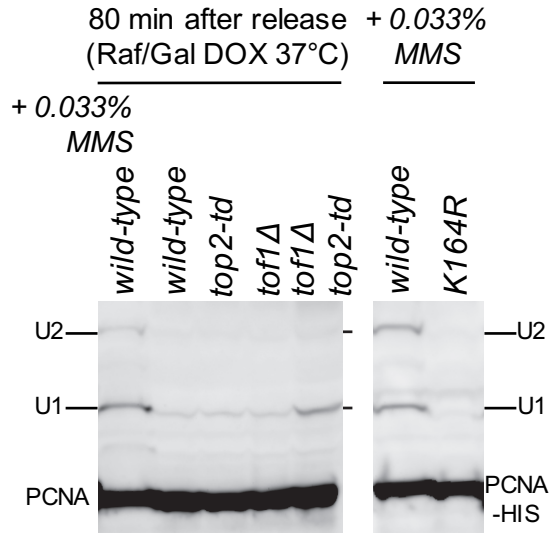
80 min after release (Raf/Gal DOX 37°C)
+ 0.033% MMS
+ 0.033% MMS
wild-type
wild-type
top2-td
tof1Δ
tof1Δ
top2-td
wild-type
K164R
U2
U1
PCNA
U2
U1
PCNA -HIS

Figure 7.5: Excessive fork rotation and DNA pre-catenation result in DNA damage in the newly replicated chromatids, followed by activation of the DNA damage checkpoint and extensive post-replicative repair.
Exponentially growing cells were arrested in G1 using alpha factor mating pheromone and subjected to restrictive conditions (YP + 2% raffinose + 2% galactose; 37°C + 25 µg/ml doxycycline) and released into media containing nocodazole. **A**) Samples were prepared at indicated time points for western blot analysis of phosphorylation of H2A S129. FACS for DNA content is also depicted. Pgk1 western blot of the same lanes is indicated for loading comparison. **B**) Samples were analysed for Rad53 activation using the Rad53 autophosphorylation assay. Exponential *top2-td* and *rad53Δ top2-td* cells were treated with MMS (methyl methanesulphonate) and analysed by western blot for Rad53 activation as control samples. FACS for DNA content is also depicted. **C**) Samples were taken 80 min following release and prepared for PCNA ubiquitylation by western blotting. His-tagged wild-type PCNA and His-tagged K164R were treated with MMS and analysed by western blot for PCNA as control samples, which confirmed the specificity of the PCNA antibody for mono-ubiquitylated PCNA (U1) or poly-ubiquitylated PCNA (U2).

7.5 Effect of Checkpoint Pathways in Cells Held in Pre-Mitotic Arrest

I observed that *tof1Δ top2-td* cells were arrested before chromosome segregation. As mentioned earlier, this is presumably because of the defects accumulating in the newly replicated chromatids in these cells, which trigger cell cycle checkpoints that prevent mitosis. It is known that when the S phase checkpoint is activated, it leads to the stabilization of the securin, Pds1. Pds1 stabilization arrests cells at the metaphase-anaphase transition (see introduction; section 1.3.2.2.5). In this case, the cells should be released from pre-mitotic arrest, i.e. they should enter into mitosis, in the absence of the checkpoint components. Therefore, to investigate whether any checkpoint pathways hold the cells in pre-mitotic arrest, I analysed the cell cycle progression and genome stability in *tof1Δ rad9Δ top2-td*, *tof1Δ tel1Δ top2-td*, *tof1Δ rad9Δ tel1Δ top2-td* and *tof1Δ tel1Δ mec1-40 top2-td* strains using FACS. These strains used for this experiment were constructed as described in section 2.1.3 of the Materials and Methods (Table 2.1).

If any of these checkpoint strains are holding the *tof1Δ top2-td* cells in pre-mitotic arrest, the cells should be released from pre-mitotic arrest in the absence of the

chosen checkpoint components in *tof1Δ top2-td* background cells between 100 and 160 min. In this experiment, exponentially growing cells were blocked in G1 and exposed to YP + 2% raffinose + 2% galactose and under 37°C + 25 µg/ml doxycycline before being released synchronously into the cell cycle. Cell samples for FACS analysis were taken every 20 min for 4 h.

Previously, Foss (2001) showed that in the absence of both *TOF1* and *RAD9*, checkpoint signalling is impaired (Foss, 2001). Thus, I predicted that *tof1Δ rad9Δ top2-td* cells should be released from the pre-mitotic arrest observed in *tof1Δ top2-td* cells. Strains *top2-td* and *tof1Δ top2-td* were also used as controls in this assay. As shown in Figure 7.6, I found that *tof1Δ rad9Δ top2-td* cells, similar to *top2-td* and *tof1Δ top2-td* cells, began to exit G1 40 min after alpha-factor release, with almost all cells having reached G2/M by 80 min. By 120 min, a large subset of the *top2-td* cells had continued back through the cell cycle to G1. However, *tof1Δ rad9Δ top2-td* cells, similar to *tof1Δ top2-td* cells, were arrested in G2/M. This result indicated that Rad9 is not involved in holding the cells in pre-mitotic arrest. Furthermore, I examined the cell cycle progression in *tof1Δ tel1Δ top2-td* and *tof1Δ rad9Δ tel1Δ top2-td* cells. I also observed that both strains went through the S phase with normal kinetics and similar to *tof1Δ top2-td* cells, were arrested in G2/M (Figure 7.6). This result suggested that neither Tel1 alone nor Rad9 and Tel1 together are involved in holding the cells in pre-mitotic arrest. Finally, I was interested in determining whether knocking out two upstream protein kinases that are involved in response to DNA damage would release the cells from pre-mitotic arrest. FACS analysis of *tof1Δ tel1Δ mec1-40 top2-td* cells revealed that this strain went through the S phase with normal kinetics and again, similar to *tof1Δ top2-td* cells, was arrested in G2/M (Figure 7.6). This data suggested that *MEC1* and *Tel1* are not involved in holding the cells in pre-mitotic arrest. Therefore, while I determined that unrestricted fork rotation and DNA pre-catenation led to DNA damage during the S phase, I could not identify the conditions under which prevention of checkpoint activation allowed cells to progress through mitosis. My inability to see passage through mitosis in these mutants could be due to the chromosomes being so entangled that they did not come apart quickly, even when the checkpoint signals were removed (see conclusions; section 7.7).

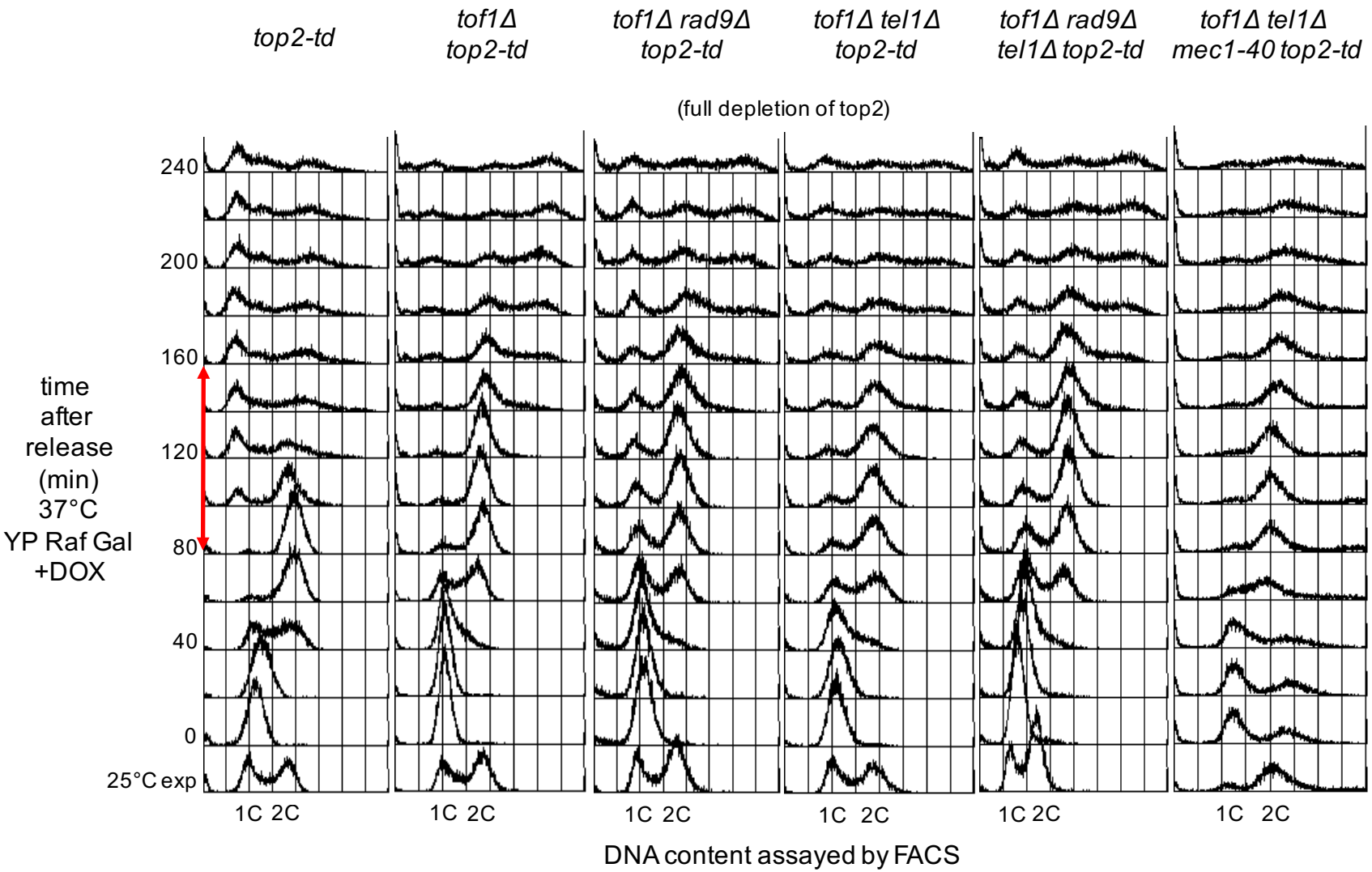
top2-td
tof1Δ top2-td
tof1Δ rad9Δ top2-td
tof1Δ tel1Δ top2-td
tof1Δ rad9Δ tel1Δ top2-td
tof1Δ tel1Δ mec1-40 top2-td
(full depletion of top2)
time after release (min) 37°C YP Raf Gal +DOX
240
200
160
120
80
40
0
25°C exp
1C 2C
DNA content assayed by FACS

Figure 7.6: Deletion of neither of the examined checkpoint components releases the cells from pre-mitotic arrest.
FACS data showing the progression of *top2-td*, *tof1Δ top2-td*, *tof1Δ rad9Δ top2-td*, *tof1Δ tel1Δ top2-td*, *tof1Δ rad9Δ tel1Δ top2-td* and *tof1Δ tel1Δ mec1-40 top2-td* cells through the cell cycle. Exponentially growing cells were arrested in G1 using alpha factor mating pheromone and placed under restrictive conditions (YP + 2% raffinose + 2% galactose; 37°C + 25 µg/ml doxycycline) before being released synchronously into the cell cycle. Cell samples for FACS analysis were taken just before release (0 min) and every 20 min after for 240 min.

7.6 Sites of DNA Damage after Deregulation of Fork Rotation

As shown in Figure 7.5A, unrestricted fork rotation and DNA pre-catenation during DNA replication leads to accumulation of gamma-H2A. Moreover, Szilard et al. (2010) previously found that gamma-H2A is enriched at the yeast equivalent of mammalian fragile sites in wild-type yeast cells (Szilard et al., 2010). Surprisingly, this set consists of the replication-pausing loci that Stephanie Schalbetter found to be inducing fork rotation, such as tRNAs (Chapter 3 of the results section). Based on these findings, I predicted that if the DNA damage detected at these fragile sites in unchallenged cells was due to excessive DNA pre-catenation during DNA replication, deletion of Top2 and/or Tof1 should exacerbate H2AS129 phosphorylation during DNA replication at these protein-DNA pausing complexes and not at non-pausing loci. In an attempt to confirm this prediction, Stephanie Schalbetter conducted ChIP analysis for H2AS129P, which revealed that DNA damage was markedly higher in the absence of Top2 and/or Tof1 at two distinct genomic tRNA pausing sites in comparison with that at the two tested euchromatic sites (Figure 7.7). These cells were arrested using nocodazole to prevent detection of damage formed during mitosis. This data indicated that elevated levels of DNA damage and fragile-site instability is associated with high levels of fork rotation and DNA pre-catenation that take place at stable protein-DNA fragile sites.

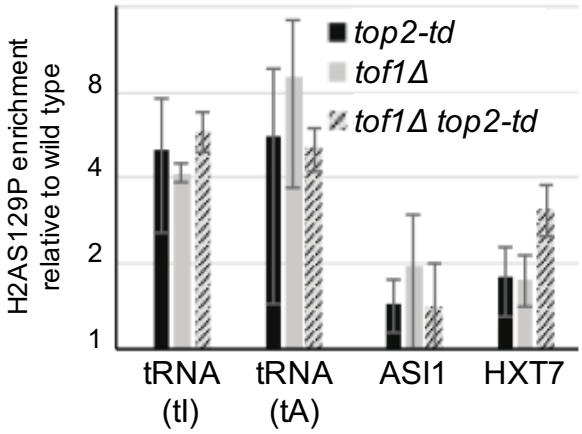

Figure 7.7: Excessive fork rotation and DNA pre-catenation leads to DNA damage at two tRNA loci and not at euchromatic loci.
Chromatin immunoprecipitation of H2AS129 phosphorylation in *top2-td, tof1Δ* and *tof1Δ top2-td* strains 80 min after release at two tRNAs and two euchromatic loci tI(AAU)N1 and tA(UGC)L. ChIP signal was normalized to input DNA before calculation of the relative change at each locus compared with wild-type cells.

Next, in order to identify the loci enriched in gamma-H2A, i.e. where the damage signals are located in wild-type*, top2-td, tof1Δ and tof1Δ top2-td* cells (Table 7.1), I set out to perform whole genome gamma-H2A chromatin immunoprecipitation high-throughput DNA sequencing (ChIP-Seq). This work was carried out in collaboration with the Zegerman lab. In order to learn the ChIP-Seq technique, I carried out the first set of experiments in the Zegerman lab at the University of Cambridge. With the knowledge acquired, I then set up and repeated the whole set of experiments in the Baxter lab at the University of Sussex.

Table 7.1 Genotypes of strains used for gamma-H2A ChIP-Seq.

Strain name	Samples sent for sequencing
wild-type	Gamma-H2A, Input
top2-td	Gamma-H2A, Input
tof1Δ	Gamma-H2A, Input
tof1Δ top2-td	Gamma-H2A, Input

The first experimental part of the ChIP-Seq experiment consisted of synchronising cells of all four strains described in Table 7.1 in the G1 phase using alpha factor. The cells were then switched to restrictive conditions (YP + 2% raffinose + 2% galactose; 37°C + 25 µg/ml doxycycline) before being released

into the S phase in the presence of nocodazole (to prevent detection of damage formed during mitosis) and collected after 90 min. Next, the harvested samples were processed as outlined in the Materials and Methods section (2.4.3). The arrest in this experiment was confirmed using FACS (Figure 7.8).

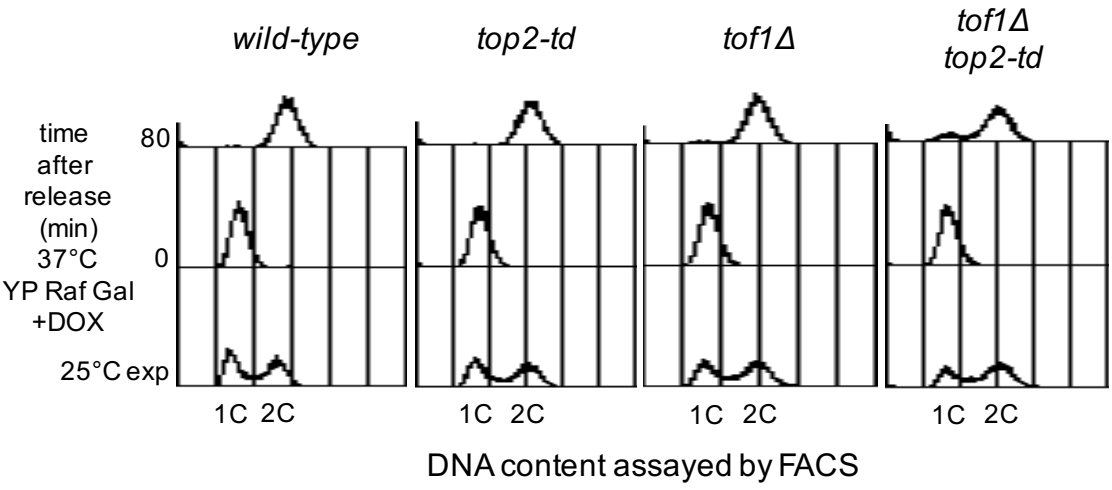

Figure 7.8: Representative FACS data showing the progression of wild-type*, top2-td, tof1Δ and tof1Δ top2-td* cells through the block and release protocol.
'exp' = exponentially growing population. '0 min' time point just prior to release from G1 block. '90 min' time point when cells reached G2/M, as assessed by the budding index.

After the first experimental part, I proceeded to perform the ChIP experiment to enrich DNA fragments associated with a protein of interest (Figure 7.9A). First, the protein was crosslinked to DNA *in vivo* using formaldehyde, which lead to the protein of interest remaining attached with chromatin through the rest of the process. After crosslinking, the cells were lysed and the chromatin was sheared by sonication into small fragments; the ideal size was 250 bp. DNA shearing was carried out using the Covaris M220 system (section 2.4.3.1). I ran cell-lysis solutions through 4, 8, 12, 16 and 20 min sonication to determine the length of time required to achieve optimal DNA strand length. As can be seen in Figure 7.9B, the sizes of DNA bands ranged broadly from nearly 100 bp all the way up to very large bands near the top of the gel after 4 min of sonication; however, the majority of the DNA smear fell within the region of optimal DNA strand size after 20 min of sonication. Hence, I determined that the ideal DNA strand length could be achieved after 20 min of sonication. Once the DNA was sheared, an antibody

specific to the protein of interest (gamma-H2A antibody) was used to immunoprecipitate the DNA-protein complex. Finally, the crosslinks were reversed and the released DNA was examined to identify the sequences bound by the protein (Figure 7.9A).

The construction of the ChIP-Seq library was carried out from the immunoprecipitated DNA fragments for this antibody sample and an input sample that carries two adapter sequences at both ends. The input sample corresponded to the genomic DNA before precipitation of gamma-H2A and served as the control for data analysis (Table 7.1). The PCR-amplified library was subjected to size selection in the ~250–370 bp range. Figure 7.9C schematically represents the main steps in ChIP-Seq library preparation. For the second repeat at the University of Sussex, I finally dispatched the prepared library to the University of Cambridge for sequencing. The ChIP-Seq analysis was done by George Allen (Bioinformatics Core, Gurdon Institute, University of Cambridge).

One important observation that could be made from the Top2 and/or Tof1 gamma-H2A ChIP-Seq profiles without further computational analysis was that high levels of constitutive damage could be detected in the *tof1Δ* cells. Depletion of Top2 alone resulted in less gamma-H2A than that observed in the *tof1Δ* cells; however, strong gamma-H2A peaks were detected on most of the chromosomes in the *tof1Δ top2-td* strain in comparison with that in wild-type*, top2-td* and *tof1Δ* strains, which suggested that DNA damage was exacerbated upon deletion of Tof1 and depletion of Top2 (Figure 7.10A). As shown in Figure 7.10B, a similar trend was also observed in two independent experiments, which indicated that the gamma-H2A signal was stronger in the *tof1Δ top2-td* strain; this result is also consistent with our previous data (Figure 7.5A). However, further analysis is required to identify the loci enriched for gamma-H2A. Figure 7.10 shows one representative chromosome for which ChIP-Seq was carried out in both Cambridge and Sussex Universities. In summary, this experiment revealed that excessive fork rotation and DNA pre-catenation lead to elevated levels of DNA damage at particular loci; these particular loci need to be identified and analysed in future studies.

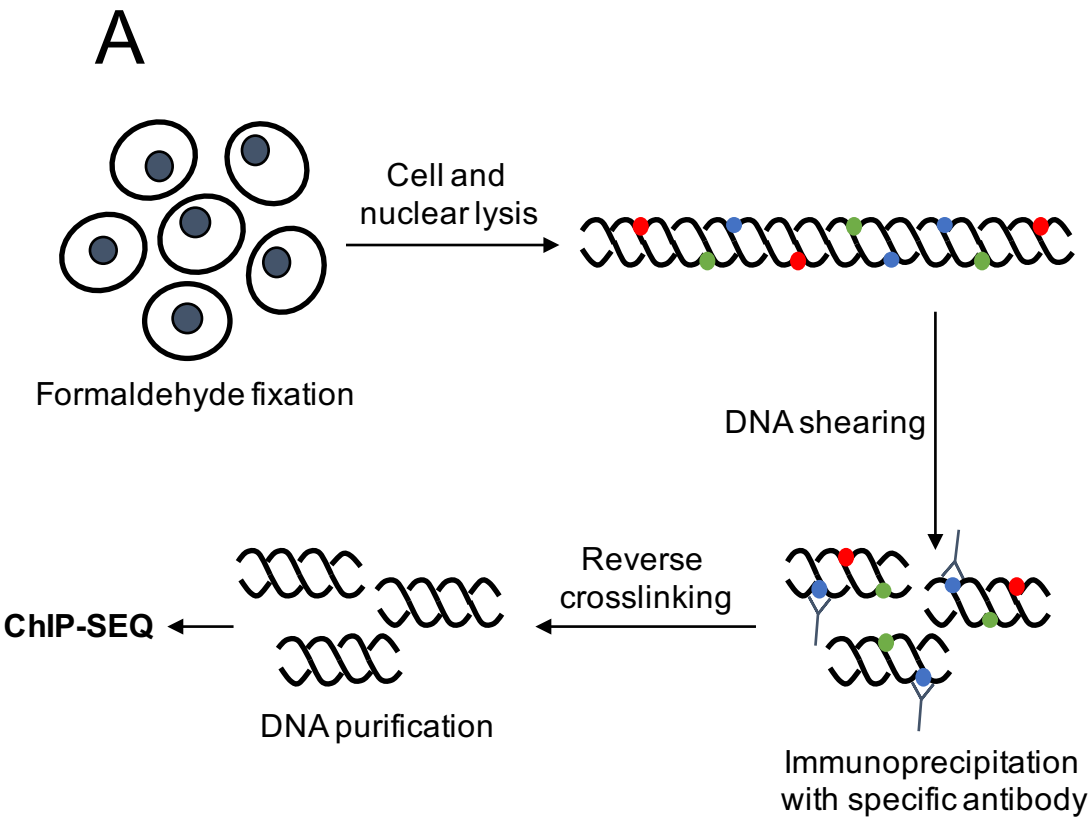
A
Cell and
nuclear lysis
Formaldehyde fixation
DNA shearing
Reverse
crosslinking
ChIP-SEQ
DNA purification
Immunoprecipitation
with specific antibody

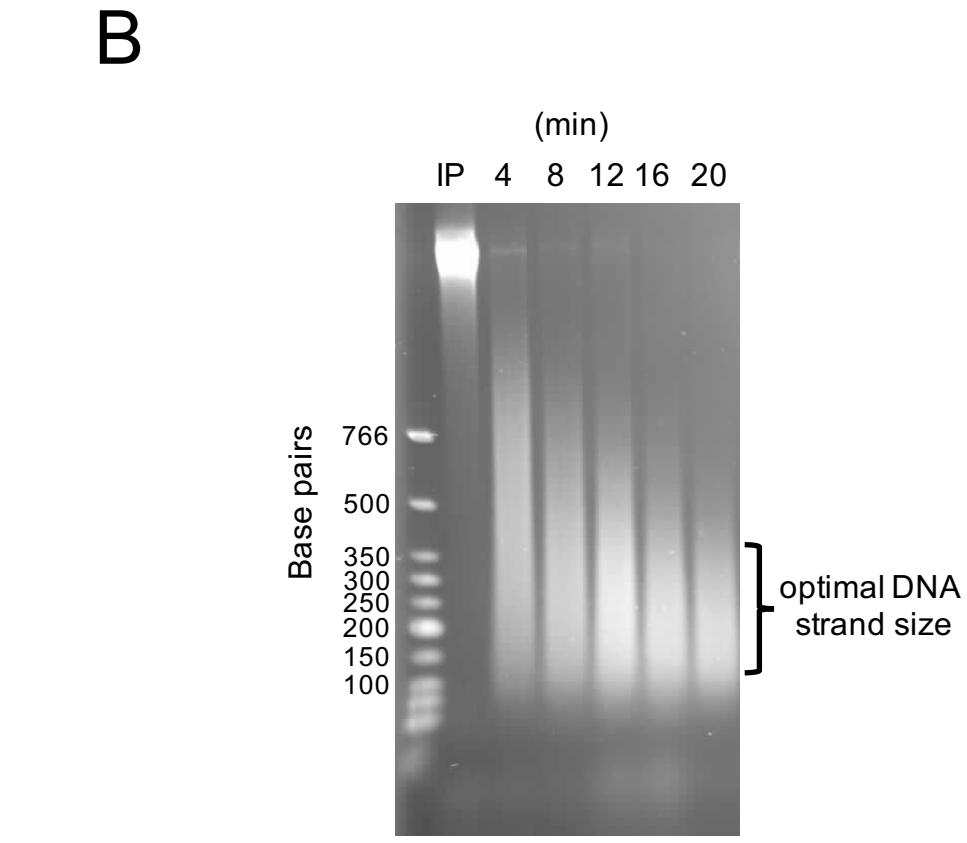
B
(min)
IP 4 8 12 16 20
Base pairs
766
500
350
300
250
200
150
100
optimal DNA
strand size

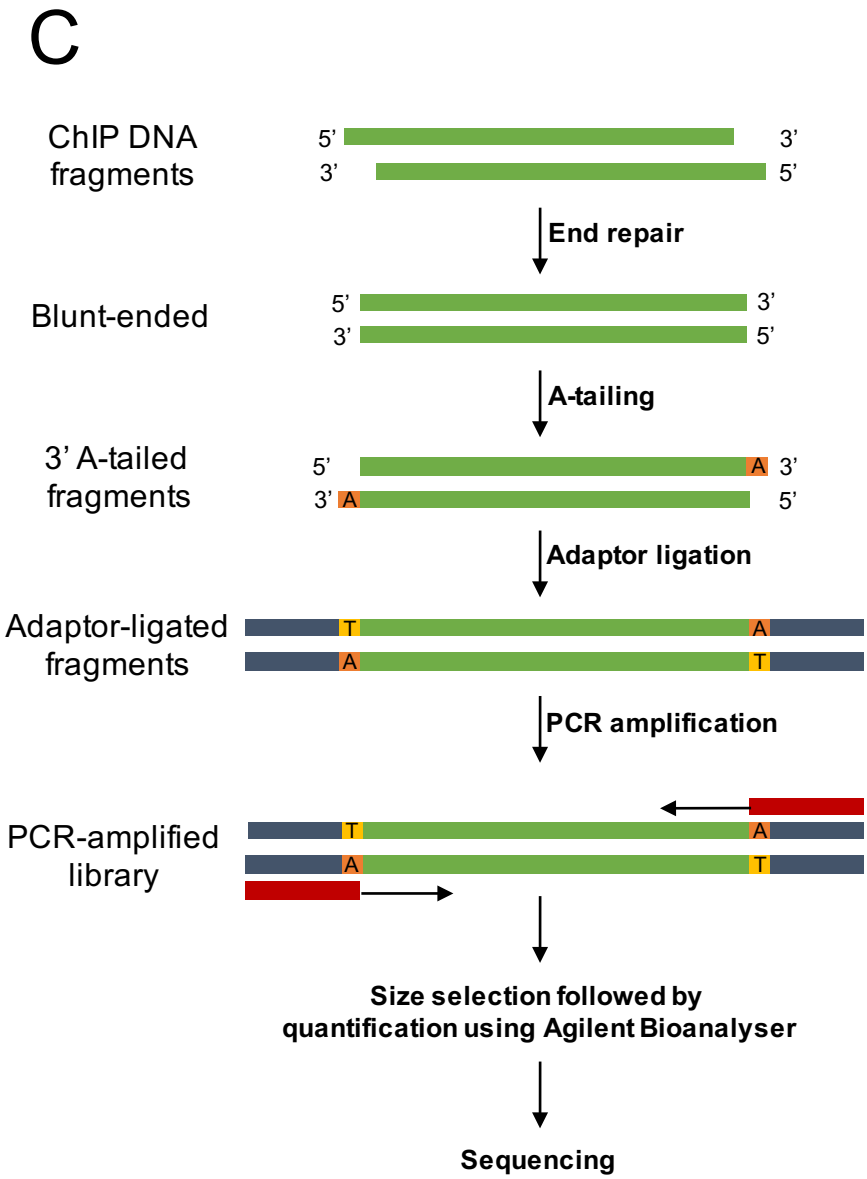

Figure 7.9: Schematic representation of the ChIP-Seq experimental design. **A**) Cartoon indicating different stages of the ChIP process. Budding yeast arrested in G2/M were fixed with formaldehyde, lysed and sonicated to shear the DNA. The protein of interest was immunoprecipitated with a specific antibody. Finally, the crosslinks were reversed. **B**) Test to determine the sonication time required to obtain optimal DNA fragment length of 250 bp. One 300 ml culture of cells was equally split into 6 separate cultures and processed through fixation and cell lysis. Supernatant from the lysed cells were then placed in the Covaris M220 system for the appropriate durations (4, 8, 12, 16 and 20 min). DNA was de-crosslinked, purified and run on a 2% agarose gel alongside a low molecular weight DNA ladder. **C**) Schematic diagram indicating the main steps of ChIP-Seq library preparation.

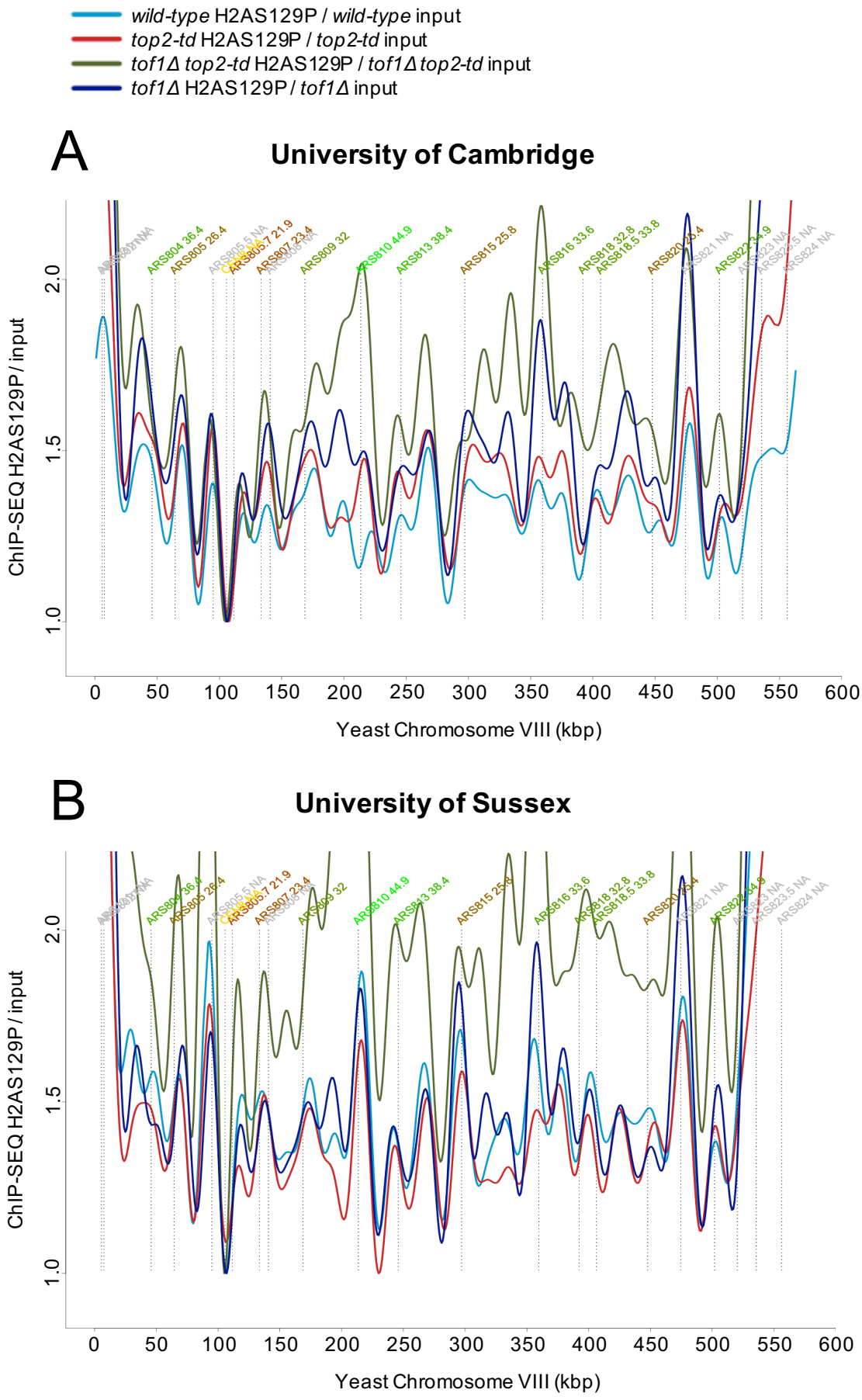
wild-type H2AS129P / wild-type input
top2-td H2AS129P / top2-td input
tof1Δ top2-td H2AS129P / tof1Δ top2-td input
tof1Δ H2AS129P / tof1Δ input
A
University of Cambridge
ChIP-SEQ H2AS129P / input
Yeast Chromosome VIII (kbp)
B
University of Sussex
ChIP-SEQ H2AS129P / input
Yeast Chromosome VIII (kbp)

Figure 7.10: A and B) Excessive fork rotation and DNA pre-catenation in *tof1Δ top2-td* cells lead to significant levels of DNA damage on most of the chromosomes.
Gamma-H2A ChIP-Seq profiles for chromosome VIII in G2/M arrested in restrictive condition wild-type-blue, *top2-td*-red, *tof1Δ*-navy and *tof1Δ top2-td*-green cells are indicated. The x-axis indicates chromosomal positions and the y-axis depicts the log ratio of the gamma-H2A signal normalised to the input signal.

7.7 Conclusions

In this chapter, I observed that *tof1Δ* cells strongly interacted synthetically with partial loss of Top2 activity, which was induced by transcriptional repression of the *top2-td* allele. Furthermore, aneuploidy and the "cut" phenotype was detected in *tof1Δ* cells under partial loss of Top2 using FACS and cytological analysis, respectively. However, these phenotypes were not observed in *mrc1Δ* cells under partial loss of Top2. Therefore, I concluded that deletion of *TOF1*, and not *MRC1*, leads to excessive fork rotation on endogenous chromosomes. I then found that *tof1Δ* cells under full depletion of Top2 show stable G2/M arrest in the cell cycle, which suggested the formation of defects in the newly replicated chromatids in *tof1Δ top2-td* cells; this in turn resulted in checkpoint activation and inhibition of mitosis. Studies in our lab conducted to explain the G2/M arrest indicated that constitutive DNA damage was significantly increased on the newly replicated chromatids in these cells as a result of excessive fork rotation and DNA pre-catenation during DNA replication, which caused the activation of the DNA damage checkpoint and extensive DNA repair. However, I could not determine the conditions under which prevention of checkpoint activation allowed cells to progress through mitosis. This could have been because the assay we used for analysing cell cycle progression (FACS) was not sensitive enough to detect the loss of any checkpoint inhibition of the mutants. It could also be due to the triggering of the spindle assembly checkpoint (SAC) in *tof1Δ top2-td* cells. It is known that both DNA damage checkpoint and SAC act through the stabilization of the securin, Pds1. Future research on this issue should be focused on examining the stabilization of Pds1 in each of these strains to examine if a checkpoint is activated and to identify the pathway activating the checkpoint.

Further research using ChIP-qPCR assay in our lab showed that gamma-H2A, a marker of DNA damage, was enriched at two distinct genomic tRNA pausing sites and not at two tested euchromatic sites in the absence of Top2 and/or Tof1. Therefore, in this chapter, I performed whole genome high throughput DNA sequencing for gamma-H2A to identify the loci enriched in gamma-H2A in cells lacking Top2 and/or Tof1. The primary analysis indicated that DNA damage was dramatically higher on most of the chromosomes in the *tof1Δ top2-td* cells; however, further computational analysis needs to be carried out to identify the loci enriched for gamma-H2A. This data is still undergoing analysis for final confirmation of the structures that may be particularly susceptible to fork rotation-dependent DNA damage.

Chapter 8

Discussion

8.1 Occurrence of Fork Rotation in Certain Chromosomal Contexts

Previous *in vitro* findings in bacterial replication systems have indicated that the occurrence of fork rotation is more frequent during elongation, which leads to the formation of extensive pre-catenanes behind the elongating forks (Hiasa et al., 1994, Peter et al., 1998, Lucas et al., 2001). Consequently, the topological stress created by DNA unwinding is relaxed during elongation either by topoisomerase action ahead of the fork or by fork rotation and DNA decatenation behind the fork (Bermejo et al., 2012, Postow et al., 2001a). However, in contrast to replication complexes created in *in vitro* systems and viral replisomes, in eukaryotic cells, the occurrence of fork rotation and pre-catenation seems to be less frequent due to the presence of various proteins and activities required for efficient DNA synthesis (Baxter, 2015).

Studies examining the termination of DNA replication in Simian virus 40 (SV40) have shown that fork rotation and formation of DNA pre-catenanes is the primary pathway causing DNA unwinding when two replication forks converge at the termination of DNA replication to unwind the final 100–150 bp. In this context, very little space is present between the converging forks, which is not sufficient for the topoisomerases to access and relax the torsional stress. Thus, fork rotation remains the sole pathway for DNA unwinding, failing which the high levels of torsional stress created would potentially arrest replication in its final stages. Topoisomerase II is then utilized to resolve the catenated molecules to form the fully replicated daughter chromosomes (Sundin and Varshavsky, 1980, Sundin and Varshavsky, 1981). If the enzyme in question fails to resolve either the pre-catenanes or full DNA catenation formed at the completion of DNA replication, aneuploidy, chromosome bridging, and non-disjunction can occur as a consequence of the unresolved intertwines. Therefore, it is crucial to unwind and remove all the intertwines between the two strands of the template DNA double-helix before the replicated chromosomes are pulled apart during cell division (Baxter, 2015).

In the third chapter of this thesis, I identified other scenarios where fork rotation is required outside of termination for DNA unwinding and preventing the torsional stress from arresting the replication progression. Upon conducting plasmid DNA catenation assays in budding yeast, I found that this DNA catenation assay facilitated a direct assessment of fork rotation and pre-catenation of the replicons. I then showed that increasing the size of plasmid replicons does not enhance the frequency of fork rotation events during DNA replication. Therefore, one can argue that fork rotation on a simple replicon primarily occurs during termination of DNA replication and does not generally occur during the elongation phase of DNA replication. Other data from our lab indicated that the frequency of fork rotation is increased at stable protein-DNA complexes such as tRNA genes and possibly centromeres during replication elongation by a mechanism similar to that thought to occur at termination. In this model, as the replisome converges at a stable protein-DNA complex, the access of topoisomerases ahead of the fork is impeded between the converging replisome and the complex, which leads to fork rotation and DNA pre-catenation at these hard-to-replicate and fragile loci in order to allow ongoing replication (Figure 8.1). Therefore, in eukaryotic cells, it appears that fork rotation and DNA pre-catenation is the preferential pathway in certain chromosomal contexts where the action of topoisomerases is inhibited from acting ahead of the fork, such as at termination and at stable protein-DNA complexes. In other genomic contexts such as at sites of converging genes, the action of topoisomerases could also be potentially impeded (Jeppsson et al., 2014), which would lead to elevated levels of topological stress. Thus, fork rotation appears to facilitate replication in these chromosomal contexts, leading to high levels of DNA pre-catenation.

8.2 Influence of Architectural Replisome Factors on Fork Rotation

In the fourth chapter of this thesis, I found that fork rotation is actively inhibited by the evolutionarily conserved Timeless/Tipin homologs, Tof1/Csm3, during DNA replication in budding yeast. This finding suggests that the relaxation of topological stress ahead of the fork is promoted by Tof1/Csm3, thus restricting the frequency of fork rotation, at least in budding yeast. Fork rotation seems to

take place only under certain chromosomal contexts where it is absolutely required, such as at termination or at stable protein-DNA complexes or wherever the activity of topoisomerases is limited, and fork rotation in these cases is the only pathway to unwind DNA. How Tof1/Csm3 mechanistically restrict fork rotation remains currently unknown. One possibility is through the interaction of Tof1 with eukaryotic topoisomerase I. This interaction has been shown both in yeast two-hybrid assays and *in vitro* (Park and Sternglanz, 1999) and it might promote the resolution of topological stress by topoisomerase I ahead of the fork and thus restrict excessive fork rotation. Timeless/Tipin proteins have been shown to be involved in coordinating the actions of the helicase and the leading strand polymerase (Errico et al., 2009, Bando et al., 2009, Cho et al., 2013). Therefore, the second possibility is that the replisome structure is disrupted in the absence of Timeless/Tipin orthologues, which could potentially lead to excessive fork rotation compared to that in the wild-type. This explanation would suggest that the presence of Tof1/Csm3 typically preserves the replisome structure in a conformation that is resistant to rotation.

It has been shown that DDK interacts with Tof1/Csm3 in fission and budding yeasts (Matsumoto et al., 2005, Murakami and Keeney, 2014). Moreover, one *in vivo* study has indicated that, when DDK is inactivated, Tof1 is released from the chromatin fractions (Bastia et al., 2016); the *in vitro* experiment in the same study also showed that DDK phosphorylates Mcm2-7 and CMG, which causes the recruitment of phosphorylated Tof1 at the replisome (Bastia et al., 2016). However, it is unclear whether DDK phosphorylates Tof1 (Bastia et al., 2016). Interestingly, I found that Cdc7 potentially restricts fork rotation during DNA replication. One possibility is that Cdc7 phosphorylates Tof1 and that this phosphorylation increases the efficiency of Tof1 function in inhibiting fork rotation. However, future studies need to be conducted to confirm this data and hypothesis.

Furthermore, in the fourth and in the fifth chapter, I found that deletion of *MRC1* or the lagging strand DNA polymerase, *POL32*, decreases fork rotation during DNA replication in plasmids containing pausing sites. Moreover, the phenotype of *mrc1-AQ* (the checkpoint-deficient mutant) was similar to that of wild-type

MRC1 throughout the S phase, which suggested that the effect of Mrc1 on fork rotation does not depend on its role in checkpoint signalling. One possible explanation for why Mrc1 and Pol32 promotes fork rotation is included in the following section.

8.3 Influence of Checkpoint Activation and Checkpoint Kinases on Fork Rotation

As discussed above, the structure and stability of the replisome provided by Tof1/Csm3 could be preventing excessive fork rotation. Under conditions of replication stress, checkpoint kinases are also thought to stabilize the replisome (Branzei and Foiani, 2006). Therefore, in the sixth chapter, I aimed to determine the influence of checkpoint activation and checkpoint kinases on fork rotation under topological stress. I found that when the replication fork progression stalls under HU treatment, the frequency of fork rotation is reduced. Tof1 has been shown to be phosphorylated by Mec1 and Tel1 (Bastos de Oliveira et al., 2015). Thus, it was possible that Mec1/Tel1 changed fork rotation through Tof1 in unchallenged cells. However, the frequency of fork rotation and DNA pre-catenation did not strongly change in the absence of *MEC1* alone or in the absence of *MEC1*/*TEL1* together during DNA replication. Therefore, I could argue that fork rotation during DNA replication is not inhibited by Mec1 and Tel1 in unchallenged cells. I further observed that deletion of *RAD53*, which is essential for replisome stabilization in challenged and unchallenged cells, did not alter the frequency of fork rotation. These data suggested that checkpoint kinases do not alter the frequency of fork rotation in unchallenged cells.

I observed three contexts, where the frequency of fork rotation is reduced—in cells lacking *MRC1*, cells lacking *POL32*, and cell under HU treatment. A possible explanation for the reduced fork rotation under these conditions could be the activity of Top3, which would lead to a decrease in the number of DNA catenanes. In general, Top3 is activated in the presence of ssDNA behind the fork, since type III enzyme requires single-stranded regions as a substrate (Harmon et al., 1999), and it hence passes single-stranded regions through the double-stranded regions to resolve DNA catenation. In the third chapter of this thesis, I further showed that

Top3, in the context of wild-type replisome does not influence fork rotation (Figure 3.5B). However, in situations where ssDNA might be generated due to the uncoupling of the helicase and the polymerase or due to deficiencies in the leading and lagging strand polymerases (Branzei and Foiani, 2005), sufficient ssDNA behind the fork may be generated to allow Top3 to decatenate the pre-catenanes. It is possible that ssDNA appears in the leading strand in *mrc1Δ* cells and in the lagging strand in *pol32Δ* cells; finally, potentially, in both strands, when replication fork progression is slowed under HU treatment, Top3 is activated and subsequently may act on the single stranded regions behind the fork.

8.4 Outcomes of Topological Stress on Replication— Fork Reversal versus Fork Rotation

So far, I have explained about fork rotation and the possible chromosomal contexts that it may occur in during DNA replication. As detailed in the first chapter of this thesis, the topological stress occurring in the unreplicated region ahead of the fork during DNA replication can be transferred to the replicated region behind the fork to inhibit replication fork stalling. However, several findings *in vitro* and *in vivo* have revealed that fork reversal of arrested forks can also happen in response to high levels of topological stress. Fork reversal is also known as fork regression and has been identified as one of the crucial mechanisms involved in the repair of arrested forks. During this process, nascent DNA strands are unwound and separated from the template strands and then annealed to each other. This leads to the formation of four-way replication structures. It is also important to note that fork reversal likely occurs following destabilization of the replisome (Postow et al., 2001b, Olavarrieta et al., 2002, Bermejo et al., 2011, Ray Chaudhuri et al., 2012). In an attempt to determine when fork rotation or fork reversal likely occurs in response to topological stress, Keszthelyi et al. (2016) hypothesized that when the torsional stress is at a level where it does not completely arrest, but only obstructs the ongoing DNA replication, it is resolved by fork rotation. Therefore, in this situation, fork rotation is potentially used as the primary pathway of DNA unwinding. In contrast, when the levels of topological stress completely arrest ongoing DNA replication, fork reversal might be the preferential pathway (Keszthelyi et al., 2016). In this case,

the replication fork is thought to be stabilized by fork reversal until the replication block is removed (Atkinson and McGlynn, 2009).

8.5 Genome Instability and Topological Stress

In general, loss of Top1 and Top2 together immediately arrests replication fork progression due to the formation of extensive unresolved topological stress ahead of the fork. However, replication fork progression is less affected in the absence of either Top1 or Top2 (Brill et al., 1987, Bermejo et al., 2007, Baxter and Diffley, 2008). Besides topoisomerase action, in some chromosomal contexts fork rotation is required to unwind the parental DNA during DNA replication, because the function of both topoisomerases ahead of the fork in these chromosomal contexts would not be sufficient to relax the torsional stress formed. It was then found that fork rotation is potentially utilized to inhibit the arresting of the forks and thus allows replication fork progression. Notably, these certain chromosomal contexts are known as fragile sites in higher eukaryotes, where the ongoing DNA replication can be slowed or inhibited; the DNA also tends to break at these sites in response to replication stress (Zeman and Cimprich, 2014). These fragile sites include stable protein-DNA complexes (Ivessa et al., 2003), long genes (Helmrich et al., 2011), highly transcribed genes (Barlow et al., 2013), and DNA prone to secondary structures (Thys et al., 2015). Although the reason for DNA breakage at these regions is not clear so far (Dillon et al., 2010), it has been predicted to occur due to inappropriate processing of the arrested forks (Carr and Lambert, 2013). Another reason can be the formation of unreplicated regions of DNA that occurs as a consequence of elevated levels of fork arrest, potentially leading to DNA breakage during cell division (Goodwin et al., 1999). It was also hypothesized that the potential fork arrest and double-strand breakage occur due to the high levels of torsional stress at these fragile sites. A possible solution in this case would be to resolve the topological stress by immediate fork rotation at these sites to potentially prevent fork stalling and double-strand breakage (Keszthelyi et al., 2016).

In this thesis, I showed that loss of *TOF1* leads to excessive fork rotation and formation of DNA catenation, which causes high levels of endogenous DNA

damage in cells and activates post-replication repair pathways. Hence, based on the observations, I believe that there might be a relationship between excessive fork rotation and endogenous DNA damage, as both DNA catenation and DNA damage accumulate at yeast fragile sites and are regulated by Tof1 and Top2 activity. In this context, the damage can be rapidly observed following the S phase before mitosis; therefore, the detected DNA damage is not due to the breakage of catenated DNA in mitosis. It is also speculated that the association between excessive fork rotation and endogenous DNA damage is through one of the following two pathways. First, in a population of cells, both fork reversal (Postow et al., 2001b) and fork rotation (Peter et al., 1998) may occur as a result of elevated levels of topological stress ahead of the fork and the damage can potentially take place as a consequence of inappropriate processing of the reversed forks. Second, the observed DNA damage is possibly due to the presence of massive DNA pre-catenation in the newly replicated chromatids (Figure 8.1), which potentially leads to the inhibition of several processes such as Okazaki fragment maturation behind the fork, thus forming gaps in the newly replicated chromosomes that need repair. This is consistent with our observation of high levels of PCNA ubiquitylation in cells where there is excessive fork rotation (*tof1Δ top2-td*). Cohesion establishment and intra-S checkpoint signalling also seems to be prevented in this model. This is the preferred hypothesis as loss of Tof1/Timeless is known to cause mitotic cohesion defects, loss of checkpoint signalling, and gaps in replicated chromosomes (Leman and Noguchi, 2012).

In summary, our data suggests that fork rotation can have both advantageous and disadvantageous influences on genome stability *in vivo*. The advantage of fork rotation is that it unwinds the final few turns of parental DNA to prevent fork stalling in response to torsional stress in certain chromosomal contexts, which leads to replication fork progression. On the other hand, the disadvantage of fork rotation is that excessive fork rotation and formation of DNA catenation may lead to high levels of endogenous DNA damage potentially at fragile sites. Thus, it could be interesting to attempt to identify sites of DNA damage following deregulation of fork rotation by using genome-wide assays in future studies. In addition, it will be interesting in the future to investigate the functions of homologs

of Tof1 and Csm3 in fork rotation at protein–DNA complexes in higher eukaryotes.

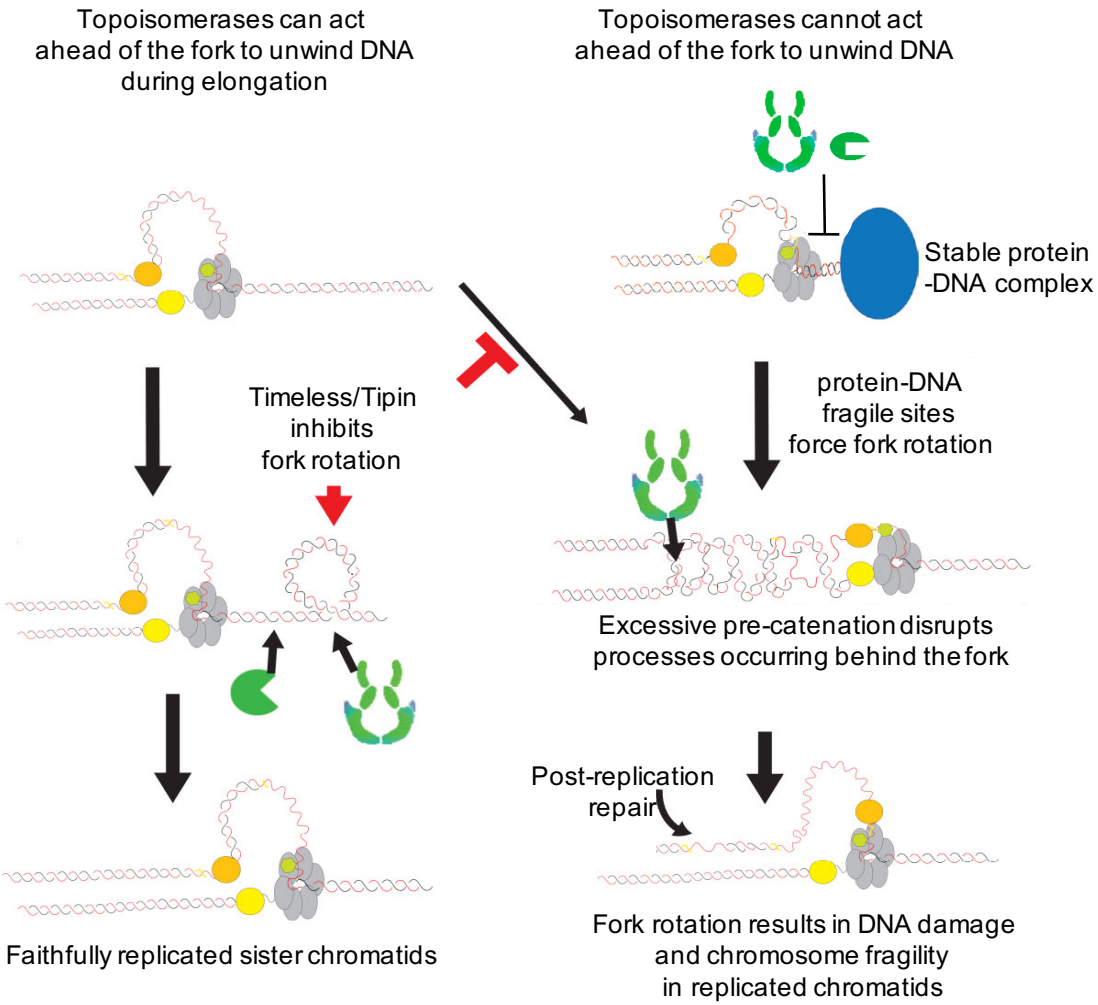

Figure 8.1: Model of the causes and consequences of fork rotation and pre-catenation.
Fork rotation is impeded by the action of topoisomerases ahead of the fork and by the function of Tof1/Csm3 during normal DNA replication (*left*). The action of topoisomerases is inhibited ahead of the fork in certain chromosomal contexts such as at stable protein-DNA complexes (*Right Top*). Thus, fork rotation is used to unwind DNA, leading to high levels of pre-catenation. Elevated levels of pre-catenation inhibit several processes such as Okazaki fragment maturation behind the fork, thus forming gaps in the newly replicated chromatids and leaving the chromatids fragile; these chromatids will consequently require repair.

Bibliography

ABBAS, T., KEATON, M. A. & DUTTA, A. 2013. Genomic instability in cancer. *Cold Spring Harb Perspect Biol,* 5**,** a012914.

AGUILERA, A. & GOMEZ-GONZALEZ, B. 2008. Genome instability: a mechanistic view of its causes and consequences. *Nat Rev Genet,* 9**,** 204-17.

ALANI, E., THRESHER, R., GRIFFITH, J. D. & KOLODNER, R. D. 1992. Characterization of DNA-binding and strand-exchange stimulation properties of y-RPA, a yeast single-strand-DNA-binding protein. *J Mol Biol,* 227**,** 54-71.

ALBERTS, B. J., A. LEWIS, J. RAFF, M. ROBERTS, K. AND WALTER, P. 2002. *Molecular Biology of the Cell [Book and CD-ROM]. Garland Science, 4 edition.*

ALCASABAS, A. A., OSBORN, A. J., BACHANT, J., HU, F., WERLER, P. J., BOUSSET, K., FURUYA, K., DIFFLEY, J. F., CARR, A. M. & ELLEDGE, S. J. 2001. Mrc1 transduces signals of DNA replication stress to activate Rad53. *Nat Cell Biol,* 3**,** 958-65.

ALLEN, J. B., ZHOU, Z., SIEDE, W., FRIEDBERG, E. C. & ELLEDGE, S. J. 1994. The SAD1/RAD53 protein kinase controls multiple checkpoints and DNA damage-induced transcription in yeast. *Genes Dev,* 8**,** 2401-15.

ANAND, R. P., SHAH, K. A., NIU, H., SUNG, P., MIRKIN, S. M. & FREUDENREICH, C. H. 2012. Overcoming natural replication barriers: differential helicase requirements. *Nucleic Acids Res,* 40**,** 1091-105.

APARICIO, O. M., WEINSTEIN, D. M. & BELL, S. P. 1997. Components and dynamics of DNA replication complexes in S. cerevisiae: redistribution of MCM proteins and Cdc45p during S phase. *Cell,* 91**,** 59-69.

ARAKI, H., HAMATAKE, R. K., JOHNSTON, L. H. & SUGINO, A. 1991a. DPB2, the gene encoding DNA polymerase II subunit B, is required for chromosome replication in Saccharomyces cerevisiae. *Proc Natl Acad Sci U S A,* 88**,** 4601-5.

ARAKI, H., HAMATAKE, R. K., MORRISON, A., JOHNSON, A. L., JOHNSTON, L. H. & SUGINO, A. 1991b. Cloning DPB3, the gene encoding the third subunit of DNA polymerase II of Saccharomyces cerevisiae. *Nucleic Acids Res,* 19**,** 4867-72.

ARGUESO, J. L., WESTMORELAND, J., MIECZKOWSKI, P. A., GAWEL, M., PETES, T. D. & RESNICK, M. A. 2008. Double-strand breaks associated

with repetitive DNA can reshape the genome. *Proc Natl Acad Sci U S A,* 105**,** 11845-50.

ATKINSON, J. & MCGLYNN, P. 2009. Replication fork reversal and the maintenance of genome stability. *Nucleic Acids Res,* 37**,** 3475-92.

AYLON, Y. & KUPIEC, M. 2004. DSB repair: the yeast paradigm. *DNA Repair (Amst),* 3**,** 797-815.

BAHLER, J., WU, J. Q., LONGTINE, M. S., SHAH, N. G., MCKENZIE, A., 3RD, STEEVER, A. B., WACH, A., PHILIPPSEN, P. & PRINGLE, J. R. 1998. Heterologous modules for efficient and versatile PCR-based gene targeting in Schizosaccharomyces pombe. *Yeast,* 14**,** 943-51.

BAKER, N. M., RAJAN, R. & MONDRAGON, A. 2009. Structural studies of type I topoisomerases. *Nucleic Acids Res,* 37**,** 693-701.

BALL, H. L., MYERS, J. S. & CORTEZ, D. 2005. ATRIP binding to replication protein A-single-stranded DNA promotes ATR-ATRIP localization but is dispensable for Chk1 phosphorylation. *Mol Biol Cell,* 16**,** 2372-81.

BANDO, M., KATOU, Y., KOMATA, M., TANAKA, H., ITOH, T., SUTANI, T. & SHIRAHIGE, K. 2009. Csm3, Tof1, and Mrc1 form a heterotrimeric mediator complex that associates with DNA replication forks. *J Biol Chem,* 284**,** 34355-65.

BARLOW, J. H., FARYABI, R. B., CALLEN, E., WONG, N., MALHOWSKI, A., CHEN, H. T., GUTIERREZ-CRUZ, G., SUN, H. W., MCKINNON, P., WRIGHT, G., CASELLAS, R., ROBBIANI, D. F., STAUDT, L., FERNANDEZ-CAPETILLO, O. & NUSSENZWEIG, A. 2013. Identification of early replicating fragile sites that contribute to genome instability. *Cell,* 152**,** 620-32.

BASTIA, D., SRIVASTAVA, P., ZAMAN, S., CHOUDHURY, M., MOHANTY, B. K., BACAL, J., LANGSTON, L. D., PASERO, P. & O'DONNELL, M. E. 2016. Phosphorylation of CMG helicase and Tof1 is required for programmed fork arrest. *Proc Natl Acad Sci U S A,* 113**,** E3639-48.

BASTOS DE OLIVEIRA, F. M., KIM, D., CUSSIOL, J. R., DAS, J., JEONG, M. C., DOERFLER, L., SCHMIDT, K. H., YU, H. & SMOLKA, M. B. 2015. Phosphoproteomics reveals distinct modes of Mec1/ATR signaling during DNA replication. *Mol Cell,* 57**,** 1124-32.

BATES, A. D. & MAXWELL, A. 2005. *DNA topology,* New York: Oxford University Press.

BAXTER, J. 2015. "Breaking up is hard to do": the formation and resolution of sister chromatid intertwines. *J Mol Biol,* 427**,** 590-607.

BAXTER, J. & ARAGON, L. 2012. A model for chromosome condensation based on the interplay between condensin and topoisomerase II. *Trends Genet,* 28**,** 110-7.

BAXTER, J. & DIFFLEY, J. F. 2008. Topoisomerase II inactivation prevents the completion of DNA replication in budding yeast. *Mol Cell,* 30**,** 790-802.

BAXTER, J., SEN, N., MARTINEZ, V. L., DE CARANDINI, M. E., SCHVARTZMAN, J. B., DIFFLEY, J. F. & ARAGON, L. 2011. Positive supercoiling of mitotic DNA drives decatenation by topoisomerase II in eukaryotes. *Science,* 331**,** 1328-32.

BELL, S. P. & DUTTA, A. 2002. DNA replication in eukaryotic cells. *Annu Rev Biochem,* 71**,** 333-74.

BELL, S. P. & KAGUNI, J. M. 2013. Helicase loading at chromosomal origins of replication. *Cold Spring Harb Perspect Biol,* 5.

BELL, S. P. & LABIB, K. 2016. Chromosome Duplication in Saccharomyces cerevisiae. *Genetics,* 203**,** 1027-67.

BELLAOUI, M., CHANG, M., OU, J., XU, H., BOONE, C. & BROWN, G. W. 2003. Elg1 forms an alternative RFC complex important for DNA replication and genome integrity. *Embo j,* 22**,** 4304-13.

BELLI, G., GARI, E., PIEDRAFITA, L., ALDEA, M. & HERRERO, E. 1998. An activator/repressor dual system allows tight tetracycline-regulated gene expression in budding yeast. *Nucleic Acids Res,* 26**,** 942-7.

BERG, J. M., TYMOCZKO, J. L. & STRYER, L. 2002. *Biochemistry,* New York: W H Freeman.

BERGER, J. M., FASS, D., WANG, J. C. & HARRISON, S. C. 1998. Structural similarities between topoisomerases that cleave one or both DNA strands. *Proc Natl Acad Sci U S A,* 95**,** 7876-81.

BERMEJO, R., CAPRA, T., JOSSEN, R., COLOSIO, A., FRATTINI, C., CAROTENUTO, W., COCITO, A., DOKSANI, Y., KLEIN, H., GOMEZ-GONZALEZ, B., AGUILERA, A., KATOU, Y., SHIRAHIGE, K. & FOIANI, M. 2011. The replication checkpoint protects fork stability by releasing transcribed genes from nuclear pores. *Cell,* 146**,** 233-46.

BERMEJO, R., DOKSANI, Y., CAPRA, T., KATOU, Y. M., TANAKA, H., SHIRAHIGE, K. & FOIANI, M. 2007. Top1- and Top2-mediated topological transitions at replication forks ensure fork progression and stability and prevent DNA damage checkpoint activation. *Genes Dev,* 21**,** 1921-36.

BERMEJO, R., LAI, M. S. & FOIANI, M. 2012. Preventing replication stress to maintain genome stability: resolving conflicts between replication and transcription. *Mol Cell,* 45**,** 710-8.

BERMUDEZ, V. P., MANIWA, Y., TAPPIN, I., OZATO, K., YOKOMORI, K. & HURWITZ, J. 2003. The alternative Ctf18-Dcc1-Ctf8-replication factor C complex required for sister chromatid cohesion loads proliferating cell nuclear antigen onto DNA. *Proc Natl Acad Sci U S A,* 100**,** 10237-42.

BLOOM, J. & CROSS, F. R. 2007. Multiple levels of cyclin specificity in cell-cycle control. *Nat Rev Mol Cell Biol,* 8**,** 149-60.

BOUSSET, K. & DIFFLEY, J. F. 1998. The Cdc7 protein kinase is required for origin firing during S phase. *Genes Dev,* 12**,** 480-90.

BRANZEI, D. & FOIANI, M. 2005. The DNA damage response during DNA replication. *Curr Opin Cell Biol,* 17**,** 568-75.

BRANZEI, D. & FOIANI, M. 2006. The Rad53 signal transduction pathway: Replication fork stabilization, DNA repair, and adaptation. *Exp Cell Res,* 312**,** 2654-9.

BRANZEI, D. & FOIANI, M. 2007. Interplay of replication checkpoints and repair proteins at stalled replication forks. *DNA Repair (Amst),* 6**,** 994-1003.

BRANZEI, D. & FOIANI, M. 2010. Maintaining genome stability at the replication fork. *Nat Rev Mol Cell Biol,* 11**,** 208-19.

BREWER, B. J. & FANGMAN, W. L. 1988. A replication fork barrier at the 3' end of yeast ribosomal RNA genes. *Cell,* 55**,** 637-43.

BRILL, S. J., DINARDO, S., VOELKEL-MEIMAN, K. & STERNGLANZ, R. 1987. Need for DNA topoisomerase activity as a swivel for DNA replication for transcription of ribosomal RNA. *Nature,* 326**,** 414-6.

BURGERS, P. M. 2009. Polymerase dynamics at the eukaryotic DNA replication fork. *J Biol Chem,* 284**,** 4041-5.

BURGERS, P. M. & GERIK, K. J. 1998. Structure and processivity of two forms of Saccharomyces cerevisiae DNA polymerase delta. *J Biol Chem,* 273**,** 19756-62.

BYLUND, G. O. & BURGERS, P. M. 2005. Replication protein A-directed unloading of PCNA by the Ctf18 cohesion establishment complex. *Mol Cell Biol,* 25**,** 5445-55.

CAIRNS, J. 1963. The bacterial chromosome and its manner of replication as seen by autoradiography. *J Mol Biol,* 6**,** 208-13.

CALZADA, A., HODGSON, B., KANEMAKI, M., BUENO, A. & LABIB, K. 2005. Molecular anatomy and regulation of a stable replisome at a paused eukaryotic DNA replication fork. *Genes Dev,* 19**,** 1905-19.

CARR, A. M. & LAMBERT, S. 2013. Replication stress-induced genome instability: the dark side of replication maintenance by homologous recombination. *J Mol Biol,* 425**,** 4733-44.

CHA, R. S. & KLECKNER, N. 2002. ATR homolog Mec1 promotes fork progression, thus averting breaks in replication slow zones. *Science,* 297**,** 602-6.

CHAMPOUX, J. J. 2001. DNA topoisomerases: structure, function, and mechanism. *Annu Rev Biochem,* 70**,** 369-413.

CHAMPOUX, J. J. & BEEN, M. D. 1980. *Topoisomerases and the swivel problem,* Academic, New York.

CHAMPOUX, J. J. & DULBECCO, R. 1972. An activity from mammalian cells that untwists superhelical DNA--a possible swivel for DNA replication (polyoma-ethidium bromide-mouse-embryo cells-dye binding assay). *Proc Natl Acad Sci U S A,* 69**,** 143-6.

CHAN, D. W., YE, R., VEILLETTE, C. J. & LEES-MILLER, S. P. 1999. DNA-dependent protein kinase phosphorylation sites in Ku 70/80 heterodimer. *Biochemistry,* 38**,** 1819-28.

CHEN, S. H. & ZHOU, H. 2009. Reconstitution of Rad53 activation by Mec1 through adaptor protein Mrc1. *J Biol Chem,* 284**,** 18593-604.

CHILKOVA, O., JONSSON, B. H. & JOHANSSON, E. 2003. The quaternary structure of DNA polymerase epsilon from Saccharomyces cerevisiae. *J Biol Chem,* 278**,** 14082-6.

CHO, W. H., KANG, Y. H., AN, Y. Y., TAPPIN, I., HURWITZ, J. & LEE, J. K. 2013. Human Tim-Tipin complex affects the biochemical properties of the replicative DNA helicase and DNA polymerases. *Proc Natl Acad Sci U S A,* 110**,** 2523-7.

CHOU, D. M. & ELLEDGE, S. J. 2006. Tipin and Timeless form a mutually protective complex required for genotoxic stress resistance and checkpoint function. *Proc Natl Acad Sci U S A,* 103**,** 18143-7.

CHRISTIANSON, T. W., SIKORSKI, R. S., DANTE, M., SHERO, J. H. & HIETER, P. 1992. Multifunctional yeast high-copy-number shuttle vectors. *Gene,* 110**,** 119-22.

CIMPRICH, K. A. & CORTEZ, D. 2008. ATR: an essential regulator of genome integrity. *Nat Rev Mol Cell Biol,* 9**,** 616-27.

COBB, J. A., BJERGBAEK, L., SHIMADA, K., FREI, C. & GASSER, S. M. 2003. DNA polymerase stabilization at stalled replication forks requires Mec1 and the RecQ helicase Sgs1. *Embo j,* 22**,** 4325-36.

COOPER, G. M. 2000. The Cell: A Molecular Approach. The Eukaryotic Cell Cycle. Sunderland (MA): Sinauer Associates; 2000. 2nd edition.

CORBETT, K. D. & BERGER, J. M. 2003. Emerging roles for plant topoisomerase VI. *Chem Biol,* 10**,** 107-11.

CORTEZ, D. 2005. Unwind and slow down: checkpoint activation by helicase and polymerase uncoupling. *Genes Dev,* 19**,** 1007-12.

CORTEZ, D., WANG, Y., QIN, J. & ELLEDGE, S. J. 1999. Requirement of ATM-dependent phosphorylation of brca1 in the DNA damage response to double-strand breaks. *Science,* 286**,** 1162-6.

COSTANZO, V., ROBERTSON, K., BIBIKOVA, M., KIM, E., GRIECO, D., GOTTESMAN, M., CARROLL, D. & GAUTIER, J. 2001. Mre11 protein complex prevents double-strand break accumulation during chromosomal DNA replication. *Mol Cell,* 8**,** 137-47.

CRISONA, N. J., STRICK, T. R., BENSIMON, D., CROQUETTE, V. & COZZARELLI, N. R. 2000. Preferential relaxation of positively supercoiled DNA by E. coli topoisomerase IV in single-molecule and ensemble measurements. *Genes Dev,* 14**,** 2881-92.

DAI, J., CHUANG, R. Y. & KELLY, T. J. 2005. DNA replication origins in the Schizosaccharomyces pombe genome. *Proc Natl Acad Sci U S A,* 102**,** 337-42.

DALGAARD, J. Z. & KLAR, A. J. 2000. swi1 and swi3 perform imprinting, pausing, and termination of DNA replication in S. pombe. *Cell,* 102**,** 745-51.

DE PICCOLI, G., KATOU, Y., ITOH, T., NAKATO, R., SHIRAHIGE, K. & LABIB, K. 2012. Replisome stability at defective DNA replication forks is independent of S phase checkpoint kinases. *Mol Cell,* 45**,** 696-704.

DELBRUCK, M. 1954. on the replication of desoxyribonucleic acid (DNA). *Proc Natl Acad Sci U S A,* 40**,** 783-788.

DESANY, B. A., ALCASABAS, A. A., BACHANT, J. B. & ELLEDGE, S. J. 1998. Recovery from DNA replicational stress is the essential function of the S-phase checkpoint pathway. *Genes Dev,* 12**,** 2956-70.

DESHPANDE, A. M. & NEWLON, C. S. 1996. DNA replication fork pause sites dependent on transcription. *Science,* 272**,** 1030-3.

DHAR, M. K., SEHGAL, S. & KAUL, S. 2012. Structure, replication efficiency and fragility of yeast ARS elements. *Res Microbiol,* 163**,** 243-53.

DILLON, L. W., BURROW, A. A. & WANG, Y. H. 2010. DNA instability at chromosomal fragile sites in cancer. *Curr Genomics,* 11**,** 326-37.

DONALDSON, A. D., FANGMAN, W. L. & BREWER, B. J. 1998. Cdc7 is required throughout the yeast S phase to activate replication origins. *Genes Dev,* 12**,** 491-501.

DOWNS, J. A., LOWNDES, N. F. & JACKSON, S. P. 2000. A role for Saccharomyces cerevisiae histone H2A in DNA repair. *Nature,* 408**,** 1001-4.

DUA, R., LEVY, D. L. & CAMPBELL, J. L. 1999. Analysis of the essential functions of the C-terminal protein/protein interaction domain of Saccharomyces cerevisiae pol epsilon and its unexpected ability to support growth in the absence of the DNA polymerase domain. *J Biol Chem,* 274**,** 22283-8.

DUCH, A., PALOU, G., JONSSON, Z. O., PALOU, R., CALVO, E., WOHLSCHLEGEL, J. & QUINTANA, D. G. 2011. A Dbf4 mutant contributes to bypassing the Rad53-mediated block of origins of replication in response to genotoxic stress. *J Biol Chem,* 286**,** 2486-91.

DUGUET, M. 1997. When helicase and topoisomerase meet! *J Cell Sci,* 110 (Pt 12)**,** 1345-50.

EATON, M. L., GALANI, K., KANG, S., BELL, S. P. & MACALPINE, D. M. 2010. Conserved nucleosome positioning defines replication origins. *Genes Dev,* 24**,** 748-53.

EKLUND, H., UHLIN, U., FARNEGARDH, M., LOGAN, D. T. & NORDLUND, P. 2001. Structure and function of the radical enzyme ribonucleotide reductase. *Prog Biophys Mol Biol,* 77**,** 177-268.

EMILI, A. 1998. MEC1-dependent phosphorylation of Rad9p in response to DNA damage. *Mol Cell,* 2**,** 183-9.

ERRICO, A., COSENTINO, C., RIVERA, T., LOSADA, A., SCHWOB, E., HUNT, T. & COSTANZO, V. 2009. Tipin/Tim1/And1 protein complex promotes Pol alpha chromatin binding and sister chromatid cohesion. *Embo j,* 28**,** 3681-92.

ERRICO, A., COSTANZO, V. & HUNT, T. 2007. Tipin is required for stalled replication forks to resume DNA replication after removal of aphidicolin in Xenopus egg extracts. *Proc Natl Acad Sci U S A,* 104**,** 14929-34.

FANNING, E., KLIMOVICH, V. & NAGER, A. R. 2006. A dynamic model for replication protein A (RPA) function in DNA processing pathways. *Nucleic Acids Res,* 34**,** 4126-37.

FARINA, A., SHIN, J. H., KIM, D. H., BERMUDEZ, V. P., KELMAN, Z., SEO, Y. S. & HURWITZ, J. 2008. Studies with the human cohesin establishment factor, ChlR1. Association of ChlR1 with Ctf18-RFC and Fen1. *J Biol Chem,* 283**,** 20925-36.

FENG, W. & D'URSO, G. 2001. Schizosaccharomyces pombe cells lacking the amino-terminal catalytic domains of DNA polymerase epsilon are viable but require the DNA damage checkpoint control. *Mol Cell Biol,* 21**,** 4495-504.

FOLTMAN, M., EVRIN, C., DE PICCOLI, G., JONES, R. C., EDMONDSON, R. D., KATOU, Y., NAKATO, R., SHIRAHIGE, K. & LABIB, K. 2013. Eukaryotic replisome components cooperate to process histones during chromosome replication. *Cell Rep,* 3**,** 892-904.

FONG, C. M., ARUMUGAM, A. & KOEPP, D. M. 2013. The Saccharomyces cerevisiae F-box protein Dia2 is a mediator of S-phase checkpoint recovery from DNA damage. *Genetics,* 193**,** 483-99.

FORD, E. 2015. *Chip-seq library construction using truseq adapters.* [Online]. Available: https: //ethanomics.files.wordpress.com/2012/09/chip_truseq.pdf. [Accessed].

FORSBURG, S. L. & NURSE, P. 1991. Cell cycle regulation in the yeasts Saccharomyces cerevisiae and Schizosaccharomyces pombe. *Annu Rev Cell Biol,* 7**,** 227-56.

FORTERRE, P., GRIBALDO, S., GADELLE, D. & SERRE, M. C. 2007. Origin and evolution of DNA topoisomerases. *Biochimie,* 89**,** 427-46.

FOSS, E. J. 2001. Tof1p regulates DNA damage responses during S phase in Saccharomyces cerevisiae. *Genetics,* 157**,** 567-77.

FRAGKOS, M., GANIER, O., COULOMBE, P. & MECHALI, M. 2015. DNA replication origin activation in space and time. *Nat Rev Mol Cell Biol,* 16**,** 360-74.

FRIEDEL, A. M., PIKE, B. L. & GASSER, S. M. 2009. ATR/Mec1: coordinating fork stability and repair. *Curr Opin Cell Biol,* 21**,** 237-44.

GAMBUS, A., JONES, R. C., SANCHEZ-DIAZ, A., KANEMAKI, M., VAN DEURSEN, F., EDMONDSON, R. D. & LABIB, K. 2006. GINS maintains association of Cdc45 with MCM in replisome progression complexes at eukaryotic DNA replication forks. *Nat Cell Biol,* 8**,** 358-66.

GAMBUS, A., VAN DEURSEN, F., POLYCHRONOPOULOS, D., FOLTMAN, M., JONES, R. C., EDMONDSON, R. D., CALZADA, A. & LABIB, K. 2009. A key role for Ctf4 in coupling the MCM2-7 helicase to DNA polymerase alpha within the eukaryotic replisome. *Embo j,* 28**,** 2992-3004.

GANGLOFF, S., DE MASSY, B., ARTHUR, L., ROTHSTEIN, R. & FABRE, F. 1999. The essential role of yeast topoisomerase III in meiosis depends on recombination. *Embo j,* 18**,** 1701-11.

GANGLOFF, S., MCDONALD, J. P., BENDIXEN, C., ARTHUR, L. & ROTHSTEIN, R. 1994. The yeast type I topoisomerase Top3 interacts with Sgs1, a DNA helicase homolog: a potential eukaryotic reverse gyrase. *Mol Cell Biol,* 14**,** 8391-8.

GARDNER, R., PUTNAM, C. W. & WEINERT, T. 1999. RAD53, DUN1 and PDS1 define two parallel G2/M checkpoint pathways in budding yeast. *Embo j,* 18**,** 3173-85.

GELLERT, M., MIZUUCHI, K., O'DEA, M. H. & NASH, H. A. 1976. DNA gyrase: an enzyme that introduces superhelical turns into DNA. *Proc Natl Acad Sci U S A,* 73**,** 3872-6.

GEORGESCU, R. E., LANGSTON, L., YAO, N. Y., YURIEVA, O., ZHANG, D., FINKELSTEIN, J., AGARWAL, T. & O'DONNELL, M. E. 2014. Mechanism of asymmetric polymerase assembly at the eukaryotic replication fork. *Nat Struct Mol Biol,* 21**,** 664-70.

GERIK, K. J., LI, X., PAUTZ, A. & BURGERS, P. M. 1998. Characterization of the two small subunits of Saccharomyces cerevisiae DNA polymerase delta. *J Biol Chem,* 273**,** 19747-55.

GERRING, S. L., SPENCER, F. & HIETER, P. 1990. The CHL 1 (CTF 1) gene product of Saccharomyces cerevisiae is important for chromosome transmission and normal cell cycle progression in G2/M. *Embo j,* 9**,** 4347-58.

GILBERT, D. M. 2001. Making sense of eukaryotic DNA replication origins. *Science,* 294**,** 96-100.

GOODWIN, A., WANG, S. W., TODA, T., NORBURY, C. & HICKSON, I. D. 1999. Topoisomerase III is essential for accurate nuclear division in Schizosaccharomyces pombe. *Nucleic Acids Res,* 27**,** 4050-8.

GOTO, T. & WANG, J. C. 1982. Yeast DNA topoisomerase II. An ATP-dependent type II topoisomerase that catalyzes the catenation, decatenation, unknotting, and relaxation of double-stranded DNA rings. *J Biol Chem,* 257**,** 5866-72.

GOTTER, A. L., SUPPA, C. & EMANUEL, B. S. 2007. Mammalian TIMELESS and Tipin are evolutionarily conserved replication fork-associated factors. *J Mol Biol,* 366**,** 36-52.

GOTTIFREDI, V. & PRIVES, C. 2005. The S phase checkpoint: when the crowd meets at the fork. *Semin Cell Dev Biol,* 16**,** 355-68.

GREENFEDER, S. A. & NEWLON, C. S. 1992. Replication forks pause at yeast centromeres. *Mol Cell Biol,* 12**,** 4056-66.

HAERING, C. H. & NASMYTH, K. 2003. Building and breaking bridges between sister chromatids. *Bioessays,* 25**,** 1178-91.

HANNA, J. S., KROLL, E. S., LUNDBLAD, V. & SPENCER, F. A. 2001. Saccharomyces cerevisiae CTF18 and CTF4 are required for sister chromatid cohesion. *Mol Cell Biol,* 21**,** 3144-58.

HANNA, M., BALL, L. G., TONG, A. H., BOONE, C. & XIAO, W. 2007. Pol32 is required for Pol zeta-dependent translesion synthesis and prevents double-strand breaks at the replication fork. *Mutat Res,* 625**,** 164-76.

HARACSKA, L., UNK, I., JOHNSON, R. E., JOHANSSON, E., BURGERS, P. M., PRAKASH, S. & PRAKASH, L. 2001. Roles of yeast DNA polymerases delta and zeta and of Rev1 in the bypass of abasic sites. *Genes Dev,* 15**,** 945-54.

HARASHIMA, H., DISSMEYER, N. & SCHNITTGER, A. 2013. Cell cycle control across the eukaryotic kingdom. *Trends Cell Biol,* 23**,** 345-56.

HARDY, C. F., DRYGA, O., SEEMATTER, S., PAHL, P. M. & SCLAFANI, R. A. 1997. mcm5/cdc46-bob1 bypasses the requirement for the S phase activator Cdc7p. *Proc Natl Acad Sci U S A,* 94**,** 3151-5.

HARMON, F. G., DIGATE, R. J. & KOWALCZYKOWSKI, S. C. 1999. RecQ helicase and topoisomerase III comprise a novel DNA strand passage function: a conserved mechanism for control of DNA recombination. *Mol Cell,* 3**,** 611-20.

HARPER, J. W. & ELLEDGE, S. J. 2007. The DNA damage response: ten years after. *Mol Cell,* 28**,** 739-45.

HARRISON, J. C. & HABER, J. E. 2006. Surviving the breakup: the DNA damage checkpoint. *Annu Rev Genet,* 40**,** 209-35.

HARTWELL, L. H. & WEINERT, T. A. 1989. Checkpoints: controls that ensure the order of cell cycle events. *Science,* 246**,** 629-34.

HELMRICH, A., BALLARINO, M. & TORA, L. 2011. Collisions between replication and transcription complexes cause common fragile site instability at the longest human genes. *Mol Cell,* 44**,** 966-77.

HIASA, H., DIGATE, R. J. & MARIANS, K. J. 1994. Decatenating activity of Escherichia coli DNA gyrase and topoisomerases I and III during oriC and pBR322 DNA replication in vitro. *J Biol Chem,* 269**,** 2093-9.

HIASA, H. & MARIANS, K. J. 1994. Topoisomerase III, but not topoisomerase I, can support nascent chain elongation during theta-type DNA replication. *J Biol Chem,* 269**,** 32655-9.

HIASA, H. & MARIANS, K. J. 1996. Two distinct modes of strand unlinking during theta-type DNA replication. *J Biol Chem,* 271**,** 21529-35.

HODGSON, B., CALZADA, A. & LABIB, K. 2007. Mrc1 and Tof1 regulate DNA replication forks in different ways during normal S phase. *Mol Biol Cell,* 18**,** 3894-902.

HOLM, C., GOTO, T., WANG, J. C. & BOTSTEIN, D. 1985. DNA topoisomerase II is required at the time of mitosis in yeast. *Cell,* 41**,** 553-63.

HUANG, M., ZHOU, Z. & ELLEDGE, S. J. 1998. The DNA replication and damage checkpoint pathways induce transcription by inhibition of the Crt1 repressor. *Cell,* 94**,** 595-605.

HUANG, M. E., RIO, A. G., GALIBERT, M. D. & GALIBERT, F. 2002. Pol32, a subunit of Saccharomyces cerevisiae DNA polymerase delta, suppresses genomic deletions and is involved in the mutagenic bypass pathway. *Genetics,* 160**,** 1409-22.

HUBSCHER, U. 2009. DNA replication fork proteins. *Methods Mol Biol,* 521**,** 19-33.

HUDSON, B. & VINOGRAD, J. 1967. Catenated Circular DNA Molecules in HeLa Cell Mitochondria. *Nature,* 216**,** 647-652.

HUSTEDT, N., GASSER, S. M. & SHIMADA, K. 2013. Replication checkpoint: tuning and coordination of replication forks in s phase. *Genes (Basel),* 4**,** 388-434.

IVESSA, A. S., LENZMEIER, B. A., BESSLER, J. B., GOUDSOUZIAN, L. K., SCHNAKENBERG, S. L. & ZAKIAN, V. A. 2003. The Saccharomyces cerevisiae helicase Rrm3p facilitates replication past nonhistone protein-DNA complexes. *Mol Cell,* 12**,** 1525-36.

JANKE, C., MAGIERA, M. M., RATHFELDER, N., TAXIS, C., REBER, S., MAEKAWA, H., MORENO-BORCHART, A., DOENGES, G., SCHWOB, E., SCHIEBEL, E. & KNOP, M. 2004. A versatile toolbox for PCR-based tagging of yeast genes: new fluorescent proteins, more markers and promoter substitution cassettes. *Yeast,* 21**,** 947-62.

JAZAYERI, A., FALCK, J., LUKAS, C., BARTEK, J., SMITH, G. C., LUKAS, J. & JACKSON, S. P. 2006. ATM- and cell cycle-dependent regulation of ATR in response to DNA double-strand breaks. *Nat Cell Biol,* 8**,** 37-45.

JEPPSSON, K., CARLBORG, K. K., NAKATO, R., BERTA, D. G., LILIENTHAL, I., KANNO, T., LINDQVIST, A., BRINK, M. C., DANTUMA, N. P., KATOU, Y., SHIRAHIGE, K. & SJOGREN, C. 2014. The chromosomal association of the Smc5/6 complex depends on cohesion and predicts the level of sister chromatid entanglement. *PLoS Genet,* 10**,** e1004680.

JOSHI, R. S., PINA, B. & ROCA, J. 2012. Topoisomerase II is required for the production of long Pol II gene transcripts in yeast. *Nucleic Acids Res,* 40**,** 7907-15.

KANEMAKI, M., SANCHEZ-DIAZ, A., GAMBUS, A. & LABIB, K. 2003. Functional proteomic identification of DNA replication proteins by induced proteolysis in vivo. *Nature,* 423**,** 720-4.

KANG, Y. H., GALAL, W. C., FARINA, A., TAPPIN, I. & HURWITZ, J. 2012. Properties of the human Cdc45/Mcm2-7/GINS helicase complex and its action with DNA polymerase epsilon in rolling circle DNA synthesis. *Proc Natl Acad Sci U S A,* 109**,** 6042-7.

KANNOUCHE, P. L., WING, J. & LEHMANN, A. R. 2004. Interaction of human DNA polymerase eta with monoubiquitinated PCNA: a possible mechanism for the polymerase switch in response to DNA damage. *Mol Cell,* 14**,** 491-500.

KATOU, Y., KANOH, Y., BANDO, M., NOGUCHI, H., TANAKA, H., ASHIKARI, T., SUGIMOTO, K. & SHIRAHIGE, K. 2003. S-phase checkpoint proteins Tof1 and Mrc1 form a stable replication-pausing complex. *Nature,* 424**,** 1078-83.

KESTI, T., FLICK, K., KERANEN, S., SYVAOJA, J. E. & WITTENBERG, C. 1999. DNA polymerase epsilon catalytic domains are dispensable for DNA replication, DNA repair, and cell viability. *Mol Cell,* 3**,** 679-85.

KESZTHELYI, A., MINCHELL, N. E. & BAXTER, J. 2016. The Causes and Consequences of Topological Stress during DNA Replication. *Genes (Basel),* 7.

KHODURSKY, A. B., PETER, B. J., SCHMID, M. B., DERISI, J., BOTSTEIN, D., BROWN, P. O. & COZZARELLI, N. R. 2000. Analysis of topoisomerase function in bacterial replication fork movement: use of DNA microarrays. *Proc Natl Acad Sci U S A,* 97**,** 9419-24.

KIM, E. M. & BURKE, D. J. 2008. DNA damage activates the SAC in an ATM/ATR-dependent manner, independently of the kinetochore. *PLoS Genet,* 4**,** e1000015.

KIM, R. A. & WANG, J. C. 1989. Function of DNA topoisomerases as replication swivels in Saccharomyces cerevisiae. *J Mol Biol,* 208**,** 257-67.

KIM, S. T., LIM, D. S., CANMAN, C. E. & KASTAN, M. B. 1999. Substrate specificities and identification of putative substrates of ATM kinase family members. *J Biol Chem,* 274**,** 37538-43.

KIRKEGAARD, K. & WANG, J. C. 1985. Bacterial DNA topoisomerase I can relax positively supercoiled DNA containing a single-stranded loop. *J Mol Biol,* 185**,** 625-37.

KNOP, M., SIEGERS, K., PEREIRA, G., ZACHARIAE, W., WINSOR, B., NASMYTH, K. & SCHIEBEL, E. 1999. Epitope tagging of yeast genes using a PCR-based strategy: more tags and improved practical routines. *Yeast,* 15**,** 963-72.

KOMATA, M., BANDO, M., ARAKI, H. & SHIRAHIGE, K. 2009. The direct binding of Mrc1, a checkpoint mediator, to Mcm6, a replication helicase, is essential for the replication checkpoint against methyl methanesulfonate-induced stress. *Mol Cell Biol,* 29**,** 5008-19.

KOUPRINA, N., KROLL, E., BANNIKOV, V., BLISKOVSKY, V., GIZATULLIN, R., KIRILLOV, A., SHESTOPALOV, B., ZAKHARYEV, V., HIETER, P., SPENCER, F. & ET AL. 1992. CTF4 (CHL15) mutants exhibit defective DNA metabolism in the yeast Saccharomyces cerevisiae. *Mol Cell Biol,* 12**,** 5736-47.

KREBS, J. E., GOLDSTEIN, E. S. & KILPATRICK, S. T. 2011. *LEWIN'S GENES X,* Jones and Bartlett publishers, LLC.

KRINGS, G. & BASTIA, D. 2004. swi1- and swi3-dependent and independent replication fork arrest at the ribosomal DNA of Schizosaccharomyces pombe. *Proc Natl Acad Sci U S A,* 101**,** 14085-90.

KUBOTA, T., HIRAGA, S., YAMADA, K., LAMOND, A. I. & DONALDSON, A. D. 2011. Quantitative proteomic analysis of chromatin reveals that Ctf18 acts in the DNA replication checkpoint. *Mol Cell Proteomics,* 10**,** M110.005561.

KUMAR, S. & BURGERS, P. M. 2013. Lagging strand maturation factor Dna2 is a component of the replication checkpoint initiation machinery. *Genes Dev,* 27**,** 313-21.

LABIB, K. 2010. How do Cdc7 and cyclin-dependent kinases trigger the initiation of chromosome replication in eukaryotic cells? *Genes Dev,* 24**,** 1208-19.

LABIB, K. & DE PICCOLI, G. 2011. Surviving chromosome replication: the many roles of the S-phase checkpoint pathway. *Philos Trans R Soc Lond B Biol Sci,* 366**,** 3554-61.

LABIB, K. & DIFFLEY, J. F. 2001. Is the MCM2-7 complex the eukaryotic DNA replication fork helicase? *Curr Opin Genet Dev,* 11**,** 64-70.

LANGSTON, L. D., ZHANG, D., YURIEVA, O., GEORGESCU, R. E., FINKELSTEIN, J., YAO, N. Y., INDIANI, C. & O'DONNELL, M. E. 2014. CMG helicase and DNA polymerase epsilon form a functional 15-subunit holoenzyme for eukaryotic leading-strand DNA replication. *Proc Natl Acad Sci U S A,* 111**,** 15390-5.

LEE, Y. D., WANG, J., STUBBE, J. & ELLEDGE, S. J. 2008. Dif1 is a DNA-damage-regulated facilitator of nuclear import for ribonucleotide reductase. *Mol Cell,* 32**,** 70-80.

LEMAN, A. R., NOGUCHI, C., LEE, C. Y. & NOGUCHI, E. 2010. Human Timeless and Tipin stabilize replication forks and facilitate sister-chromatid cohesion. *J Cell Sci,* 123**,** 660-70.

LEMAN, A. R. & NOGUCHI, E. 2012. Local and global functions of Timeless and Tipin in replication fork protection. *Cell Cycle,* 11**,** 3945-55.

LENGRONNE, A., MCINTYRE, J., KATOU, Y., KANOH, Y., HOPFNER, K. P., SHIRAHIGE, K. & UHLMANN, F. 2006. Establishment of sister chromatid cohesion at the S. cerevisiae replication fork. *Mol Cell,* 23**,** 787-99.

LEONARD, A. C. & MECHALI, M. 2013. DNA replication origins. *Cold Spring Harb Perspect Biol,* 5**,** a010116.

LEVINE, C., HIASA, H. & MARIANS, K. J. 1998. DNA gyrase and topoisomerase IV: biochemical activities, physiological roles during chromosome replication, and drug sensitivities. *Biochim Biophys Acta,* 1400**,** 29-43.

LI, Y. & ARAKI, H. 2013. Loading and activation of DNA replicative helicases: the key step of initiation of DNA replication. *Genes Cells,* 18**,** 266-77.

LI, Y., PURSELL, Z. F. & LINN, S. 2000. Identification and cloning of two histone fold motif-containing subunits of HeLa DNA polymerase epsilon. *J Biol Chem,* 275**,** 31554.

LICHTEN, M. 2001. Meiotic recombination: breaking the genome to save it. *Curr Biol,* 11**,** R253-6.

LINSKENS, M. H. & HUBERMAN, J. A. 1988. Organization of replication of ribosomal DNA in Saccharomyces cerevisiae. *Mol Cell Biol,* 8**,** 4927-35.

LIU, L., MO, J., RODRIGUEZ-BELMONTE, E. M. & LEE, M. Y. 2000a. Identification of a fourth subunit of mammalian DNA polymerase delta. *J Biol Chem,* 275**,** 18739-44.

LIU, L. F. & WANG, J. C. 1987. Supercoiling of the DNA template during transcription. *Proc Natl Acad Sci U S A,* 84**,** 7024-7.

LIU, Q. & WANG, J. C. 1998. Identification of active site residues in the "GyrA" half of yeast DNA topoisomerase II. *J Biol Chem,* 273**,** 20252-60.

LIU, Y., VIDANES, G., LIN, Y. C., MORI, S. & SIEDE, W. 2000b. Characterization of a Saccharomyces cerevisiae homologue of Schizosaccharomyces pombe Chk1 involved in DNA-damage-induced M-phase arrest. *Mol Gen Genet,* 262**,** 1132-46.

LOHMAN, T. M. 1993. Helicase-catalyzed DNA unwinding. *J Biol Chem,* 268**,** 2269-72.

LONDON, T. B., BARBER, L. J., MOSEDALE, G., KELLY, G. P., BALASUBRAMANIAN, S., HICKSON, I. D., BOULTON, S. J. & HIOM, K. 2008. FANCJ is a structure-specific DNA helicase associated with the maintenance of genomic G/C tracts. *J Biol Chem,* 283**,** 36132-9.

LOPES, M., COTTA-RAMUSINO, C., PELLICIOLI, A., LIBERI, G., PLEVANI, P., MUZI-FALCONI, M., NEWLON, C. S. & FOIANI, M. 2001. The DNA replication checkpoint response stabilizes stalled replication forks. *Nature,* 412**,** 557-61.

LOPEZ-MOSQUEDA, J., MAAS, N. L., JONSSON, Z. O., DEFAZIO-ELI, L. G., WOHLSCHLEGEL, J. & TOCZYSKI, D. P. 2010. Damage-induced phosphorylation of Sld3 is important to block late origin firing. *Nature,* 467**,** 479-83.

LOU, H., KOMATA, M., KATOU, Y., GUAN, Z., REIS, C. C., BUDD, M., SHIRAHIGE, K. & CAMPBELL, J. L. 2008. Mrc1 and DNA polymerase epsilon function together in linking DNA replication and the S phase checkpoint. *Mol Cell,* 32**,** 106-17.

LUCAS, I., GERME, T., CHEVRIER-MILLER, M. & HYRIEN, O. 2001. Topoisomerase II can unlink replicating DNA by precatenane removal. *Embo j,* 20**,** 6509-19.

MA, J. L., LEE, S. J., DUONG, J. K. & STERN, D. F. 2006. Activation of the checkpoint kinase Rad53 by the phosphatidyl inositol kinase-like kinase Mec1. *J Biol Chem,* 281**,** 3954-63.

MACULINS, T., NKOSI, P. J., NISHIKAWA, H. & LABIB, K. 2015. Tethering of SCF(Dia2) to the Replisome Promotes Efficient Ubiquitylation and Disassembly of the CMG Helicase. *Curr Biol,* 25**,** 2254-9.

MAKOVETS, S., HERSKOWITZ, I. & BLACKBURN, E. H. 2004. Anatomy and dynamics of DNA replication fork movement in yeast telomeric regions. *Mol Cell Biol,* 24**,** 4019-31.

MARAHRENS, Y. & STILLMAN, B. 1992. A yeast chromosomal origin of DNA replication defined by multiple functional elements. *Science,* 255**,** 817-23.

MARIC, M., MACULINS, T., DE PICCOLI, G. & LABIB, K. 2014. Cdc48 and a ubiquitin ligase drive disassembly of the CMG helicase at the end of DNA replication. *Science,* 346**,** 1253596.

MARINI, J. C., MILLER, K. G. & ENGLUND, P. T. 1980. Decatenation of kinetoplast DNA by topoisomerases. *J Biol Chem,* 255**,** 4976-9.

MARTINEZ-ROBLES, M. L., WITZ, G., HERNANDEZ, P., SCHVARTZMAN, J. B., STASIAK, A. & KRIMER, D. B. 2009. Interplay of DNA supercoiling and catenation during the segregation of sister duplexes. *Nucleic Acids Res,* 37**,** 5126-37.

MASAI, H., MATSUMOTO, S., YOU, Z., YOSHIZAWA-SUGATA, N. & ODA, M. 2010. Eukaryotic chromosome DNA replication: where, when, and how? *Annu Rev Biochem,* 79**,** 89-130.

MATSUMOTO, S., OGINO, K., NOGUCHI, E., RUSSELL, P. & MASAI, H. 2005. Hsk1-Dfp1/Him1, the Cdc7-Dbf4 kinase in Schizosaccharomyces pombe, associates with Swi1, a component of the replication fork protection complex. *J Biol Chem,* 280**,** 42536-42.

MAYER, M. L., GYGI, S. P., AEBERSOLD, R. & HIETER, P. 2001. Identification of RFC(Ctf18p, Ctf8p, Dcc1p): an alternative RFC complex required for sister chromatid cohesion in S. cerevisiae. *Mol Cell,* 7**,** 959-70.

MAYER, M. L., POT, I., CHANG, M., XU, H., ANELIUNAS, V., KWOK, T., NEWITT, R., AEBERSOLD, R., BOONE, C., BROWN, G. W. & HIETER, P. 2004. Identification of protein complexes required for efficient sister chromatid cohesion. *Mol Biol Cell,* 15**,** 1736-45.

MCINTOSH, D. & BLOW, J. J. 2012. Dormant origins, the licensing checkpoint, and the response to replicative stresses. *Cold Spring Harb Perspect Biol,* 4.

MILES, J. & FORMOSA, T. 1992. Evidence that POB1, a Saccharomyces cerevisiae protein that binds to DNA polymerase alpha, acts in DNA metabolism in vivo. *Mol Cell Biol,* 12**,** 5724-35.

MIYABE, I., KUNKEL, T. A. & CARR, A. M. 2011. The major roles of DNA polymerases epsilon and delta at the eukaryotic replication fork are evolutionarily conserved. *PLoS Genet,* 7**,** e1002407.

MIYAKE, T., LOCH, C. M. & LI, R. 2002. Identification of a multifunctional domain in autonomously replicating sequence-binding factor 1 required for transcriptional activation, DNA replication, and gene silencing. *Mol Cell Biol,* 22**,** 505-16.

MOHANTY, B. K., BAIRWA, N. K. & BASTIA, D. 2006. The Tof1p-Csm3p protein complex counteracts the Rrm3p helicase to control replication termination of Saccharomyces cerevisiae. *Proc Natl Acad Sci U S A,* 103**,** 897-902.

MOLDOVAN, G. L., PFANDER, B. & JENTSCH, S. 2007. PCNA, the maestro of the replication fork. *Cell,* 129**,** 665-79.

MORAIS CABRAL, J. H., JACKSON, A. P., SMITH, C. V., SHIKOTRA, N., MAXWELL, A. & LIDDINGTON, R. C. 1997. Crystal structure of the breakage-reunion domain of DNA gyrase. *Nature,* 388**,** 903-6.

MORGAN, D. O. 1995. Principles of CDK regulation. *Nature,* 374**,** 131-4.

MOROHASHI, H., MACULINS, T. & LABIB, K. 2009. The amino-terminal TPR domain of Dia2 tethers SCF(Dia2) to the replisome progression complex. *Curr Biol,* 19**,** 1943-9.

MORROW, D. M., TAGLE, D. A., SHILOH, Y., COLLINS, F. S. & HIETER, P. 1995. TEL1, an S. cerevisiae homolog of the human gene mutated in ataxia telangiectasia, is functionally related to the yeast checkpoint gene MEC1. *Cell,* 82**,** 831-40.

MURAKAMI, H. & KEENEY, S. 2014. Temporospatial coordination of meiotic DNA replication and recombination via DDK recruitment to replisomes. *Cell,* 158**,** 861-73.

MYERS, J. S. & CORTEZ, D. 2006. Rapid activation of ATR by ionizing radiation requires ATM and Mre11. *J Biol Chem,* 281**,** 9346-50.

NATSUME, T., MULLER, C. A., KATOU, Y., RETKUTE, R., GIERLINSKI, M., ARAKI, H., BLOW, J. J., SHIRAHIGE, K., NIEDUSZYNSKI, C. A. & TANAKA, T. U. 2013. Kinetochores coordinate pericentromeric cohesion and early DNA replication by Cdc7-Dbf4 kinase recruitment. *Mol Cell,* 50**,** 661-74.

NEDELCHEVA, M. N., ROGUEV, A., DOLAPCHIEV, L. B., SHEVCHENKO, A., TASKOV, H. B., SHEVCHENKO, A., STEWART, A. F. & STOYNOV, S. S. 2005. Uncoupling of unwinding from DNA synthesis implies regulation of MCM helicase by Tof1/Mrc1/Csm3 checkpoint complex. *J Mol Biol,* 347**,** 509-21.

NICHOLS, M. D., DEANGELIS, K., KECK, J. L. & BERGER, J. M. 1999. Structure and function of an archaeal topoisomerase VI subunit with homology to the meiotic recombination factor Spo11. *Embo j,* 18**,** 6177-88.

NICK MCELHINNY, S. A., GORDENIN, D. A., STITH, C. M., BURGERS, P. M. & KUNKEL, T. A. 2008. Division of labor at the eukaryotic replication fork. *Mol Cell,* 30**,** 137-44.

NIEDUSZYNSKI, C. A., HIRAGA, S., AK, P., BENHAM, C. J. & DONALDSON, A. D. 2007. OriDB: a DNA replication origin database. *Nucleic Acids Res,* 35**,** D40-6.

NIEDUSZYNSKI, C. A., KNOX, Y. & DONALDSON, A. D. 2006. Genome-wide identification of replication origins in yeast by comparative genomics. *Genes Dev,* 20**,** 1874-9.

NOGUCHI, E., NOGUCHI, C., DU, L. L. & RUSSELL, P. 2003. Swi1 prevents replication fork collapse and controls checkpoint kinase Cds1. *Mol Cell Biol,* 23**,** 7861-74.

NOGUCHI, E., NOGUCHI, C., MCDONALD, W. H., YATES, J. R., 3RD & RUSSELL, P. 2004. Swi1 and Swi3 are components of a replication fork protection complex in fission yeast. *Mol Cell Biol,* 24**,** 8342-55.

NORDLUND, P. & REICHARD, P. 2006. Ribonucleotide reductases. *Annu Rev Biochem,* 75**,** 681-706.

NURSE, P. 1997. Regulation of the eukaryotic cell cycle. *Eur J Cancer,* 33**,** 1002-4.

NURSE, P., LEVINE, C., HASSING, H. & MARIANS, K. J. 2003. Topoisomerase III can serve as the cellular decatenase in Escherichia coli. *J Biol Chem,* 278**,** 8653-60.

O'DONNELL, M., LANGSTON, L. & STILLMAN, B. 2013. Principles and concepts of DNA replication in bacteria, archaea, and eukarya. *Cold Spring Harb Perspect Biol,* 5.

OHYA, T., KAWASAKI, Y., HIRAGA, S., KANBARA, S., NAKAJO, K., NAKASHIMA, N., SUZUKI, A. & SUGINO, A. 2002. The DNA polymerase domain of pol(epsilon) is required for rapid, efficient, and highly accurate chromosomal DNA replication, telomere length maintenance, and normal cell senescence in Saccharomyces cerevisiae. *J Biol Chem,* 277**,** 28099-108.

OHYA, T., MAKI, S., KAWASAKI, Y. & SUGINO, A. 2000. Structure and function of the fourth subunit (Dpb4p) of DNA polymerase epsilon in Saccharomyces cerevisiae. *Nucleic Acids Res,* 28**,** 3846-52.

OLAVARRIETA, L., MARTINEZ-ROBLES, M. L., SOGO, J. M., STASIAK, A., HERNANDEZ, P., KRIMER, D. B. & SCHVARTZMAN, J. B. 2002. Supercoiling, knotting and replication fork reversal in partially replicated plasmids. *Nucleic Acids Res,* 30**,** 656-66.

OSBORN, A. J. & ELLEDGE, S. J. 2003. Mrc1 is a replication fork component whose phosphorylation in response to DNA replication stress activates Rad53. *Genes Dev,* 17**,** 1755-67.

PARISH, J. L., ROSA, J., WANG, X., LAHTI, J. M., DOXSEY, S. J. & ANDROPHY, E. J. 2006. The DNA helicase ChlR1 is required for sister chromatid cohesion in mammalian cells. *J Cell Sci,* 119**,** 4857-65.

PARK, H. & STERNGLANZ, R. 1999. Identification and characterization of the genes for two topoisomerase I-interacting proteins from Saccharomyces cerevisiae. *Yeast,* 15**,** 35-41.

PAULOVICH, A. G. & HARTWELL, L. H. 1995. A checkpoint regulates the rate of progression through S phase in S. cerevisiae in response to DNA damage. *Cell,* 82**,** 841-7.

PELLICIOLI, A. & FOIANI, M. 2005. Signal transduction: how rad53 kinase is activated. *Curr Biol,* 15**,** R769-71.

PELLICIOLI, A., LUCCA, C., LIBERI, G., MARINI, F., LOPES, M., PLEVANI, P., ROMANO, A., DI FIORE, P. P. & FOIANI, M. 1999. Activation of Rad53 kinase in response to DNA damage and its effect in modulating phosphorylation of the lagging strand DNA polymerase. *Embo j,* 18**,** 6561-72.

PENG, H. & MARIANS, K. J. 1993. Decatenation activity of topoisomerase IV during oriC and pBR322 DNA replication in vitro. *Proc Natl Acad Sci U S A,* 90**,** 8571-5.

PEREZ-CHEEKS, B. A., LEE, C., HAYAMA, R. & MARIANS, K. J. 2012. A role for topoisomerase III in Escherichia coli chromosome segregation. *Mol Microbiol,* 86**,** 1007-22.

PETER, B. J., ULLSPERGER, C., HIASA, H., MARIANS, K. J. & COZZARELLI, N. R. 1998. The structure of supercoiled intermediates in DNA replication. *Cell,* 94**,** 819-27.

POLI, J., TSAPONINA, O., CRABBE, L., KESZTHELYI, A., PANTESCO, V., CHABES, A., LENGRONNE, A. & PASERO, P. 2012. dNTP pools determine fork progression and origin usage under replication stress. *Embo j,* 31**,** 883-94.

POSTOW, L., CRISONA, N. J., PETER, B. J., HARDY, C. D. & COZZARELLI, N. R. 2001a. Topological challenges to DNA replication: conformations at the fork. *Proc Natl Acad Sci U S A,* 98**,** 8219-26.

POSTOW, L., HARDY, C. D., ARSUAGA, J. & COZZARELLI, N. R. 2004. Topological domain structure of the Escherichia coli chromosome. *Genes Dev,* 18**,** 1766-79.

POSTOW, L., ULLSPERGER, C., KELLER, R. W., BUSTAMANTE, C., VOLOGODSKII, A. V. & COZZARELLI, N. R. 2001b. Positive torsional strain causes the formation of a four-way junction at replication forks. *J Biol Chem,* 276**,** 2790-6.

PUTNAM, C. D., HAYES, T. K. & KOLODNER, R. D. 2009. Specific pathways prevent duplication-mediated genome rearrangements. *Nature,* 460**,** 984-9.

RAGHURAMAN, M. K., WINZELER, E. A., COLLINGWOOD, D., HUNT, S., WODICKA, L., CONWAY, A., LOCKHART, D. J., DAVIS, R. W., BREWER, B. J. & FANGMAN, W. L. 2001. Replication dynamics of the yeast genome. *Science,* 294**,** 115-21.

RANDELL, J. C., BOWERS, J. L., RODRIGUEZ, H. K. & BELL, S. P. 2006. Sequential ATP hydrolysis by Cdc6 and ORC directs loading of the Mcm2-7 helicase. *Mol Cell,* 21**,** 29-39.

RANDELL, J. C., FAN, A., CHAN, C., FRANCIS, L. I., HELLER, R. C., GALANI, K. & BELL, S. P. 2010. Mec1 is one of multiple kinases that prime the Mcm2-7 helicase for phosphorylation by Cdc7. *Mol Cell,* 40**,** 353-63.

RAO, H. & STILLMAN, B. 1995. The origin recognition complex interacts with a bipartite DNA binding site within yeast replicators. *Proc Natl Acad Sci U S A,* 92**,** 2224-8.

RAY CHAUDHURI, A., HASHIMOTO, Y., HERRADOR, R., NEELSEN, K. J., FACHINETTI, D., BERMEJO, R., COCITO, A., COSTANZO, V. & LOPES, M. 2012. Topoisomerase I poisoning results in PARP-mediated replication fork reversal. *Nat Struct Mol Biol,* 19**,** 417-23.

REMUS, D., BEURON, F., TOLUN, G., GRIFFITH, J. D., MORRIS, E. P. & DIFFLEY, J. F. 2009. Concerted loading of Mcm2-7 double hexamers around DNA during DNA replication origin licensing. *Cell,* 139**,** 719-30.

ROEDER, G. S. & FINK, G. R. 1980. DNA rearrangements associated with a transposable element in yeast. *Cell,* 21**,** 239-49.

ROWLEY, A., COCKER, J. H., HARWOOD, J. & DIFFLEY, J. F. 1995. Initiation complex assembly at budding yeast replication origins begins with the recognition of a bipartite sequence by limiting amounts of the initiator, ORC. *Embo j,* 14**,** 2631-41.

SALE, J. E. 2013. Translesion DNA synthesis and mutagenesis in eukaryotes. *Cold Spring Harb Perspect Biol,* 5**,** a012708.

SALE, J. E., BATTERS, C., EDMUNDS, C. E., PHILLIPS, L. G., SIMPSON, L. J. & SZUTS, D. 2009. Timing matters: error-prone gap filling and translesion synthesis in immunoglobulin gene hypermutation. *Philos Trans R Soc Lond B Biol Sci,* 364**,** 595-603.

SALE, J. E., LEHMANN, A. R. & WOODGATE, R. 2012. Y-family DNA polymerases and their role in tolerance of cellular DNA damage. *Nat Rev Mol Cell Biol,* 13**,** 141-52.

SAMBROOK, J., FRITSCH, E. & MANIATIS, T. 1989. *Molecular Cloning: A Laboratory Manual.*, Cold spring harbor, NY, Cold spring harbor laboratory press.

SAMORA, C. P., SAKSOUK, J., GOSWAMI, P., WADE, B. O., SINGLETON, M. R., BATES, P. A., LENGRONNE, A., COSTA, A. & UHLMANN, F. 2016. Ctf4 Links DNA Replication with Sister Chromatid Cohesion Establishment by Recruiting the Chl1 Helicase to the Replisome. *Mol Cell,* 63**,** 371-84.

SANCHEZ, Y., BACHANT, J., WANG, H., HU, F., LIU, D., TETZLAFF, M. & ELLEDGE, S. J. 1999. Control of the DNA damage checkpoint by chk1 and rad53 protein kinases through distinct mechanisms. *Science,* 286**,** 1166-71.

SANCHEZ, Y., DESANY, B. A., JONES, W. J., LIU, Q., WANG, B. & ELLEDGE, S. J. 1996. Regulation of RAD53 by the ATM-like kinases MEC1 and TEL1 in yeast cell cycle checkpoint pathways. *Science,* 271**,** 357-60.

SANTOCANALE, C. & DIFFLEY, J. F. 1998. A Mec1- and Rad53-dependent checkpoint controls late-firing origins of DNA replication. *Nature,* 395**,** 615-8.

SANTOCANALE, C., SHARMA, K. & DIFFLEY, J. F. 1999. Activation of dormant origins of DNA replication in budding yeast. *Genes Dev,* 13**,** 2360-4.

SCHALBETTER, S. A., MANSOUBI, S., CHAMBERS, A. L., DOWNS, J. A. & BAXTER, J. 2015. Fork rotation and DNA precatenation are restricted during DNA replication to prevent chromosomal instability. 112**,** E4565-70.

SCLAFANI, R. A. & HOLZEN, T. M. 2007. Cell cycle regulation of DNA replication. *Annu Rev Genet,* 41**,** 237-80.

SEGURADO, M., DE LUIS, A. & ANTEQUERA, F. 2003. Genome-wide distribution of DNA replication origins at A+T-rich islands in Schizosaccharomyces pombe. *EMBO Rep,* 4**,** 1048-53.

SEGURADO, M. & DIFFLEY, J. F. 2008. Separate roles for the DNA damage checkpoint protein kinases in stabilizing DNA replication forks. *Genes Dev,* 22**,** 1816-27.

SEGURADO, M. & TERCERO, J. A. 2009. The S-phase checkpoint: targeting the replication fork. *Biol Cell,* 101**,** 617-27.

SENGUPTA, S., VAN DEURSEN, F., DE PICCOLI, G. & LABIB, K. 2013. Dpb2 integrates the leading-strand DNA polymerase into the eukaryotic replisome. *Curr Biol,* 23**,** 543-52.

SHEN, Z. 2011. Genomic instability and cancer: an introduction. *J Mol Cell Biol,* 3**,** 1-3.

SHEU, Y. J. & STILLMAN, B. 2010. The Dbf4-Cdc7 kinase promotes S phase by alleviating an inhibitory activity in Mcm4. *Nature,* 463**,** 113-7.

SHIMMOTO, M., MATSUMOTO, S., ODAGIRI, Y., NOGUCHI, E., RUSSELL, P. & MASAI, H. 2009. Interactions between Swi1-Swi3, Mrc1 and S phase kinase, Hsk1 may regulate cellular responses to stalled replication forks in fission yeast. *Genes Cells,* 14**,** 669-82.

SHIOTANI, B. & ZOU, L. 2009. Single-stranded DNA orchestrates an ATM-to-ATR switch at DNA breaks. *Mol Cell,* 33**,** 547-58.

SHIRAHIGE, K., HORI, Y., SHIRAISHI, K., YAMASHITA, M., TAKAHASHI, K., OBUSE, C., TSURIMOTO, T. & YOSHIKAWA, H. 1998. Regulation of DNA-replication origins during cell-cycle progression. *Nature,* 395**,** 618-21.

SIDDIQUI, K., ON, K. F. & DIFFLEY, J. F. 2013. Regulating DNA replication in eukarya. *Cold Spring Harb Perspect Biol,* 5.

SIKORSKI, R. S. & HIETER, P. 1989. A system of shuttle vectors and yeast host strains designed for efficient manipulation of DNA in Saccharomyces cerevisiae. *Genetics,* 122**,** 19-27.

SKIBBENS, R. V. 2004. Chl1p, a DNA helicase-like protein in budding yeast, functions in sister-chromatid cohesion. *Genetics,* 166**,** 33-42.

SMELKOVA, N. & MARIANS, K. J. 2001. Timely release of both replication forks from oriC requires modulation of origin topology. *J Biol Chem,* 276**,** 39186-91.

SMITH, K. D., FU, M. A. & BROWN, E. J. 2009. Tim-Tipin dysfunction creates an indispensible reliance on the ATR-Chk1 pathway for continued DNA synthesis. *J Cell Biol,* 187**,** 15-23.

SMITH-ROE, S. L., PATEL, S. S., ZHOU, Y., SIMPSON, D. A., RAO, S., IBRAHIM, J. G., CORDEIRO-STONE, M. & KAUFMANN, W. K. 2013. Separation of intra-S checkpoint protein contributions to DNA replication fork protection and genomic stability in normal human fibroblasts. *Cell Cycle,* 12**,** 332-45.

SOMMARIVA, E., PELLNY, T. K., KARAHAN, N., KUMAR, S., HUBERMAN, J. A. & DALGAARD, J. Z. 2005. Schizosaccharomyces pombe Swi1, Swi3, and Hsk1 are components of a novel S-phase response pathway to alkylation damage. *Mol Cell Biol,* 25**,** 2770-84.

SPECK, C., CHEN, Z., LI, H. & STILLMAN, B. 2005. ATPase-dependent cooperative binding of ORC and Cdc6 to origin DNA. *Nat Struct Mol Biol,* 12**,** 965-71.

STILLMAN, B. 2008. DNA polymerases at the replication fork in eukaryotes. *Mol Cell,* 30**,** 259-60.

STINCHCOMB, D. T., STRUHL, K. & DAVIS, R. W. 1979. Isolation and characterisation of a yeast chromosomal replicator. *Nature,* 282**,** 39-43.

SUNDIN, O. & VARSHAVSKY, A. 1980. Terminal stages of SV40 DNA replication proceed via multiply intertwined catenated dimers. *Cell,* 21**,** 103-14.

SUNDIN, O. & VARSHAVSKY, A. 1981. Arrest of segregation leads to accumulation of highly intertwined catenated dimers: dissection of the final stages of SV40 DNA replication. *Cell,* 25**,** 659-69.

SWEENEY, F. D., YANG, F., CHI, A., SHABANOWITZ, J., HUNT, D. F. & DUROCHER, D. 2005. Saccharomyces cerevisiae Rad9 acts as a Mec1 adaptor to allow Rad53 activation. *Curr Biol,* 15**,** 1364-75.

SYLJUASEN, R. G., SORENSEN, C. S., HANSEN, L. T., FUGGER, K., LUNDIN, C., JOHANSSON, F., HELLEDAY, T., SEHESTED, M., LUKAS, J. & BARTEK, J. 2005. Inhibition of human Chk1 causes increased initiation of DNA replication, phosphorylation of ATR targets, and DNA breakage. *Mol Cell Biol,* 25**,** 3553-62.

SZILARD, R. K., JACQUES, P. E., LARAMEE, L., CHENG, B., GALICIA, S., BATAILLE, A. R., YEUNG, M., MENDEZ, M., BERGERON, M., ROBERT, F. & DUROCHER, D. 2010. Systematic identification of fragile sites via genome-wide location analysis of gamma-H2AX. *Nat Struct Mol Biol,* 17**,** 299-305.

SZYJKA, S. J., VIGGIANI, C. J. & APARICIO, O. M. 2005. Mrc1 is required for normal progression of replication forks throughout chromatin in S. cerevisiae. *Mol Cell,* 19**,** 691-7.

TAKAYAMA, Y., KAMIMURA, Y., OKAWA, M., MURAMATSU, S., SUGINO, A. & ARAKI, H. 2003. GINS, a novel multiprotein complex required for chromosomal DNA replication in budding yeast. *Genes Dev,* 17**,** 1153-65.

TANAKA, K. & RUSSELL, P. 2001. Mrc1 channels the DNA replication arrest signal to checkpoint kinase Cds1. *Nat Cell Biol,* 3**,** 966-72.

TANAKA, S. & ARAKI, H. 2013. Helicase activation and establishment of replication forks at chromosomal origins of replication. *Cold Spring Harb Perspect Biol,* 5**,** a010371.

TANAKA, S., UMEMORI, T., HIRAI, K., MURAMATSU, S., KAMIMURA, Y. & ARAKI, H. 2007. CDK-dependent phosphorylation of Sld2 and Sld3 initiates DNA replication in budding yeast. *Nature,* 445**,** 328-32.

TERCERO, J. A. & DIFFLEY, J. F. 2001. Regulation of DNA replication fork progression through damaged DNA by the Mec1/Rad53 checkpoint. *Nature,* 412**,** 553-7.

TERCERO, J. A., LONGHESE, M. P. & DIFFLEY, J. F. 2003. A central role for DNA replication forks in checkpoint activation and response. *Mol Cell,* 11**,** 1323-36.

THEIS, J. F. & NEWLON, C. S. 1997. The ARS309 chromosomal replicator of Saccharomyces cerevisiae depends on an exceptional ARS consensus sequence. *Proc Natl Acad Sci U S A,* 94**,** 10786-91.

THU, Y. M. & BIELINSKY, A. K. 2014. MCM10: one tool for all-Integrity, maintenance and damage control. *Semin Cell Dev Biol,* 30**,** 121-30.

THYS, R. G., LEHMAN, C. E., PIERCE, L. C. & WANG, Y. H. 2015. DNA secondary structure at chromosomal fragile sites in human disease. *Curr Genomics,* 16**,** 60-70.

TOURRIERE, H., VERSINI, G., CORDON-PRECIADO, V., ALABERT, C. & PASERO, P. 2005. Mrc1 and Tof1 promote replication fork progression and recovery independently of Rad53. *Mol Cell,* 19**,** 699-706.

TSE, Y. & WANG, J. C. 1980. E. coli and M. luteus DNA topoisomerase I can catalyze catenation of decatenation of double-stranded DNA rings. *Cell,* 22**,** 269-76.

UHLMANN, F. & NASMYTH, K. 1998. Cohesion between sister chromatids must be established during DNA replication. *Curr Biol,* 8**,** 1095-101.

UMEK, R. M. & KOWALSKI, D. 1988. The ease of DNA unwinding as a determinant of initiation at yeast replication origins. *Cell,* 52**,** 559-67.

UNSAL-KACMAZ, K., CHASTAIN, P. D., QU, P. P., MINOO, P., CORDEIRO-STONE, M., SANCAR, A. & KAUFMANN, W. K. 2007. The human Tim/Tipin complex coordinates an Intra-S checkpoint response to UV that slows replication fork displacement. *Mol Cell Biol,* 27**,** 3131-42.

URTISHAK, K. A., SMITH, K. D., CHANOUX, R. A., GREENBERG, R. A., JOHNSON, F. B. & BROWN, E. J. 2009. Timeless Maintains Genomic Stability and Suppresses Sister Chromatid Exchange during Unperturbed DNA Replication. *J Biol Chem,* 284**,** 8777-85.

UZUNOVA, S. D., ZARKOV, A. S., IVANOVA, A. M., STOYNOV, S. S. & NEDELCHEVA-VELEVA, M. N. 2014. The subunits of the S-phase checkpoint complex Mrc1/Tof1/Csm3: dynamics and interdependence. *Cell Div,* 9**,** 4.

VALLET, J. M., RAHIRE, M. & ROCHAIX, J. D. 1984. Localization and sequence analysis of chloroplast DNA sequences of Chlamydomonas reinhardii that promote autonomous replication in yeast. *Embo j,* 3**,** 415-21.

VAN DER LELIJ, P., CHRZANOWSKA, K. H., GODTHELP, B. C., ROOIMANS, M. A., OOSTRA, A. B., STUMM, M., ZDZIENICKA, M. Z., JOENJE, H. & DE WINTER, J. P. 2010. Warsaw breakage syndrome, a cohesinopathy associated with mutations in the XPD helicase family member DDX11/ChlR1. *Am J Hum Genet,* 86**,** 262-6.

VOS, S. M., TRETTER, E. M., SCHMIDT, B. H. & BERGER, J. M. 2011. All tangled up: how cells direct, manage and exploit topoisomerase function. *Nat Rev Mol Cell Biol,* 12**,** 827-41.

WAGA, S. & STILLMAN, B. 1998. The DNA replication fork in eukaryotic cells. *Annu Rev Biochem,* 67**,** 721-51.

WALLIS, J. W., CHREBET, G., BRODSKY, G., ROLFE, M. & ROTHSTEIN, R. 1989. A hyper-recombination mutation in S. cerevisiae identifies a novel eukaryotic topoisomerase. *Cell,* 58**,** 409-19.

WANG, J. C. 1971. Interaction between DNA and an Escherichia coli protein omega. *J Mol Biol,* 55**,** 523-33.

WANG, J. C. 1996. DNA topoisomerases. *Annu Rev Biochem,* 65**,** 635-92.

WANG, J. C. 2002. Cellular roles of DNA topoisomerases: a molecular perspective. *Nat Rev Mol Cell Biol,* 3**,** 430-40.

WARREN, C. D., ECKLEY, D. M., LEE, M. S., HANNA, J. S., HUGHES, A., PEYSER, B., JIE, C., IRIZARRY, R. & SPENCER, F. A. 2004. S-phase checkpoint genes safeguard high-fidelity sister chromatid cohesion. *Mol Biol Cell,* 15**,** 1724-35.

WATSON, J. D. & CRICK, F. C. 1993. GEnetical implications of the structure of deoxyribonucleic acid. *JAMA,* 269**,** 1967-1969.

WATSON, J. D. & CRICK, F. H. 1953a. The structure of DNA. *Cold Spring Harb Symp Quant Biol,* 18**,** 123-31.

WATSON, J. D. & CRICK, F. H. C. 1953b. Molecular Structure of Nucleic Acids: A Structure for Deoxyribose Nucleic Acid. *Nature,* 171**,** 737-738.

WEINERT, T. A. & HARTWELL, L. H. 1988. The RAD9 gene controls the cell cycle response to DNA damage in Saccharomyces cerevisiae. *Science,* 241**,** 317-22.

WEINERT, T. A., KISER, G. L. & HARTWELL, L. H. 1994. Mitotic checkpoint genes in budding yeast and the dependence of mitosis on DNA replication and repair. *Genes Dev,* 8**,** 652-65.

WYRICK, J. J., APARICIO, J. G., CHEN, T., BARNETT, J. D., JENNINGS, E. G., YOUNG, R. A., BELL, S. P. & APARICIO, O. M. 2001. Genome-wide distribution of ORC and MCM proteins in S. cerevisiae: high-resolution mapping of replication origins. *Science,* 294**,** 2357-60.

XU, H., BOONE, C. & KLEIN, H. L. 2004. Mrc1 is required for sister chromatid cohesion to aid in recombination repair of spontaneous damage. *Mol Cell Biol,* 24**,** 7082-90.

YABUKI, N., TERASHIMA, H. & KITADA, K. 2002. Mapping of early firing origins on a replication profile of budding yeast. *Genes Cells,* 7**,** 781-9.

YOSHIZAWA-SUGATA, N. & MASAI, H. 2007. Human Tim/Timeless-interacting protein, Tipin, is required for efficient progression of S phase and DNA replication checkpoint. *J Biol Chem,* 282**,** 2729-40.

ZECHIEDRICH, E. L. & COZZARELLI, N. R. 1995. Roles of topoisomerase IV and DNA gyrase in DNA unlinking during replication in Escherichia coli. *Genes Dev,* 9**,** 2859-69.

ZECHIEDRICH, E. L., KHODURSKY, A. B., BACHELLIER, S., SCHNEIDER, R., CHEN, D., LILLEY, D. M. & COZZARELLI, N. R. 2000. Roles of topoisomerases in maintaining steady-state DNA supercoiling in Escherichia coli. *J Biol Chem,* 275**,** 8103-13.

ZEGERMAN, P. 2015. Evolutionary conservation of the CDK targets in eukaryotic DNA replication initiation. *Chromosoma,* 124**,** 309-21.

ZEGERMAN, P. & DIFFLEY, J. F. 2007. Phosphorylation of Sld2 and Sld3 by cyclin-dependent kinases promotes DNA replication in budding yeast. *Nature,* 445**,** 281-5.

ZEGERMAN, P. & DIFFLEY, J. F. 2009. DNA replication as a target of the DNA damage checkpoint. *DNA Repair (Amst),* 8**,** 1077-88.

ZEGERMAN, P. & DIFFLEY, J. F. 2010. Checkpoint-dependent inhibition of DNA replication initiation by Sld3 and Dbf4 phosphorylation. *Nature,* 467**,** 474-8.

ZEMAN, M. K. & CIMPRICH, K. A. 2014. Causes and consequences of replication stress. *Nat Cell Biol,* 16**,** 2-9.

ZHAO, X., CHABES, A., DOMKIN, V., THELANDER, L. & ROTHSTEIN, R. 2001. The ribonucleotide reductase inhibitor Sml1 is a new target of the Mec1/Rad53 kinase cascade during growth and in response to DNA damage. *Embo j,* 20**,** 3544-53.

ZHAO, X., MULLER, E. G. & ROTHSTEIN, R. 1998. A suppressor of two essential checkpoint genes identifies a novel protein that negatively affects dNTP pools. *Mol Cell,* 2**,** 329-40.

ZHAO, X. & ROTHSTEIN, R. 2002. The Dun1 checkpoint kinase phosphorylates and regulates the ribonucleotide reductase inhibitor Sml1. *Proc Natl Acad Sci U S A,* 99**,** 3746-51.

ZHU, W., UKOMADU, C., JHA, S., SENGA, T., DHAR, S. K., WOHLSCHLEGEL, J. A., NUTT, L. K., KORNBLUTH, S. & DUTTA, A. 2007. Mcm10 and And-1/CTF4 recruit DNA polymerase alpha to chromatin for initiation of DNA replication. *Genes Dev,* 21**,** 2288-99.

ZOU, L. & ELLEDGE, S. J. 2003. Sensing DNA damage through ATRIP recognition of RPA-ssDNA complexes. *Science,* 300**,** 1542-8.

ZOU, L. & STILLMAN, B. 2000. Assembly of a complex containing Cdc45p, replication protein A, and Mcm2p at replication origins controlled by S-phase cyclin-dependent kinases and Cdc7p-Dbf4p kinase. *Mol Cell Biol,* 20**,** 3086-96.

ZUO, S., GIBBS, E., KELMAN, Z., WANG, T. S., O'DONNELL, M., MACNEILL, S. A. & HURWITZ, J. 1997. DNA polymerase delta isolated from Schizosaccharomyces pombe contains five subunits. *Proc Natl Acad Sci U S A,* 94**,** 11244-9.

Appendix